THE GEOCHEMISTRY AND PETROLOGY OF THE ROOFROCKS OF THE BUSHVELD COMPLEX EAST OF GROBLERSDAL

BY

GÜNTHER JOHANN KLEEMANN

Submitted in partial fulfilment of
the requirements for the degree of
MASTER OF SCIENCE
in the faculty of Science,
University of Pretoria

JUNE 1985

ACKNOWLEDGEMENTS

The author would like to thank the Council for Scientific and Industrial Research, the Council for Research Priorities of Southwest Africa and the Institute for Geological Research on the Bushveld Complex for the financing of this study.

Sincere thanks are due to Prof. G. Von Gruenewaldt and Dr. D. Twist for supervision and continued interest in this study.

Dr. M.R. Sharpe and Mr. J.P. Engelbrecht are thanked for assistance in the data processing and XRF analyses and Mrs M. Potgieter for drafting the diagrams.

The family J.J. Dreyer of Rooikraal is thanked for accomodation during field work.

Rand Mines Limited made available the core of the bore-holes drilled on Varschwater 23JS.

Dr. C. Frick of the Geological Survey of South Africa gave permission to use the SEM and the microprobe.

Mr S.B. Gain of the Mining Corporation gave access to geochemical data on the Lebowa Granite Suite.

Last but not least thanks are due to my wife for her patience and encouragement and to my parents for financial support.

Abstract

The area investigated extends west of longitude 29°55' and south of latitude 25°00'. The major acid components of the Bushveld Complex, the Rashoop Granophyre Suite and the Lebowa Granite Suite and the volcanic rocks of the Rooiberg Felsite Group are exposed. Rocks of the Rustenburg Layered Suite occur in the south-eastern sector of the area.

Stavoren Granophyre and Rooiberg Felsite occupy the western part of the study area. A detailed petrographical description of the granophyres was undertaken and several granophyric intergrowth forms were distinguished. The granophyres are fairly homogenous in composition throughout the 2000 metre thick sheet, while the felsites display a differentiation trend. It seems that the two rocktypes are related. Either the granophyres represent a partial melt extracted from the felsites on metamorphism by the Rustenburg Layered Suite or the felsites and granophyres represent one co-magmatic suite.

The Lebowa Granite Suite occurs in the western half of the study area and consists of the Nebo Granite and several Klipkloof Granite types. A mineral gradation, differences in grain size and colour, and geochemical fractionation is observeable from bottom to top in the Nebo Granite sheet. The Klipkloof Granite occurs in the stratigraphically higher portions of the Nebo Granite sheet, where it forms undulating, flat-lying sills and dykes, which are intrusive into the Nebo Granite.

The Nebo Granite is characterized by a well defined differentiation trend, whereas the Klipkloof Granite, being highly differentiated, plots randomnly near the end of the Nebo Granite trends. The majority of the geochemical plots presented suggest that the Klipkloof Granite is a late-stage

evolved phase of the Nebo Granite. There is, however, a difference between the two with respect to their Al_2O_3, TiO_2 and Zr concentrations, which seems to reflect some late metasomatic alteration of the Klipkloof Granite.

The upper portions of the tin-specialized albitized Klipkloof Granite were probably lost by erosion. Therefore no significant tin concentrations could be found. The possibility for more molybdenum and copper mineralization exist, where the mineralizing fluids were trapped by Klipkloof Granite sills. The Stavoren Granophyre could also have served as a trap for mineralization.

The albitized Klipkloof Granite of the study area has the same fractionation pattern for Rb, Ba and Sr as was observed in the highly metasomatized tin-bearing granites of the Zaaiplaats area. The fractionation pattern in the unmineralized slightly altered Klipkloof Granite, however, appears to be the normal pattern for the Bushveld Granite. These differences could thus be useful in the identification of target areas for tin mineralization.

Samevatting

Die studiegebied strek wes van lengtegraad 29°55' en suid van breedtegraad 25°00'. Die belangrikste suurgesteentes van die Bosveldkompleks, die Suite Rashoopgranofier Suite Lebowagraniet en die vulkaniese gesteentes van die Groep Rooiberg is in die gebied ontwikkel. Gesteentes van die Gelaagde Suite Rustenburg dagsoom in die suid-oostelike deel van die gebied.

Stavorengranofier en Rooibergfelsiet beslaan die westelike gedeelte van die studiegebied. 'n Breedvoerige petrografiese beskrywing van die granofiere is gedoen en verskeie granofiriese vergroeiings is onderskei. Die granofiere is taamlik homogeen in samestelling in die 2000 meter dik opeenvolging, terwyl die felsiete 'n differensiasie neiging vertoon. Dit wil voorkom asof die twee gesteentetipes verwant aanmekaar is. Die granofiere verteenwoordig of 'n gedeeltelike smeltsel geekstraheer uit die felsiete tydens metamorfose tydens indringing van die Gelaagde Suite Rustenburg of die felsiete en granofiere verteenwoordig een ko-magmatiese suite.

Die Lebowagraniet dagsoom in die westelike gedeelte van die studiegebied en bestaan uit die Nebograniet en verskeie Klipkloofgraniet tipes. 'n Mineraal gradasie, verskille in korrelgrootte en kleur, en geochemiese fraksionasie is waarneembaar van onder na bo in die Nebograniet laag. Die Klipkloofgraniet is in die stratigrafies hoër gedeeltes van die Nebograniet en selfs tot in die Stavorengranofier ontwikkel en vorm 'n aantal opeenvolgende golwende, plat-lêende plate en gange.

Die Nebograniet word gekarakteriseer deur 'n goed-gedefinieerde differensiasie neiging, terwyl die Klipkloof-graniet, wat hoogs gedifferensieerd is, onreelmatig aan die einde van die Nebograniet differensiasiepatroon stip.

Die meerderheid van die geochemiese diagramme dui daarop dat die Klipkloofgraniet 'n laatfase van die Nebograniet is. Daar is egter 'n verskil in Al_2O_3, TiO_2 and Zr konsentrasie tussen die twee graniete, wat op moontlike laat metasomatiese verandering van die Klipkloofgraniet dui.

Die boonste gedeeltes van die tin gespesialiseerde ge-albitiseerde Klipkloofgraniet het heelwaarskynlik as gevolg van erosie verlore gegaan aangesien geen belangrike tin konsentrasies daarin gevind word nie. Die moontlikheid vir meer molibdeen en koper mineralisasie bestaan waar mineraliserende vloeistowwe vasgevang is deur Klipkloofgraniet plate. Die Stavorengranofier kan ook dien as 'n ondeurdringbare laag waaronder mineralisasie kan plaasvind.

Die ge-albitiseerde Klipkloofgraniet van die studiegebied toon dieselfde fraksionasieneiging vir Rb, Ba en Sr as die in hoogs gemetasomatiseerde tin-draende graniete van die Zaaiplaatsgebied. Die fraksionasieneiging van die ongemineraliseerde, minder metasomaties veranderde Klipkloofgraniet, blyk die normale neiging vir die Bosveldgraniete te wees. Hierdie verskille kan gebruik word in die identifikasie van teikengebiede vir tinmineralisasie.

CONTENTS

LIST OF FIGURES IN THE TEXT

LIST OF TABLES IN THE TEXT

1. Introduction.

The present study was undertaken to describe and investigate the geology and geochemistry of the Bushveld Complex in the area immediately east of Groblersdal. Here the major acid components of the complex, the Rashoop Granophyre Suite and the Lebowa Granite Suite, as well as the acid volcanic roofrocks, the felsites of the Rooiberg Group, are exposed (Fig.1.1). Part of the area was mapped for an Honours project during July 1980. Further mapping, covering some 400 square kilometres and extending west of longitude 29°55' and south of latitude 25°00', was conducted with the aid of aerial photographs (scale 1:30000) during the summer months of 1981. The information gathered was transferred to 1:50000 topographic maps (2529AB Groblersdal and 2529BA Maleoskop) from which a final geological map was compiled (Folder 1, back folder).

A total of 270 samples were collected, of which 230 were selected (for location see Folder 2, back folder) and analysed for major and trace elements on the Siemens SRS-1 X-ray fluorescence spectrometer in the Departement of Geology, University of Pretoria. The scanning electron microscope and the electron microprobe of the Geological Survey of South Africa were used for the mineralogical investigation of some of these samples.

The aims of the present study are to provide a detailed description of the petrography of the rock types; to investigate the geochemical evolution of the Bushveld granite magmas in the region and the possible mineralization in the younger intrusives; to elucidate the geochemical specialization of the Klipkloof Granite; and to correlate the granites of the study area with those of the Zaaiplaats area.

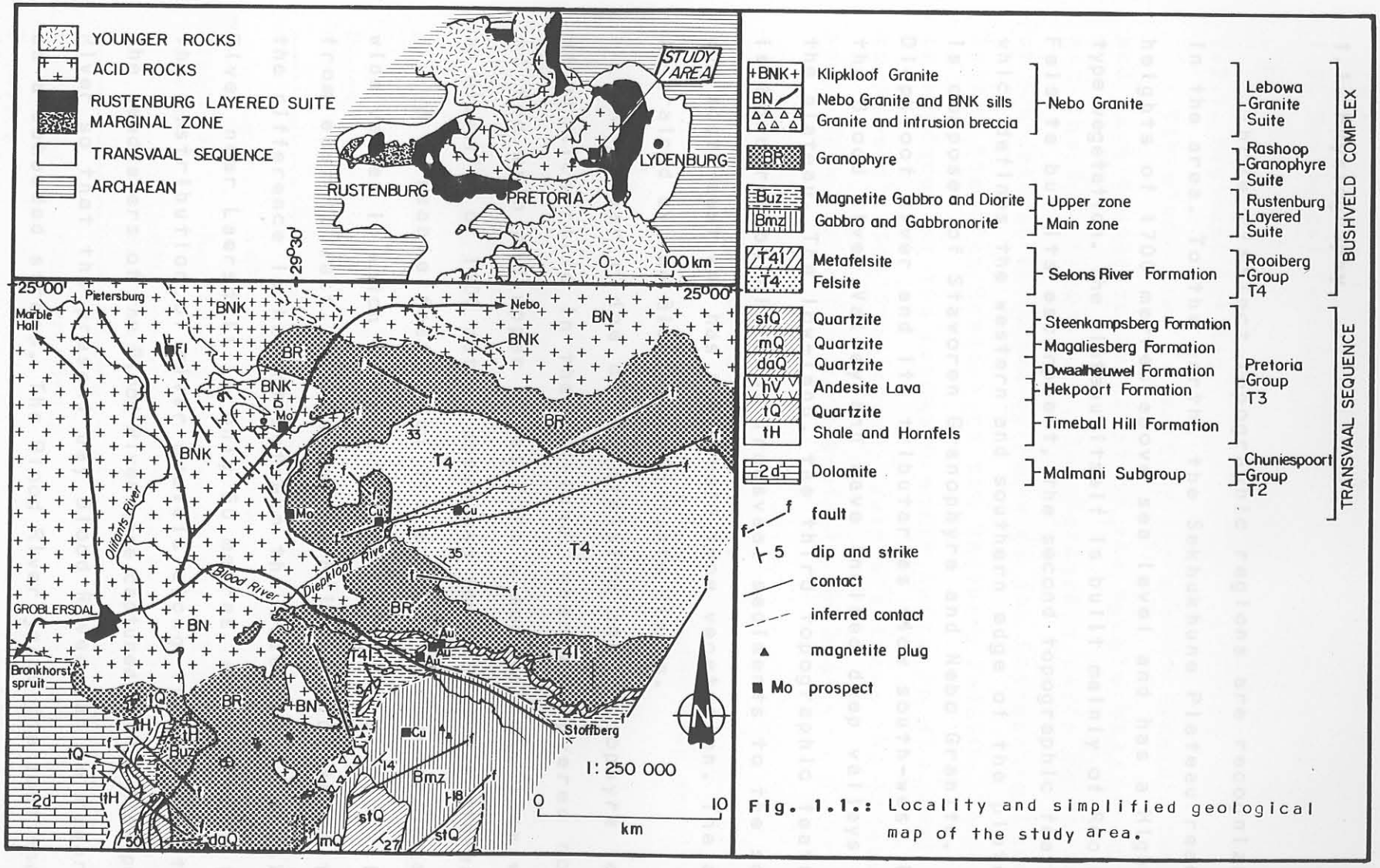

Fig. 1.1.: Locality and simplified geological map of the study area.

1.1. Physiography.

Three distinct topographic regions are recognizable in the area. To the north, the Sekhukhune Plateau reaches heights of 1700 metres above sea level and has a Highveld type vegetation. The plateau itself is built mainly of Rooiberg Felsite but its escarpment, the second topographic feature, which defines the western and southern edge of the plateau, is composed of Stavoren Granophyre and Nebo Granite. The Diepkloof River and its tributaries flow south-west into the Blood River Valley and have incised deep valleys into the plateau. The low-land, the third topographic feature, is bordered by hills of Transvaal sediments to the south and south-east and has a Bushveld type vegetation. The area is drained by the Blood- and Olifants Rivers.

A linear ridge of metafelsite and granophyre forms an erosion relic in the low-land, whereas layered rocks of the main and upper zones form a mountainous area with an elevation of 1400 metres above sea level in the south-east.

A noteable feature of the area is the exceptionally wide valley in which the Blood River, a minor stream, flows from east to west. Willemse and Frick (1970) found that the difference in height between the Steelpoort and Blood River near Laersdrif is only 50 metres, and concluded from the distribution of river gravels along the divide that the headwaters of the Blood River were captured by the Steelpoort River so that the present day Blood River can be regarded as a beheaded stream. The Blood River joins the south-north flowing Olifants River near Groblersdal.

1.2. Geological Setting.

1.2.1. Regional Setting.

The study area is part of the eastern Bushveld Complex and is situated to the east of the Marble Hall fragment and the Dennilton dome. The Maleoskop basin to the east of Groblersdal is formed by rocks of the Rustenburg Layered Suite, Stavoren Granophyre and Rooiberg Felsite. The basin is bordered by the Lebowa Granite Suite to the west and south-west. The Steelpoort fault displaces the Maleoskop basin from the Tauteshoogte basin in the east.

1.2.2. Major geological components.

The geological formations present in the area are listed in Table 1.1.

Table 1.1. Geological formations developed in the study area.

Sequence or Era	Group or Suite	Formation or Unit
Recent		Alluvium and soil
Karoo		Karoo dolerite
Bushveld Complex	Lebowa Granite Suite	Klipkloof Granite
		Nebo Granite
	Rustenburg Layered Suite	upper zone
		main zone
	Rashoop Granophyre Suite	Stavoren Granophyre
	Marico Diabase Suite	Pre-Bushveld Sills
Transvaal Sequence	Rooiberg Group	Selons River
	Pretoria Group	Timeball Hill
		Hekpoort
		Dwaalheuwel
		Magaliesberg
		Steenkampsberg

Only those formations not discussed in detail in the following chapters are described briefly below.

1.2.3. The Pretoria Group.

Quartzites and shales of the Pretoria Group, the oldest rocks in this area, are restricted to the south-western and southern parts of the area. Pre-Bushveld sills are intrusive into this sequence.

The Timeball Hill Formation dips at 50° to the east and consists of a lower shale member, a 120 metres thick quartzite member and an upper shale member. Low- to medium grade metamorphism of the lower and upper shale members by diabase sills and the Rustenburg Layered Suite resulted in the formation of muscovite hornfels.

Overlying the Timeball Hill Formation are lavas of the Hekpoort Formation, which attain a thickness of about 20 metres. Button (1973) has shown the Hekpoort lavas of the eastern Transvaal to be transitional between continental basalt and andesite compositions. Sharpe et al. (1983) found that the Hekpoort lavas of the western and eastern Transvaal are of andesite composition on some classification systems, whereas on others they belong to the basaltic andesites or even tholeiitic basalts.

The Hekpoort Formation is overlain by quartzite, which has a thickness of about 100 metres and dips at 45° to the east. According to Button (1973) this quartzite member, the Dwaalheuwel Formation, is always present overlying the Hekpoort Formation in the Transvaal basin north of Pretoria.

The Magaliesberg and Steenkampsberg Formations occur in the south-east of the study area and were described in some detail by Von Gruenewaldt (1966).

1.2.4. The Rustenburg Layered Suite.

The main and upper zones of the Rustenburg Layered Suite are represented in the area. The outcrops of the upper zone are generally weathered and magnetite plugs are sometimes

the only indication of the presence of the mafic rocks, as for instance on Weltevreden 165JS.

Gabbros and gabbronorites are the predominant rock types of the main zone in the area. Dips measured on the stratification in anorthosite layers show the rocks to dip at 12 to 14° to the south-east, whereas a dip measurement on the Tennisball-marker was found to be 18° to the east. A fault could be responsible for the difference in dip.

The upper zone is represented by olivine diorite and magnetite plugs. Magnetite layer 21 crops out along the foot of the escarpement on Weltevreden 165JS and Haakdoringdraai 169JS, where it underlies the metafelsites and granophyres. A magnetite plug on Weltevreden 165JS was found to pierce the roof of metafelsite.

The Rustenburg Layered Suite is developed on both sides of the prominent ridge of fine-grained acid roofrocks on Weltevreden 165JS. However, the only indication of the presence of these rocks on the western side of the ridge are magnetite plugs and chips of gabbro recovered from old percussion drill holes.

The intrusion breccia on Rietkloof 166JS contains all the different rock types of the main and upper zones found in the area. A fine-grained mafic rock, possibly a sill of critical zone composition (M.R. Sharpe, pers. comm.), constitutes the largest part of the breccia.

Rocks of the Rustenburg Layered Suite are also developed on Kalkfontein 49JS, where a magnetite plug seems to be intrusive into the rocks of the Transvaal Sequence.

Granodiorites, representing highly contaminated upper zone liquids, occur as a sheet underlying the Stavoren Granophyre and as irregular veins and pockets in the metafelsite. They are composed of quartz, perthite, oligoclase, hornblende, biotite and fayalite. Accessory phases are clinopyroxene,

apatite, zircon, magnetite, ilmenite, sphene, allanite and fluorite.

The first minerals to crystallize in the granodiorites were feldspars and quartz with hornblende interstitial between these grains. Hornblende is dark green, pleochroic and probably a hastingsite.

Olivine, another early crystallizing phase, is present in the granodiorite as a minor constituent compared to diorites of the upper zone, where it is abundant. It is altered to iddingsite or iron oxides and only the original outline of the olivine grain is usually recognizable.

Coarse granophyric intergrowth is present in the granodiorites and the content thereof increases as the granophyre is approached. The transitional rock was called a melanogranophyre by Von Gruenewaldt (1971).

Zircons in the granodiorite are zoned and two phases of growth can usually be distinguished in most grains. Most zircon grains are cracked and contain inclusions.

Allanite is a major accessory phase in the granodiorites and forms irregular patches or well developed zoned crystals.

1.2.5. Structural features.

The structure of the area is dominated by the Maleoskop basin (Clubley-Armstrong and Sharpe, 1979). Rooiberg Felsite, Stavoren Granophyre and the underlying basic rocks of the Rustenburg Layered Suite form this basin.

The structure of the Transvaal Sequence in this area is dominated by broad, open folding and by a number of major faults.

A magnetite plug crops out on Kalkfontein 49JS underlying the quartzite member of the Timeball Hill Formation. The relation of upper zone rocks in the area with critical zone further south is not understood. The occurrence of basic

rocks, especially a magnetite plug, explains the gravity-high over this farm (Hattingh, 1977).

The intrusion breccia on Rietkloof 166JS is located at the intersection of faults and the extension of the ridge of fine-grained acid roofrocks (Folder 1, back folder). The intersection of faults produced a weakness in the crust, which resulted in the forceful intrusion of the granitic magma. The ridge of fine-grained acid roofrocks together with the upper zone next to it, represents a downfaulted block.

A postulated WNW-ESE striking fault, to the north of and parallel to the Blood River (Von Gruenewaldt, 1966) is considered responsible for the difference in dip and strike between the ridge of fine-grained acid roof rocks to the south and the rocks of the Maleoskop basin to the north.

1.3. Previous Work.

Previous work in this area has been carried out by Hall (1913), who gives an explanation of the regional geology; by Wagner (1929), who noted the occurrence of platinoids in the rocks of the Layered Suite on Blaauwbank 168JS; by B.V. Lombaard (1934) who concluded from his work in the Blood River valley that the granite, granophyre and rhyolite represent textural modifications of the same magma; by A.F. Lombaard (1949), who investigated the relationships between various rocks in the Blood River area; by Von Gruenewaldt (1966,1971), who did extensive work to the south and east respectively, drawing regional correlations and proposing a model for the origin of the roof rocks; and by MacCaskie (1983), who mapped the area and did extensive geochemical research on the Lebowa Granite Suite.

The felsites of the Rooiberg Group were mainly investigated

by Lombaard (1932), who proposed a classification for these rocks; by Wolhuter (1954); by Von Gruenewaldt (1968), who investigated the felsites north of Middelburg; by Clubley-Armstrong (1977), who recognized the Damwal and Selons River Formation in the Loskop Dam area and by Twist (1984), who did research on the geochemistry of these rocks and recognized three magma types.

The granophyres have been the subject of detailed investigations by Von Gruenewaldt (1971) and Walraven (1982), who reached markedly different conclusions on the origin of these rocks. Von Gruenewaldt (op. cit.) argued that the granophyres crystallized from a magma which formed during the melting of felsite due to the intrusion of the Layered Suite magma. Walraven (op. cit.), however, claimed that the Rooiberg Felsite and Stavoren Granophyre respectively represent the volcanic and hypabyssal counterparts of one co-magmatic igneous suite.

Most detailed geochemical work on the Lebowa Granite Suite has been done in the Zaaiplaats area by Fourie (1969), Lenthall (1975), Lenthall and Hunter (1977), Groves and McCarthy (1978), Strydom (1983) and Coetzee (1984). Strauss and Truter (1944) and Strauss (1954) recognized four different granite types in the Zaaiplaats area: the Main Granite (Nebo Granite), the Foothills Granite, the Bobbejaankop Granite and the Lease Granite. The primary tin mineralization in the Zaaiplaats area is associated with the Bobbejaankop and Lease Granite.

1.4. Analytical Techniques.

Glass disks of the rock powders were prepared according to the method of Norrish and Hutton (1969) and analysed by XRF for all the major elements except sodium. Compressed 34 millimetre powder pellets were used to analyse for sodium

and the trace elements Nb,Zr,Y,Sr,Rb,Ba,Sc,Zn,Cu,Ni,U,Th,Pb,-Nd,Ce,La,Ga,Hf,Sn,W and Mo. The experimental parameters for major and trace element analyses are listed in Tables 1.2. and 1.3. respectively.

The analytical accuracy for major elements is better than one per cent for concentrations greater than one per cent and better than two per cent where the concentration is less than one per cent. Accuracy for trace elements is about five per cent for concentrations less than 20 ppm and about two per cent for concentrations above 50 ppm.

The precision of major and trace element analyses is similar to the accuracy at low concentration of a particular element, but is better than about 0,5 per cent at concentrations of more than five per cent for major elements and more than 50 ppm for trace elements.

Table 1.2. Experimental parameters for major element analyses.

Oxide	SiO_2	Al_2O_3	TiO_2	Fe_2O_3	MnO	MgO	CaO	K_2O	Na_2O	Cr_2O_3	NiO	P_2O_5
Tube	Cr	Cr	Cr	W	W	Cr	Cr	Cr	Cr	W	Cr	Cr
Crystal	PET	PET	LIF 220	LIF 220	LIF 220	TLAP	LIF 220	LIF 220	TLAP	LIF 220	LIF 220	Ge
Detector	FC	FC	FC	FC	FC	FC	FC	FC	FC	FC	FC	FC
Aperture	Au	Au	Au	Au	Au	Au	Au	Au	Au	Au	Au	Au
Collimator (Deg)	0,4	0,4	0,15	0,15	0,15	0,4	0,15	0,4	0,4	0,15	0,15	0,4
2θ-Angle	109,155	145,195	86,125	85,775	95,222	45,137	113,135	136,758	55,110	107,200	71,290	140,760
Count-time (sec)	100	100	20	20	40	100	20	20	100	100	100	100
Detection-lim (%)	0,048	0,029	0,007	0,032	0,012	0,143	0,009	0,003	0,080	0,011	0,011	0,025

Table 1.3. Experimental parameters for trace element analyses.

Element	Tube	Aperture	Detector	Crystal	Collimator	Count-time (sec)	2θ-Angle	Detection-lim (ppm)
Ba	Cr	Cr	FC	LIF 200	0,15	200	87,146	3
Rb	W	Cr	SC	LIF 220	0,15	100	37,942	2
Sr	W	Cr	SC	LIF 220	0,15	100	35,830	2
Y	W	Cr	SC	LIF 220	0,15	100	33,868	2
Zr	W	Cr	SC	LIF 220	0,15	100	32,090	2
Nb	W	Cr	SC	LIF 220	0,15	200	30,430	2
La	W	Au	FC	LIF 220	0,15	100	139,042	2
Ce	W	Au	FC	LIF 220	0,15	400	111,770	4
Nd	W	Au	FC	LIF 220	0,15	200	112,832	3
Th	W	Cr	SC	LIF 220	0,15	200	39,300	4
U	W	Cr	SC	LIF 220	0,15	200	37,400	4
Hf	Mo	Cr	SC	LIF 200	0,15	200	39,942	4
Ga	Mo	Cr	SC	LIF 200	0,15	200	38,948	1
Sc	Cr	Cr	FC	LIF 200	0,15	200	97,700	1
Zn	Au	Au	SC	LIF 220	0,15	100	60,511	2
Cu	Au	Au	SC	LIF 220	0,15	100	65,622	2
Ni	Au	Au	SC	LIF 220	0,15	100	71,348	2
Pb	W	Cr	SC	LIF 220	0,15	200	40,400	4
Mo	Au	Au	SC	LIF 220	0,15	200	28,935	3
W	Mo	Cr	SC	LIF 220	0,15	200	62,525	6
Sn	Mo	Cr	SC	LIF 220	0,15	200	19,920	6

2. The Rooiberg Felsite Group.

2.1. Field Relationships.

East of Groblersdal the Rooiberg Group occupies a synformal structure which Clubley-Armstrong and Sharpe (1979) and Walraven (1982) respectively termed the Maleoskop and Angewezen basin. The felsites are intruded by a thick sill of Stavoren Granophyre, which separates an upper unit of comparatively unaltered felsites from a lower unit of metafelsites. The metafelsites overlie the upper zone of the Rustenburg Layered Suite along the foot of the escarpment on the farms Weltevreden 165JS and Haakdoringdraai 169JS, and thicken towards the east.

Several investigators have attempted to subdivide the Rooiberg Felsite Group into different stratigraphic units. Von Gruenewaldt (1968) proposed a three-fold division for an area north of Middelburg which he subsequently applied to the area to the east of the study area (Von Gruenewaldt, 1971). The following subdivision was suggested:

1. A lower felsite zone, which is in contact with rocks of the upper zone of the Layered Sequence and therefore consists mostly of metafelsite.

2. A middle felsite zone, consisting of a thin layer of amygdaloidal lava, occurs immediately above the Stavoren Granophyre, which separates it from the lower felsite zone.

3. An upper felsite zone of massive, porphyritic and non-porphyritic varieties, forming the bulk of the felsites outcropping on the Sekhukhune Plateau.

Clubley-Armstrong (1977) suggested a broad subdivision of the felsites in the Loskopdam-Middelburg region, including the areas mapped by Von Gruenewaldt (1968, 1971), into a lower Damwal Formation and an upper Selons River Formation.

Details of Clubley-Armstrong's classification are presented in Table 2.1., where some tentative correlations with Von Gruenewaldt's stratigraphic units are proposed.

Metafelsites, constitute the lowest portion of the Rooiberg felsite. The metamorphosed lavas include dark brown porphyritic types, massive magnetite-rich types and dark brown micrographic types. These are highly recrystallized and partially melted rock types and their original textures are therefore largely obliterated. Flow-banding and agglomeratic textures, however, are still recognizable in these rocks (Fig.2.1 and 2.2).

In the linear metafelsite and granophyre ridge on Weltevreden 165JS and Rietkloof 166JS (Fig.2.3), only a thin layer of metafelsite, dipping at 5° to the west, is present on the western side of the ridge. Microgranophyre is in contact with mafic rocks where metafelsite is absent.

Different stages of recrystallization, reflected by the increasing coarseness of micrographic intergrowth, can be recognized in the metafelsite horizon. Features such as veins of leucocratic microgranite, cutting irregulary through the metafelsite, and veins and pockets of granodiorite with inclusions of metafelsite were observed (Fig.2.4 and 2.5). A detailed description of these features was provided by Von Gruenewaldt (1971) and is therefore not included here.

A thin layer of amygdaloidal felsite, recognized by Von Gruenewaldt (1971) in the area to the east, peters out to the west. This amygdaloidal felsite is the only rocktype representative of the middle felsite zone. It crops out near the contact with granophyre on the farm Hartbeestlaagte 162JS and attains a thickness of 100 metres.

The upper felsite zone, which apparently corresponds to the lower Selons River Formation, represents the bulk

Table 2.1. Correlations of Clubley-Armstrong's (1977) and Von Gruenewaldt's (1968 and 1971) classification of the Roolberg Felsite.

		Loskopdam and Middelburg Clubley-Armstrong (1977)	North of Middelburg Von Gruenewaldt (1968)	Sekhukhune Plateau Von Gruenewaldt (1971) and this study
SELONSRIVER FORMATION	Klipnek Felsite Member	red porphyritic felsite mainly flowbanded		
	Doornkloof Felsite Member	dark, laminated mudstone Union Tin tuff member black felsite and amygdaloidal felsite underlain by porphyritic variety and impersistent pyroclastics	shale, well-bedded	
		red porphyritic felsite mainly massive with occasional sandstone layers, tuff and quartzite xenoliths	purple agglomerate reddish-brown porphyritic felsite agglomerate quartzite amygdaloidal felsite	red-brown porphyritic felsite quartzite layer red porphyritic felsite mainly massive with impersistent pyroclastics and quartzite xenoliths thin amygdaloidal felsite
		sandstone/quartzite layer	dual-marker: quartzite	
DAMWAL FORMATION		agglomerate, sandstone layers black felsite large discshaped amygdales	with agglomerate below black and glassy porphyritic felsite amygdales up to 30 centimeter in diameter	
		black variable felsite mainly porphyritic and pseudospherulitic interbedded with discontinous layers of black glassy felsite, amygdaloidal felsite, agglomerate, tuff and sandstone	black amygdaloidal felsite pseudospherulitic felsite irregular lenses of quartzite	
		granophyric red felsite micrographic felsite leptite	microgranophyre, granophyre and microgranite leptite	microgranophyre, granophyre and microgranite metafelsite (leptite)

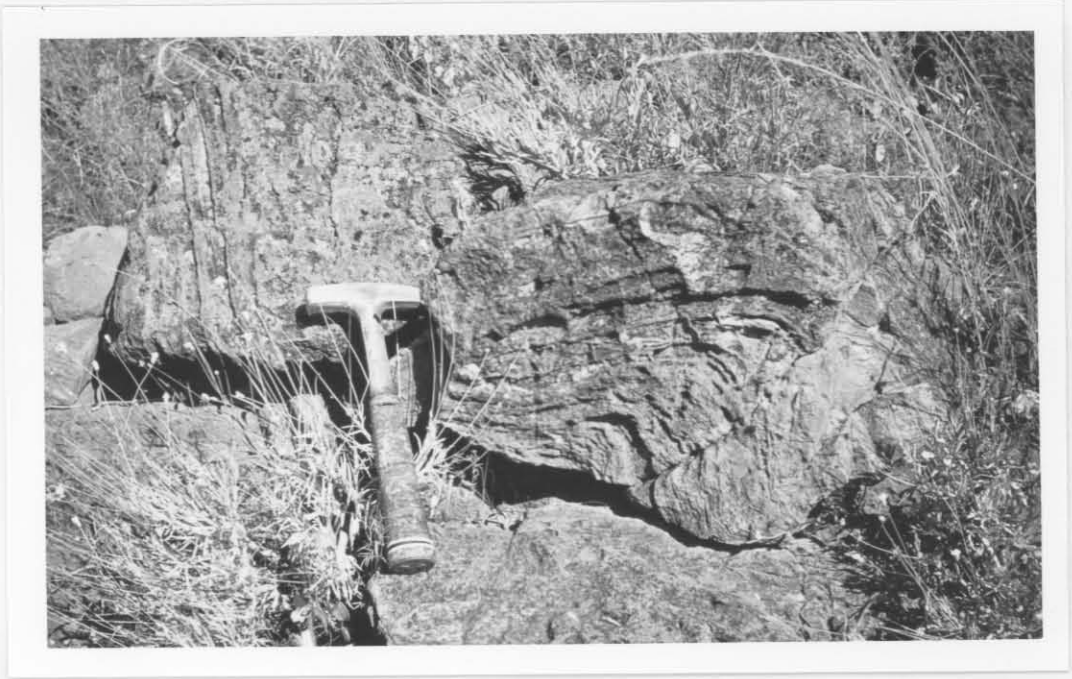

Fig. 2.1.: Flowbanding preserved in metafelsite. Weltevreden 165JS.

Fig. 2.2.: Agglomeratic textures recognizable in metafelsite. Weltevreden 165JS.

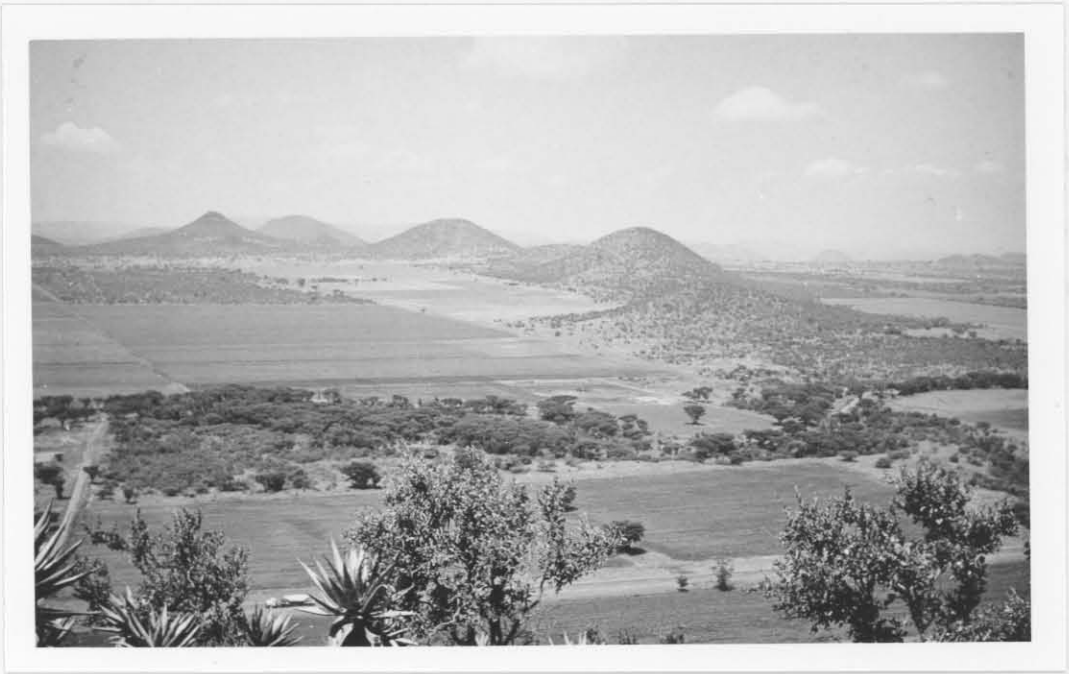

Fig. 2.3.: The metafelsite ridge on Weltevreden 165JS and the three prominent magnetite plugs on Rietkloof 166JS in the background.

Fig. 2.4.: Veins of leucocratic microgranite (to the left of the hammer) cutting irregulary through metafelsite. Weltevreden 165JS.

of the felsites in the Aangewezen basin. These rocks comprise porphyritic and non-porphyritic, massive red and black felsites, sometimes flow-banded (Fig.2.6) and/or amygdaloidal, and interstratified with occasional layers of agglomerate (Fig.2.7) and tuff (Fig.2.8).

Because of the gentle centripetal dips of the felsites in the Aangewezen basin, about 5-10° in the north and 30° in the south, the variety of rock types exposed is limited. This makes it difficult to correlate the sequence with that of areas like Loskopdam, where the dips are steep and a thick succession is exposed.

It should be noted that the metafelsites are not a specific stratigraphic unit in the Rooiberg Group. Depending on the depth at which the layered rocks intruded and on the amount of melting of felsite (Von Gruenewaldt, 1971), the metafelsite unit may be developed at any level in the Rooiberg Group.

2.2. Petrography of the felsite.

The felsites of the Aangewezen basin are mainly massive and porphyritic to glomeroporphyritic with altered plagioclase phenocrysts (0,5 to 3,0 mm) and rare quartz phenocrysts (0,5 to 1,0 mm) set in a fine-grained groundmass. The groundmass is composed of quartz, feldspar, hornblende and opaque particles.

Magnetite is the major opaque mineral and contains exsolution lamellae of ilmenite. Apatite, calcite, rutile, sphene and zircon were found as accessory minerals in these rocks. Most of the accessory phases were analysed with the SEM, because microscopic identification was not possible in the fine-grained groundmass.

Quartz needles (0,5 to 1,0 mm), pseudomorphous after tridymite, are common in some varieties. It is evident that

Fig. 2.5.: Inclusion of metafelsite in granodiorite. Weltevreden 165JS.

Fig. 2.6.: Intense flowbanding in Rooiberg Felsite. Kwaggavoetpad 163JS.

Fig. 2.7.: Agglomerate. Mooiplaats 121JS.

Fig. 2.8.: Tuff. Hartbeestlaagte 162JS.

they formed by the inversion of tridymite to quartz, because every needle can consist of different orientations of quartz (Fig.2.9). Clusters of quartz needles with the same extinction (Fig.2.10) are also considered to represent quartz after tridymite. In such cases the original small tridymite needles were replaced by quartz, resulting in a group with the same orientation.

Amygdales in the felsites (Fig.2.11) are composed of quartz and rarely calcite. They may be surrounded by spherulites which show characteristic extinction crosses.

Agglomerates are sericitized and it is difficult to make out the original features of these rocks (Fig.2.12).

2.3. Petrography of the metafelsite.

The metafelsites are recrystallized felsites, with the degree of recrystallization depending on the distance from the contact with the rocks of the upper zone. Melting of the rocks has taken place where they were in contact with the magma of the Rustenburg Layered Suite, resulting in the development of granitic veinlets and patches of restite or basic fronts.

The metafelsites may be derived from porphyritic felsites, fine-grained massive felsites with or without flow-banding, amygdaloidal and spherulitic varieties or pyroclastic rocks.

Recrystallization of porphyritic felsite typically produces a granoblastic polygonal groundmass comprising quartz, feldspar, clinopyroxene, chlorite, magnetite and sphene and containing relict altered phenocrysts, presumably altered feldspar (Fig.2.13). The sphene content is variable and in some instances it is only an accessory phase. Hornblende may be a major constituent of the rocks, depending on the metamorphic grade and the original composition of the rock. Other accessory minerals in the metafelsites are apatite, ilmenite,

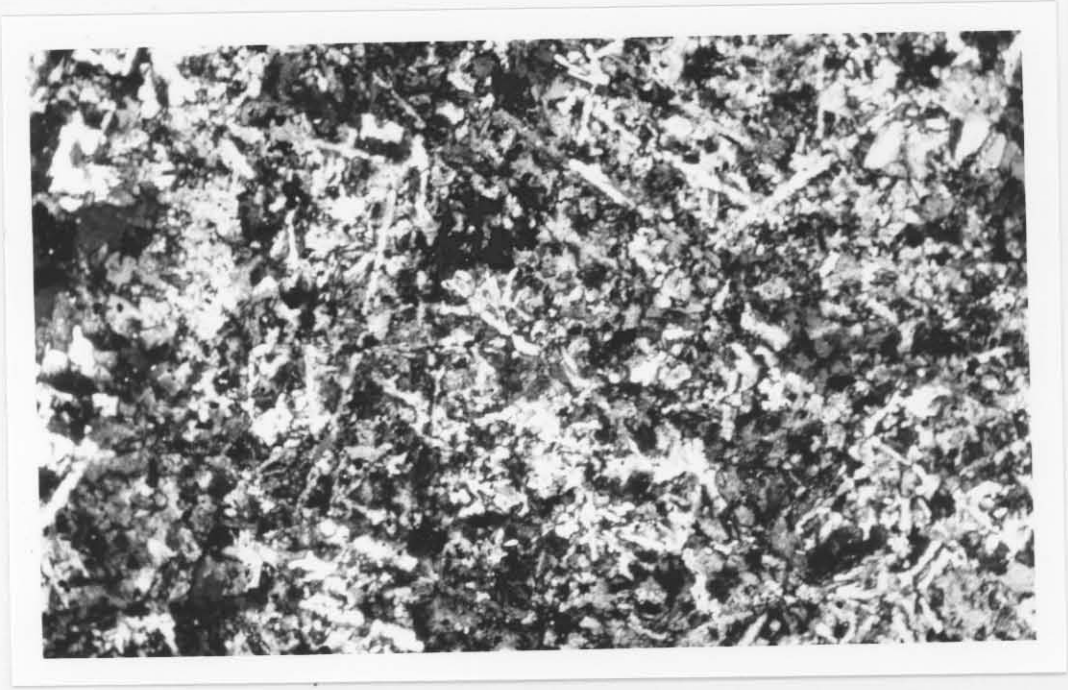

Fig. 2.9.: Tridymite needles in Rooiberg Felsite, where segments with different optical orientations are developed in one needle. F-67. X-Nicols. 63x. Kwaggavoetpad 163JS.

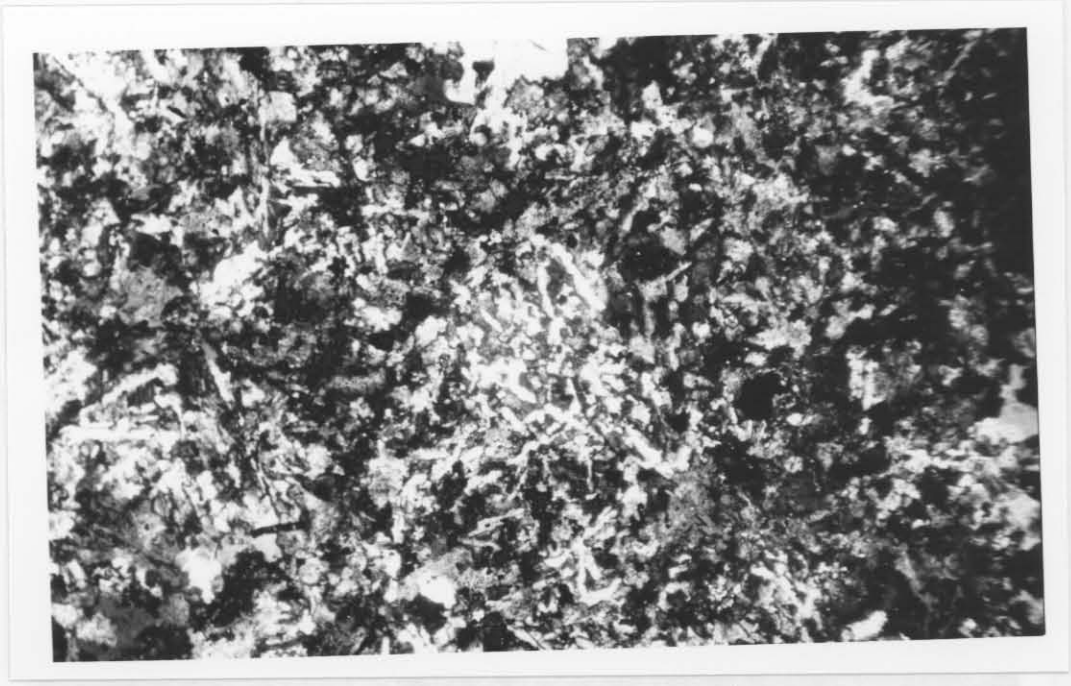

Fig. 2.10.: A group of tridymite needles with uniform extinction in Rooiberg Felsite, representing a secondary quartz grain. F-60. X-Nicols. 63x. Kwaggavoetpad 163JS.

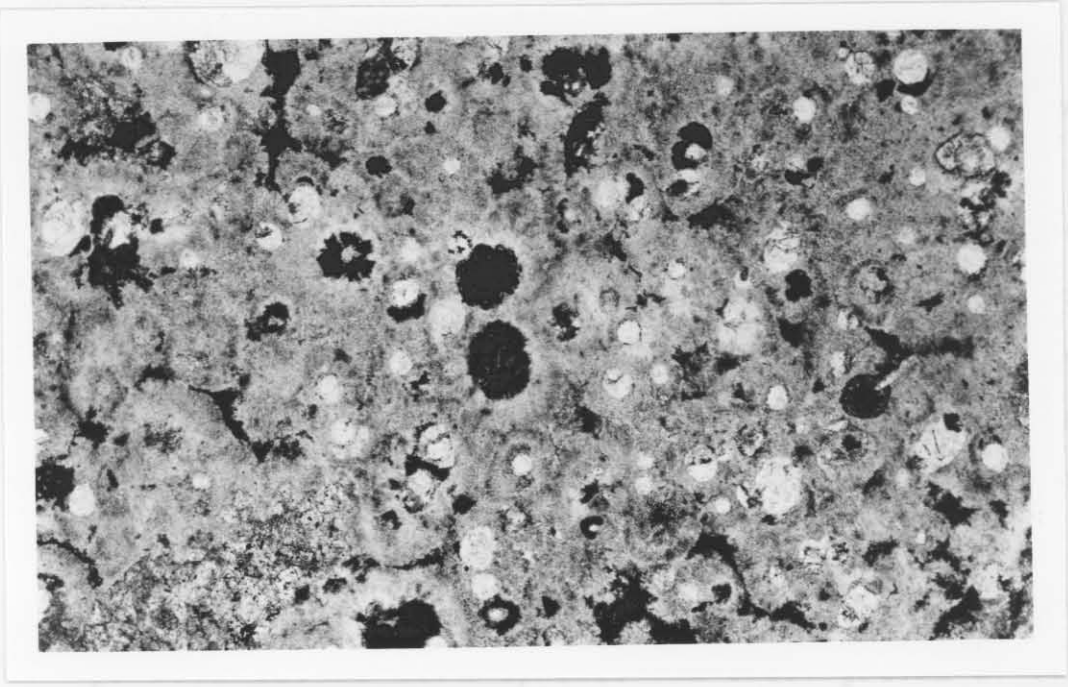

Fig. 2.11.: Spherulites around amygdales in felsite. F-80. 25x. Kwaggavoetpad 163JS.

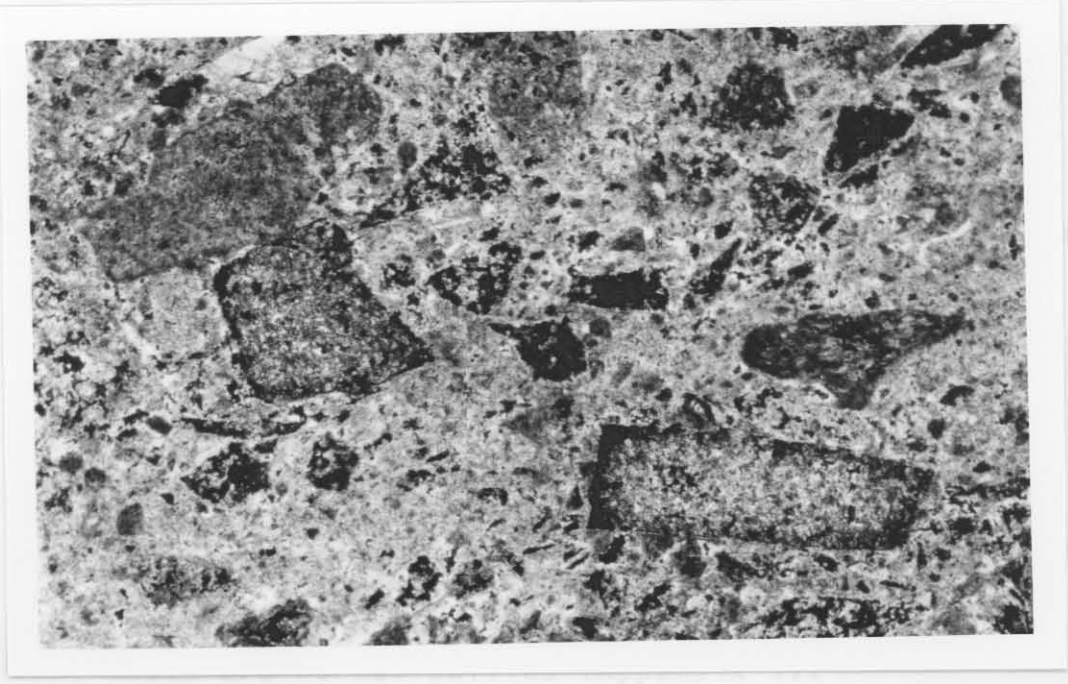

Fig. 2.12.: Agglomerate. F-81. 25x. Kwaggavoetpad 163JS.

pyrite and zircon.

The abundance of sphene in the metafelsites is probably caused by the replacement of magnetite by sphene. The sphene usually forms rims around magnetite (Fig.2.14), but in some cases the magnetite is completely replaced. Sphene rims and magnetite grains are closely associated with apatite (Fig.2.15).

Microprobe analyses revealed the magnetite rimmed by sphene to contain about twice the TiO_2 concentration of their unrimmed counterparts (Appendix 1). Magnetite grains rimmed by sphene are always larger (>0,2 mm in diameter) than the unrimmed grains. It is considered that the large magnetite grains with sphene rims were present in the rock before metamorphism and that they reacted in the presence of H_2O with CaO to form sphene. The small grains of Ti-poor magnetite crystallized in the original Fe-rich glassy groundmass during metamorphism.

A similar feature was observed by Janardan Rao et al. (1973) in the Hyderabad Granites, Andhra Pradesh, India. However, in this case the sphene coronas formed by metamorphic reaction involving the breakdown of hornblende to plagioclase with the release of iron to form magnetite and release of Ca and Ti to form the sphene coronas around the magnetite. They concluded that the rims of sphene around magnetite originated during regional metamorphism at elevated temperatures in a water deficient environment.

The clinopyroxene in the metafelsite which, together with magnetite, quartz and feldspars forms a granoblastic polygonal texture (Fig.2.13), is considered to have formed as a result of the metamorphic breakdown of hornblende and biotite. Microprobe analyses of the clinopyroxenes show that these are normal salites (Appendix 1).

Pool textures consisting of quartz and feldspar surrounded

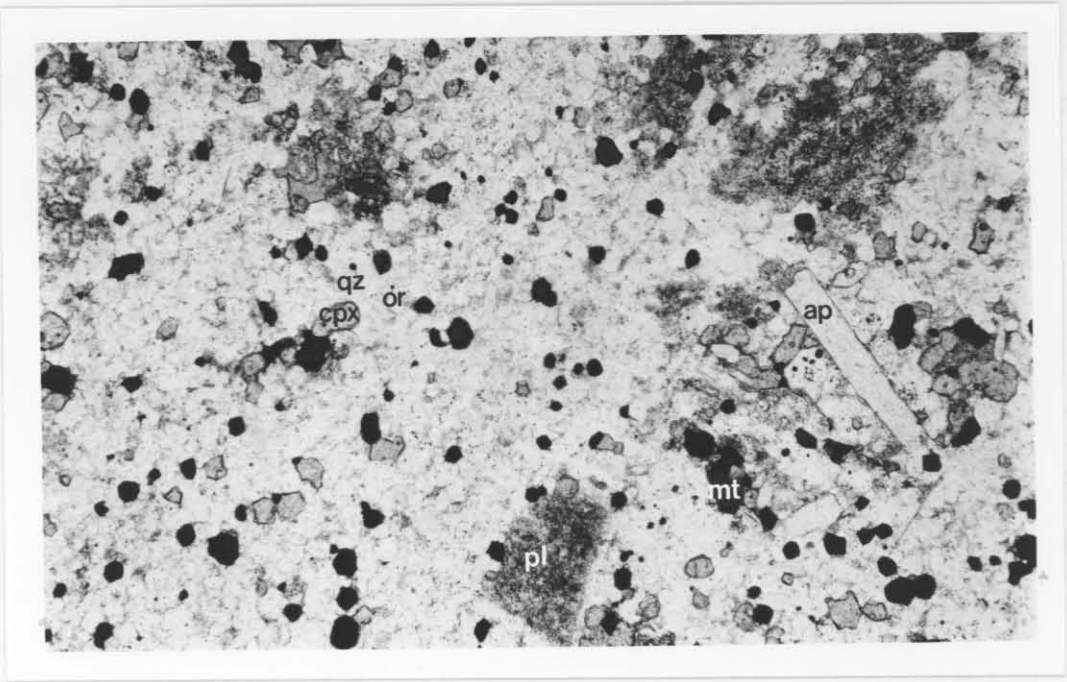

Fig. 2.13.: Granoblastic polygonal texture in metafelsite composed of altered plagioclase phenocrysts (pl), clinopyroxene (cpx), magnetite (mt) and apatite phenocrysts (ap). The white areas are represented by quartz (qz) and K-feldspar (or). GR-80. 63x. Haakdoorndraai 169JS.

Fig. 2.14.: Sphene rim around magnetite in metafelsite. GR-86. 25x. Haakdoorndraai 169JS.

by areas enriched in mafic minerals were observed in some sections (Fig.2.16). These may have formed by melting of felsite, where the areas rich in mafic minerals represent the restite and the pools of quartz and feldspar areas of incipient melting, which may eventually have coalesced to form the veins of leucogranite that cut irregularly through the metafelsite.

Micrographic varieties of the metafelsite (Fig.2.17) tend to become coarser towards the contact with the layered rocks (Von Gruenewaldt 1968). The development of micrographic intergrowths seems to depend on the nature of the source rock. Where the source rock was spherulitic it could have produced a micrographic intergrowth on metamorphism, whereas a glassy source rock probably produced a granitic or granoblastic polygonal texture. They differ from the Stavoren Granophyre in that they contain an irregular intergrowth without the hourglass texture or radiating fringe texture (see Chapter 3.2), which characterizes the latter. Because most samples contain corroded and very altered phenocrysts of plagioclase and clinopyroxene as major constituents, and a different type of quartz-feldspar intergrowth compared to the Stavoren Granophyre, these rocks are considered to have originated by metamorphism of porphyritic felsite by the Layered Suite. They are the equivalents of the so-called micrographic felsites of Von Gruenewaldt (1968).

Similar, fayalite-bearing micrographic varieties are present on Loskop Suid 53JS, where they overlie the Nebo Granite. The presence of fayalite in these rocks may point to a different origin, as this mineral was not found elsewhere in the felsites or the metafelsites.

Some metafelsites are rich in mafic minerals (Fig.2.18), like clinopyroxene and chlorite; the chlorite in such rocks is probably of retrograde metamorphic origin.

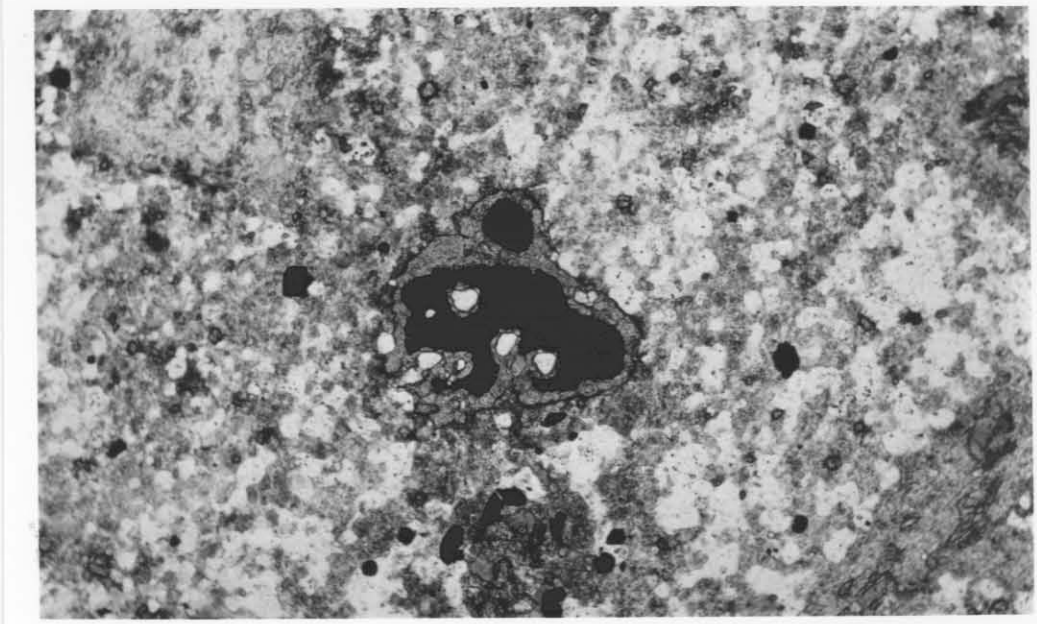

Fig. 2.15.: Magnetite rimmed by sphene with which apatite is closely associated. Metafelsite. GR-86. 63x. Haakdoorndraai 169JS.

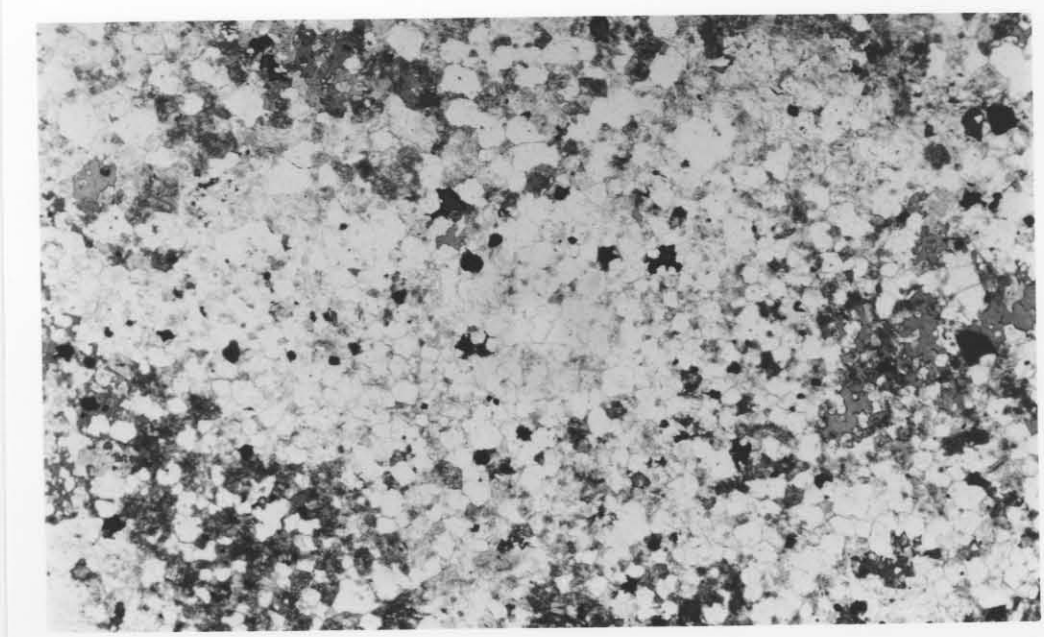

Fig. 2.16.: K-feldspar-quartz pool texture in metafelsite. GR-55. 25x. Weltevreden 165JS.

Fig. 2.17.: Micrographic intergrowth in metafelsite. GR-48. X-Nicols. 25x. Weltevreden 165JS.

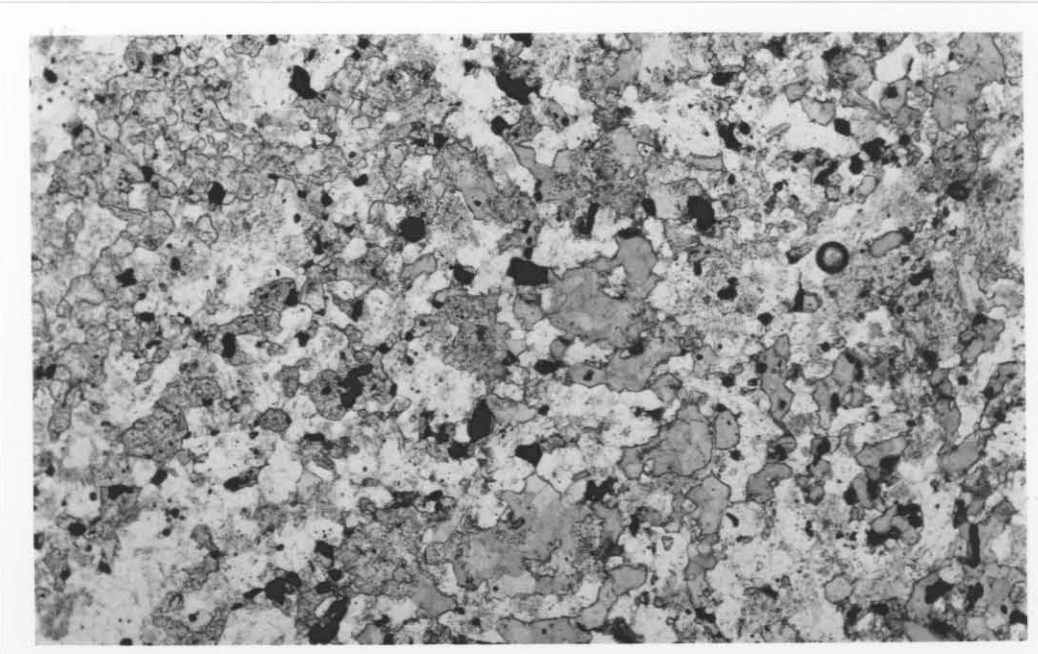

Fig. 2.18.: Chlorite- and clinopyroxene-rich metafelsite. GR-43. 63x. Weltevreden 165JS.

3. The Rashoop Granophyre Suite.

3.1. Field Relationships.

The Stavoren Granophyre, of the Rashoop Granophyre Suite, dated at 2084 ± 62 Ma (Walraven et al. 1981), is developed throughout the area and occupies different positions in relation to other rocks.

It occurs mainly as a sheet intrusive into Rooiberg Felsite Group (Fig.3.1), with a thickness of about 2300 metres on Probeeren 164JS. The intrusive relationship is obvious from an intrusion breccia in the riverbed of the Boekenhoutkloof River on the farm Mooiplaats 121JS, where angular blocks of felsite up to 40 centimetres in diameter are present in micro-granophyre (Fig.3.2). Intrusive relationships of granophyre into felsite were also observed on the farms Probeeren 164JS and Boekenhoutkloof 124JS.

The Stavoren Granophyre is also developed between Nebo Granite and Transvaal Sequence rocks, and it was also found intrusive into the upper shale member of the Timeball Hill Formation on the farm Loskop Suid 53JS. Intrusive relationships of Nebo Granite into granophyre are present in many localities, with a particularly good example in a riverbed (29°30'W, 25°15'S) on Rietkloof 166JS.

On Rietkloof 166JS the granophyre seems to be intruded by rocks of the Layered Sequence, because an inclusion of granophyre is present in rocks of the upper zone near the prominent magnetite plugs on this farm. This would imply that the granophyre predates the mafic sequence.

The Stavoren Granophyre is fairly homogeneous throughout the area. It displays a range in colour from brick-red to grey, where the red colour is due to oxidation of the iron in the feldspars. Grain size decreases towards the top of the granophyre sheet on the farms Boekenhoutkloof 124JS

Fig. 3.1.: The contact between Stavoren Granophyre on the left and Rooiberg Felsite on the right. Boekenhoutkloof 124JS.

Fig. 3.2.: Intrusion breccia of Stavoren Granophyre into Rooiberg Felsite in the Boekenhoutkloof riverbed on the farm Mooiplaats 121JS. Chemical analyses of these rocks, samples GR-155G and GR-155F respectively, are listed in Appendix 2.

and Tafelkop 120JS in the northern part of the area, where extensive outcrops of microgranophyre dipping at about 5°N are in contact with the felsite. Microgranophyres are not always present as a roof-facies of the granophyre in contact with the Rooiberg felsite. On Kwaggavoetpad 163JS the granophyre in contact with felsite is coarse-grained, but deeper in the sheet on Hartbeestlaagte 162JS microgranophyre is developed within the succession of coarse-grained granophyre. It is possible that granophyre intruded the microgranophyre at this horizon.

3.2. Petrography of the Stavoren Granophyre.

3.2.1. The granophyric intergrowth.

Granophyric intergrowth consists mainly of roughly equal amounts of quartz and perthite. These textures vary from specimen to specimen and are generally believed to have resulted from the simultaneous and sometimes rapid crystallization of quartz and feldspar.

Barker (1971) distinguished several types of intergrowth, viz. spherulitic, plumose, radiating fringe, vermicular, cuneiform and insular (Fig.3.3).

The plumose type, representing a mass of small spherulites, is fine-grained, while the spherulitic type is a coarse-grained version of the former. Radiating fringe types consist of homogeneous feldspar surrounded by granophyric intergrowth. Vermicular types resemble those found in myrmekitic textures, but the intergrowth is not restricted to grain boundaries. The cuneiform is similar to the type found in graphic granite, whereas the insular type consists of islands of quartz with feldspar in the centre of the island, set in a matrix of feldspar, suggesting a complex history of formation. Some intergrowths are more complex than those described above.

The radiating fringe type of granophyric intergrowth,

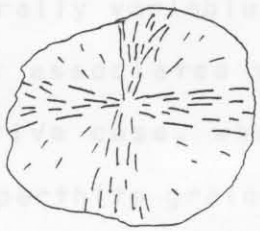

spherulitic

plumose

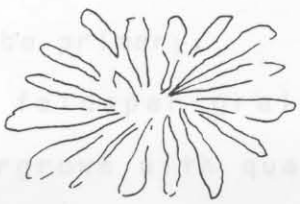

radiating fringe

cuneiform

insular

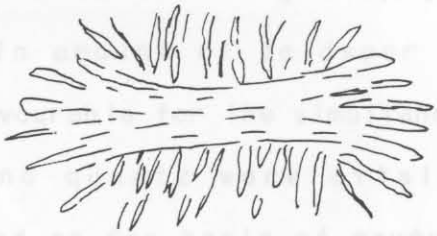

hourglass texture

exploding bomb

Fig. 3.3.: The different varieties of granophyric intergrowth after Barker (1971) and this study.

where the quartz coarsens as the rim of the intergrowth is approached, is the most common in the granophyres studied. K-feldspar or plagioclase may form the nucleus of this texture. Quartz as a nucleus to the intergrowth is extremely rare and was only observed in one sample (Fig.3.4). The intergrowths are generally variable and different domains of quartz are normally associated with one continous perthite grain. The alternative case, where a domain of quartz spreads over several perthite grains, was observed in a few thin sections. According to Smith (1974) it is possible that some extinction domains of quartz in an optically continous K-feldspar grain may result from recrystallization of the quartz, whereas some may be primary.

The feldspar grains forming the nuclei are usually not intergrown with quartz but are in optical continuity with the perthite intergrown with quartz. This may represent one feldspar grain, where the nucleus crystallized under conditions unfavourable to the formation of granophyric intergrowth. Accordingly, a certain amount of feldspar had to crystallize before conditions favourable for the simultaneous crystallization of K-feldspar and quartz were attained (Fig.3.5). Walraven (1976) suggested on the basis of textural evidence that the crystallization of quartz was delayed until the composition of the melt moved some distance into the stability field of quartz in the quartz-albite- orthoclase system.

Intergrowth-free perthite phenocrysts do not always form nuclei of the intergrowth (Fig.3.6), nor are perthite grains at the centre of the intergrowth always in optical continuity with the perthite of the granophyric intergrowth (Fig.3.6). This may indicate that the formation of granophyric intergrowth is dependent on the structural state of the perthite involved.

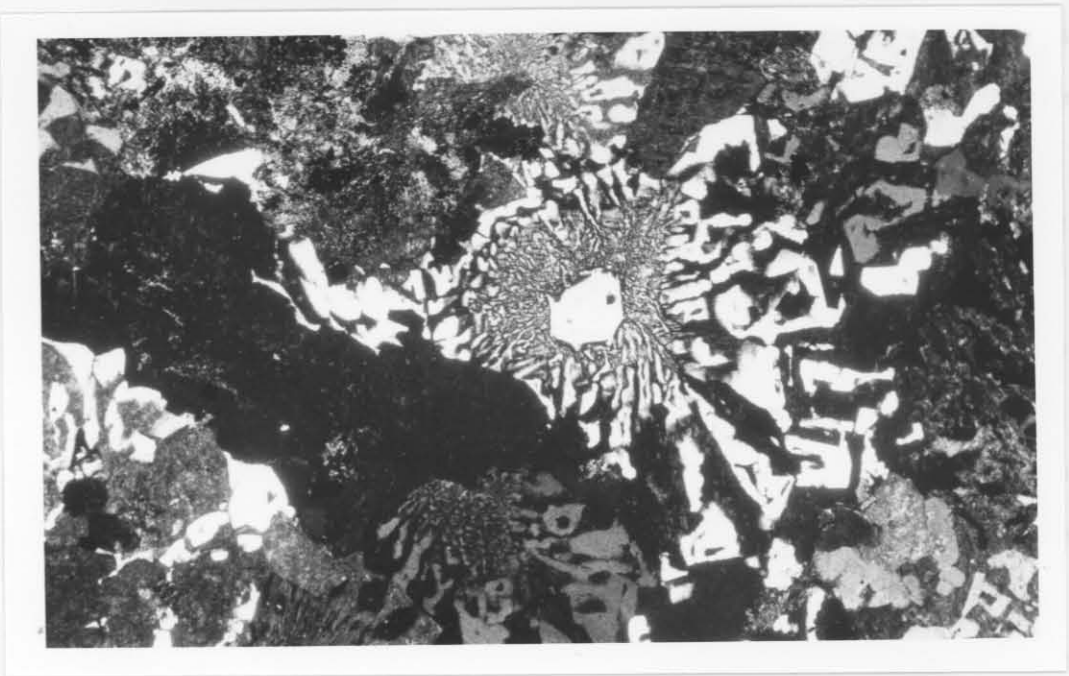

Fig. 3.4.: A quartz phenocryst forms the nucleus to a radiating fringe granophyric intergrowth. GR-268. X-Nicols. 25x. Hartbeestlaagte 162JS.

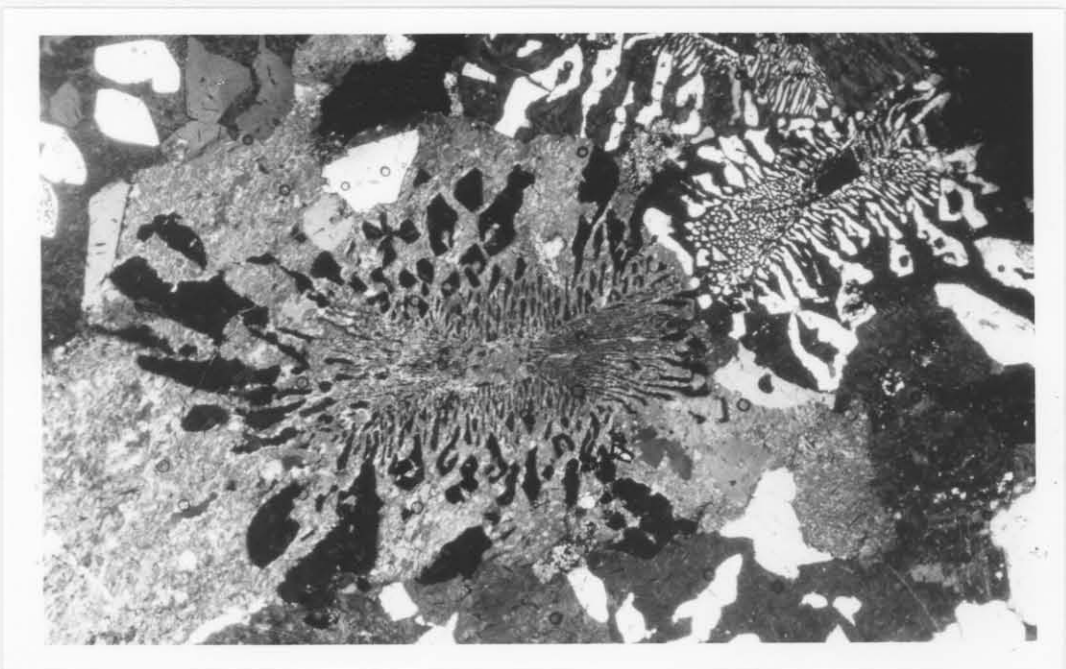

Fig.3.5.: Two hourglass textures, both containing a nucleus of K-feldspar, which is in optical continuity with the intergrown perthite. It is noteworthy that the perthite of the intergrowth extends beyond the domains of quartz. GR-54. X-Nicols. 25x. Weltevreden 165JS.

Sample GR-262 contains feldspar phenocrysts intergrown with quartz, with a rim free of intergrowth (Fig.3.7), separating it from more coarse-grained intergrown quartz and feldspar. A puzzling aspect of this texture is that the phenocryst is part of a larger feldspar grain with the same optical orientation.

The cuneiform texture, commonly found in graphic granite, is rarely developed (e.g. sample GR-242).

Insular types, with inclusions of feldspar in the quartz, are present in different forms (Fig.3.8) indicative of a complex growth history. The intergrowth shown in the photograph may also be called a cuneiform texture with inclusions of feldspar in quartz.

The microgranophyres consist of spherulite-like and microgranophyric intergrowth, in which it is difficult to distinguish between quartz and feldspar, even at very high magnifications. These spherulites, which display characteristic extinction crosses under crossed nicols, are set in a fine-grained groundmass of quartz and feldspar (Fig.3.9). The amount of groundmass between the spherulites varies and some rocks are composed almost entirely of spherulites. Orb textures of interlocking small spherulites are developed in some specimens (Fig.3.10).

The spherulite-like textures were formed by rapid crystallization during quenching of the granophyre magma when it intruded beneath the felsites. A gradual coarsening of the granophyric intergrowth in the spherulites and normal intergrown grains is observed as the distance from the contact with the felsites increases (compare Fig.3.9 and 3.11).

The hourglass texture represents part of a spherulite and homogeneous K-feldspar crystals may form the nucleus of the texture (Fig.3.5). Orientation of quartz and feldspar

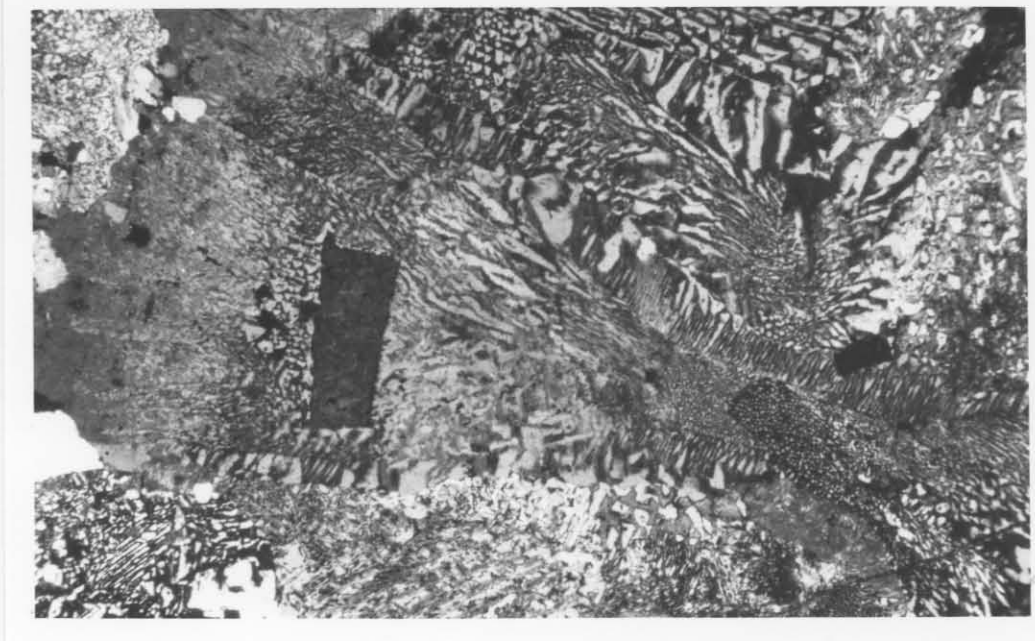

Fig. 3.6.: A complex intergrowth, where two phenocrysts of K-feldspar at the centre of the hourglass texture are intergrown with quartz, whereas another phenocryst (black) is not intergrown. GR-266. X-Nicols. 25x. Mooiplaats 121JS.

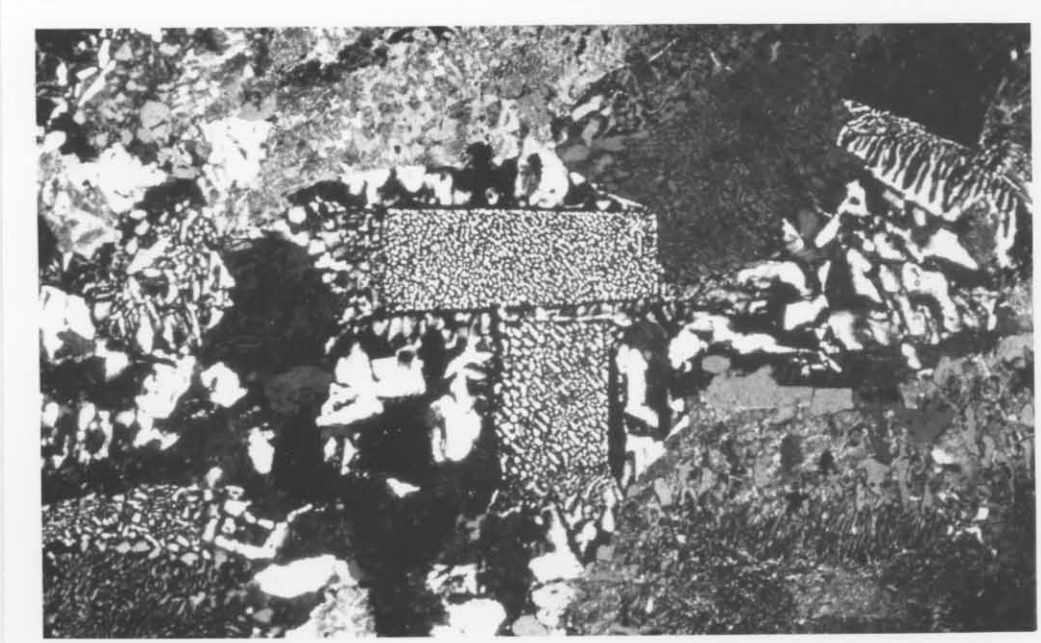

Fig. 3.7.: Two granophyrically intergrown phenocrysts, bordered by a thin rim which is not intergrown with quartz. GR-262. X-Nicols. 25x. Tafelkop 120JS.

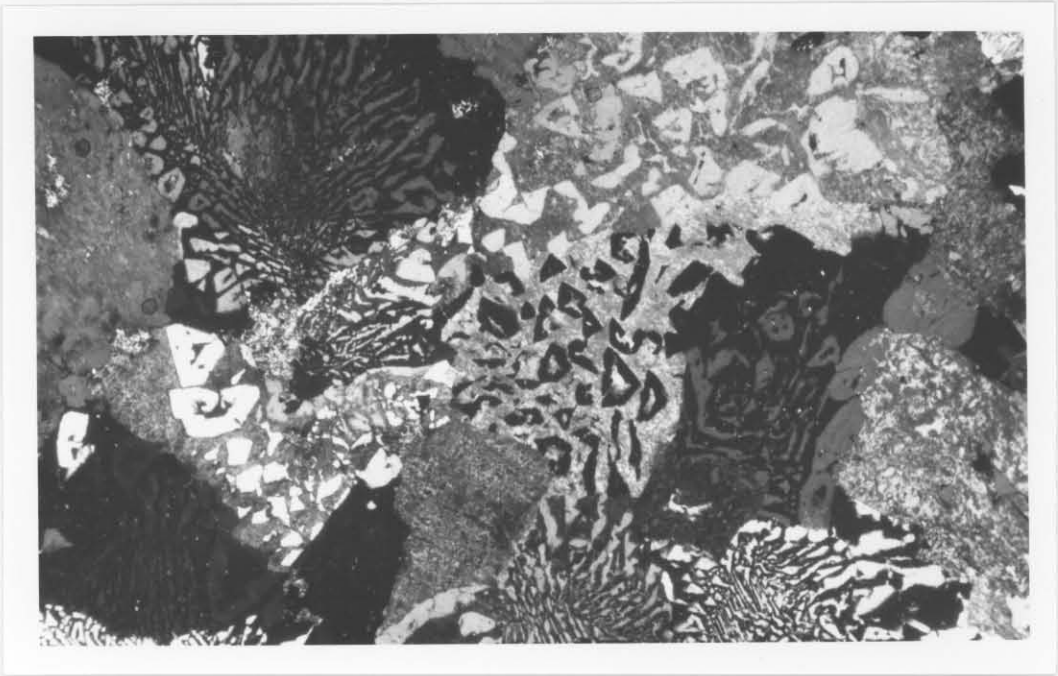

Fig. 3.8.: The insular type of granophyric intergrowth with cuneiform outlines. GR-70. X-Nicols. 25x. Kwaggavoetpad 163JS.

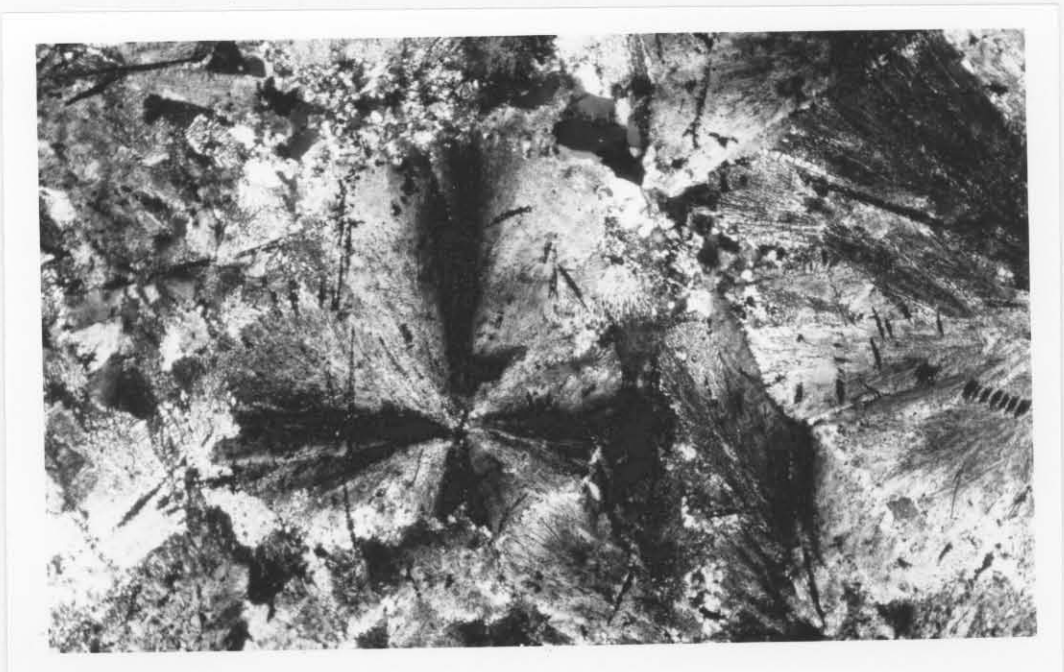

Fig. 3.9.: A spherulite with extinction cross in microgranophyre of the Stavoren Granophyre. GR-133. X-Nicols. 25x. Tafelkop 120JS.

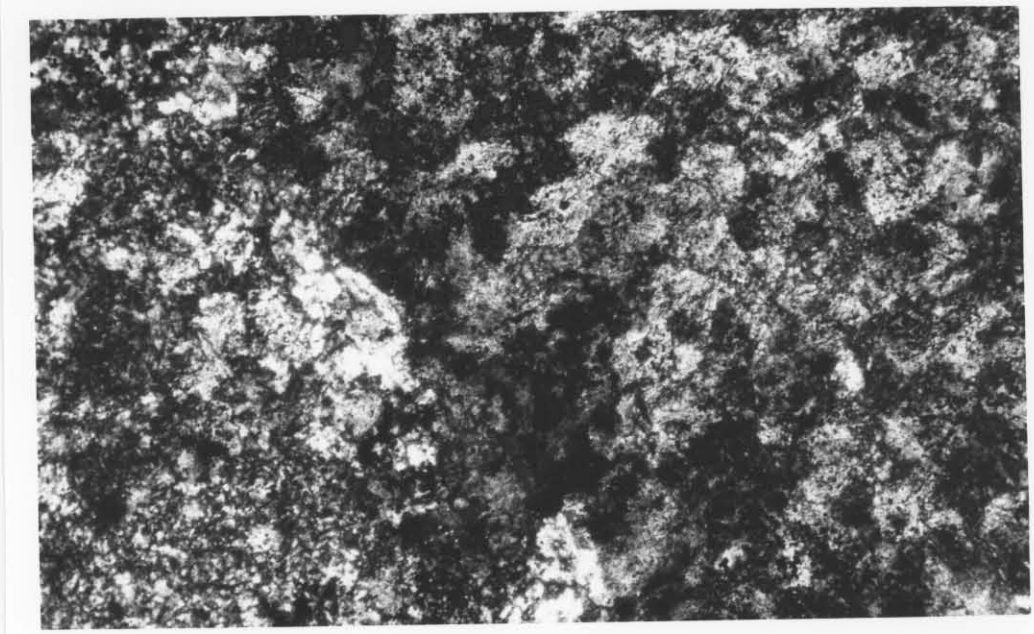

Fig. 3.10.: Orb texture in microgranophyre of the Stavoren Granophyre. GR-234. X-Nicols. 63x. Boekenhoutkloof 124JS.

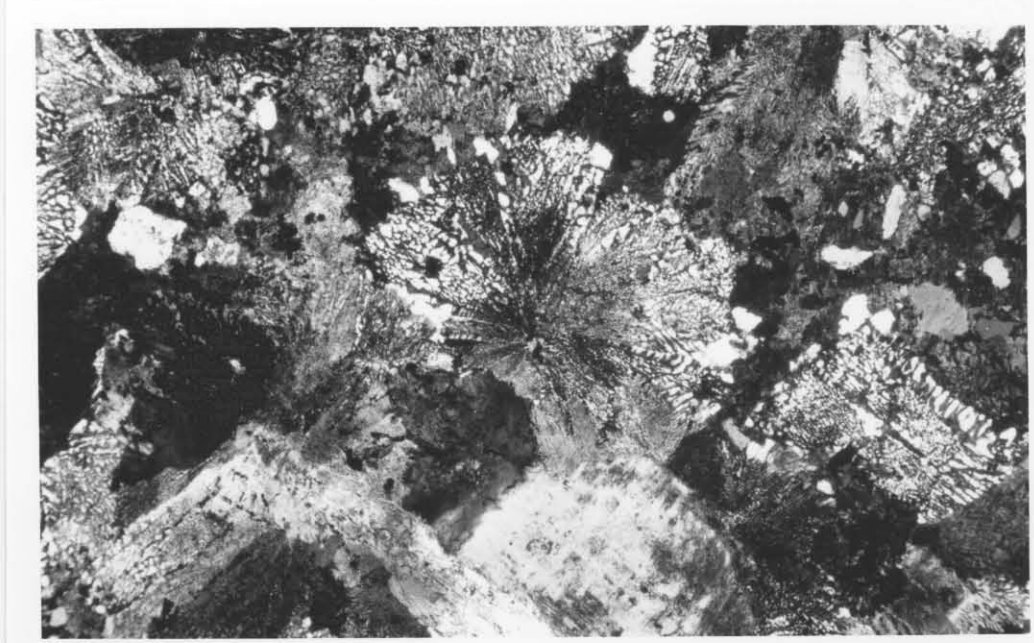

Fig. 3.11.: "Coarse-grained" spherulite in microgranophyre of the Stavoren Granophyre. GR-221. X-Nicols. 25x. Tafelkop 120JS.

within the intergrowth can vary.

The feldspars that form intergrowths with quartz in the microgranophyres are strongly zoned e.g. in sample GR-54. Here a plagioclase phenocryst is surrounded by a rim of K-feldspar, representing an intermediate zone, which in turn, is surrounded by perthite intergrown with quartz (Fig.3.12). This texture can be described as an anti-rapakivi texture. Similar features were also described by Barker (1970), where the feldspar changed in composition from a sodic plagioclase in the core to albite in the intermediate zone and K-feldspar in the outer zone. Abbot (1978) also described this feature in hornblende granophyres from the Red Beach Granite in extreme eastern Maine. According to him it appears that during the formation of anti-rapakivi texture the liquid portion of the magma remained in equilibrium with more than one feldspar only long enough for the plagioclase to become completely rimmed. After the formation of the anti-rapakivi phenocrysts the last liquids to crystallize were in equilibrium with two feldspars.

3.2.2. Minor and accessory constituents.

Clinopyroxene, hornblende, biotite and rarely fayalite may be present within the granophyre. The major mafic mineral is a clinopyroxene. It has a light-green color and a large extinction angle $Z\hat{}c$ of 45°. Microprobe analyses show that the MgO content is extremely low (Appendix 1) and that the clinopyroxene is a hedenbergite. Together with plagioclase, hedenbergite was the first mineral to crystallize from the melt. The crystallization was evidently rapid, as indicated by its occurrence as long thin crystals throughout the rock (Fig.3.13), and as thin needles in the spherulite-like textures and in the granitic groundmass of the microgranophyre. In most granophyres the clinopyroxene occurs as long stem-like

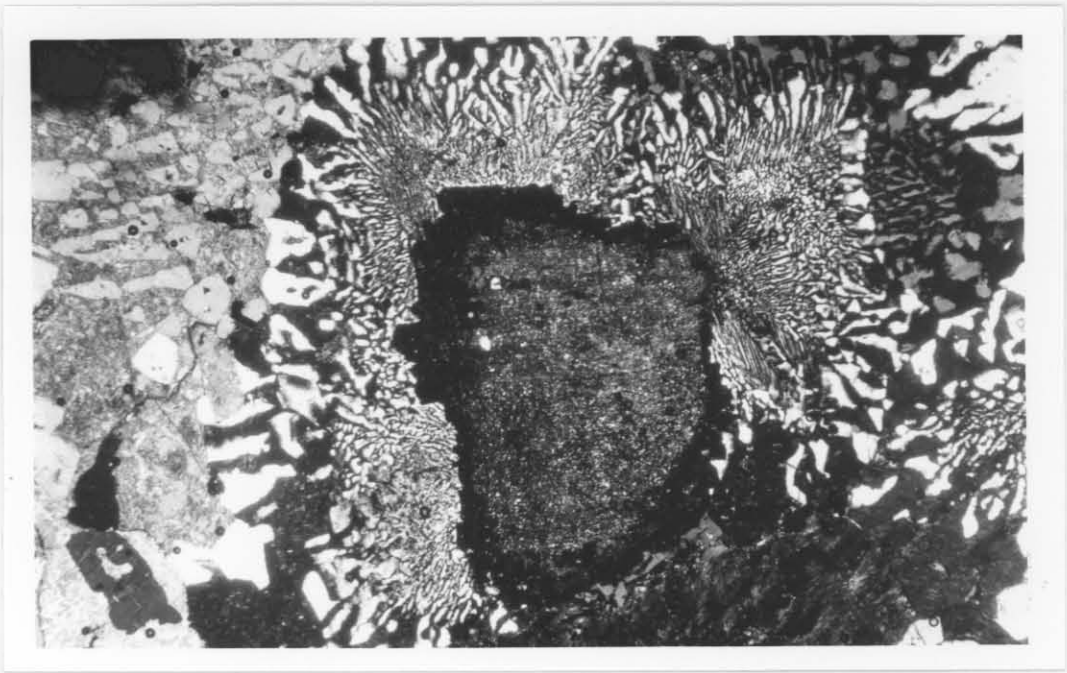

Fig. 3.12.: Strongly zoned phenocryst consisting of a plagioclase core rimmed by K-feldspar and an outer part of granophyrically intergrown perthite. GR-54. X-Nicols. 25x. Weltevreden 165JS.

Fig. 3.13.: Laths of clinopyroxene in granophyre. The large extinction angle of 45° can be seen from the position of one clinopyroxene lath. GR-43. X-Nicols. 25x. Tussenin 21JS.

crystals. It is readily altered to hornblende and different stages of this transformation have been observed.

Some granophyres contain hornblende as a major mafic mineral. This hornblende is pleochroic with X = light brown-green, Y = dark olive-green and Z = very dark olive-green, has an extinction angle $Z \wedge c$ of $\pm 10^{o}$ and is probably a ferro-hastingsite. It did not originate through the transformation from clinopyroxene but occupies interstitial spaces between the intergrowth rosettes and therefore represents a primary late-crystallized phase.

Fayalite was only observed in a few samples. It is usually altered to iddingsite which is reddish-brown in thin section and which has a higher birefringence than olivine. An olivine grain in one of the granophyres is altered to an isotropic mineral, probably chlorophaeite (Deer, Howie and Zussman Vol 1, 1962). Fayalite, which crystallized early, is always associated with clinopyroxene (Fig.3.14).

Biotite is a subordinate mineral and occurs interstitially or associated with magnetite.

Sphene is an important accessory constituent, especially in the microgranophyres. The colour is brownish-yellow with slight pleochroism, indicative of an iron(III)-rich variety (Tröger, 1969).

Fluorite, which occurs as small interstitial patches, is present in every thin section investigated. It also occurs as patches in interstitial hornblende. The fluorite is apparantly a primary magmatic mineral.

The few zircons of the granophyres are generally very small and carry inclusions of foreign material. Secondary overgrowth is developed in some grains and radioactive halos are present.

Other accessory minerals are allanite, apatite, calcite, magnetite and ilmenite.

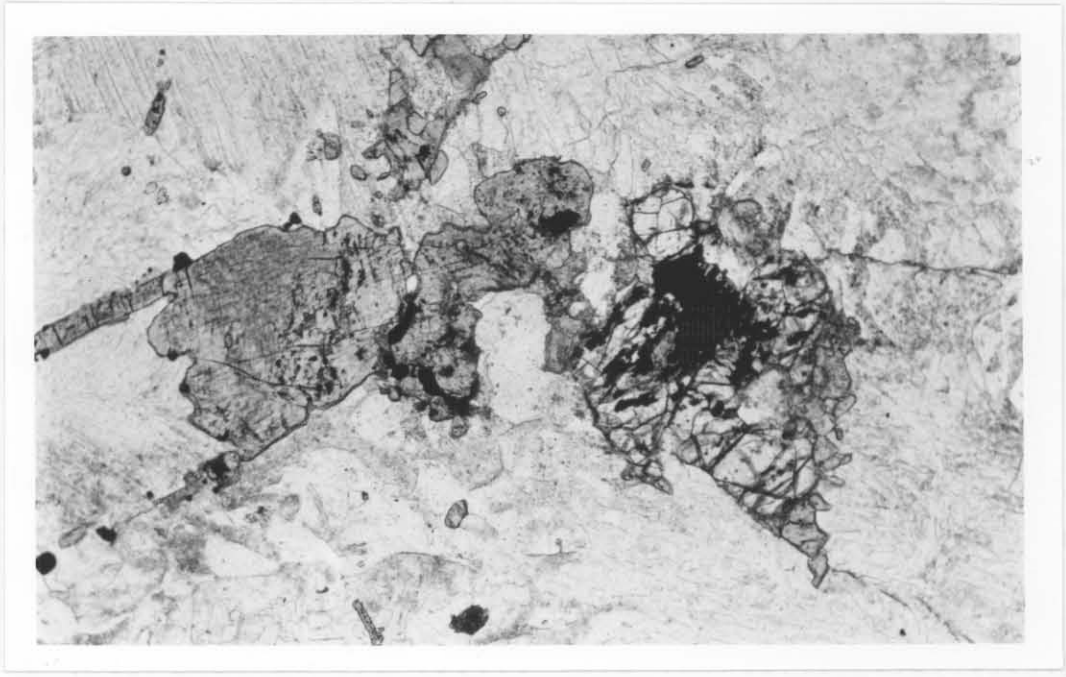

Fig. 3.14.: Clinopyroxene and olivine in Stavoren Granophyre. GR-43. 63x. Tussenin 21JS.

4. The Lebowa Granite Suite.

4.1. Field Relationships.

The Lebowa Granite forms a sheet-like composite pluton which underlies the Stavoren Granophyre and overlies the layered mafic rocks. In this area it is composed of various Klipkloof Granite types and the Nebo Granite. The Klipkloof types of granite are best developed in the northern and north-western sector, whereas Nebo Granite occurs throughout the larger part of the area. This is therefore an ideal area to study the relationship between Nebo- and Klipkloof Granite, and the relation of these granites with the overlying granophyres.

The variety of rock types which form part of the Lebowa Granite Suite in this area are listed in Table 4.1.

4.1.1. The Nebo Granite.

The Nebo Granite with an age of 2052 ± 48 Ma (Walraven 1982) intrudes the Stavoren Granophyre dated at 2084 ± 62 Ma (Walraven et al. 1981). This intrusive relationship was observed at various localities, e.g. in a riverbed (29°30'W, 25°15'S) on Rietkloof 166JS. The contact of Nebo Granite with Stavoren Granophyre is sharp, but may be gradational in places, as for instance on Mooiplaats 121JS, where a coarse-grained granophyric granite marks the transition between the two rock types.

The escarpment of the Sekhukhune Plateau is formed by Nebo Granite, overlain by granophyre and then by felsite. Where mafic rocks are present, Nebo Granite is not developed beneath the Stavoren Granophyre.

Due to a lack of outcrop in the low-lying areas, the exact contact between the Nebo Granite and the rocks of the Layered Suite on Weltevreden 165JS could not be found.

Table 4.1. The various rock types of the Lebowa Granite Suite in the area, listed in chronological order.

LEBOWA	GRANITE	SUITE	Klipkloof Granite	**Fine- to medium-grained:** (a) aplite dykes: Intrusive into all the Klipkloof Granite types as well as the Nebo Granite. Extremely leucocratic, fine-grained and albitized granite. Fluorite contents is variable. Contains pegmatite lenses and tourmaline spheroids. Sharp contact with other varieties. (b) aplite sheets: Developed at different horizons in upper part of the Nebo Granite. Tourmaline spheroids are present if the granite is albitized. Clots of biotite and pegmatite lenses are developed. The amount of fluorite varies. Granophyric intergrowth is common. Intrusive into Nebo Granite.
				Porphyritic: Perthite(2-8 mm) and quartz(2-5 mm) phenocrysts in a fine-grained groundmass. Grey to red coloured. Granophyric intergrowth present. High concentration of white fluorite. Gradational contact with aplite sheets and sharp contact with aplite dykes.
				Medium- to coarse-grained: Leucocratic granite with high fluorite content. Always red coloured. Mafic minerals altered to chlorite. Interlocking quartz grains. Pegmatite lenses. Gradational contact with Nebo Granite.
			Nebo Granite	Coarse-grained grey to red granite with red varieties common in the upper parts of the sheet. Decrease in mafic mineral content and grain size from bottom to top in the sheet. Increase in biotite/hornblende ratio and fluorite content from bottom to top. Intrusive into Stavoren Granophyre. Intrusion breccia in Rustenburg Layered Suite.

Hereabout the lowest stratigraphic portion of the Nebo Granite in the whole area is exposed. On the farm Tussenin 21JS in the north-western part of the area the stratigraphically highest portion of the Nebo Granite occurs.

A mineral gradation characterizes the Nebo Granite sheet, wherein the amount of hornblende, the hornblende to biotite ratio, and the total mafic mineral content all decrease from bottom to top. The amount of free quartz and fluorite displays a concomitant increase, whilst the grain size shows a corresponding decrease upwards through the Nebo Granite sheet.

An intrusion breccia of a medium-grained hornblende granite into mafic rocks of the Layered Suite on Rietkloof 166JS (Fig.4.1) probably represents the least differentiated Nebo Granite magma recognized in the area (Chapter 6).

4.1.2. The Klipkloof Granite.

The Klipkloof Granite, the youngest member of the Lebowa Granite Suite in the area mapped, has been dated at 2036 ± 50 Ma (Walraven et al. 1981). Several different textural types are present. They include fine- to medium-grained equigranular and porphyritic types, which are reddish, grey or white coloured and may contain clots of biotite and pegmatite lenses. These granites are closely related to the Nebo Granite and seem to constitute a highly fractionated aplitic phase of the latter.

The Klipkloof Granite occurs in the stratigraphically higher portions of the Nebo Granite sheet, where it forms undulating flat-lying sills as well as dykes and veins which are intrusive into Nebo Granite (Fig.4.2). An extensive outcrop of Klipkloof Granite is also present between the Nebo Granite and the Stavoren Granophyre, where it forms dykes and sills intruding the latter rock type.

Fig. 4.1.: The intrusion breccia of granite into the Rustenburg Layered Suite on Rietkloof 166JS. Different rocktypes are present, viz. gabbro, gabbronorite, norite, anorthosite, magnetite-gabbro and magnetite. Large quantities of a fine-grained mafic rock, probably a sill of critical zone composition (Sharpe, pers. comm.), constitute the largest number of the fragments (large block at handle of hammer).

4.1.2.1. Fine- to medium-grained Klipkloof Granite.

This rock type forms the largest part, by volume, of the Klipkloof intrusives. It occurs as aplite sills, dykes and thin veins in the Nebo Granite or as second-generation aplite dykes or veins in the Klipkloof aplite sills (Fig.4.3). The dykes and veins dip steeply and terminate abruptly. Klipkloof Granite sills are developed at different horizons within the upper parts of the Nebo Granite sheet: at each level dykes and veins originate which may terminate at or intrude overlying Klipkloof Granite sills.

The rock is always leucocratic and contains only minor amounts of chloritized biotite, which forms clots in some localities. Primary, magmatic fluorite is ubiquitous and the grain size varies, being fine-grained in dykes and veins and fine- to medium-grained in sills. This rock type resembles the Lease Granite of the Zaaiplaats area (Crocker, pers. comm.; authors observation).

Associated with the dykes and sills are plug-like bodies of albitized Klipkloof Granite (Fig.4.4). These are reddish in colour when albitization is not advanced and white if a high degree of albitization has occurred.

Tourmaline spheroids with a diameter of 4 to 15 centimetres and a concentration of one to three spheroids per square metre occur in both the reddish and white albitized Klipkloof Granite (Fig.4.5). The majority of spheroids are nearly perfect spheres enclosed by granitic rims depleted in mafic constituents. Some spheroids contain visible 1 to 2 centimetre long tourmaline crystals of the schorl type.

4.1.2.2. Porphyritic Klipkloof Granite.

This rock type invariably forms a marginal phase to the other types of Klipkloof Granite wherever these are in contact with Nebo Granite. Contacts with other Klipkloof

Fig. 4.2.: The contact between Nebo Granite and an overlying Klipkloof Granite sill (white arrows). Roadcut on Varschwater 23JS.

Fig. 4.3.: Two aplite dykes intrude Nebo Granite. The steeply dipping dyke carried the mineralizing fluids, which were trapped by the overlying Klipkloof Granite sill. The molybdenite mineralization occurs both as massive and disseminated ore in the aplite dyke and the surrounding Nebo Granite. Roadcut on Varschwater 23JS.

Fig. 4.4.: The round, pluglike outcrop of white albitized Klipkloof Granite is clearly recognizable at the centre of the photograph. Tussenin 21JS.

Fig. 4.5.: Two merged pairs of tourmaline spheroids in white albitized Klipkloof Granite. Tussenin 21JS.

Granite varieties are gradational, as is illustrated by the decrease in phenocrysts in the rock.

The rock type is characterized by phenocrysts of quartz and perthite, up to 8 millimetres in diameter, with quartz phenocrysts usually smaller than the perthites. Mafic minerals are chloritized and the fluorite content is relatively high; however, being white-coloured, the fluorite is difficult to recognize in handspecimen.

4.1.2.3. Medium- to coarse-grained Klipkloof Granite.

This generally red coloured rock type is extremely leucocratic with minor amounts of chloritized biotite. The quartz grains are interlocking and both quartz and perthite grains are typically about 4 millimetres in diameter. The appearance of this rock type resembles that of the Bobbejaankop Granite of the Zaaiplaats area.

The contact of the sheet with the underlying Nebo Granite is difficult to locate because of the poor outcrop and the small difference in grain sizes. This granite is, however, different from the Nebo Granite in that it is generally finer grained, more leucocratic, has a much higher contents of fluorite and chloritized biotite, and contains quartz-rich pegmatite lenses.

4.2. Petrography of the Nebo Granite.

The Nebo Granite is an equigranular coarse-grained rock with hornblende and biotite forming the major mafic minerals. It has a grey colour in the lower part of the sheet and displays a red colour in its upper part.

Quartz, perthite, plagioclase, hornblende and biotite are the major rock-forming minerals. Plagioclase and perthite were the first major phases to crystallize in the least

differentiated Nebo Granite. Nebo Granite higher in the sheet is more differentiated and here quartz appears to be the first major mineral to crystallize. Hornblende and biotite always occur as interstitial grains indicating that they were late in the crystallization sequence.

4.2.1. Perthite.

All the primary K-feldspars are perthitic. Some are macroperthitic, but most are microperthitic. They are slightly zoned and partially seritizised.

Interlocking-, string-, vein-, patch- and microcline perthites are developed. The perthite is usually rimmed by albite, which is in optical continuity with the albite component of the perthite grain, except where the albite rim is developed between perthite and plagioclase when the albite is in optical continuity with the plagioclase. A peculiar situation arises if two albite rims are developed around adjacent perthite grains, where the rim surrounding one grain appears to acquire the optical orientation of the albite component of the adjoining perthite grain (Fig.4.6).

4.2.2. Plagioclase.

Plagioclase is less abundant than perthite and accounts for 5 to 7 per cent of the modal composition. The grains are strongly zoned and saussuritization of the core is common. Two types of plagioclase occur in the Nebo Granite. Firstly, early-formed crystals of oligoclase that are sometimes twinned according to pericline law and secondly, relatively late-formed grains of oligoclase composition which are interstitial between quartz and perthite.

The anorthite content of late-formed plagioclase cores is about 10 to 15 per cent in undifferentiated rocks, but below 10 per cent in more differentiated counterparts, with

(a)

(b)

(c)

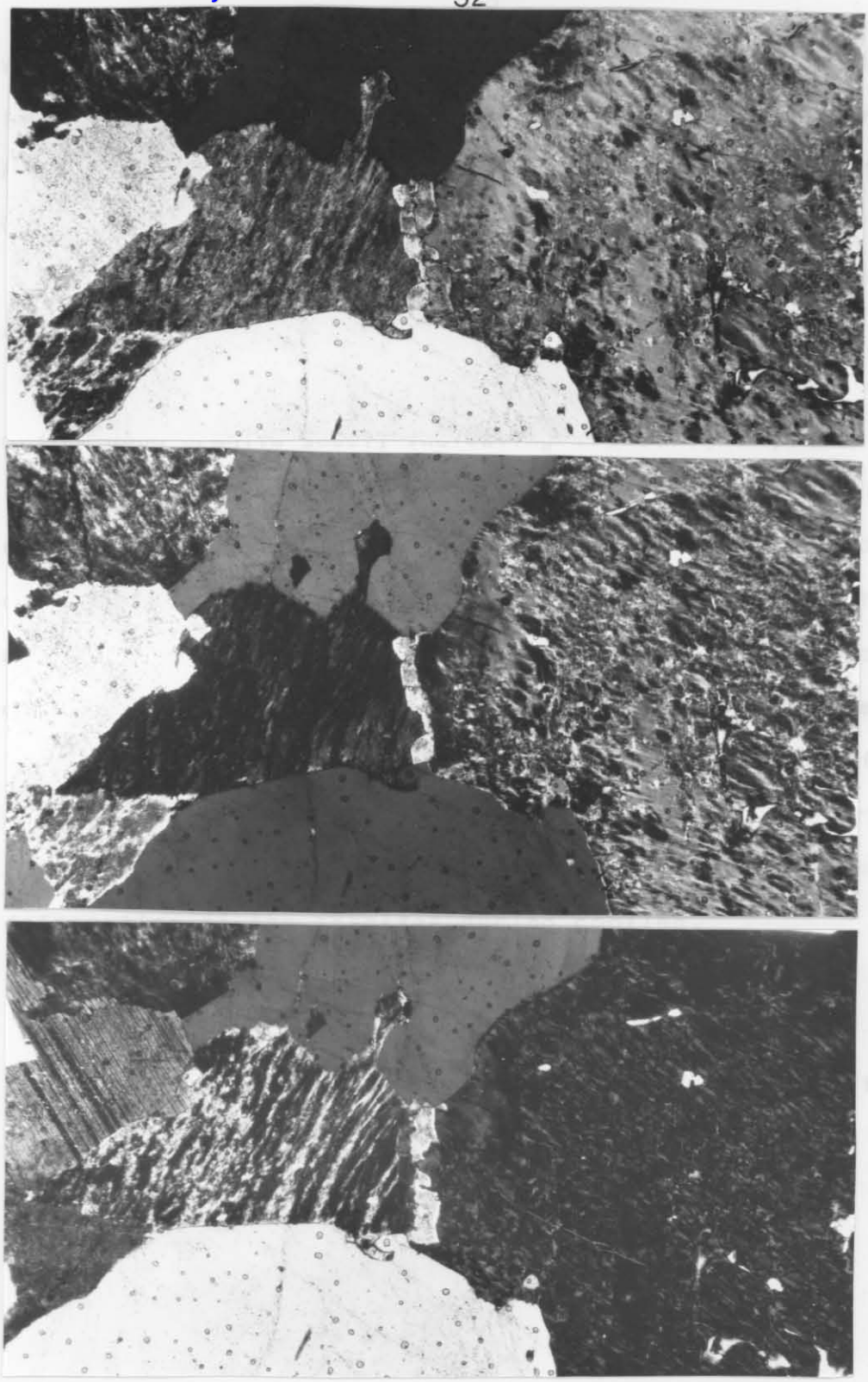

Fig. 4.6.: Two albite rims are present in Nebo Granite if two perthite grains are in contact (a). "Swapped rims", ie. the rims are in optical continuity with the albite component of the adjoining grains. The large perthite grain on the right is of the interlocking variety (b). With rotation of the stage through 180°, the other albite rim is now in optical continuity with the adjoining perthite grain (c). GN-12. X-Nicols. 25x. Varschwater 23JS.

values as low as An_{1-5} in the most differentiated varieties (Appendix 1). There is therefore a marked decrease in the An content of plagioclase with differentiation of the Nebo Granite magma.

4.2.3. Quartz.

Quartz forms subidiomorphic crystals in the upper parts of the Nebo Granite sheet, indicating its early crystallization. In the lower parts of the granite body, no subidiomorphic quartz grains are present and feldspar crystallized before quartz. Clusters of quartz of variable orientation are common in the Nebo Granite, especially in the upper parts of the sheet. This feature was considered by Hara et al. (1980), who investigated the origin of granites of Japan, as being a secondary feature produced by dynamic recrystallization of large single quartz grains caused by high-temperature deformation of the granites during cooling.

Sagenitic quartz, containing opaque needles, possibly rutile, occurs in some specimens.

Myrmekitic textures are developed at perthite grain boundaries; these textures usually occur in one of the two albite rims referred to earlier (Section 4.2.1.).

4.2.4. Hornblende and Biotite.

The major mafic minerals in the lower part of the Nebo Granite comprise mainly hornblende with minor biotite. The abundance of biotite increases upwards through the granite sheet, with a concomitant decrease in total mafic mineral content.

Hornblende and biotite occur interstitially to quartz and feldspar, indicating their late crystallization. Hornblende has the absorbtion formula X= brown green, Y= olive green and Z= dark olive green. According to the terminology of

Leake (1978), the amphibole is a ferro-edenite (Appendix 1) belonging to the group of calcic amphiboles with the end-member formula $NaCa_2Fe_5Si_7AlO_{22}(OH)_2$. The $Mg/(Mg+Fe^{2+})$ ratio is low and has a value of 0,04. Zircons, opaque minerals, apatite and other accessory minerals are enclosed by hornblende, again confirming its late crystallization.

Biotite, present as small flakes, has the absorption formula X= brown, Y= Z= dark brown. The biotites of the Nebo Granite are annite-rich (Appendix 1.). Annite is an uncommon biotite (Eugster and Wones, 1962) because a certain amount of substitution of Mg for Fe^{2+} is usually present.

4.2.5. Zircon.

Zircons are comparatively abundant and occur in three settings. The majority of zircons are enclosed in hornblende grains, together with opaque minerals and apatite. Some zircon crystals are enclosed in quartz, perthite and plagioclase, and a few zircons are situated along grain boundaries between quartz, perthite and plagioclase. Zircons crystallized early and were evidently dispersed throughout the melt. Crystallizing quartz and feldspar grains do not readily include the zircon crystals because of the large difference in surface tension between them (Spry 1979, p 171); this explains why the majority of zircons are found in the late crystallizing hornblende.

Most zircons are zoned and secondary overgrowths on the primary zircon are common. The overgrowth results in pleochroic halos in hornblende, as it is reasonable to assume that the late overgrowths probably contain the highest U and Th concentrations.

Pupin (1980) states that zircon crystallization is not confined to the first stages of crystallization of a magma, but continues to the hydrothermal stage. This is substantiated by the development of late overgrowths, which

may distort the cleavage of late biotite grains (Fig.4.7), thereby indicating that the overgrowth formed when the silicates had already crystallized.

4.2.6. Accessory minerals.

Accessory minerals that occur in the Nebo Granite are allanite, apatite, calcite, fluorite, magnetite, ilmenite, sphalerite, galena, arsenopyrite, chalcopyrite, molybdenite, thorite, sphene and tourmaline. Allanite, ilmenite and magnetite are the most abundant accessories.

Allanite from the lower parts of the sheet is lighter in colour than that from the upper parts. Subidiomorphic allanite is rare and irregular grains are more common.

Thorite is a rare constituent. Due to its high Th content, it produces a halo in the host mineral.

4.3. Petrography of the Klipkloof Granite.

4.3.1. Fine- to medium-grained and porphyritic Klipkloof Granite.

Quartz, perthite, minor plagioclase with a low An content (Appendix 1), biotite and accessory amounts of hornblende form an equigranular 0,5 to 1,5 millimetre matrix. Phenocrysts of quartz, perthite and rarely plagioclase, between 5 and 8 millimetres in diameter, occur evenly distributed in the fine- to medium-grained matrix.

Microcline-, string- and patch perthites are the predominant types of perthite forming both phenocrysts and groundmass. Swapped albite rims are present between perthite grains.

Quartz phenocrysts are smaller than the perthite phenocrysts and have subidiomorphic crystal outlines. They are frequently surrounded by a thin rim of granophyric intergrowth, the quartz of which is optically continous with the phenocryst (Fig.4.8).

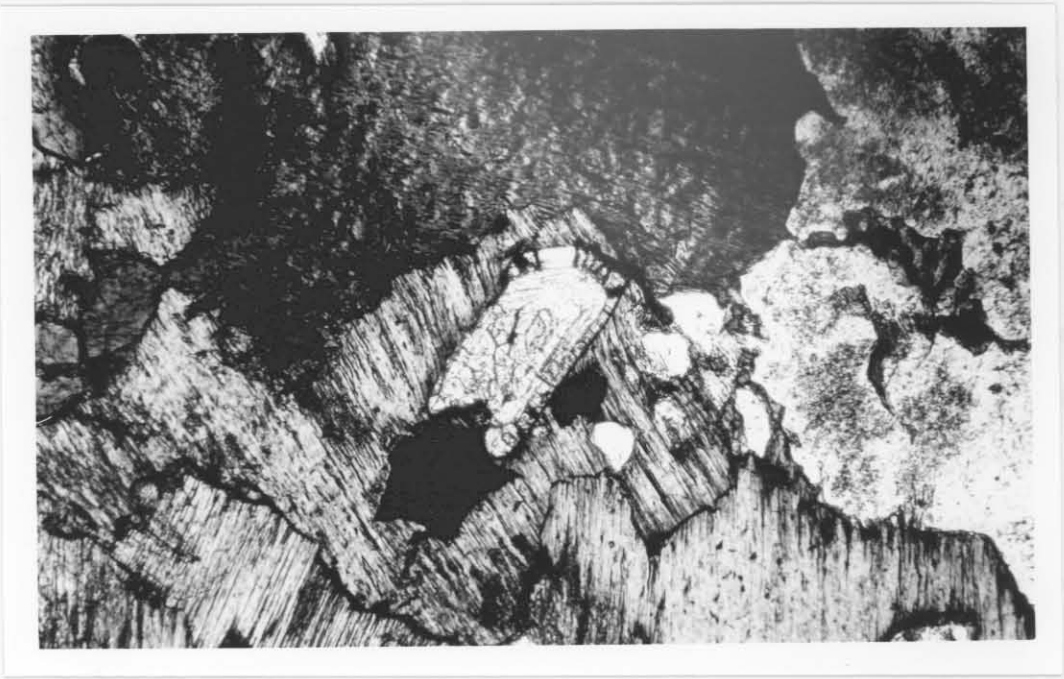

Fig. 4.7.: A zoned zircon crystal with secondary overgrowth in late crystallizing biotite. It is evident that secondary overgrowth formed very late in the crystallization sequence, because it disturbs the cleavage of biotite. GN-16. 125x. Varschwater 23JS.

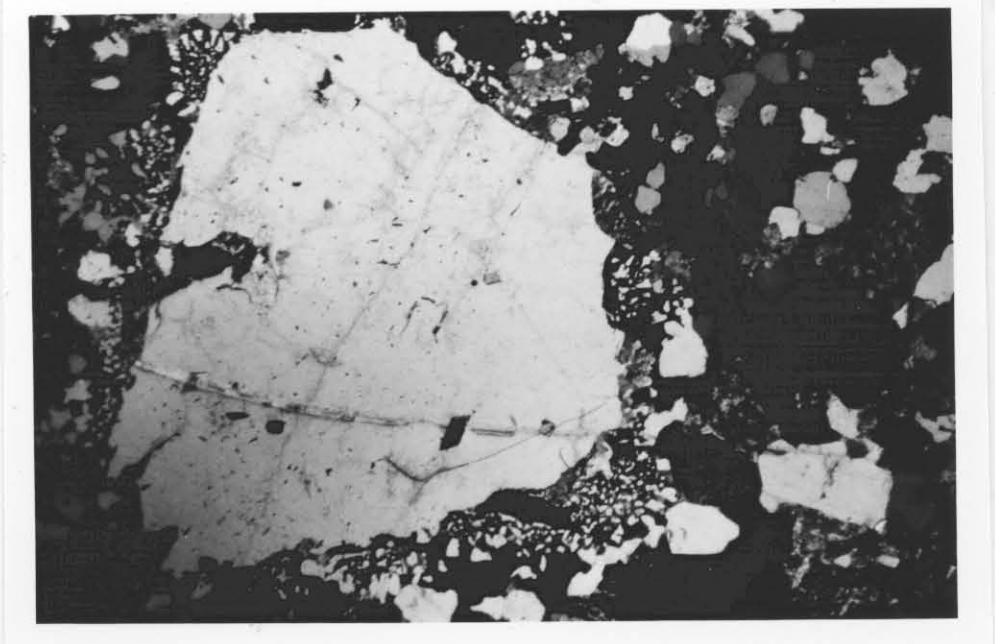

Fig. 4.8.: The small quartz domains are in optical continuity with the large quartz phenocryst. GK-29. X-Nicols. 12,5x. Varschwater 23JS.

Granophyric intergrowth around perthite phenocrysts and in the groundmass is common. The majority of these intergrowths have the appearance of an exploding bomb (Fig.4.9). Schloemer (1962) showed that mixtures of quartz and K-feldspar in a water medium at 400°C produce intergrowths of quartz and feldspar resembling the exploding bomb texture. This may suggest the possibility of hydrothermal activity in the granite.

Biotite is generally altered to chlorite and occurs interstitially to quartz and perthite. The chlorites are Mg-poor, Fe-rich varieties of thuringite which are dark green and nearly opaque (Appendix 1). Parry and Downey (1982) found that chloritic alteration in the Gold Hill quartz monzonite in Utah took place at about 200°C, and that Mg, Fe^{3+}, H^{+} and Mn are added to the rock, whilst K, Fe^{2+}, Ti, F and Cl are lost to solution. The same process evidently occurred in the Klipkloof Granite.

Accessory minerals include abundant fluorite, as well as zircon, ilmenite, thorite, monazite, allanite, muscovite, arsenopyrite, galena, chalcopyrite, sphalerite, molybdenite, rutile and tourmaline.

Zircons are extremely zoned and characterized by secondary overgrowths (Fig.4.10).

The following minerals in Klipkloof Granite were identified with the aid of the scanning electron microscope:

1) Th,Y silicate - yttrialite, which occurs next to and intergrown with zircon.
2) $ThSiO_4$ - thorite, closely associated with zircon.
3) $Ce,La,Y,Ca,Th(PO_4)$ - cheralite, where Ca and Th are substituting for REE.
4) Ca,Fe,Al,Ce,La silicate - allanite.
5) Th,Ce,Y,Ca, fluorsilicate - tritomite?
6) La,Ce silicate - cerite?

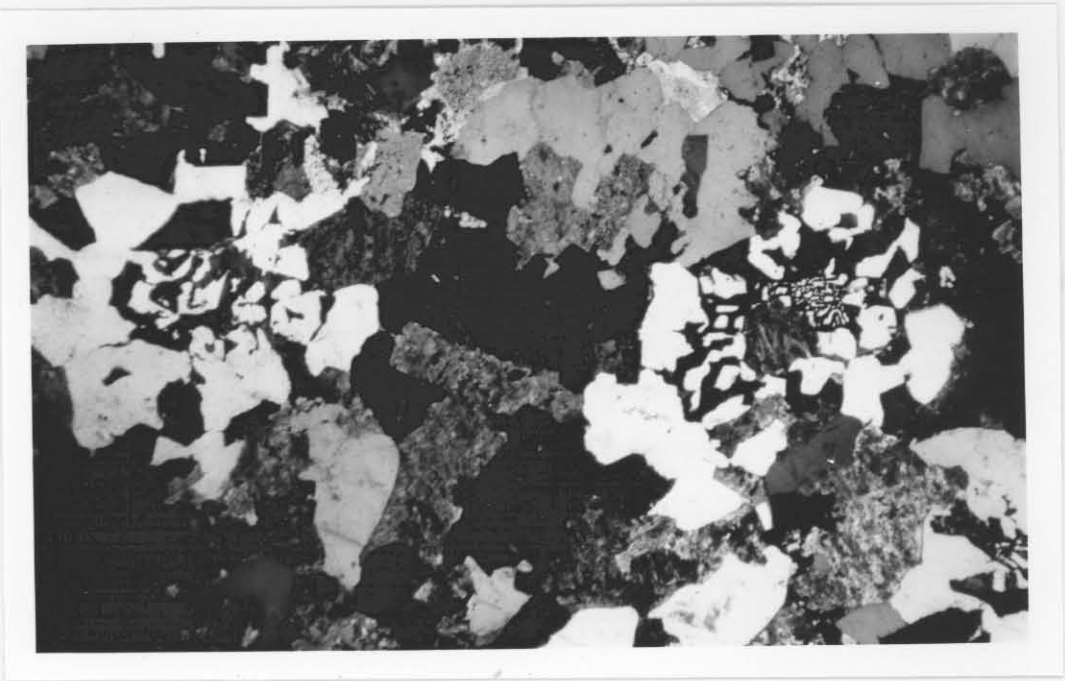

Fig. 4.9.: Exploding bomb texture in Klipkloof Granite. GK-17. X-Nicols. 12,5x. Varschwater 23JS.

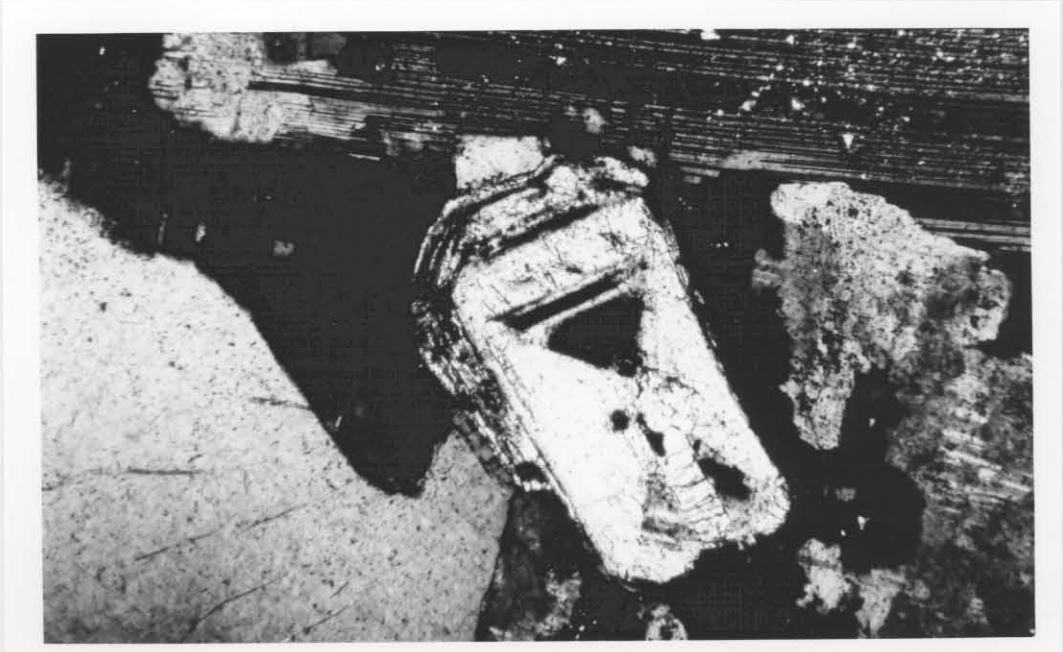

Fig. 4.10.: Secondary overgrown zircon crystal with sector zoning. GK-17. X-Nicols. 125x. Varschwater 23JS.

7) Ca,La,Ce silicate - beckelite?

8) $(Zr,Th)SiO_4$ - zircon and thorite solid solution.

9) $(Ce,La,Di)PO_4$ - monazite.

10) Ca,Ce,Fe silicate.

11) Ca,Ce,Ti,Y silicate.

12) $(Th,P)SiO_4$ - auerlite, because of P in the lattice.

Most of the above-mentioned minerals are very minute and therefore difficult to identify with a petrographic microscope. They occur mostly in hornblende. Some of them were found enclosed in plagioclase grains or on grain boundaries of quartz, perthite and plagioclase.

4.3.2. Medium- to coarse-grained Klipkloof Granite.

This type has a grain size of 2 to 4 millimetres with interlocking quartz grains and a high fluorite content. Mafic minerals are generally chloritized and the feldspars are reddish and very altered.

Subidiomorphic grains of quartz were the first to have crystallized (Fig.4.11). The amount of plagioclase is lower compared to the Nebo Granite. Granophyric intergrowth was observed in some samples.

The zircons are extremely zoned and secondary overgrowth is common. Other accessory minerals, as listed for the fine- to medium-grained and porphyritic Klipkloof Granite, also occur in this rock type.

4.3.3. Albitized Klipkloof Granite.

Albitization is due to late sodium-rich fluids, which interacted with the rock and changed its mineralogy and chemistry. The albite component of perthite increases in volume and a mesoperthite is formed (Fig.4.12).

Muscovite with slight pleochroism, indicating a celadonite composition, fluorite and tourmaline are important accessory

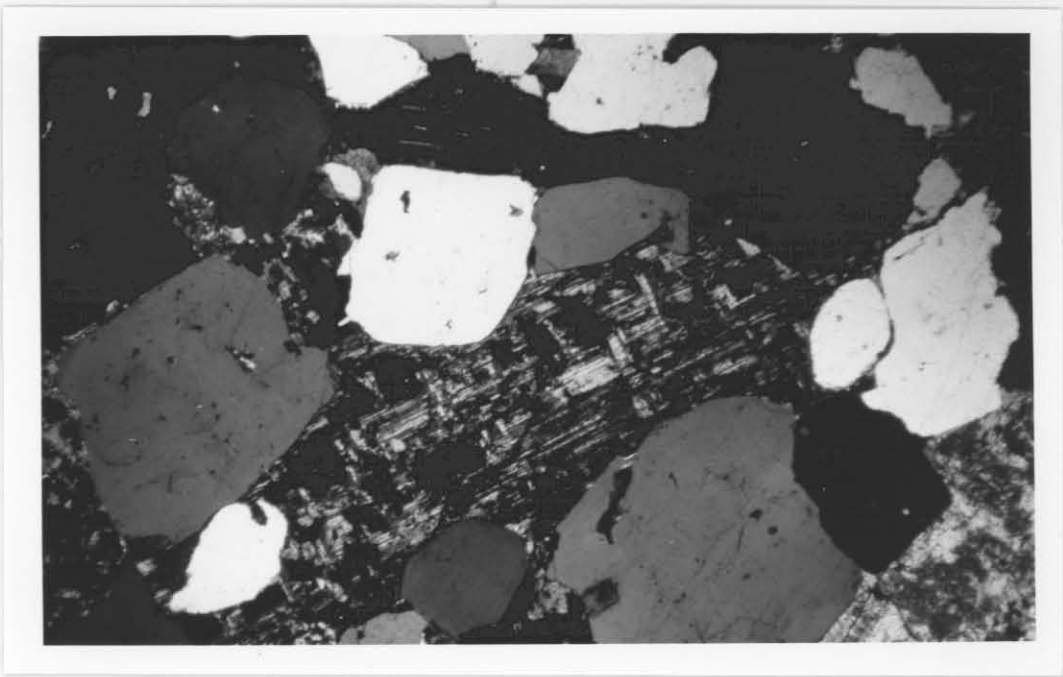

Fig. 4.11.: Subidiomorphic quartz grains which crystallized before perthite in Klipkloof Granite. GGR-362. X-Nicols. 12,5x. Tussenin 21JS.

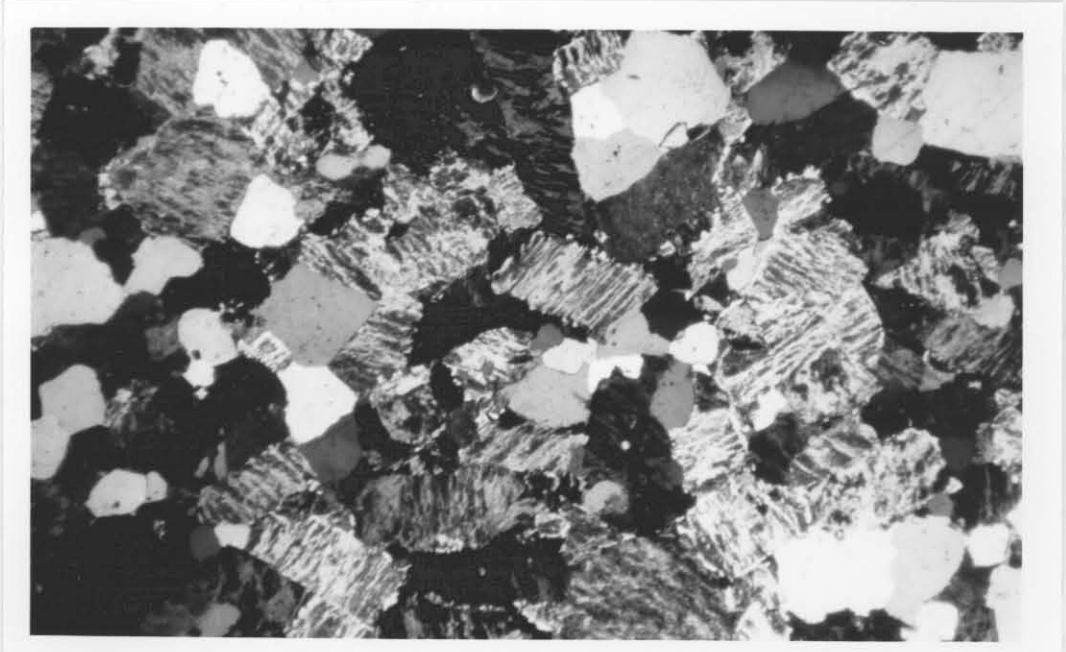

Fig. 4.12.: Albitized Klipkloof Granite is characterized by the large albite components of the perthite grains. GK-14. X-Nicols. 12,5x. Varschwater 23JS.

minerals.

Tourmaline-rich spheroids in the albitized granite are composed of tourmaline (schorl), quartz, plagioclase, perthite and topaz. Quartz occurs as irregular and subidiomorphic grains, enclosed in optically continous patches of tourmaline.

Thorite and zircon present are metamict.

4.4. Obliquity of potassium feldspars.

Obliquity values of potassium feldspars of the Nebo and Klipkloof Granite were determined using the separation of the 131 and $1\bar{3}1$ reflections (Smith and MacKenzie, 1955) (Table 4.2).

More than one factor controls the obliquity value of K-feldspar and it is difficult to ascertain the importance of any of these factors. There is a tendency for obliquity values to increase with the silica content and it may therefore be inferred that an increase in obliquity takes place during magmatic evolution, which includes lowering of consolidation temperature or increase of volatile content (Dietrich, 1962).

A range of obliquity values from low towards high values with accompanying intermediate values is an indication of one igneous suite, where the younger parts have the highest values, with pegmatites being characterized by obliquity values above 0,80. Dietrich (1962) also found that most of the Ab content must be exsolved before obliquity values above 0,85 can be fixed.

The obliquity values of K-feldspar are influenced by temperature and volatile content of the magma during crystallization, the amount of albite in solid solution, post-magmatic hydrothermal solutions and cooling rate (Lenthall and Hunter, 1977).

Table 4.2.: Obliquity values of K-feldspar.

Rocktype	Sample No.	Obliquity.
Nebo Granite	GN-56	0,689
Nebo Granite	GN-50	0,735
Medium- to coarse-grained Klipkloof Granite	GGr-146	0,786
Porphyritic Klipkloof Granite	GGr-184	0,783
Porphyritic Klipkloof Granite	GGr-261	0,823
Fine- to medium-grained Klipkloof Granite	GGr-156	0,823
Fine- to medium-grained Klipkloof Granite	GK-51	0,859
Albitized Klipkloof Granite	GK-36	0,833

Nebo Granite sample GN-56 is from the bottom of the sheet, whereas sample GN-50 is from the upper more differentiated parts. The obliquity value of GN-50 is probably higher due to the presence of volatiles, a slower cooling rate and lower overall crystallization temperature.

Obliquity values of Klipkloof Granite are higher than those of the Nebo Granite, which is possibly due to the presence of volatiles, as reflected by the higher fluorite content, or perhaps because the Klipkloof Granite magma cooled more rapidly.

4.5. Tourmaline spheroids in the Klipkloof Granite.

According to Taylor (1979, p 200) many apogranites contain clots and nests of tourmaline, which may contain minor amounts of cassiterite. The tourmaline spheroids in the Klipkloof Granite appear to be an integral part of the rock with no sign of structural control (Fig.4.5).

The tourmaline clusters or spheroids are rimmed by a wide halo of light coloured rock, due to the impoverishment of mafic constituents. The diameter of the light coloured halos are always proportional to the size of the tourmaline spheroids. The hostrock is albitized and leucocratic and total mafic minerals do not exceed three percent. The spheroids

are scattered irregularly through the rock and their diameters range from three to twenty centimetres, with the majority having a diameter of about ten centimetres. Most tourmaline accumulations are spherical, but in some instances irregularly shaped clusters of tourmaline were observed.

The chemical analyses of the spheroids, together with the hostrock (GGr-256), are presented in Table 4.3. The spheroids are enriched in Al_2O_3 and FeO, but depleted in SiO_2, CaO, Na_2O and K_2O relative to their hostrock. The amount of K-feldspar in the spheroids is low, explaining the low K_2O content of the analyses. The FeO content is higher, due to its presence in schorl.

The analyses of the tourmaline spheroids do not add up to 100 percent, which is attributed to the presence of B_2O_3. From the two spheroid analyses it can be assumed that the B_2O_3 content amounts to about 2,5 to 3,0 percent, which is a reasonable figure if the modal amount of tourmaline is considered. A modal composition of 25 per cent schorl would result in a B_2O_3 content of about 2,5 per cent.

The spheroids contain about 40 ppm Sn, which is only slightly higher than the 34 ppm in the host rock.

According to Nemec (1975), the origin of tourmaline spots and spheroids may be explained by metasomatic replacement of granite, because the mineral assemblage tourmaline and quartz is also known from greisens and pegmatites, where it developed as a result of the replacement of feldspar by tourmaline, forming a poikilitic texture with quartz. He also suggests that the material required for the development of tourmaline spheroids was imported partly from outside in the case of boron, and partly from the light halos, due to the breakdown of biotite.

Schust et al. (1970) also believe in the metasomatic origin of the spheroids, because they are similar to small

Table 4.3.: Chemical analyses of spheroids (GKSph) and host rock (GGr).

	GKSph-37	GKSph-37A	GGr-256
SiO_2	72,29	72,27	75,55
TiO_2	0,10	0,09	0,06
Al_2O_3	12,82	12,89	12,16
FeO	5,98	5,99	1,56
MnO	0,03	0,03	0,01
MgO	0,00	0,00	0,00
CaO	0,23	0,04	0,65
Na_2O	3,64	3,88	4,16
K_2O	1,27	1,25	4,73
P_2O_5	0,00	0,00	0,00
Cr_2O_3	0,03	0,04	0,04
NiO	0,00	0,00	0,01
LOI	0,76	0,64	0,65
H_2O^-	0,08	0,07	0,20
Total	97,23	97,19	99,78
Ba	5	10	33
Rb	155	163	643
Sr	3	2	9
Y	94	51	158
Zr	226	227	277
Nb	52	63	88
La	28	60	72
Ce	42	103	121
Nd	6	44	55
Th	45	41	63
U	17	10	29
Hf	7	9	13
Ga	46	49	32
Sc	0	0	0
Zn	104	99	19
Cu	1	2	6
Ni	6	4	6
Pb	10	11	30
Mo	1	1	2
W	10	6	14
Sn	45	39	34

greisen bodies. They concluded that the spheroids originated after the granite host had crystallized, because they could find no difference between textures of the host granite and the spheroid on stained varnished rockslabs.

Teuscher (1936) proposes that such spheroids originated in gas cavities, which formed whilst the granite crystallized. Oelsner (1952) believes that they formed as a result of pneumatolitic introduction of boron, while Tindle and Pearce (1981) attribute their origin to a late-stage build up and expulsion of volatiles.

Durasova and Barsukov (1973) suggest a magmatic origin for the tourmaline spherolds. According to them separation of a silicate magma enriched in boron by a mechanism of liquid immiscibility could take place at a late stage in differentiation when the boron has accumulated sufficiently. They showed that it is possible for tin and boron to be extracted from the silicate melt by liquid immiscibility in the system $CaO-B_2O_3-2SiO_2$.

Tourmaline spheroids in the Klipkloof Granite are believed to have originated by metasomatic replacement of K-feldspar by schorl. The iron necessary for the formation of tourmaline was derived from the breakdown of biotite. A build-up of volatiles probably played a role in the importation of boron.

Recknagel (1909) and Strauss (1954) state that the tourmaline nodules present in the Bobbejaankop Granite at Zaaiplaats are genetically related to the pipe-like ore bodies, and that the nodules may mark the transition between the hydrothermal and pegmatite phase. The presence of tourmaline nodules in the albitized Klipkloof Granite on the Sekhukhune Plateau, can therefore be considered as a further indication of the tin potential of these granites in this area.

4.6. The molybdenite mineralization on Varschwater 23JS.

Massive and disseminated molybdenite and chalcopyrite mineralization is exposed in a roadcutting on Varschwater 23JS (Plate 1, back folder). Crocker et al. (1977), the Mining Corporation (report by S. Gain) and Rand Mines (report by I.M. Clementson and P.A. van Straten) have investigated the deposit and surrounding area in some detail.

Three types of ore are recognizable in the deposit, viz. molybdenite-rich, chalcopyrite-rich, and REE-rich ore.

4.6.1. Molybdenite-rich ore.

Molybdenite and fluorite are the major ore minerals, with arsenopyrite, chalcopyrite, galena, sphalerite and ilmenite the accessory constituents. Allanite is generally associated with the ore.

Molybdenite occurs as large elongated aggregates with kinkbands (Fig.4.13) set in a gangue of albite, chlorite and thuringite. Fluorite with minor Y in the lattice is present in large amounts. One yttrocerite grain was identified. According to Dana (1932), yttrocerite can accommodate up to 55 per cent $(Y,Ce)F_3$ in its lattice.

Scheelite was found in some samples, where it occupies gaps between molybdenite kinkbands, whereas a bismuth-telluride (tetradymite-$Bi_2(Te,S)_3$) was found in one sample (Fig.4.13).

4.6.2. Copper ore.

The copper-ore, which consists mainly of chalcopyrite, occurs in a gangue of albite. Arsenopyrite, forming large euhedral grains, galena, covellite and molybdenite are accessory ore minerals. Inclusions of galena (Fig.4.14), iron-poor sphalerite, cassiterite (Fig.4.15), and rarely stannite occur in the chalcopyrite. Inclusions of galena were also found in arsenopyrite (Fig.4.16).

Sulphosalts are common in the copper ore. They include sulpharsenites, sulphantimonites and sulphbismuthites, as well as a Cu,Pb,Bi-sulphosalt (9,8% Cu; 29,1% Pb; 31,1% Bi; 29,4% S and 0,6% Fe). In some samples sulphosalts are present in high concentration as large grains, which are sometimes intermingled with chalcopyrite. They were also commonly observed in the cleavages of altered biotite (Fig.4.17).

Native bismuth, Pb,Bi,S-compounds, Bi-telluride-selenide and Bi-selenide were identified as minute grains in the copper ore.

Fig. 4.13.: Kinkbands of molybdenite are characteristic. Bismuth-telluride occurs in the molybdenite ore. 20 kV. 390x. VW-1. Varschwater 23JS.

Fig. 4.14.: Inclusions of galena in chalcopyrite. 20kV. 390x. VW-4. Varschwater 23JS.

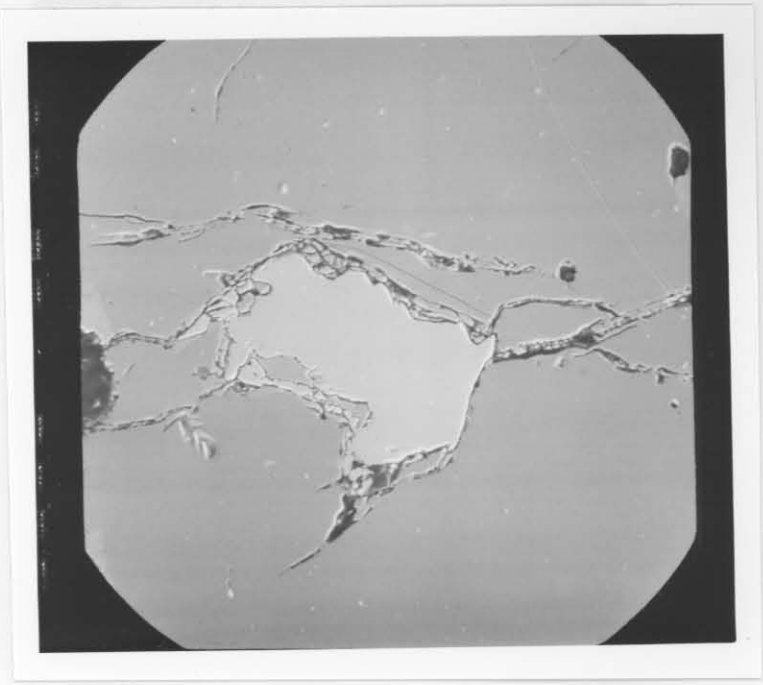

Fig. 4.15.: Inclusion of cassiterite in chalcopyrite. 20 kV. 220x. VW-4. Varschwater 23JS.

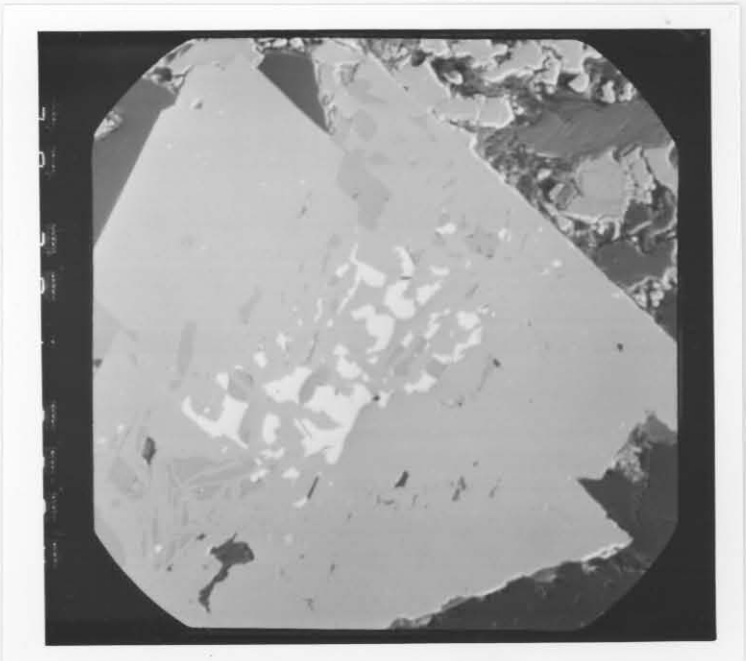

Fig. 4.16.: Inclusions of galena in arsenopyrite. 20 kV. 200x. VW-5. Varschwater 23JS.

Fig. 4.17.: Sulphosalts commonly occur in the cleavages of altered biotite. 20 kV. 110x. VW-3. Varschwater 23JS.

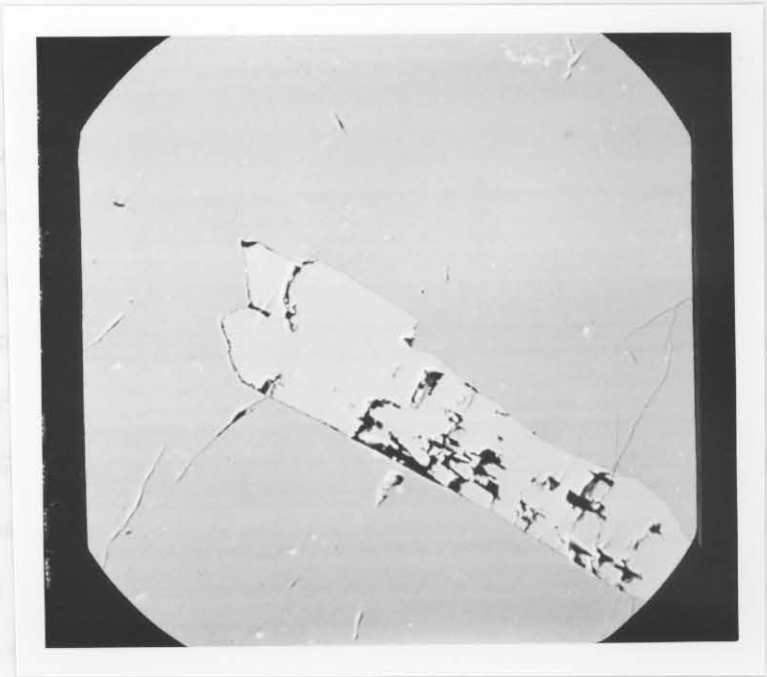

Fig. 4.18.: A well developed grain of loellingite in arsenopyrite. 20 kV. 470x. VW-5. Varschwater 23JS.

Loellingite ($FeAs_2$) commonly occurs as well defined grains in arsenopyrite (Fig.4.18). A continuous substitution of sulphur takes place between the former and latter and any composition between $FeAs_2$ and FeAsS seems possible.

Zircons, characterized by secondary overgrowths, are common. In some instances galena is present in the overgrowth (Fig.4.19). The presence of galena could be due to the radioactive decay of U to the daughter element Pb. Sulphur-rich liquid probably combined with the lead to form galena.

4.6.3. REE-rich ore.

The ores rich in REE (La,Ce,Nd,Sm and Gd) are mainly composed of allanite, which is strongly zoned (Fig.4.20 and Fig.4.21). The zone with the high reflectance is characterized by a high concentration of the heavy REE Nd,Sm and Gd.

4.6.4. The origin of the mineralization.

The mineralization is related to late Klipkloof Granite aplite dykes, which intrude both the Nebo Granite and Klipkloof Granite sills. Some Klipkloof Granite sills therefore intruded earlier than the aplite dykes.

The mineralization is present as disseminations in the Nebo Granite and as small pockets of massive ore, underlying a Klipkloof Granite sill. The mineralization occurs at this particular position because late aplite dykes, intruding the Nebo Granite along structural weaknesses, were enriched in volatiles and ore elements, which were subsequently trapped by the Klipkloof Granite sill. This is obvious from the field relationships (Fig.4.3), where the intruding aplite dyke was impeded by the Klipkloof Granite sill.

Because the Klipkloof Granite sills acted as traps for the mineralizing fluids, it is difficult to identify

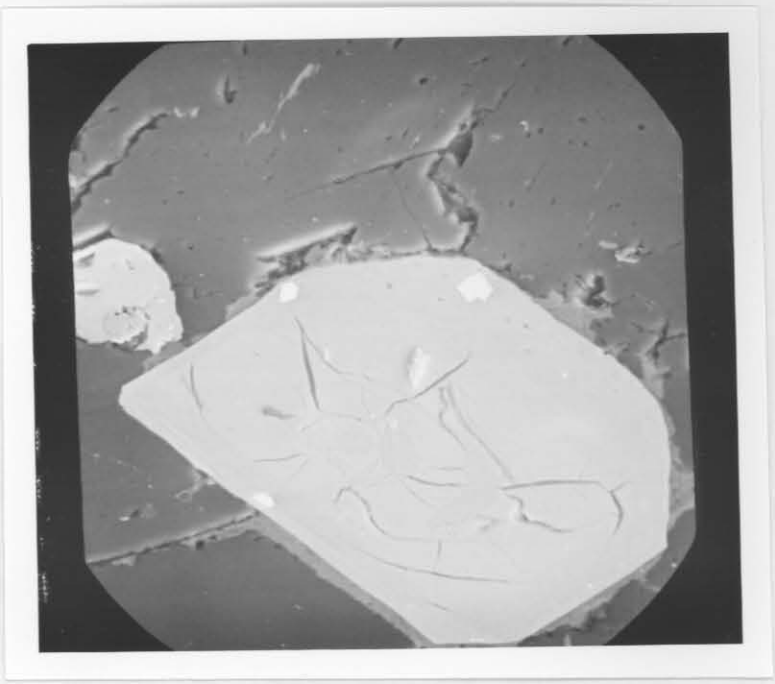

Fig. 4.19.: Grains of galena are present in the secondary overgrowth of zircons. 20 kV. 430x. VW-2. Varschwater 23JS.

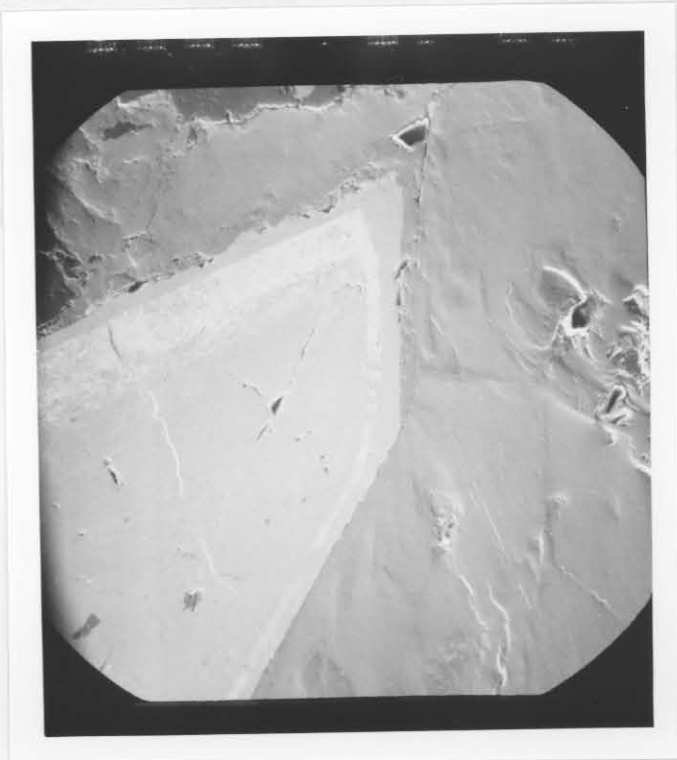

Fig. 4.20.: Strongly zoned allanite crystal. The zone with the high reflectance is characterized by a high concentration of heavy REE. 20 kV. 100x. VW-2. Varschwater 23JS.

Fig. 4.21.: Zoned allanite crystals in a host of albite. VW-10. 12.5x. Varschwater 23JS.

anomalies above these sills. Detailed geochemical exploration of specialized Klipkloof Granite would probably indicate more mineralized localities. For these reasons, it seems that the Klipkloof Granite underlying the Stavoren Granophyre is a potential target, because the contact with the granophyre is an ideal trap for mineralization.

5. Geochemistry of Rooiberg Felsite and Stavoren Granophyre.

5.1. Major element geochemistry.

The similarity in the geochemistry of Rooiberg Felsite and Stavoren Granophyre and their proposed co-magmatic origin (Walraven, 1982) is the reason why these rock types are considered together.

The major element analyses of felsites, metafelsites and granophyres are tabulated in Appendix 2.

The major oxides were plotted against the Thornton-Tuttle Differentiation Index (Thornton and Tuttle, 1960). All the diagrams display a trend for the felsites, whereas the granophyres are characterized by a cluster of points around a D.I. of 90 to 93. This relationship is clearly shown in Figure 5.1., where CaO is plotted against the D.I.

Samples of granophyres were taken in different localities throughout the area, from stratigraphically high positions, underlying the felsites, as well as from stratigraphically low positions, overlying the Nebo Granite. No differentiation trend of the Stavoren Granophyre magma could be observed. A difference in the geochemistry of major elements between the micro-granophyres and normal granophyres was not observed. Figure 5.1, however, shows some lower values of CaO for the micro-granophyres compared to the granophyres, and may be due to a higher content of plagioclase phenocrysts in the normal granophyres.

The felsites and granophyres were also plotted in the Qz-Ab-Or diagram (Fig.5.2.). The Stavoren Granophyre occupies the same compositional area as the Nebo Granite (Fig.7.5.), corresponding to the field of hypersolvus granites of Luth et al. (1964). The felsites are characterized by a larger compositional area compared to the granophyres.

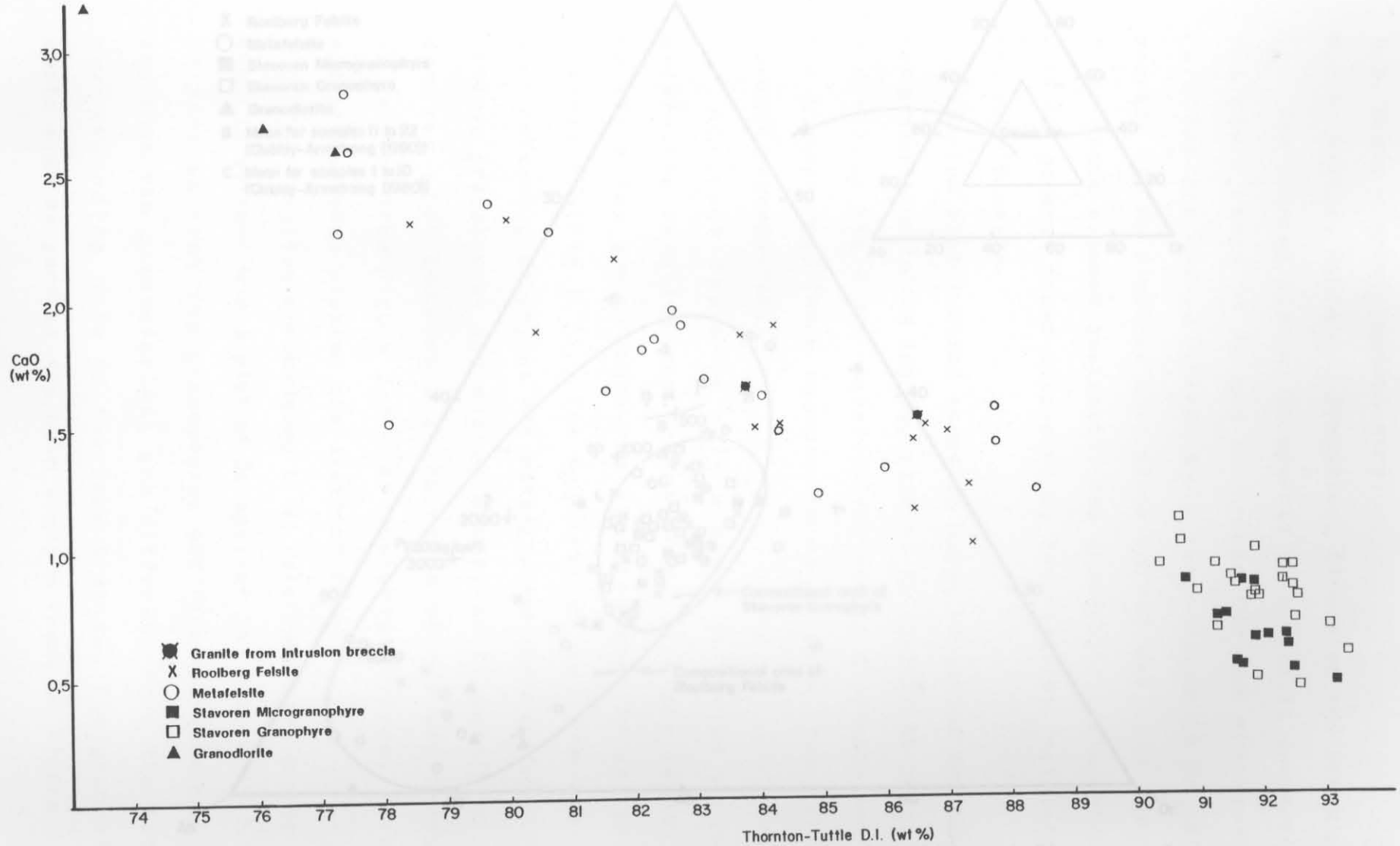

Fig. 5.1.: Plot of CaO against the Thornton-Tuttle D.I. for Roolberg Felsite, metafelsite, granodiorite and Stavoren Granophyre.

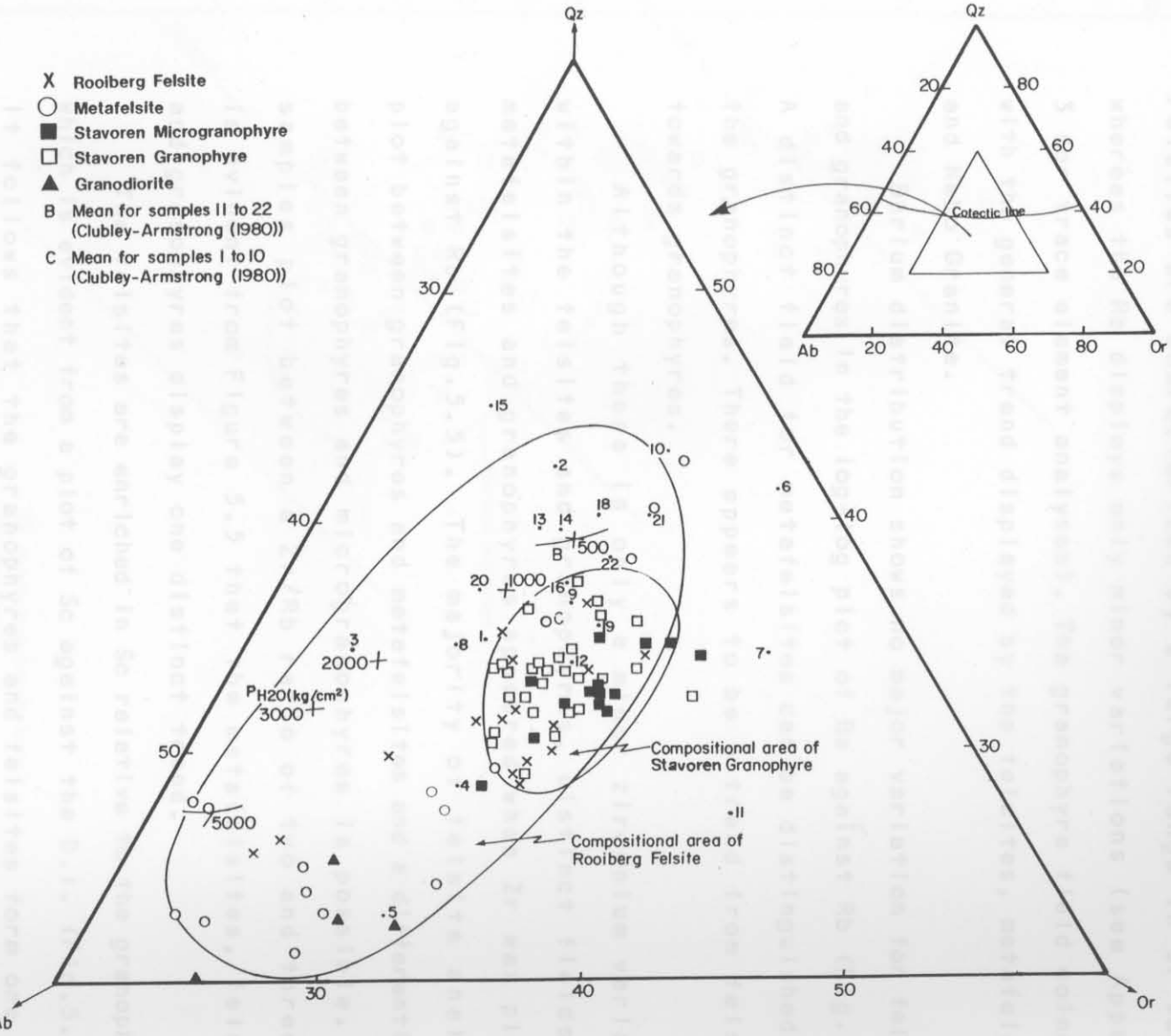

Fig. 5.2.: CIPW normative compositions of Rooiberg Felsite, metafelsite and Stavoren Granophyre in the Qz-Ab-Or diagram. The pressures indicated are in kg/cm^2 and taken from Tuttle and Bowen (1958) and Luth, Jahns and Tuttle (1964). The numbered samples are from Clubley-Armstrong (1981).

5.2. Trace element geochemistry.

5.2.1. Barium, Rubidium, Strontium, Zirconium and Scandium.

The log-log plot of Sr against Rb (Fig.5.3) demonstrates the small range in Rb and Sr values for the granophyres. Felsites are characterized by a large range in Sr values, whereas the Rb displays only minor variations (see Appendix 3 for trace element analyses). The granophyre field coincides with the general trend displayed by the felsites, metafelsites and Nebo Granite.

Barium distribution shows no major variation for felsites and granophyres in the log-log plot of Ba against Rb (Fig.5.4). A distinct field for metafelsites can be distinguished from the granophyres. There appears to be a trend from felsites towards granophyres.

Although there is only a minor zirconium variation within the felsites and granophyres, distinct fields for metafelsites and granophyres appeared when Zr was plotted against Rb (Fig.5.5). The majority of felsite analyses plot between granophyres and metafelsites and a differentiation between granophyres and microgranophyres is possible. Most samples plot between a Zr/Rb ratio of two and three. It is evident from Figure 5.5 that the metafelsites, felsites and granophyres display one distinct trend.

The felsites are enriched in Sc relative to the granophyres, which is evident from a plot of Sc against the D.I. (Fig.5.6). It follows that the granophyres and felsites form one trend and that the granodiorites are different from the latter, corresponding more to the Nebo Granite. The granophyres could also be part of the Nebo Granite trend on Figure 5.6.

5.3. Discussion.

Despite its distribution and volume the Stavoren Granophyre forms a very homogeneous suite of rocks. This was also noted

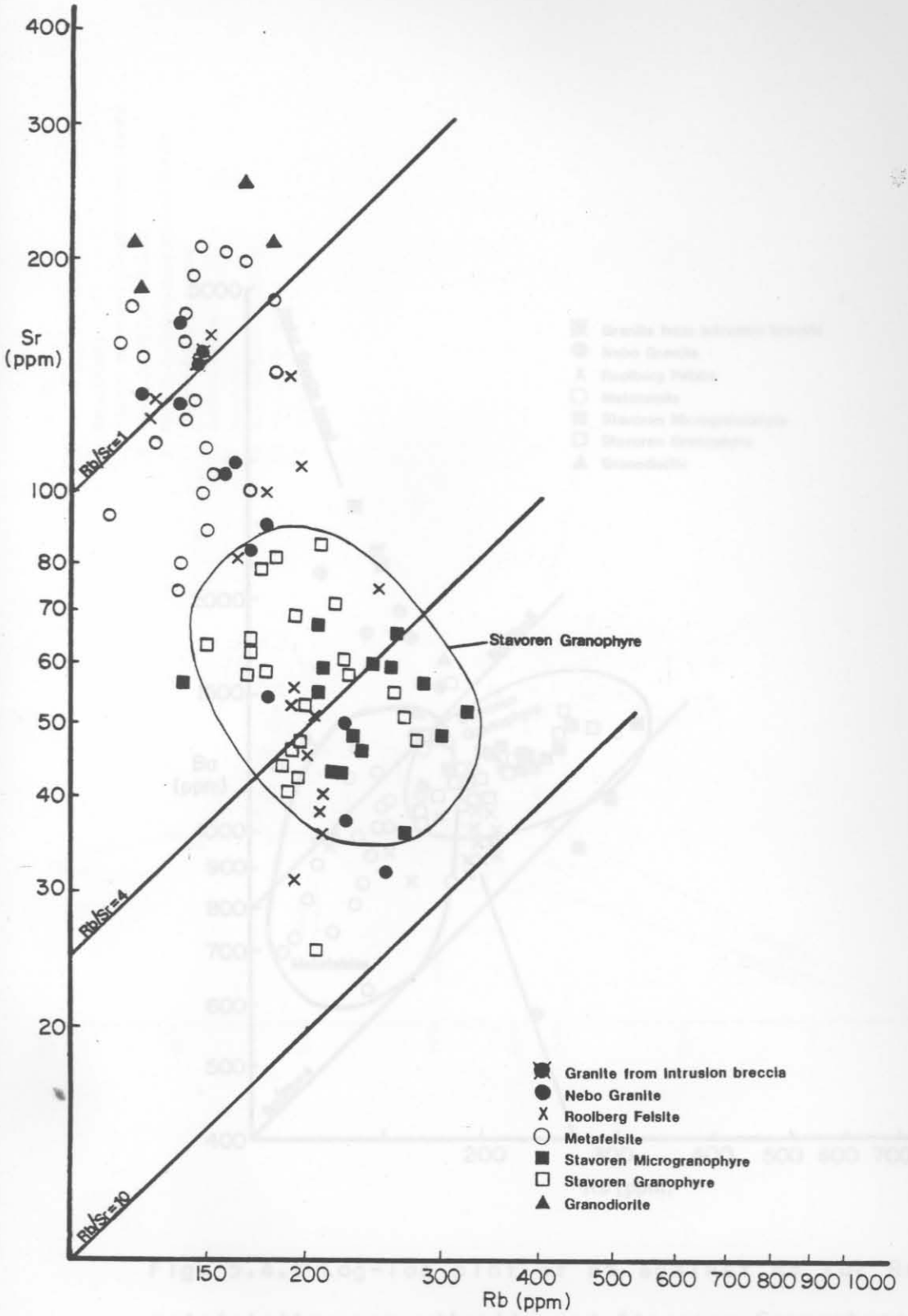

Fig. 5.3.: Log-log plot of Sr against Rb for Roolberg Felsite, metafelsite, granodiorite and Stavoren Granophyre.

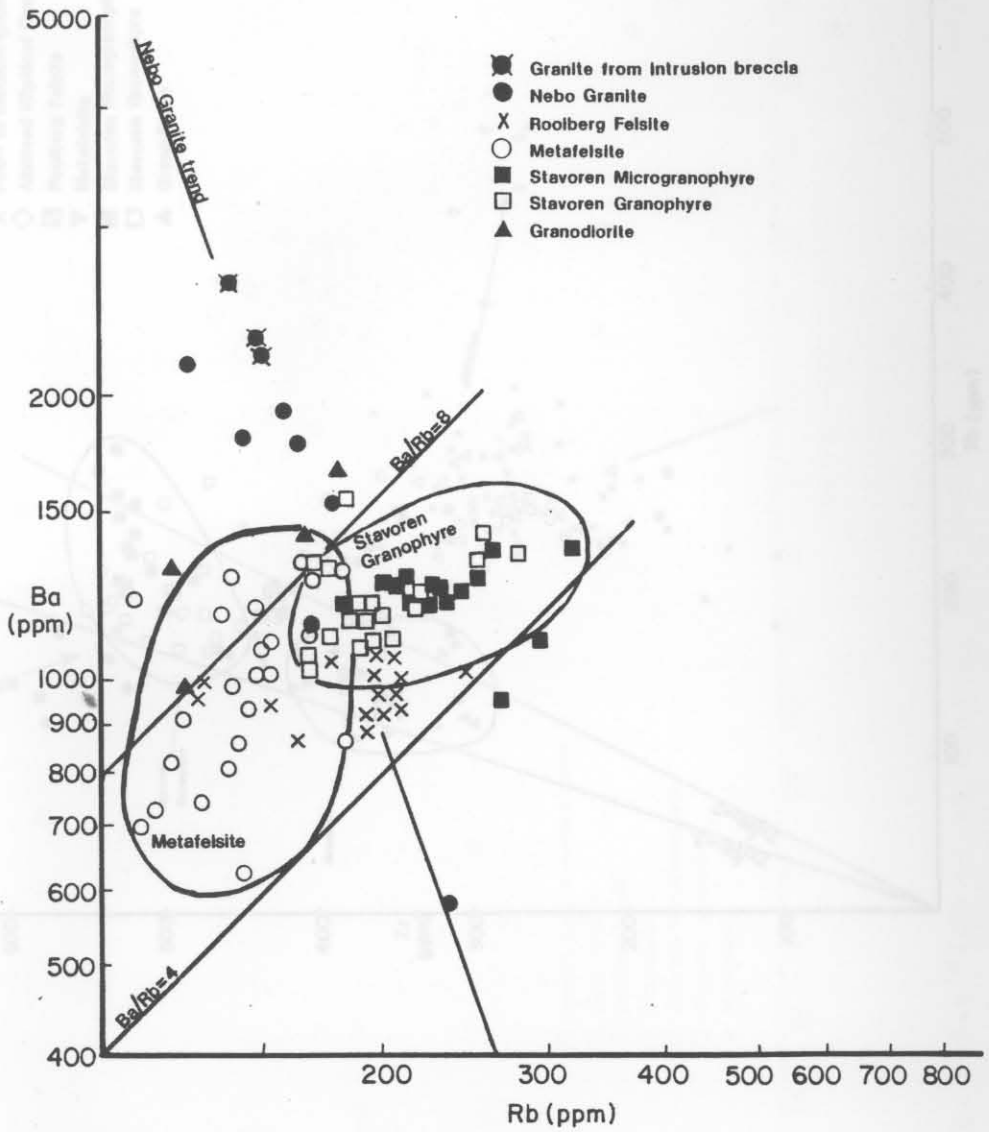

Fig. 5.4.: Log-log plot of Ba against Rb for Rooiberg Felsite, metafelsite, granodiorite and Stavoren Granophyre.

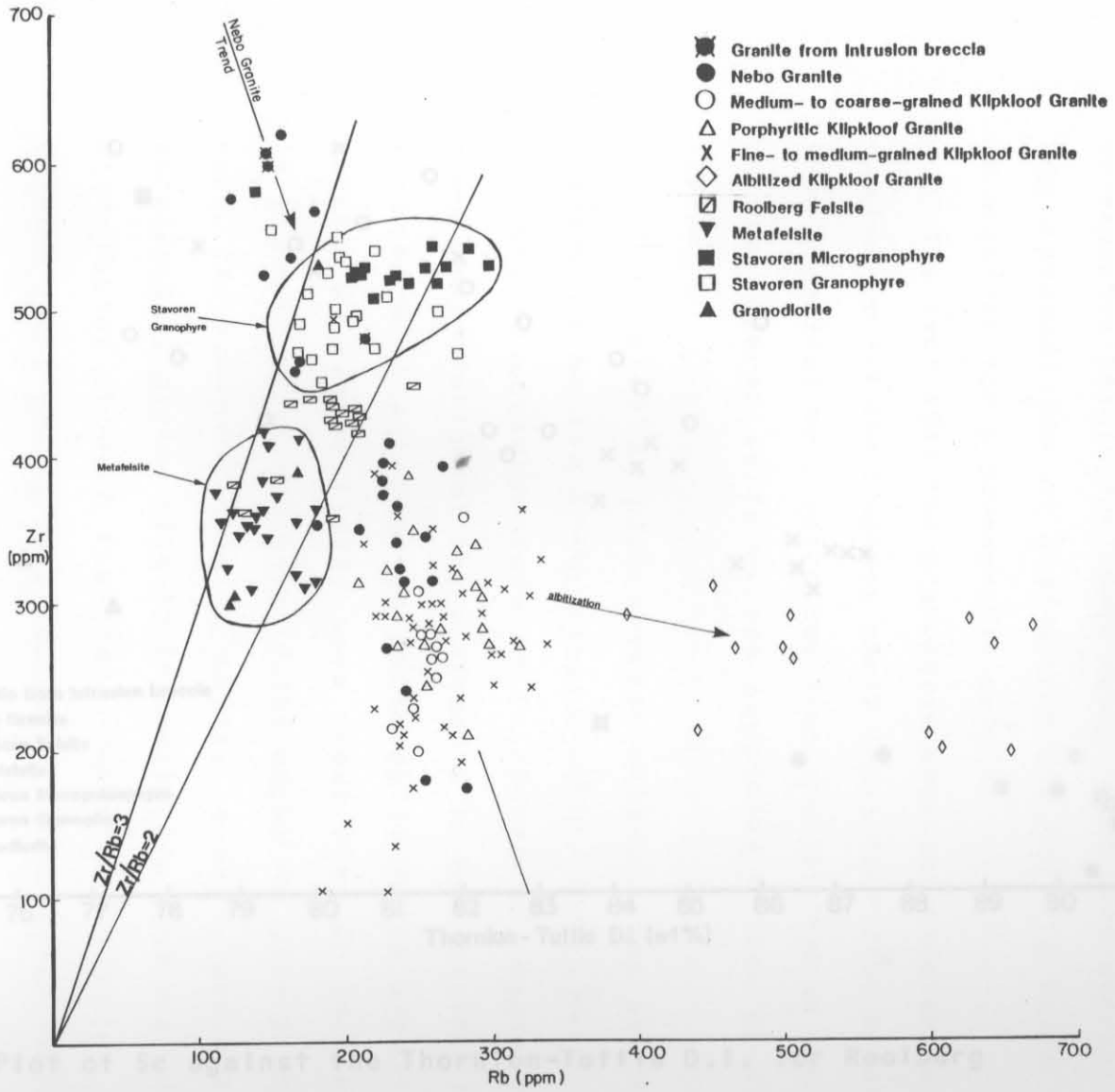

Fig. 5.5.: Plot of Zr against Rb for Roolberg Felsite, metafelsite, granodiorite, Stavoren Granophyre, Nebo and Klipkloof Granite.

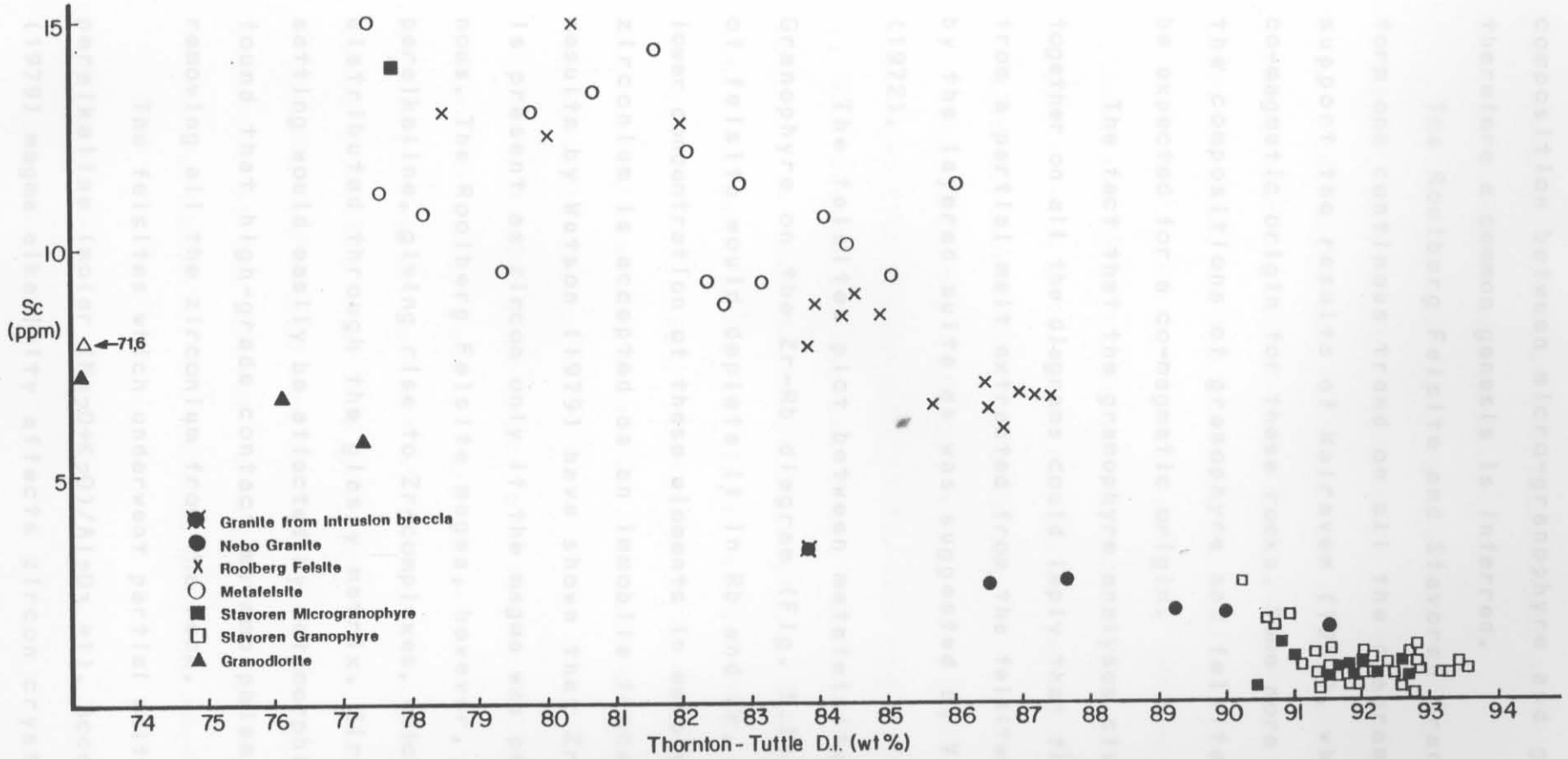

Fig. 5.6.: Plot of Sc against the Thornton-Tuttle D.I. for Roolberg Felsite, metafelsite, granodiorite, Stavoren Granophyre and Nebo Granite.

by Walraven (1982). There is only a slight difference in composition between micro-granophyre and granophyre and therefore a common genesis is inferred.

The Rooiberg Felsite and Stavoren Granophyre seem to form one continous trend on all the diagrams, which could support the results of Walraven (1982), who postulated a co-magmatic origin for these rocks. Some more overlap between the compositions of granophyre and felsite would however be expected for a co-magmatic origin.

The fact that the granophyre analyses cluster so closely together on all the diagrams could imply that they crystallized from a partial melt extracted from the felsites on metamorphism by the layered suite as was suggested by Von Gruenewaldt (1972).

The felsites plot between metafelsites and Stavoren Granophyre on the Zr-Rb diagram (Fig. 5.5). Metamorphism of felsite would deplete it in Rb and Zr, explaining the lower concentration of these elements in metafelsite. However, zirconium is accepted as an immobile trace element. But, results by Watson (1979) have shown that Zr in a rhyolite is present as zircon only if the magma was per- or metaluminous. The Rooiberg Felsite magma, however, was marginally peralkaline, giving rise to Zr-complexes, which are uniformally distributed through the glassy matrix. Zirconium in this setting would easily be affected by metamorphism. Nell (1984) found that high-grade contact metamorphism is capable of removing all the zirconium from the rock.

The felsites which underwent partial melting were slightly peralkaline (molar $(Na_2O+K_2O)/Al_2O_3 = 1$). According to Watson (1979) magma alkalinity affects zircon crystallization. He found that zircon becomes unstable due to an increase in peralkalinity, which is possible if only plagioclase crystallizes, removing the CaO from the system. This is termed

the plagioclase effect by Bowen (1945). It is known from petrographic work that plagioclase was an early crystallizing mineral in the granophyres.

Due to the high temperature (850°C) and moderate pressure (2 kbar), melting of the felsite will take place after the upper zone magma was intruded (Von Gruenewaldt, 1972). Walraven (1982), also proved by heat-modelling that the mafic magma could have melted the Rooiberg Felsite.

From Figure 5.5 it follows that the Stavoren Granophyre is enriched in Zr relative to the Rooiberg Felsite and the metafelsite. A difference between microgranophyre and granophyre is also obvious from this diagram.

The Rooiberg Felsite, which were melted by the upper zone magma (Von Gruenewaldt, 1972), were rhyolites and rhydacites of the Damwal Formation. These felsites are different in composition from Stavoren Granophyre. The melting process would however, only partially affect the rock, giving rise to restite which was incorporated in the upper zone magma and which was subsequently intruded as granodiorite into the metafelsites.

It is also important to note that only very few minute zircon crystals were observed in the granophyres, although the Zr content of the rock is high. It therefore seems possible that the granophyric magma, representing a peralkaline liquid was derived from the marginally peralkaline felsites of the Damwal Formation by partial melting due to the intrusion of the Layered Sequence magma.

6. The geochemistry of the Lebowa Granite Suite.

6.1. Introduction.

A detailed geochemical study of the Nebo Granite and Klipkloof Granite was undertaken with the aim to determine the relationship between these rock types, to study the differentiation of the Nebo Granite magma, to compare the Lebowa Granite Suite of the study area with that of the Potgietersrust area and to investigate the geochemical specialization of the Klipkloof Granite with respect to mineralization.

6.2. Major element geochemistry.

The Nebo Granite, comprising a sheet-like body, is characterized by an upward increase in SiO_2 and K_2O with increasing D.I.; TiO_2, Al_2O_3, FeO, MnO, MgO, CaO and P_2O_5 decrease with increasing D.I., whilst Na_2O shows no variation. The Nebo Granite displays a fairly large differentiation trend, ranging from a D.I. of 84 to 95 (see Appendix 2 for major element analyses).

In contrast, the Klipkloof Granite evidently crystallized from a highly fractionated liquid and displays no differentiation trend. The different rock types, viz. porphyritic, medium- to coarse-grained, fine-to medium-grained and albitized granites, plot randomly in the vicinity of the most differentiated Nebo Granite.

The concentration of MgO is very low and only the very first differentiates of the Nebo Granite contain values of about 0,05 per cent. The MgO content decreases to below the lower limit of detection for the differentiated Nebo Granite and the Klipkloof Granite. The low concentration of MgO in the rocks is apparent from the ferromagnesian minerals, hornblende and biotite, which contain at the most only one per cent MgO (Appendix 1).

A large range in SiO_2 concentration, from 69 to 76 per cent, was found from bottom to top in the Nebo Granite sheet. The Klipkloof Granite ranges between 74 and 77 per cent SiO_2 (Fig.6.1).

TiO_2 was found to decrease from 0,4 to 0,1 per cent with differentiation in the Nebo Granite. Of interest here is the fact that the Klipkloof Granite does not plot exactly at the end of the Nebo Granite trend, as seen on the plot of TiO_2 against SiO_2 (Fig.6.2).

A well defined trend results for the Nebo Granite if Al_2O_3 is plotted against the D.I. (Fig.6.3). It is not understood why the analyses of the Klipkloof Granite do not conform to this trend. The Al_2O_3 values are generally higher than those of the corresponding Nebo Granite and only the medium- to coarse-grained Klipkloof Granite plot towards the end of the Nebo Granite trend.

The decrease in FeO from five to two per cent is ascribed to the increasingly leucocratic nature of the upper parts of the Nebo Granite sheet. The bulk of the Klipkloof Granite samples contain between two and three per cent FeO, with the exception of the albitized varieties, which contain between one and two per cent.

The CaO content changes from 0,4 to 1,5 per cent from top to bottom in the Nebo Granite sheet, because the anorthite content of early crystallizing plagioclase is higher at the base of the sheet. The high fluorite content of the differentiated Nebo Granite also contributes to the total CaO content. This is also the case with the Klipkloof Granite, which contains between 0,3 and 0,8 per cent CaO.

The amount of sodium (3,8 per cent Na_2O) in the Nebo Granite stays constant with changing D.I. The majority of Klipkloof Granites plot towards the end of the differentiation trend (this plot is not presented here), except for the

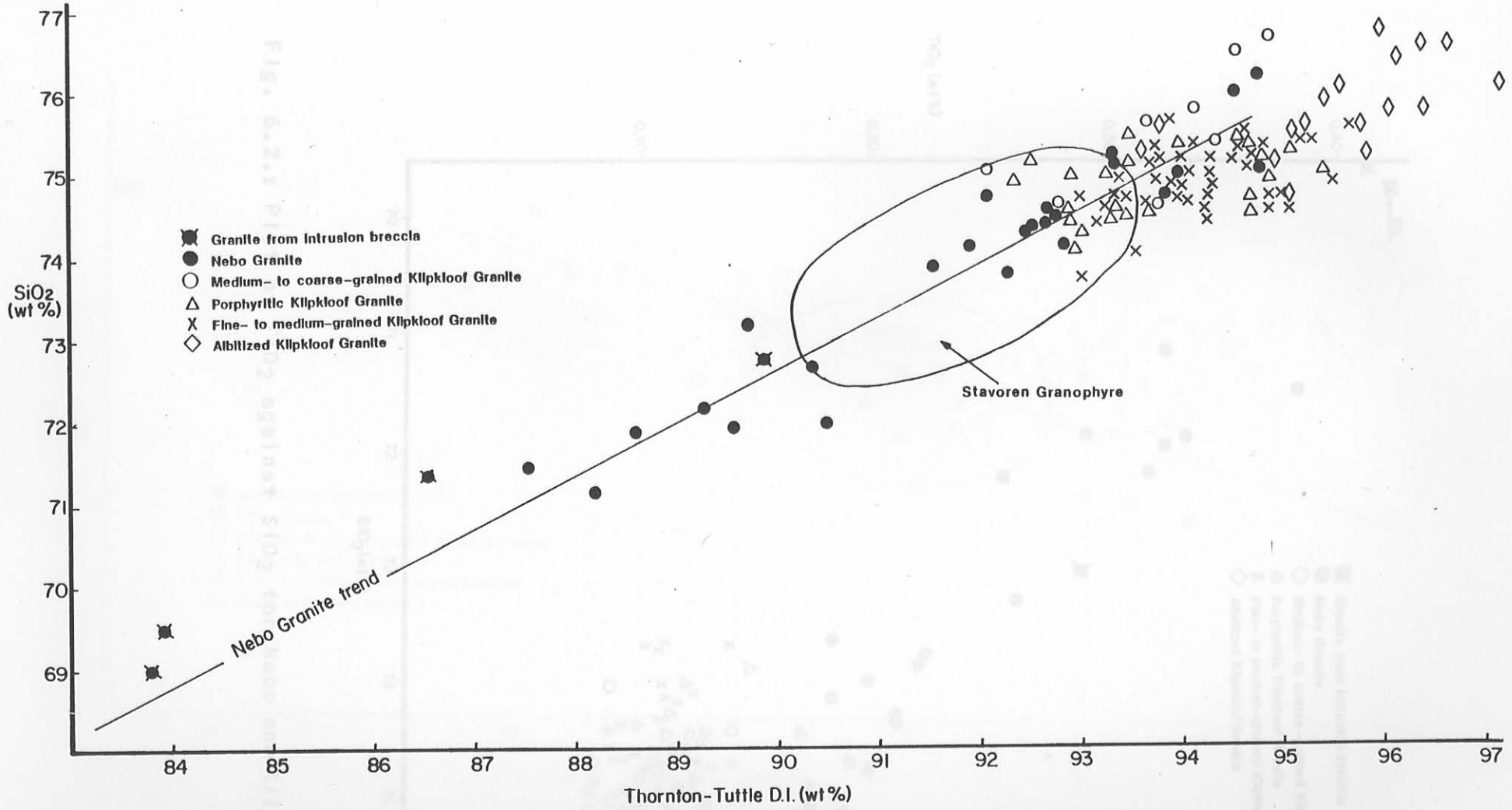

Fig. 6.1.: Plot of SiO_2 against the Thornton-Tuttle D.I. for Nebo and Klipkloof Granite. The field for Stavoren Granophyre is also indicated.

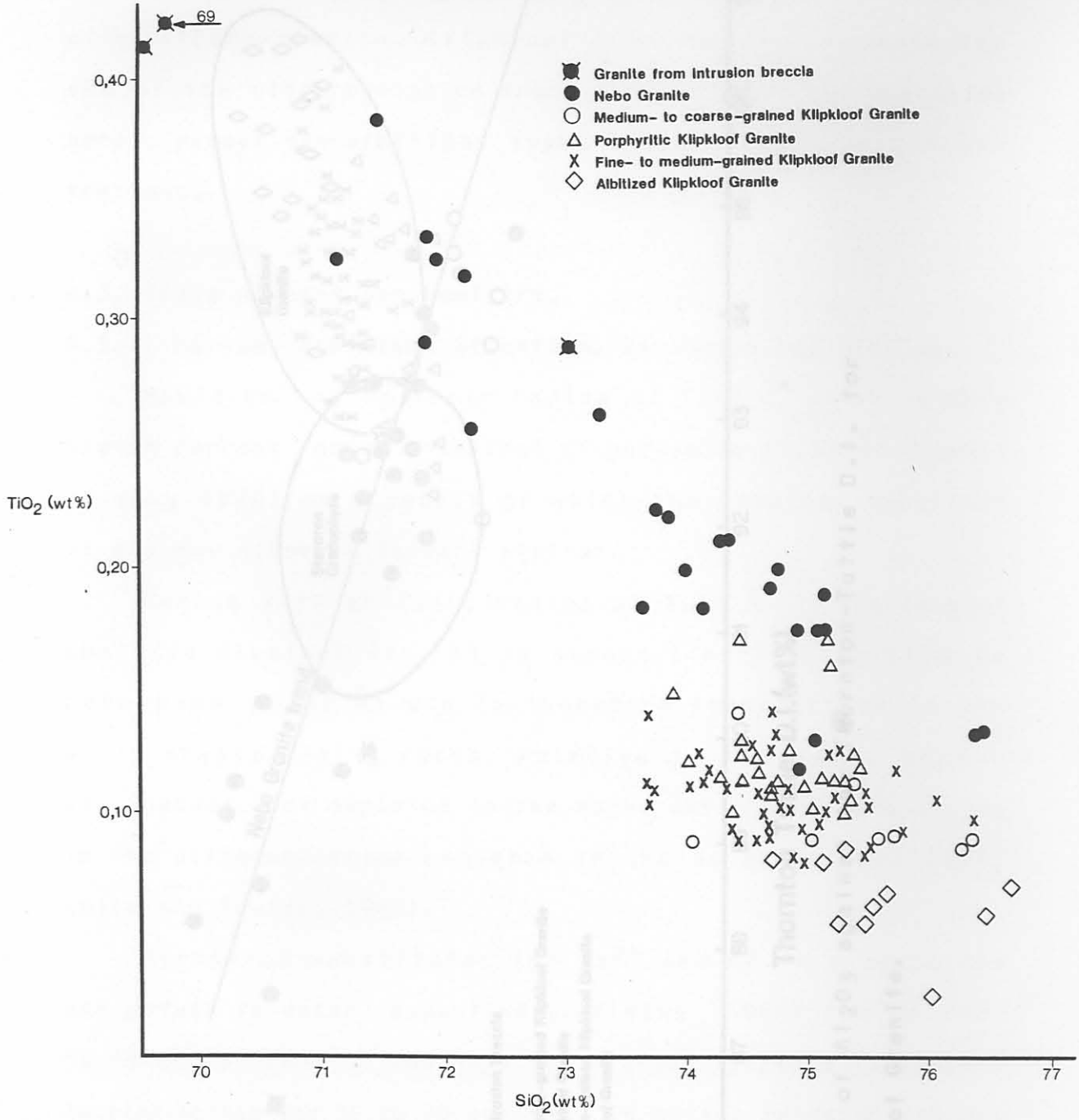

Fig. 6.2.: Plot of TiO_2 against SiO_2 for Nebo and Klipkloof Granite.

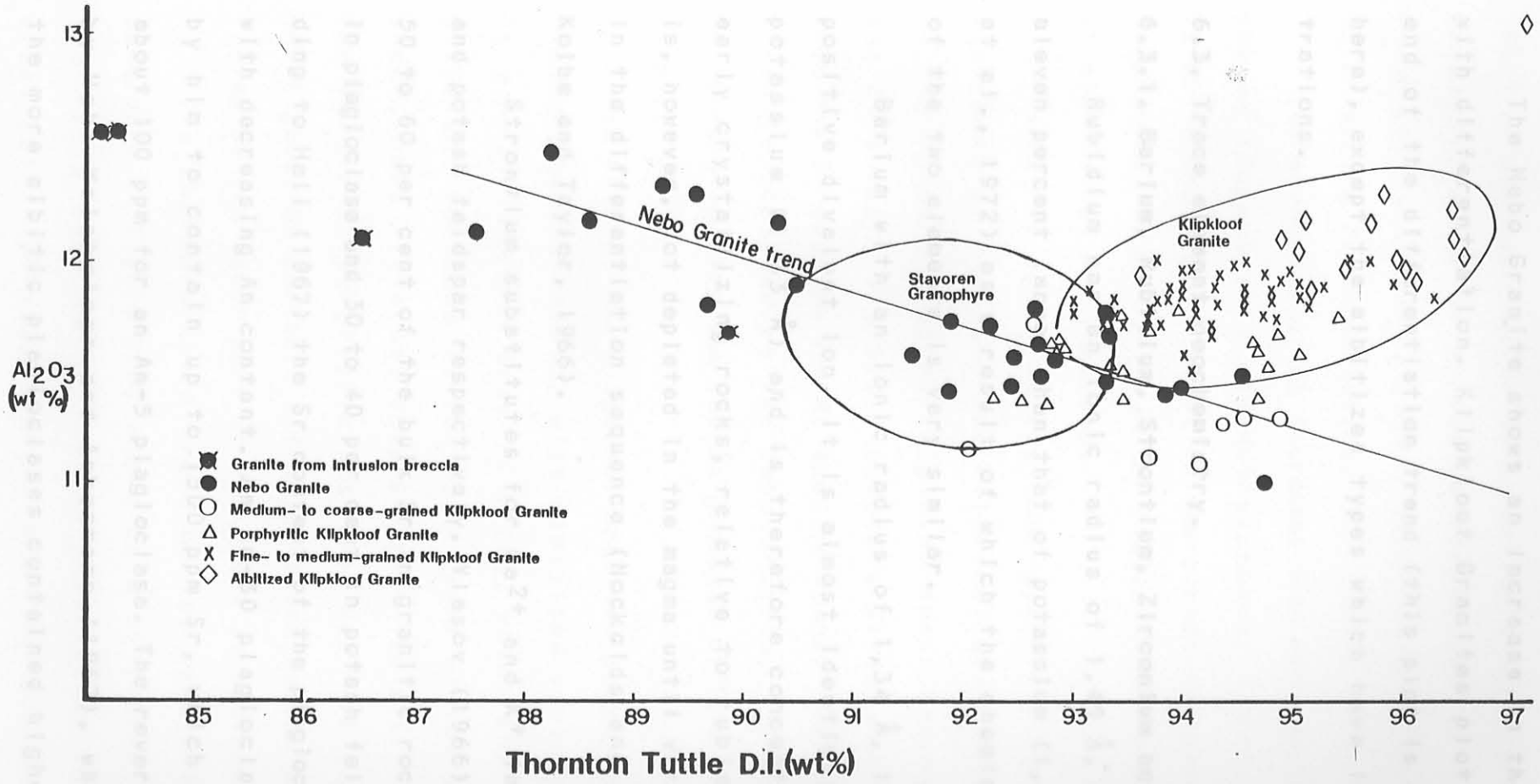

Fig. 6.3.: Plot of Al_2O_3 against the Thornton-Tuttle D.I. for Nebo and Klipkloof Granite.

albitized varieties, which have much higher values due to the large amount of albite in the rock.

The Nebo Granite shows an increase in the K_2O content with differentiation. Klipkloof Granites plot towards the end of the differentiation trend (this plot is not presented here), except the albitized types which have lower concentrations.

6.3. Trace element geochemistry.

6.3.1. Barium, Rubidium, Strontium, Zirconium and Niobium.

Rubidium has an ionic radius of 1,49 Å, which is only eleven percent larger than that of potassium (1,33 Å) (Cocco et al., 1972) as a result of which the chemical behaviour of the two elements is very similar.

Barium with an ionic radius of 1,34 Å, is the largest positive divalent ion. It is almost identical in size to potassium (1,33 Å) and is therefore concentrated in the early crystallizing rocks, relative to rubidium. Barium is, however, not depleted in the magma until very late stages in the differentiation sequence (Nockolds and Allen, 1953; Kolbe and Taylor, 1966).

Strontium substitutes for Ca^{2+} and K^{+} in plagioclase and potash feldspar respectively. Vlasov (1966) claims that 50 to 60 per cent of the bulk Sr in granitic rocks is present in plagioclase and 30 to 40 per cent in potash feldspar. According to Hall (1967) the Sr content of the plagioclase decreases with decreasing An content. An An-30 plagioclase was shown by him to contain up to 1500 ppm Sr, which decreases to about 100 ppm for an An-5 plagioclase. The reverse was noted by Hahn-Weinheimer and Ackermann (1967), who found that the more albitic plagioclases contained higher Sr values than the earlier plagioclases.

The average granite contains 175 ppm Zr (Degenhardt,

1957), which is far below the concentration found in the Lebowa Granite Suite. Zirconium may either increase (Kolbe, 1966) or decrease during differentiation of a granitic magma. Crystallization of zircon is suppressed if the magma is peralkaline (Watson, 1979), which results in an increase of Zr during differentiation.

The abundance of Nb increases from early to later intrusive phases (Mogarovskiy and Mel'nichenko, 1968), because it is an incompatible element in the common rock-forming minerals. Niobium may also serve as an indicator of mineralization, if high values are recorded.

If Ba, Rb and Sr values (see Appendix 3 for trace element analyses) of the Nebo and Klipkloof Granite are plotted on the ternary diagram (Fig.6.4) described by El Bouseily and El Sokkary (1975), a complete differentiation trend from the Ba apex to the Rb apex is found. The "normal granite" field is occupied by the Nebo Granite, which in turn can be correlated with the low-Ca granites of Turekian and Wedepohl (1961).

The bulk of the Klipkloof Granites plot in the "differentiated granite" field, with albitized varieties near the Rb apex. Klipkloof Granite sills, which are developed at different horizons in the upper part of the Nebo Granite sheet, have different compositions. The sill which occupies the lowest stratigraphic position has the lowest Rb and the highest Ba content. Sills therefore become more differentiated as the upper part of the sheet is approached.

The characteristic trend of the Nebo Granite is also developed in Figure 6.5, where data of Lenthall and Hunter (1977) is used to define the granites of the Zaaiplaats area. Point "B" represents a starting composition of 40 ppm Sr and 240 ppm Rb and the line "pure solid composition" represents the compositions of solids formed during perfect

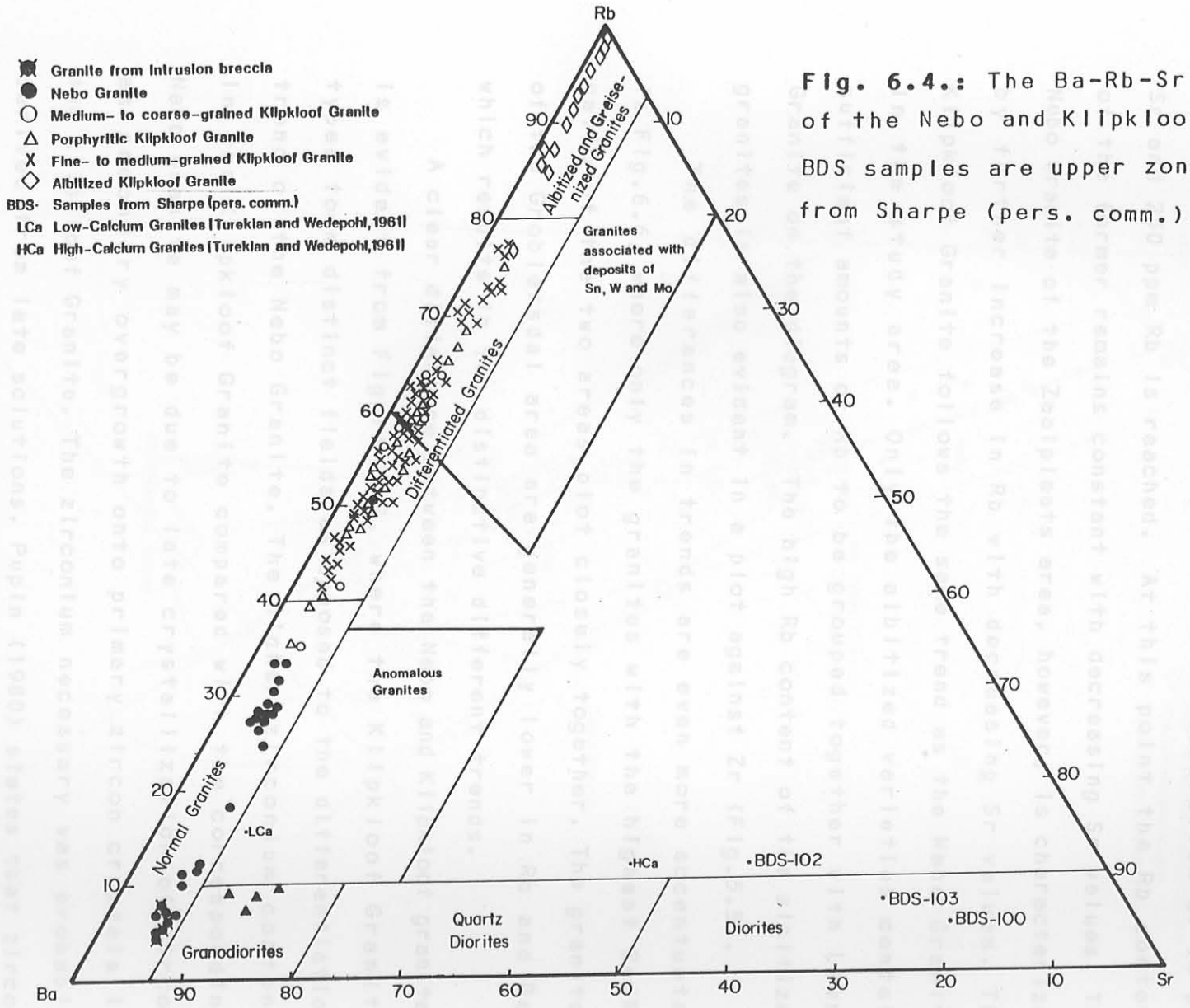

Fig. 6.4.: The Ba-Rb-Sr distribution of the Nebo and Klipkloof Granite. BDS samples are upper zone diorites from Sharpe (pers. comm.).

fractional crystallization of melt "B". The line "melt composition" connects the compositions of the equilibrium melts.

From Figure 6.5 it is evident that the Nebo Granite of the study area follows the same trend as its counterpart from the Zaaiplaats area, until a concentration of 30 ppm Sr and 250 ppm Rb is reached. At this point the Rb content of the former remains constant with decreasing Sr values. The Nebo Granite of the Zaaiplaats area, however, is characterized by further increase in Rb with decreasing Sr values. The Klipkloof Granite follows the same trend as the Nebo Granite in the study area. Only the albitized varieties contain sufficient amounts of Rb to be grouped together with Lease Granite on the diagram. The high Rb content of the albitized granites is also evident in a plot against Zr (Fig.5.5).

The differences in trends are even more accentuated in Fig.6.6, where only the granites with the highest Ba/Rb ratio of the two areas plot closely together. The granites of the Groblersdal area are generally lower in Rb and Ba, which results in two distinctive different trends.

A clear difference between the Nebo and Klipkloof granites is evident from Figure 6.7, where the Klipkloof Granite types form distinct fields as opposed to the differentiation trend of the Nebo Granite. The higher zirconium content in the Klipkloof Granite compared with the corresponding Nebo Granite may be due to late crystallization of zircon as secondary overgrowth onto primary zircon crystals in the Klipkloof Granite. The zirconium necessary was probably derived from late solutions. Pupin (1980) states that zircon growth is possible in the hydrothermal stage.

The Nb concentration of the Nebo Granite remains constant with differentiation as opposed to the Klipkloof Granite, which shows some enrichment, with values of up to 85 ppm (Appendix 3).

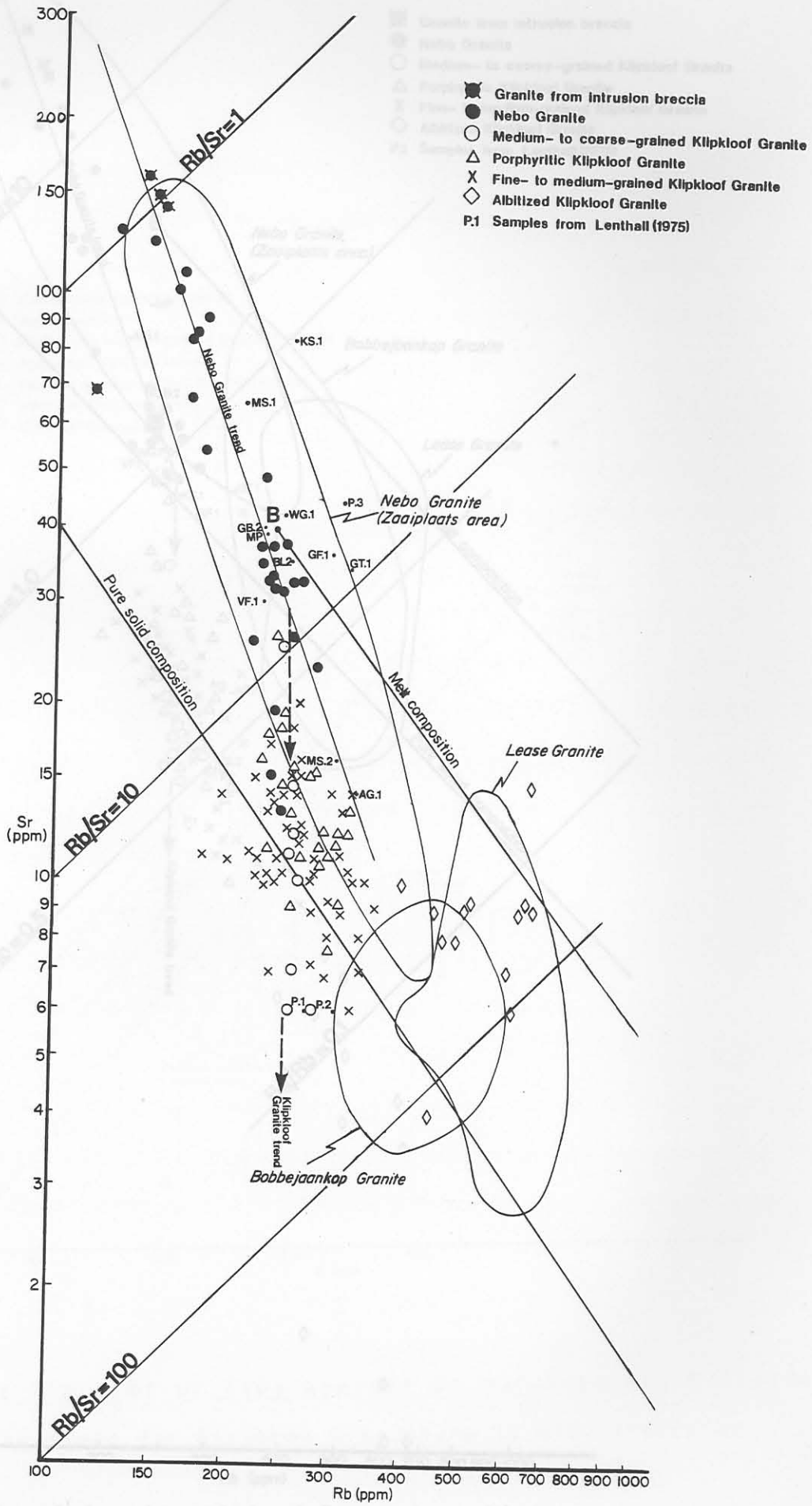

Fig. 6.5.: A log-log plot of Sr against Rb for Nebo and Klipkloof Granite.

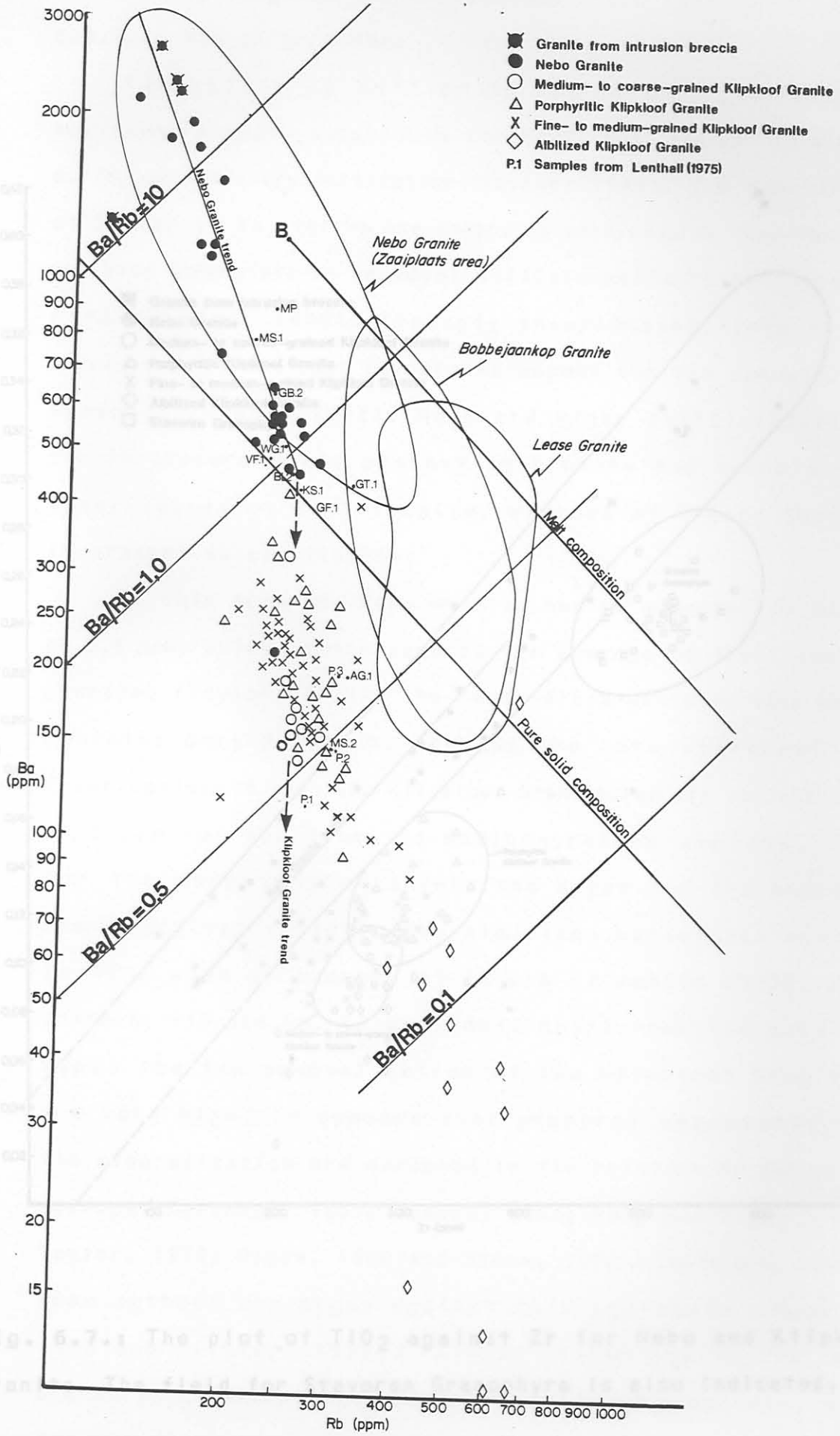

Fig. 6.6.: A log-log plot of Ba against Rb for Nebo and Klipkloof Granite.

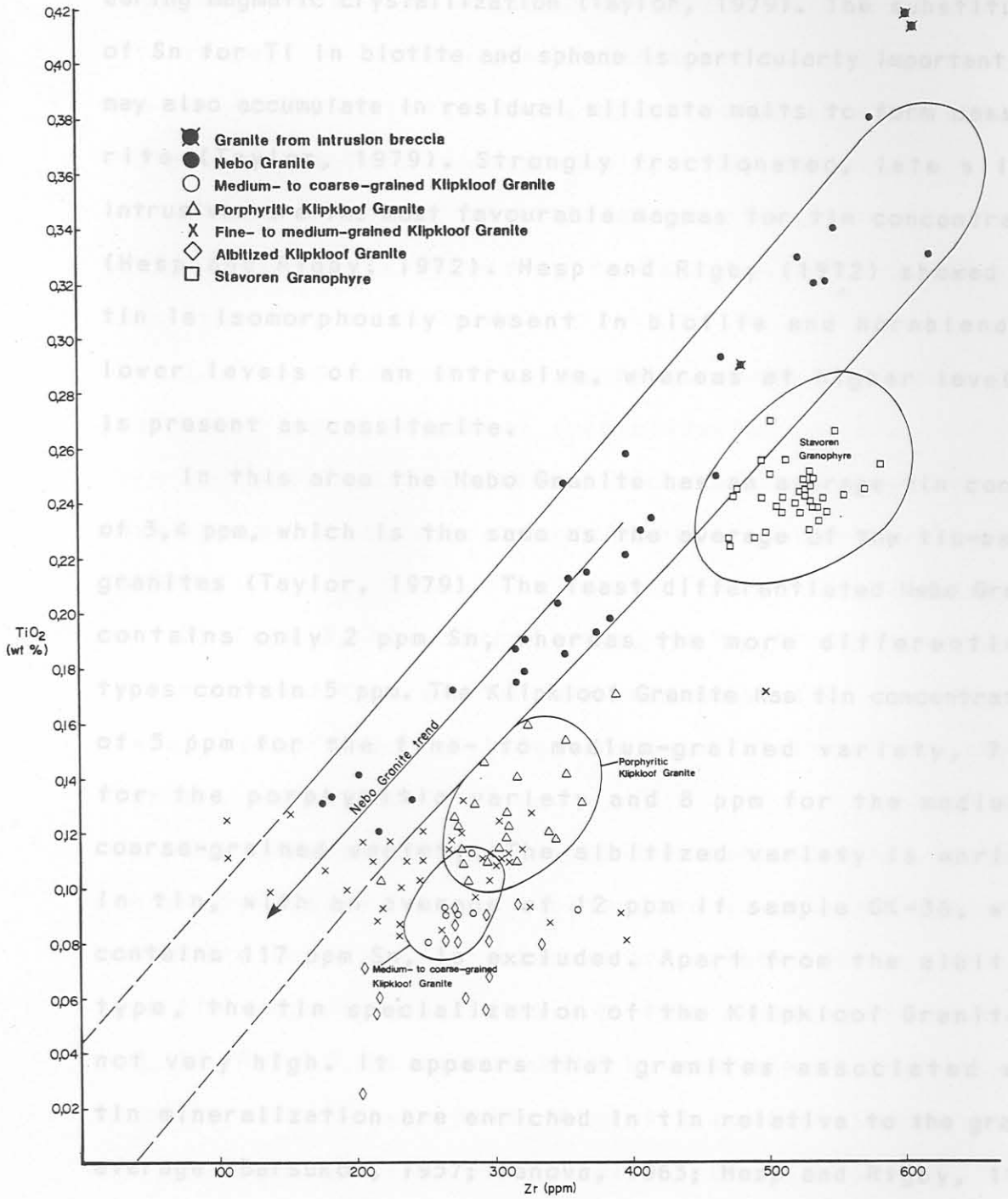

Fig. 6.7.: The plot of TiO_2 against Zr for Nebo and Klipkloof Granite. The field for Stavoren Granophyre is also indicated.

6.3.2. Tin, Tungsten and Molybdenum.

6.3.2.1. Tin in granites.

Tin exists as Sn^{4+} or in the form of complexes and may isomorphously substitute for Fe^{3+}, Mg^{2+} and Li^{+} in minerals during magmatic crystallization (Taylor, 1979). The substitution of Sn for Ti in biotite and sphene is particularly important. Tin may also accumulate in residual silicate melts to form cassiterite (Taylor, 1979). Strongly fractionated, late silicic intrusives are the most favourable magmas for tin concentration (Hesp and Rigby, 1972). Hesp and Rigby (1972) showed that tin is isomorphously present in biotite and hornblende at lower levels of an intrusive, whereas at higher levels it is present as cassiterite.

In this area the Nebo Granite has an average tin content of 3,4 ppm, which is the same as the average of the tin-barren granites (Taylor, 1979). The least differentiated Nebo Granite contains only 2 ppm Sn, whereas the more differentiated types contain 5 ppm. The Klipkloof Granite has tin concentrations of 5 ppm for the fine- to medium-grained variety, 7 ppm for the porphyritic variety and 8 ppm for the medium-to coarse-grained variety. The albitized variety is enriched in tin, with an average of 12 ppm if sample GK-36, which contains 117 ppm Sn, is excluded. Apart from the albitized type, the tin specialization of the Klipkloof Granite is not very high. It appears that granites associated with tin mineralization are enriched in tin relative to the granite average (Barsukov, 1957; Ianova, 1963; Hesp and Rigby, 1975; Taylor, 1979; Olade, 1980 and Stone, 1982). There are, however, some authors who argue against this statement (Hosking, 1968 and Flinter, 1971). Taylor (1979) states that there are very few examples of highly specialized granitoids which are not directly or indirectly associated with tin deposits. Hosking (1968), however, claims that there is no connection

between the tin content of a granite and possible mineralization. Flinter (1971), Hesp (1971) and Flinter et al. (1972) also state that the tin content of a granitoid has no bearing on the presence of mineralization. There is therefore a possibility that a granitoid which is not specialized with respect to tin can contain economic tin mineralization. Hunter (1973) states that, under favourable conditions, any granite is capable of producing a tin deposit.

Different types of tin distribution and concentration mechanisms exist. According to Taylor (1979, p 102) five such types may be defined:

1) The differentiation type, where the later phase granitoids show geochemical specialization for tin.

2) Type 2 occurs where tin content commences at a high level in more basic granitoids and then declines in acid rocks.

3) Type 3, the barren type, is typified by a decline in tin content towards the more acid members of an intrusive, where none of the granitoids are associated with tin concentration.

4) A complexity in trace element concentration is represented by Type 4, where a batholith has some intrusives which are specialized, whereas others are barren, but still have tin deposits associated with them (Hosking, 1968).

5) Type 5 is represented by the tin distribution in alkaline massifs, where the high tin content is due to the tin holding capacity of the alkaline rich minerals.

The tin specialization of a granitoid may be tested in many different ways, which include geochemical, mineralogical and petrological methods. According to Van de Pijpekamp (1982) the only tool necessary to establish the tin potential of a granitoid is the petrographic microscope. Later detailed geochemical surveys are performed on selected target areas. He

used the alteration of the rock to arrive at the "petrographical score", which is the sum of the different observations including texture, structure and newly formed minerals. A high petrographical score would therefore indicate the possible tin potential of a granitoid.

Following Van de Pijpekamp (1982), the Klipkloof Granite, especially the albitized variety, has a high petrographic score, because it contains newly formed minerals like chlorite, inclusions of fluorite in biotite and albitized perthite grains.

Flinter et al. (1972) used the Thornton-Tuttle D.I., the colour index (C.I) and the petrological index (P.I.) to identify a possible tin specialized granite. The color index represents the sum of the hornblende and biotite in the sample. The petrological index uses the initial letter of each of the granite constituents, viz. biotite and hornblende. If, for instance, the granite contains accessory biotite (<4 percent), it is a bxxx type. If it contains essential hornblende and accessory biotite, it is a Hbxxx type. Tin mineralization occurs in granitic rocks with D.I.> 85 and P.I.< 4 and a low color index.

Using major element data (D.I. and ternary diagrams) and petrographical data (C.I., petrographical score and P.I.) it appears that the Klipkloof Granite and the differentiated parts of the Nebo Granite may be specialized with respect to tin.

Sattran and Klominsky (1970), Hesp and Rigby (1974), Smith and Turek (1976) and Biste (1979) used the Köhler-Raaz indices (Köhler and Raaz, 1951) to investigate the tin specialization of a granite. According to these authors a tin-granite has Köhler- Raaz indices of +qz= 60 to 70, F= 20 to 30 and fm= 5 to 15, where +qz is free Si occurring as quartz, F is Na, K and Ca content in feldspars and fm is femic cations

and Ca in micas, pyroxenes and amphiboles. For the calculation of the indices, see Köhler and Raaz (1951) and Hesp and Rigby (1974).

If the Nebo and Klipkloof Granite are plotted on the diagram of Köhler and Raaz (1951) (Fig.6.8), it is evident that the Klipkloof Granite and the differentiated Nebo Granite qualify as tin granites.

Juniper and Kleeman (1979) found that Sn-mineralizing granites form compact groups, distinct from granites not associated with mineralization, when plotted on the ternary diagrams of SiO_2 - CaO+MgO+FeO - $Na_2O+K_2O+Al_2O_3$, Na+K - Fe - Mg, and Ca - Na - K. The field of U-mineralizing granites was introduced by Wilson and Akerblom (1982). It is evident from Figure 6.9, 6.10 and 6.11 that the granites of the Groblersdal area overlap with the fields of U- and Sn-mineralizing granites, with the exception of the least differentiated Nebo Granite.

According to several authors (Stemprok, 1970; Tauson and Kozlov, 1973; Smith and Turek, 1976; Haapala, 1977; Tischendorf, 1977; Taylor, 1979; Biste, 1979; Olade, 1980 and Yeates et al. 1982), tin-granites usually contain anomalous amounts of the trace elements Sn,F,Cl,Li,B,Rb,Nb,Th,U,REE and Cs, and are depleted in Ba, Sr and Zr. The U and Th concentrations in Klipkloof Granite are about three to four times higher than the granite average of Yeates et al. (1982), who found values of 4,8 and 17 ppm U and Th respectively to be typical. According to Yeates et al. (1982) high U (greater than 8 ppm) and Th values are normally accompanied by high Sn concentrations and mineralization may be present.

The Ba/Rb ratio has been recommended as the best indicator of mineralization (Tauson and Kozlov, 1973). The ratio is up to 80 times lower in ore bearing granites compared to the barren granites. Because of the low Ba content of albitized

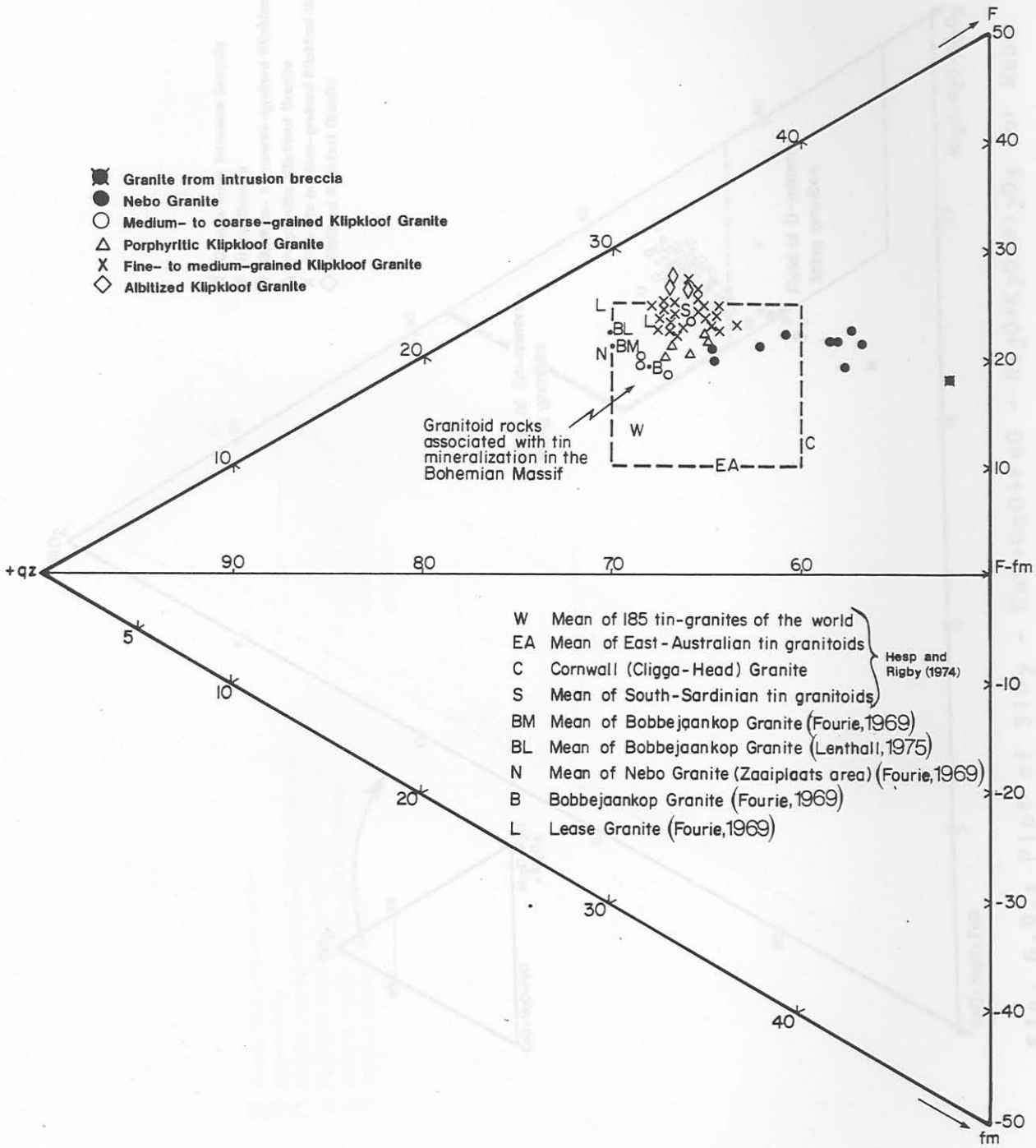

Fig. 6.8.: The Köhler-Raaz diagram indicating the tin specialization of the Bushveld granites.

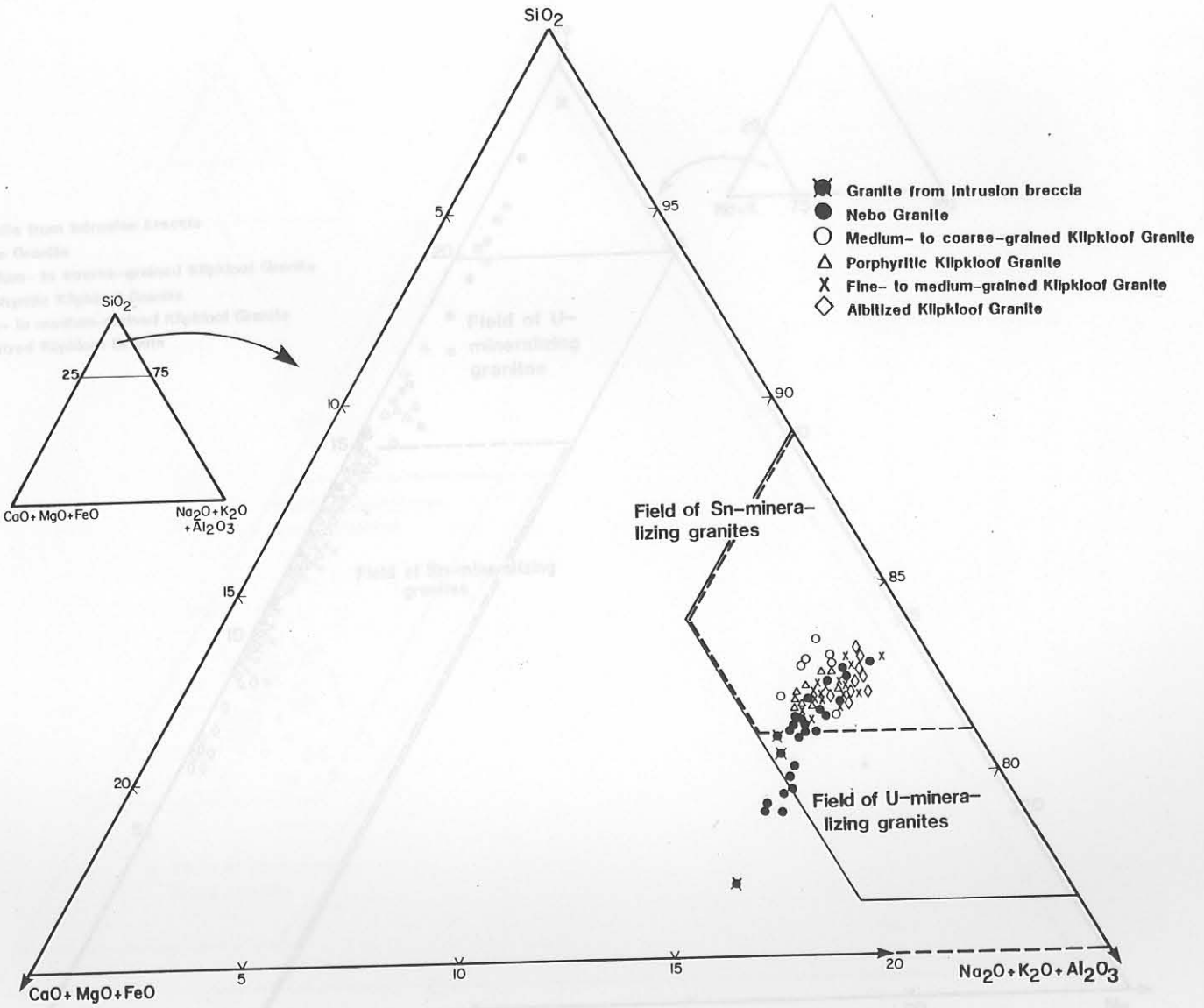

Fig. 6.9.: Plot of SiO_2 - $CaO+MgO+FeO$ - $Na_2O+K_2O+Al_2O_3$ for Nebo and Klipkloof Granite.

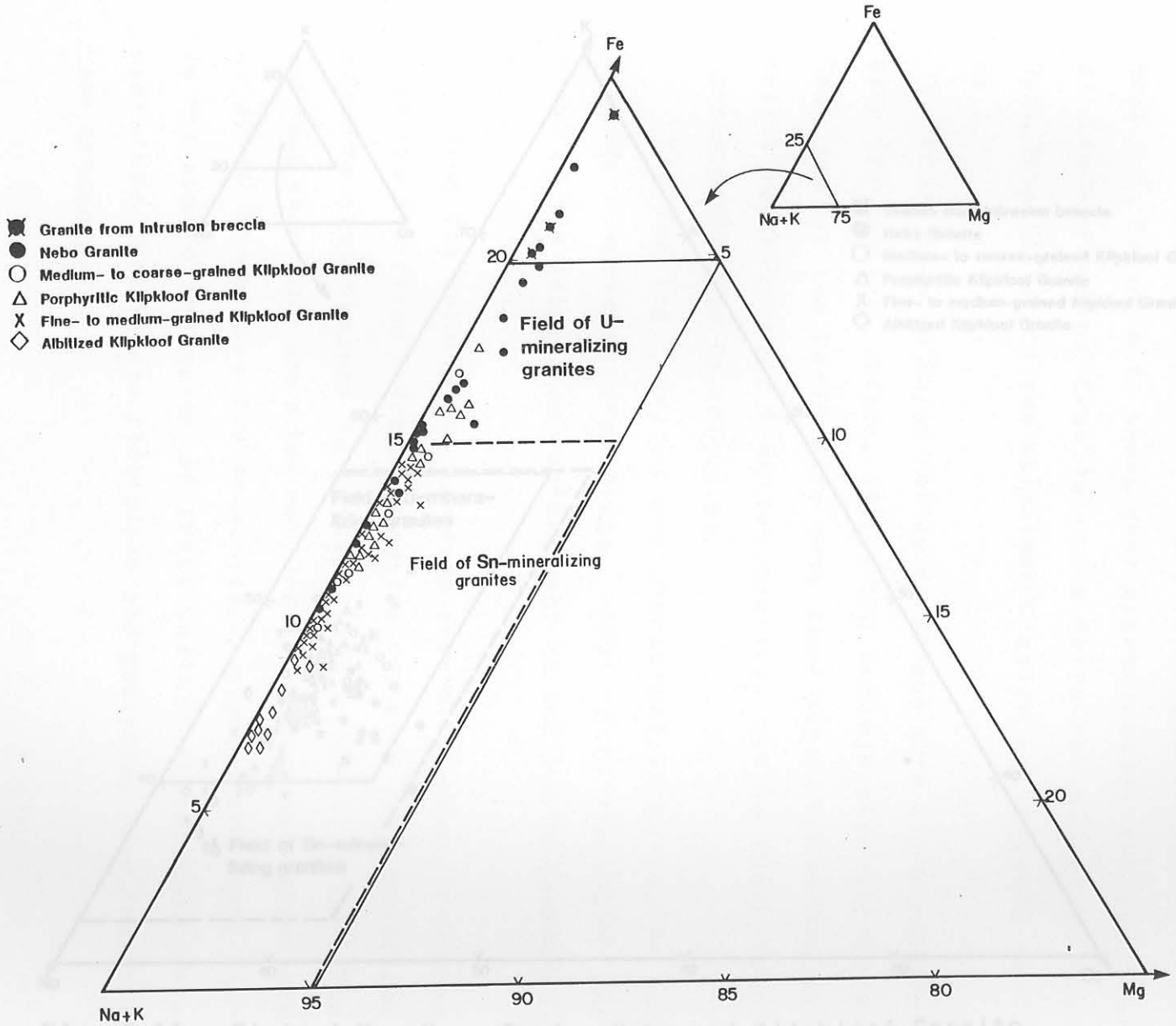

Fig. 6.10.: Plot of Fe - Na+K - Mg for Nebo and Klipkloof Granite.

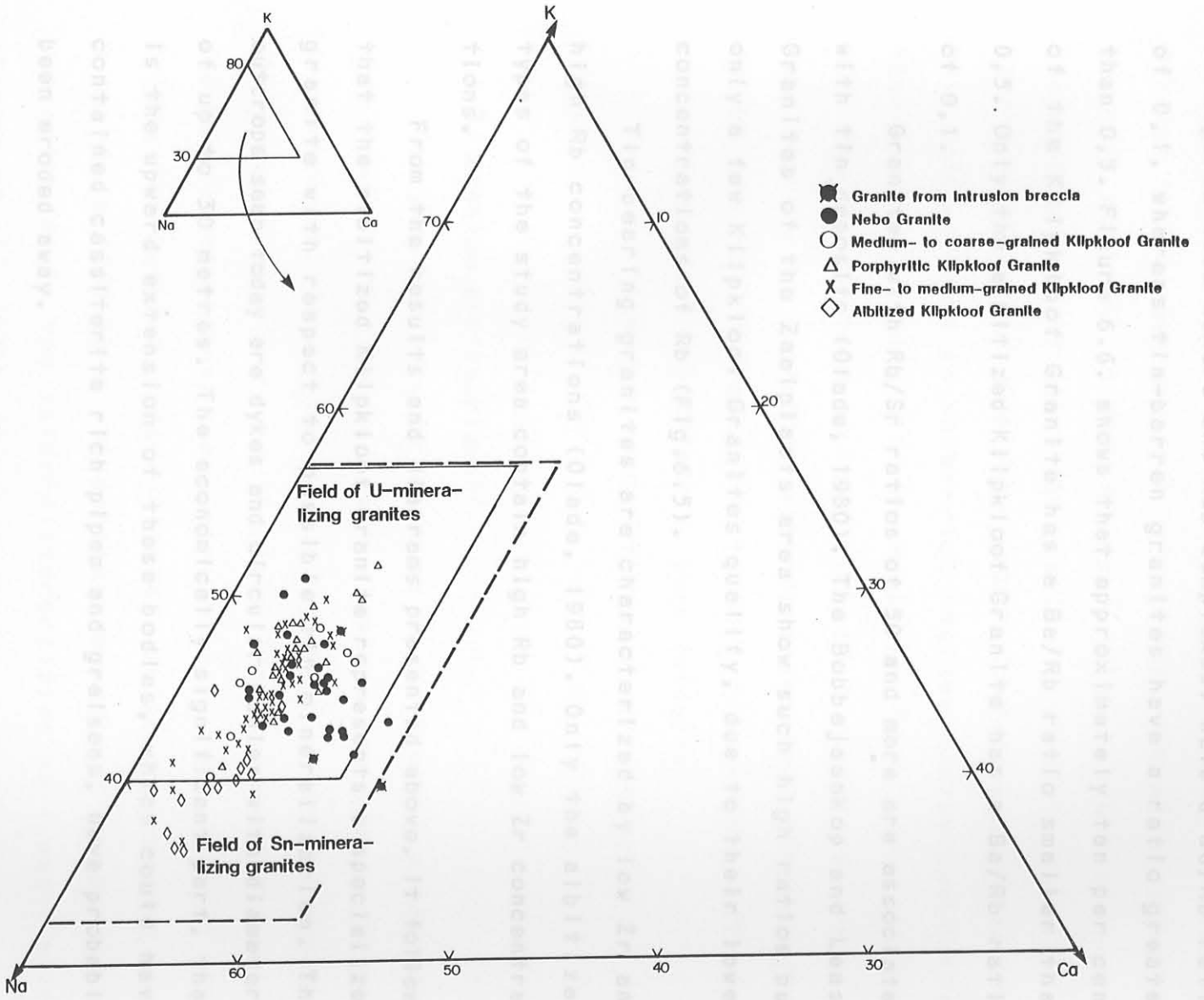

Fig. 6.11.: Plot of K - Na - Ca for Nebo and Klipkloof Granite.

and fine- to medium-grained Klipkloof Granite, the ratio is about 100 times lower than those of undifferentiated Nebo Granite. According to Olade (1980), tin-bearing granites of Nigeria (Jos Bukuru and Rob complexes) have a Ba/Rb ratio of 0,1, whereas tin-barren granites have a ratio greater than 0,5. Figure 6.6. shows that approximately ten per cent of the Klipkloof Granite has a Ba/Rb ratio smaller than 0,5. Only the albitized Klipkloof Granite has a Ba/Rb ratio of 0,1.

Granites with Rb/Sr ratios of 50 and more are associated with tin deposits (Olade, 1980). The Bobbejaankop and Lease Granites of the Zaaiplaats area show such high ratios but only a few Klipkloof Granites qualify, due to their lower concentrations of Rb (Fig.6.5).

Tin-bearing granites are characterized by low Zr and high Rb concentrations (Olade, 1980). Only the albitized types of the study area contain high Rb and low Zr concentrations.

From the results and diagrams presented above, it follows that the albitized Klipkloof Granite represents a specialized granite with respect to possible tin mineralization. The outcrops seen today are dykes and circular bodies with diameters of up to 30 metres. The economically significant part, that is the upward extension of these bodies, which could have contained cassiterite rich pipes and greisens, have probably been eroded away.

6.3.2.2. Molybdenum and Tungsten.

The chemistry of Mo and W is similar. There is, however, a difference in geochemical behaviour of the two elements, as Mo, like Cu, is strongly chalcophile (Kuroda and Sandell, 1954). This behaviour accounts for flakes of molybdenite present in many samples of Klipkloof and differentiated

Nebo Granite.

Tungsten is only found in pegmatites or high-temperature quartz veins and seldom occurs in the granite itself (Wedepohl, 1969, 74-F-2). Ivanova (1969) noted in his work in eastern Siberia that normal granites in regions of W mineralization are not enriched in this element. High concentrations of tungsten only occur where the granite is directly associated with a W deposit. Wedepohl (1969, 74-F-1) postulates that W is concentrated in water-rich residual solutions rather than in crystallizing silicate minerals.

The Mo content of the Klipkloof and differentiated Nebo Granite is sporadic, with some samples containing up to 30 ppm Mo. The molybdenite occurrences are indicated on the geological map (Plate 1, back folder).

No significant W concentrations were recorded in the area.

6.3.3. Uranium and Thorium.

The geochemistry of uranium is intimately associated with that of thorium and both elements are stable in the 4+ valences. There is also a close relationship between the crystal chemistry of thorium, uranium and zirconium and many isostructural compounds are known, e.g. $ZrSiO_4$-$ThSiO_4$-$USiO_4$ (Bayer, 1974). In the tetravalent form U is classified as a lithophile element and tends to be concentrated in the later differentiates of igneous melts (Rogers et al., 1978). It may be oxidized to the hexavalent state as the complex uranyl ion UO_2^{2+} which generally permits more extensive separation into fluid and volatile phases. This is not true in the case of Th, which cannot exist in the hexavalent state (Whitfield et al., 1959). The hexavalent U is more soluble than tetravalent Th, which explains the more rapid loss of U than Th in weathered surface samples.

The general increase of U and Th with differentiation is explained by their large size and high ionic charge, which prevents their entry into lattices of common rock-forming minerals. The Th/U ratio can either increase (Whitfield et al., 1959; Rogers and Ragland, 1961) or decrease (Larsen and Gottfried, 1961) depending on redox conditions and volatile content (Pagel, 1982). Investigations by Heier et al. (1966) have shown high Th/U ratios of greater than four to be typical of granitic rocks and ratios below three to be rare. According to them the oxidation of U^{4+} to U^{6+} is prevented if magmatic crystallization occurs in a system that is closed with respect to oxygen, in which case the Th/U ratio would stay constant throughout the crystallization history of a magma and could even decrease in strongly differentiated rocks. Most granite crystallization, however, takes place under oxidizing conditions with loss of the vapour phase (Heier and Brooks ,1966). If, however, the volatile phase of the granitic rest magma is retained during crystallization, a constant Th/U ratio would result, which would decrease in the last differentiates (Heier and Brooks, 1966).

Uranium and thorium may occur in several mineralogical settings:

1) Primary and important U- and Th-bearing minerals, such as uraninite and thorite.
2) U and Th replacing other elements in common accessory minerals, such as monazite, allanite, zircon, sphene and apatite.
3) U- and Th-bearing minerals occuring as sub-microscopic inclusions in silicates and fluorite. U may occur as molecular or ionic disseminations, where it is not tightly held, because it can be extracted by weak acids in a short time (Larsen and Gottfried, 1961).

The uranium and thorium content of the Nebo Granite increases as the rocks become more differentiated in the upper part of the sheet (Fig.6.12). The Klipkloof Granite is characterized by high U and Th concentrations, compared to the granite average of 3,5 ppm U and 12 ppm Th.

The Th/U ratio of the Klipkloof Granite is generally lower than the ratio of the Nebo Granite (Fig.6.13). This is anomalous, because in most case studies of Th and U distribution in granites it has been found that the ratio increases in more differentiated rocks (Whitfield et al., 1959; Rogers and Ragland, 1961; Heier and Rogers, 1963; Rogers et al., 1978; Rye and Roy, 1978). This is considered to be due to a loss of U as a result of increasingly oxidising conditions during crystallization of the magma. In the form UO_2^{2+}, uranium is highly soluble and is normally lost with a volatile phase. Therefore the Th/U ratio increases as the melt evolves. The lower Th/U ratio of the Klipkloof Granite may be due to crystallization in a closed system and retention of the volatile phase. If this is the case, deposits of tin and copper together with the high U values should be present. Such deposits have not yet been found, except for the small molybdenite deposit on Varschwater 23JS and a pipe-like copper deposit in felsites, which may originate from the granites below, on Kwaggavoetpad 163JS.

According to Heier and Brooks (1966), abundance of tourmaline in highly differentiated granites is an indication that the magma retained its volatile phase. Tourmaline spheroids in the albitized granite may indicate the possibility of such a process.

Heier and Brooks (1966) concluded from their study of the Heemskirk Granite, West Tasmania, that the low Th/U ratio in highly differentiated rocks of a granite batholith is due to "immersion" of the highly differentiated granite

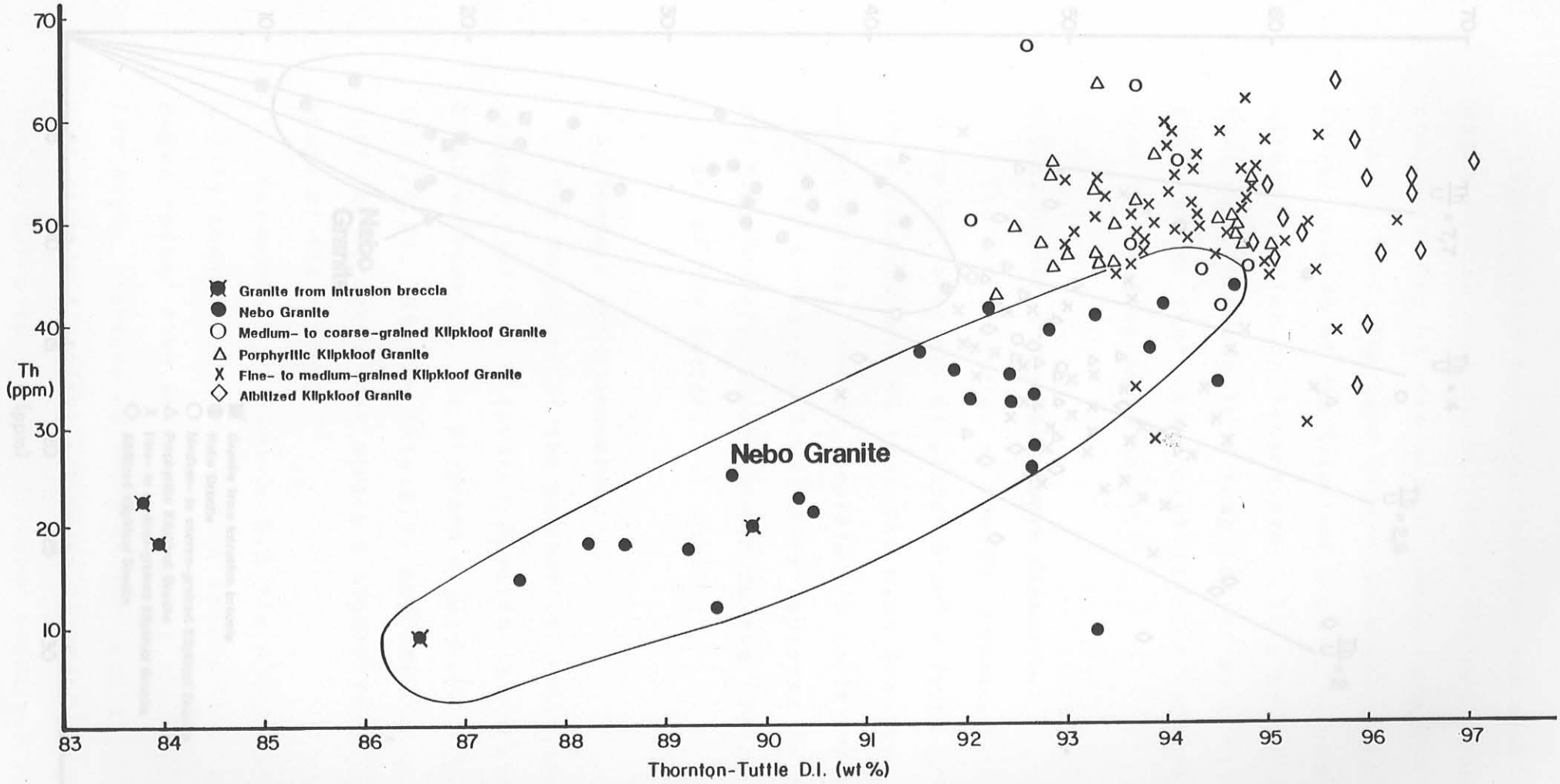

Fig. 6.12.: Plot of Th against the Thornton-Tuttle D.I. for Nebo and Klipkloof Granite.

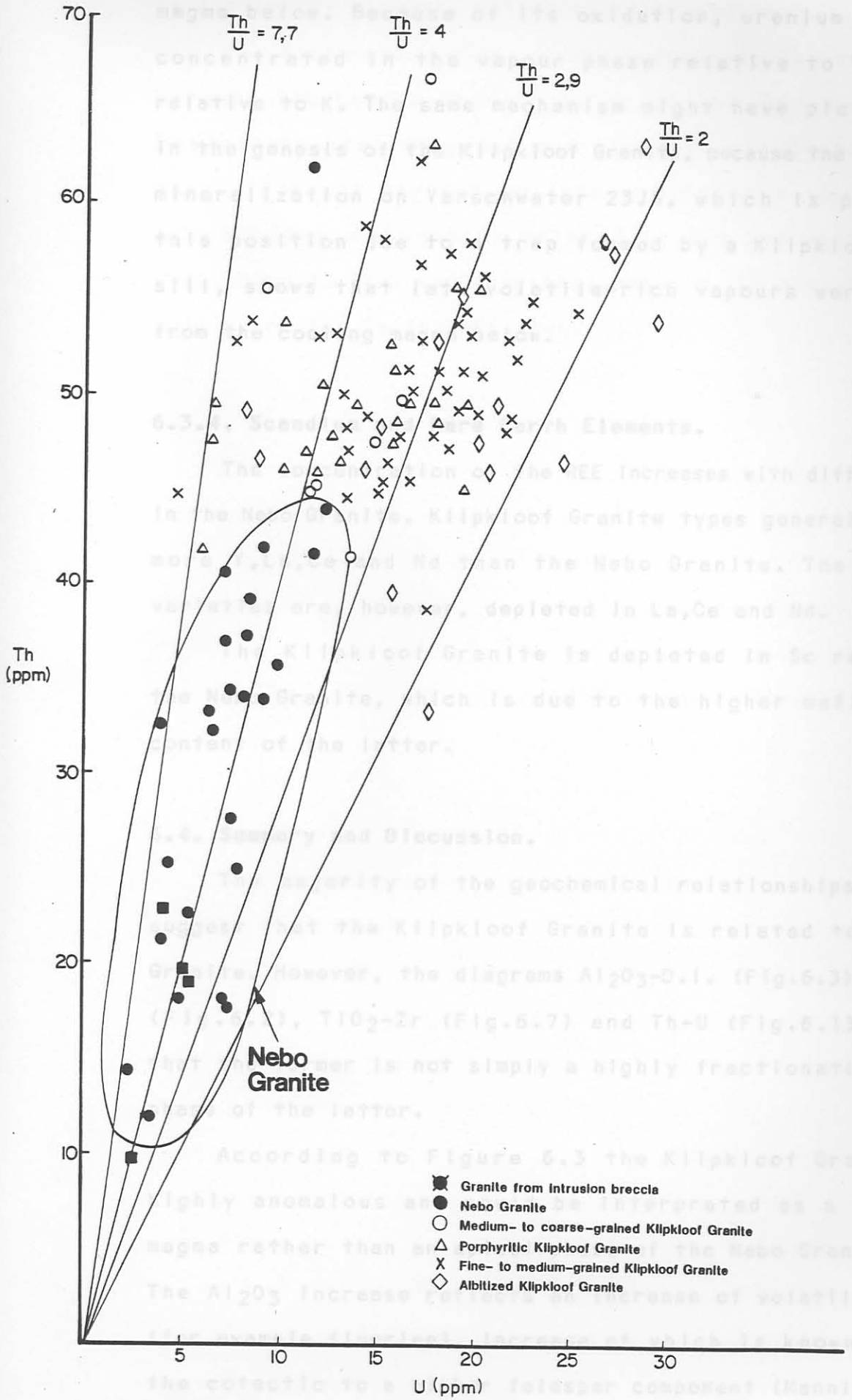

in vapour which has migrated from the slowly crystallizing magma below. Because of its oxidation, uranium should be concentrated in the vapour phase relative to Th, and Rb relative to K. The same mechanism might have played a role in the genesis of the Klipkloof Granite, because the molybdenite mineralization on Varschwater 23JS, which is present at this position due to a trap formed by a Klipkloof Granite sill, shows that late volatile-rich vapours were derived from the cooling magma below.

6.3.4. Scandium and Rare Earth Elements.

The concentration of the REE increases with differentiation in the Nebo Granite. Klipkloof Granite types generally contain more Y,La,Ce and Nd than the Nebo Granite. The albitized varieties are, however, depleted in La,Ce and Nd.

The Klipkloof Granite is depleted in Sc relative to the Nebo Granite, which is due to the higher mafic mineral content of the latter.

6.4. Summary and Discussion.

The majority of the geochemical relationships presented suggest that the Klipkloof Granite is related to the Nebo Granite. However, the diagrams Al_2O_3-D.I. (Fig.6.3), TiO_2-SiO_2 (Fig.6.2), TiO_2-Zr (Fig.6.7) and Th-U (Fig.6.13) suggest that the former is not simply a highly fractionated aplitic phase of the latter.

According to Figure 6.3 the Klipkloof Granites are highly anomalous and could be interpreted as a different magma rather than an apical phase of the Nebo Granite magma. The Al_2O_3 increase reflects an increase of volatile pressure (for example fluorine), increase of which is known to shift the cotectic to a higher feldspar component (Manning, 1981).

Taking Fig.6.2 and Fig.6.7 into account, the relationship

between Nebo and Klipkloof Granite is obscure, because it is not one of a simple differentiation sequence.

The difference in Ba, Sr and especially Rb concentration between the Lebowa Granite Suite of the Groblersdal and Zaaiplaats area (Fig.6.5 and Fig.6.6) points to the fact that different degrees of late metasomatic reaction and sub-solidus alteration existed in the two areas (Twist, pers. comm.). This could perhaps explain the high tin favourability of the Zaaiplaats area.

7. Evolution of the Bushveld granites.

7.1. Differentiation trends and mechanisms.

The geochemical study suggests that the Nebo Granite and the Klipkloof Granite are closely related and it appears that the latter is an apical phase of the former. Most of the variation diagrams presented indicate that the Klipkloof Granite forms an extension of the Nebo Granite differentiation trend although there are noteable differences in their TiO_2 and Al_2O_3 contents. The difference in TiO_2 values is probably due to the chloritization of biotite, whereas the higher Al_2O_3 values may have resulted from an increase in volatile pressure.

Post-magmatic changes have played a major role in the geochemical signature of the Klipkloof Granite. These include late hydrothermal alteration and albitization of the feldspars. Albitization had a major effect on the trace element geochemistry of the rock, wherein trace elements normally present in perthite (Ba) were lost in solution.

The granites of the Groblersdal area are not as altered as the granites of the Zaaiplaats area, which is evident from Figure 6.5 and 6.6. The first differentiates of Nebo Granite in the two areas have the same composition. Only the later differentiates are different in the respect that the rubidium content is higher in the granites of the Zaaiplaats area. The albitized Klipkloof Granites have similar rubidium contents compared with the Lease Granite of the Zaaiplaats area. It is well known that a high degree of alteration took place at Zaaiplaats (Strydom, 1983 and Coetzee, 1984), which is also reflected in the tin mineralization in the area. The plots of Sr against Rb and Ba against Rb are therefore a good exploration tool, because an increase in rubidium due to late-stage alteration, could be associated with minerali-

zation. If, on the other hand, the rubidium content in the rocks remains constant after an initial increase during differentiation, the possibility for mineralization seems low. The Lebowa Granite Suite in the study area would therefore be unfavourable for tin mineralization because no increase in rubidium took place. Only the albitized Klipkloof Granite could have some potential, but it was mentioned earlier that the economically significant roof zone of this altered granite was lost by erosion.

The majority of the diagrams used indicate that the Lebowa Granite Suite, the Stavoren Granophyre and Rociberg Felsite could be related. Whether there is a definite comagmatic relationship, or whether the relationship is only due to the fact that these granitic rocks are derived from a common zone of source-region melting, is debateable.

7.2. The "A-type granite" characteristics of the Bushveld granites.

Many contributions to the classification of granitic rocks exist in the literature (e.g. Tuttle and Bowen, 1958; Streckeisen, 1973; Chappel and White, 1974; Hine et al., 1978; Ishihara, 1981; Collins et al., 1982; Lameyre and Bowden, 1982; White and Chappel, 1982).

If the properties of I-type, S-type (Chappel and White, 1974) and A-type (Collins et al., 1982) granites are compared with the properties of the Bushveld Granites it appears that the latter represent typical A-type granites.

The following properties of the granites of the Lebowa Granite Suite correspond to those of A-type granites (Collins et al., 1982):

1) The abundance of MgO is very low and the concentration of CaO in undifferentiated Nebo Granites is only 1,5 per cent. The fluorite content of the later

differentiates is generally high.

2) Concentrations of V,Ni,Co and Cr are low, whereas the content of highly charged elements, e.g. Nb,Ga,Y,REE,U and Th, are high (Fig.7.1).

3) The Ga/Al_2O_3 ratio is always high, especially in the Klipkloof Granite (Fig.7.2).

4) According to the Shand diagram (Fig.7.3) the composition of the Bushveld Granite varies between metaluminous and peralkaline. The proposed field of A-type granites coincides with a field defined by Loiselle and Wones (in press).

5) The magma was dry, as evidenced by late precipitation of amphibole and biotite.

6) The An content of plagioclase is low with values between An-10 and An-0,8 (Appendix 1).

7) High Zr content and peralkaline affinities.

8) CIPW normative alkali metasilicate or acmite (Appendix 2).

9) Bushveld Granites are hypersolvus granites.

It therefore appears that the Nebo and Klipkloof Granites have the same characteristics as the A-type granites of Collins et al. (1982). In particular, the high Ga content and Ga/Al_2O_3 ratio are in accordance with those of A-type granites.

The high Ga/Al_2O_3 ratios are considered by Collins et al. (1982) to be due to preferential retention of An-rich plagioclase in the source region during partial melting. The Ga-oxygen bond is longer than the Al-oxygen bond, which suggests that Ga will be slightly excluded relative to Al in earlier products of magmatic crystallization and will tend to concentrate in later products of differentiation and residual minerals (Burton, 1972). This explains why the Ga content increases in the Lebowa Granite Suite from

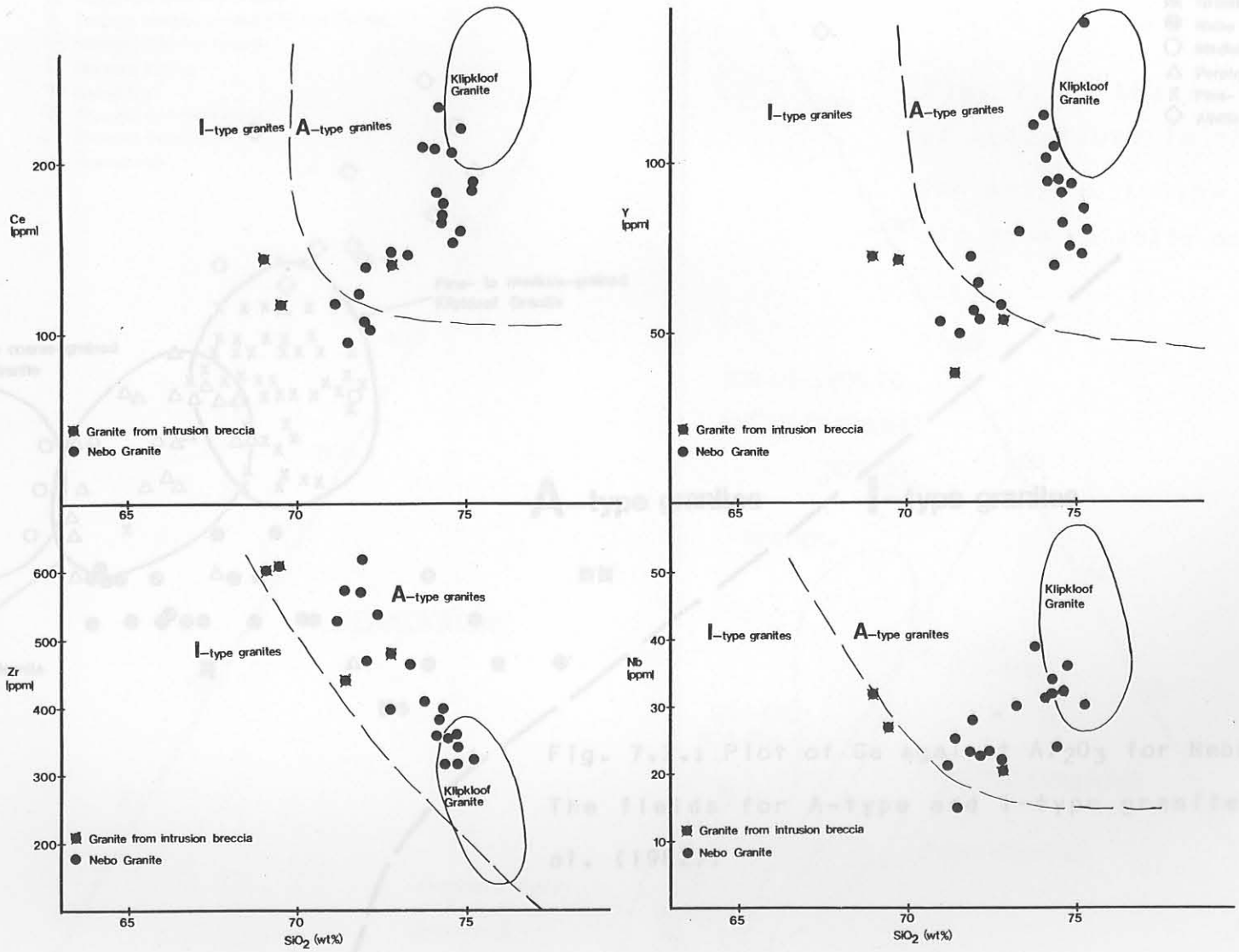

Fig. 7.1.: Harker diagrams for Ce, Y, Zr and Nb concentration in Nebo and Klipkloof Granite. The fields for A-type and I-type granites are from Collins et al. (1982).

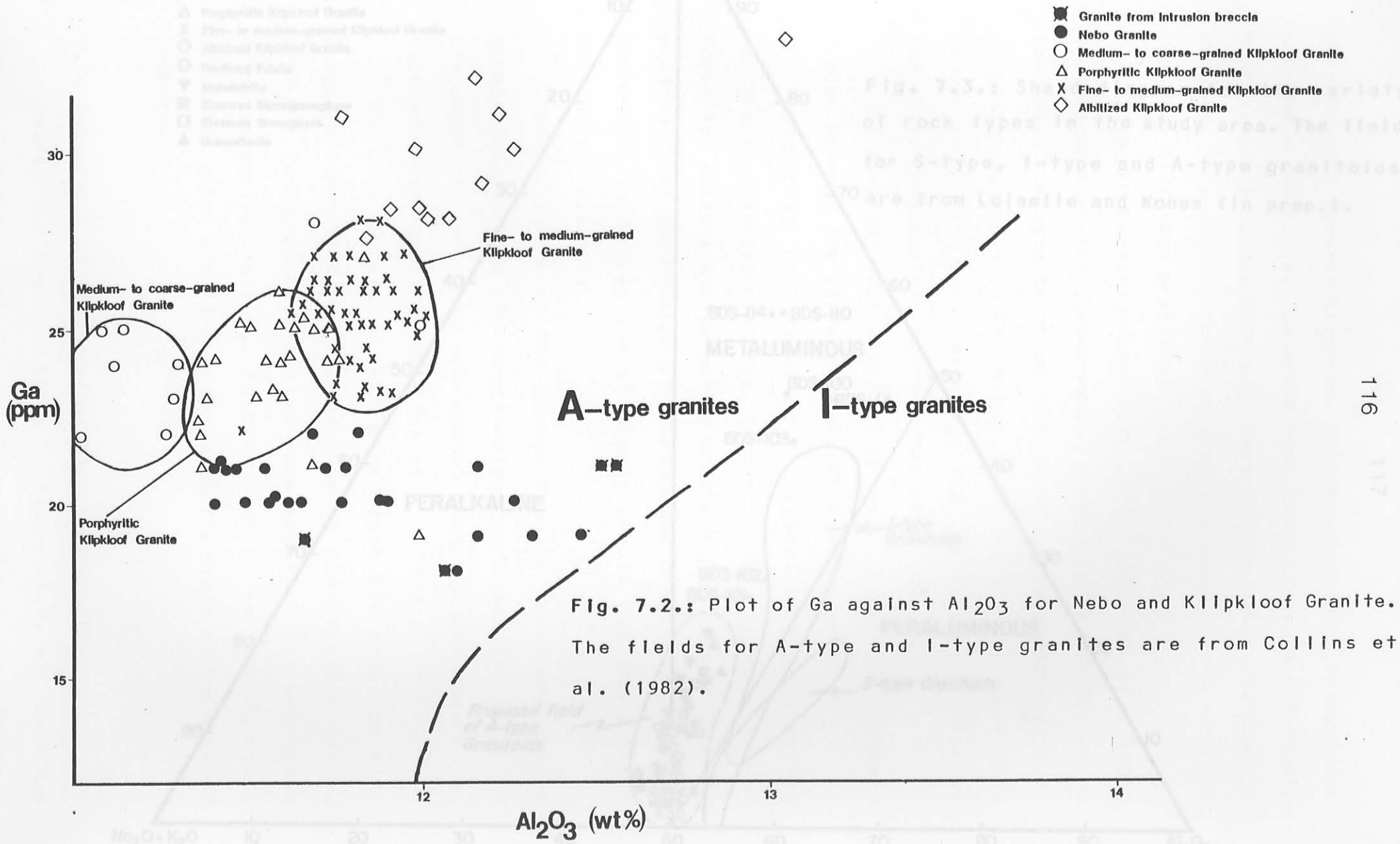

Fig. 7.2.: Plot of Ga against Al_2O_3 for Nebo and Klipkloof Granite. The fields for A-type and I-type granites are from Collins et al. (1982).

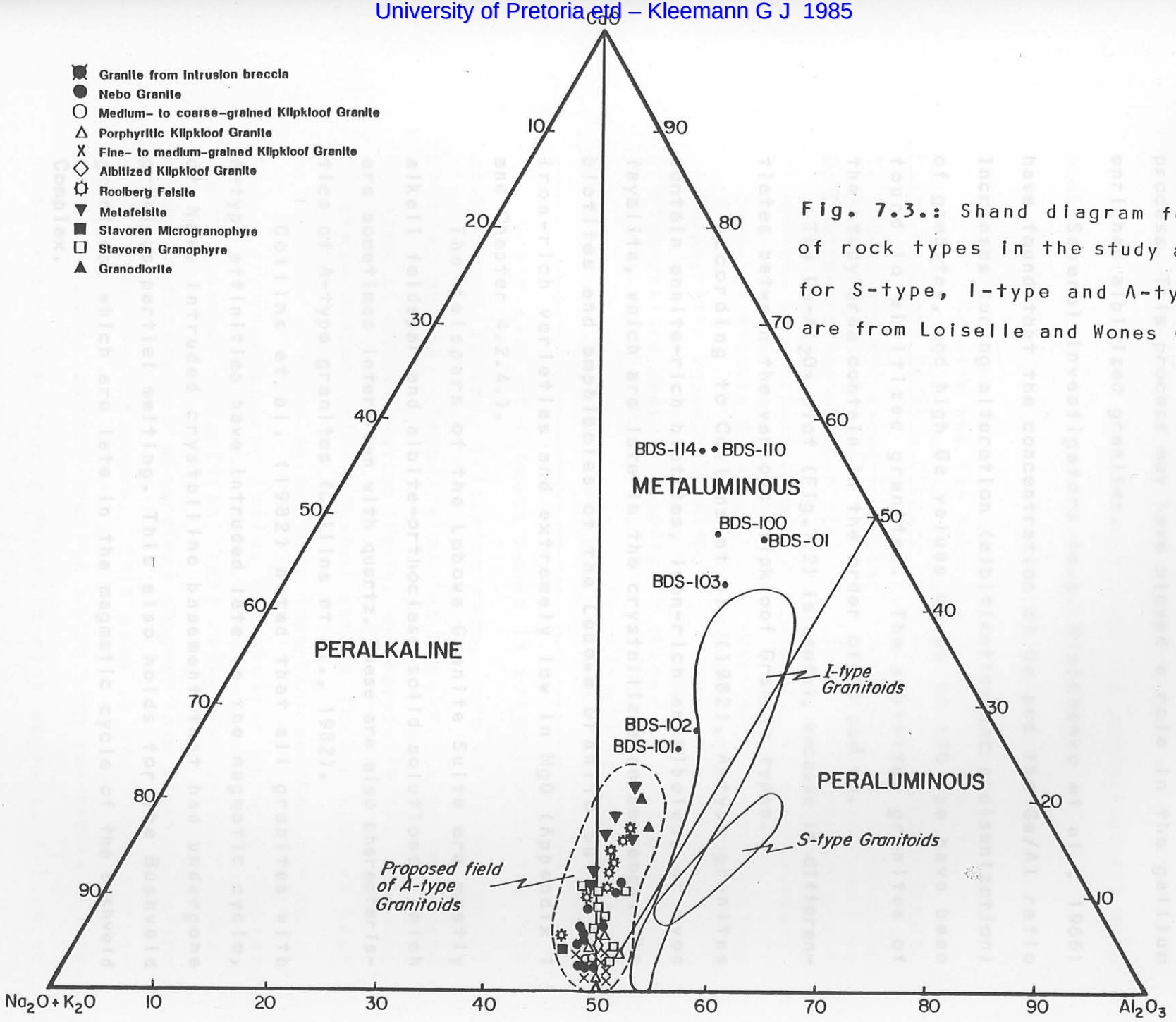

Fig. 7.3.: Shand diagram for the variety of rock types in the study area. The fields for S-type, I-type and A-type granitoids are from Loiselle and Wones (in prep.).

Nebo Granite towards Klipkloof Granite. According to Borisenok and Saukov (1960) gallium enrichment takes place in situations where volatile components were important in the crystallization process. This process may have played a role in the gallium enriched albitized granites.

Several investigators (e.g. Mishchenko et al., 1966) have found that the concentration of Ga and the Ga/Al ratio increases during alteration (albitization and greisenization) of granites, and high Ga values of up to 170 ppm have been found in albitized granites. The albitized granites of the study area contain in the order of 30 ppm Ga.

The Ga-Al_2O_3 plot (Fig.7.2) is useful, because it differentiates between the various Klipkloof Granite types.

According to Collins et al. (1982), A-type granites contain annite-rich biotites, iron-rich amphiboles, or even fayalite, which are late in the crystallization sequence. The biotites and amphiboles of the Lebowa Granite Suite are iron-rich varieties and extremely low in MgO (Appendix 1 and Chapter 4.2.4.).

The felspars of the Lebowa Granite Suite are mostly alkali feldspar and albite-orthoclase solid solutions, which are sometimes intergrown with quartz. These are also characteristics of A-type granites (Collins et al., 1982).

Collins et al. (1982) noted that all granites with A-type affinities have intruded late in the magmatic cycle, or have intruded crystalline basement that had undergone previous partial melting. This also holds for the Bushveld granites, which are late in the magmatic cycle of the Bushveld Complex.

7.3. The origin of fine-grained Klipkloof Granite.

Hawley and Wobus (1977), in their study of the Pikes Peak and Redskin Granites of Colorado, found a decrease

in grain size from the oldest to the youngest granite. Their classification bears close comparison to that of the granites of the study area (Table 7.1.). The Pikes Peak Granite is considered to represent an A-type granite suite (Collins et al., 1982) and the present study has shown that the Nebo Granite is also an A-type granite suite.

Table 7.1. Comparison between the Pikes Peak and Redskin Granite and the Nebo and Klipkloof Granite.

Pikes Peak and Redskin Granite	Nebo and Klipkloof Granite
1) Coarse-grained subequigranular Pikes Peak Granite.	Coarse-grained equigranular Nebo Granite in sheet-like body. Decrease in grain size from bottom to top in the granite sheet.
2) Coarse-grained porphyritic Pikes Peak Granite.	
3) Medium- to coarse-grained Pikes Peak Granite.	
4) Granular Redskin Granite.	Medium- to coarse-grained Klipkloof Granite.
5) Porphyritic Redskin Granite.	Porphyritic Klipkloof Granite.
6) Fine-grained Redskin Granite.	Fine- to medium-grained Klipkloof Granite consisting of sills and aplite dykes.
7) Granite aplite (Redskin).	

Grain size of igneous rocks is controlled by the rate of crystallization, diffusion rate, rate of formation of crystal nuclei, viscosity of the crystallizing magma and time-span of crystallization (Hawley and Wobus, 1977). According to these authors fine-grained border facies plutons show no evidence of chilling and more important neither the local fine- grained border facies nor similar interior facies are of quenched composition. They represent unusual rocks, whose chemistry and mineralogy suggest late crystallization from volatile-rich magma. This sums up the characteristics of the Klipkloof Granite which also represents a late phase crystalizing from a volatile-rich magma as evidenced by the high fluorite content, exploding bomb textures and the presence of tourmaline spheroids.

A commonly accepted view of the origin of fine-grained

granites involves rapid crystallization after emplacement and loss of volatiles. The process, as detailed by White (1940), involves a late-stage build up of volatiles, resulting in increased vapour pressure and finally boiling off of volatile constituents with associated heat loss and more rapid crystallization.

Following Jahns and Tuttle (1963) three mechanisms exist for the formation of igneous aplites, namely:

1) temperature quenching or chilling

2) pressure release quenching

and 3) compositional quenching.

Jahns and Tuttle (1963) believed that pressure release quenching was the probable mechanism for the formation of granite aplites. This involves loss of volatiles and may have occurred in the case of the Klipkloof Granite aplites due to pressure release along structural weaknesses (faults and cracks) formed during the cooling of the Nebo Granite magma.

Another hypothesis proposed by Hawley and Wobus (1977) involves the gradual decrease of grain size, affected by a gradual increase in viscosity caused by a complex relation of bulk and volatile element composition and hence temperature of crystallization. They plotted compositions of Pikes Peak and Redskin Granite on sections through the thermal minima at different water-vapor pressures. Figures 22 and 23 of Tuttle and Bowen (1958) were used to construct the diagram with a range of SiO_2-K+Na feldspar compositions on the x-axis and temperature on the y-axis (Fig.7.4.). Hawley and Wobus (1977) found that the granular Redskin Granite (corresponding to the medium- to coarse-grained Klipkloof Granite) has much more of a thermal minimum composition than does the coarse-grained Pikes Peak Granite (Nebo Granite).

Tuttle and Bowen (1958, p17) found that viscosity is

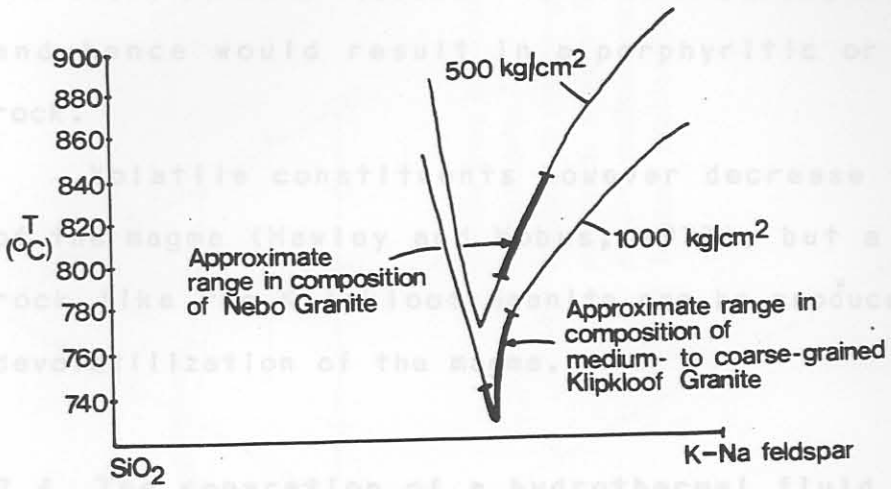

Fig. 7.4.: Compositions of Nebo and Klipkloof Granite plotted on sections through the thermal minimum at different water vapor pressures. Figures 22 and 23 of Tuttle and Bowen (1958) were used to construct the diagram.

related to ease of crystallization and that mixtures whose compositions lie along the Ab-Or sideline of the Qz-Ab-Or diagram (Fig.7.5) are the least viscous, whereas those compositions near the quartz-orthoclase eutectic and the ternary minimum are the most viscous. The Klipkloof Granite would therefore be more viscous than the Nebo Granite (Fig.7.5.) and hence would result in a porphyritic or fine-grained rock.

Volatile constituents however decrease the viscosity of the magma (Hawley and Wobus, 1977), but a fine-grained rock like the Klipkloof Granite can be produced by a sudden devolatilization of the magma.

7.4. The separation of a hydrothermal fluid from the Nebo Granite magma.

If aluminium is present in excess of that required to form Na- and K-feldspars, it occurs as corundum in the CIPW-norm. If, however, alkalis are in excess of that necessary to form Na- and K-feldspars, it occurs as acmite and/or alkali metasilicate in the CIPW-norm. From the CIPW-norm calculations (Appendix 2) it follows that no corundum is present in the granites of the study area, but that most of the samples contain CIPW normative acmite and/or alkali metasilicate. Tuttle and Bowen (1958, p89) concluded that a continous gradation from magma to hydrothermal solution exists if the alkali to aluminium ratio is such that crystallization results in concentration of alkali metasilicates. This is therefore taken as an indication that a hydrothermal fluid could have separated from the Nebo Granite magma.

7.5. Water content of the Nebo Granite magma.

It was concluded before that the Nebo Granite represents an A-type granite suite. According to Collins et al.(1982)

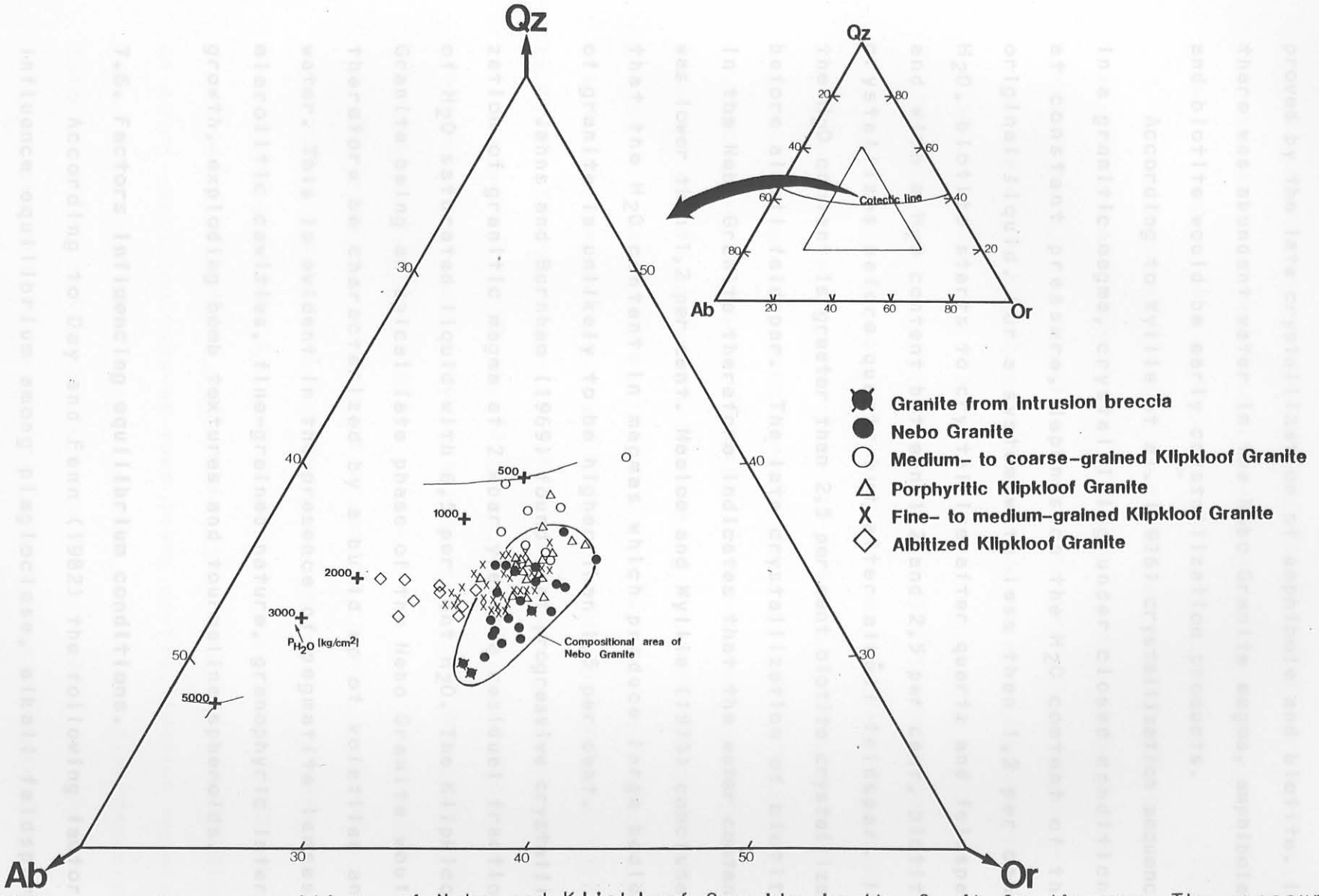

Fig. 7.5.: CIPW normative compositions of Nebo and Klipkloof Granite in the Qz-Ab-Or diagram. The pressures indicated are in kg/cm^2 and taken from Tuttle and Bowen (1958) and Luth, Jahns and Tuttle (1964).

A-type granite magmas are dry if not anhydrous, which is proved by the late crystallization of amphibole and biotite. If there was abundant water in the Nebo Granite magma, amphiboles and biotite would be early crystallization products.

According to Wyllie et al. (1976) crystallization sequence in a granitic magma, crystallizing under closed conditions at constant pressure, depends on the H_2O content of the original liquid. For a system with less than 1,2 per cent H_2O, biotite starts to crystallize after quartz and feldspar and with a H_2O content between 1,2 and 2,5 per cent, biotite crystallizes before quartz but after alkali feldspar. If the H_2O content is greater than 2,5 per cent biotite crystallizes before alkali feldspar. The late crystallization of biotite in the Nebo Granite therefore indicates that the water content was lower than 1,2 per cent. Maaloe and Wyllie (1975) concluded that the H_2O content in magmas which produce large bodies of granite is unlikely to be higher than 1,5 per cent.

Jahns and Burnham (1969) found that progressive crystallization of granitic magma at 2 kbar yields a residual fraction of H_2O saturated liquid with 6,5 per cent H_2O. The Klipkloof Granite being an apical late phase of the Nebo Granite would therefore be characterized by a build up of volatiles and water. This is evident in the presence of pegmatite lenses, miarolitic cavities, fine-grained nature, granophyric intergrowth, exploding bomb textures and tourmaline spheroids.

7.6. Factors influencing equilibrium conditions.

According to Day and Fenn (1982) the following factors influence equilibrium among plagioclase, alkali feldspar, quartz and water:

1) With increasing total pressure the two-feldspar liquidus boundary curve is shifted markedly towards more albite-rich compositions and therefore the composition field

of K-feldspar is expanded.

2) James and Hamilton (1969) found that increasing calcium in the liquid stabilizes plagioclase as the liquidus phase at the expense of K-feldspar.

3) Steiner et al. (1975) presented data which indicates that if the water content of liquids in the system Ab-Or-Q is decreased, the two-feldspar boundary curve moves so as to decrease the liquidus field of K-feldspar and stabilizing albite.

Fluorine (Bailey, 1977; Manning, 1981), rubidium (Glyuk et al., 1977) and boron (Chorlton and Martin, 1978) are capable of lowering the granite solidus by several hundred degrees centigrade. According to Manning (1981) the position of the quartz-alkali feldspar field boundary moves away from the quartz apex with increasing fluorine content. One per cent F lowers the minimum liquidus temperature of the fluorine-free system from 730°C (Tuttle and Bowen, 1958) to 690°C. With four per cent F the minimum liquidus temperature is lowered to 630°C. Addition of two per cent B_2O_3 lowers the minimum liquidus temperature from 730°C to about 650°C (Chorlton and Martin, 1978).

The combined effect of fluorine, boron, rubidium and other volatile elements would therefore lower the crystallization temperature of the Klipkloof Granite to about 550°C. The presence of tourmaline spheroids with a high concentration of boron would indicate an even lower crystallization temperature. Desborough et al. (1980) gave a crystallization temperature of 500°C and lower for the Redskin Granite, which has similar properties as the Klipkloof Granite (see Chapter 10.1).

Day and Fenn (1982) concluded that the Scituate Granite, a low Ca-granite, central Rhode Island, started to crystallize at a temperature of at least 750°C. The undifferentiated

low-Ca Nebo Granite has the same composition as the Scituate Granite on the Q-Ab-Or diagram with 3 per cent An (James and Hamilton, 1969). An initial liquidus temperature of about 800°C is therefore proposed for the Nebo Granite, with the solidus at a temperature of about 650 to 700°C.

7.7. Hypersolvus and subsolvus granites.

According to Tuttle (1952), hypersolvus granites represent water-poor magmas, whereas subsolvus granites represent water-rich magmas. He also points out that hypersolvus granites are poor in alumina, with diopside, acmite, wollastonite or alkali metasilicate in the CIPW norm and that subsolvus granites are enriched in alumina, which is represented by corundum in the CIPW norm.

Luth, Jahns and Tuttle (1964) found that hypersolvus granites plotted in the Ab-Or-Q diagram, cluster in the thermal valley leading from the isobaric minimum for low values of P_{H2O} (<0,5 kb) to the feldspar side line (the boundary separating the liquidus fields of Ab and Or), whereas subsolvus granites plot more closely to the isobaric minimum of the granite system. They further pointed out that occurrence of all plagioclase in perthite rather than as separate grains is evidence of development from a magma containing very limited amounts of water or other dissolved volatiles. According to Martin and Bonin (1976) granitic liquids will not yield a hypersolvus mineralogy at water pressures above 2,5 kbar.

The granites of the study area are hypersolvus, because they conform to all the criteria given above. The contents of plagioclase occurring as separate grains is low in the granites and the perthites are not cross-hatched microclines, which is characteristic of subsolvus granites (Martin and Bonin, 1976).

7.8. A model for the origin of Nebo and Klipkloof Granite.

Pitcher (1979) believes that plutons formed as great sheets are rather thin and emplaced forcefully. According to him the Main Donegal Granite, a sheet-like body, has a thickness of about four kilometres. According to Hyndman (1981) granitic magma must have been emplaced at a depth less than about 17 kilometres if breakdown of muscovite supplied all of its water, at less than 4 kilometres if biotite supplied the water, and at still shallower depths if hornblende supplied the water. Partial melting of a residual source containing F- and Cl-rich biotite and amphibole was suggested by Collins et al. (1982) for the production of A-type granite melts. Consequently the Nebo Granite was evidently generated by partial melting of a source that permitted emplacement at relatively shallow levels.

The Nebo Granite intruded under a cover sequence of Stavoren Granophyre, which in turn underlies Rooiberg felsites. After most of the Nebo Granite magma had crystallized, a late-stage volatile-rich liquid separated and crystallized to form the thin sill-like bodies of Klipkloof Granite in the upper part of the Nebo Granite. From Ba-Rb-Sr distribution it was concluded that the more differentiated sills occur at higher levels in the Nebo Granite. Late stage liquids from both the Nebo Granite and the Klipkloof Granite intruded into higher levels to form fine-grained Klipkloof Granite dykes. Some of these dykes had a high volatile and ore element content. Under an impermeable Klipkloof Granite sill or Stavoren Granophyre mineralization of the Varschwater type could occur (Fig.7.6).

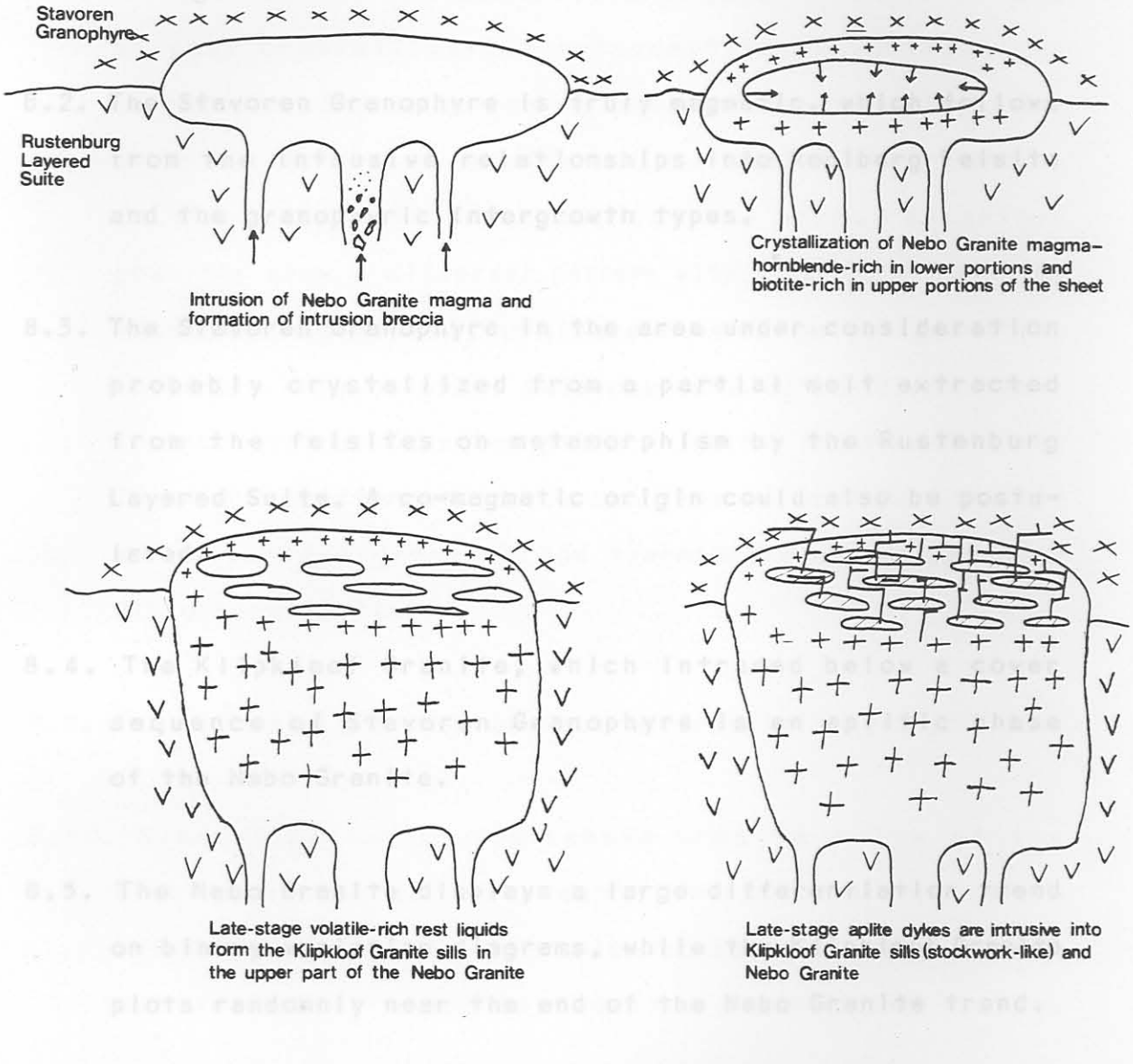

Fig. 7.6.: A model for the origin of Nebo and Klipkloof Granite.

8. Conclusions.

8.1. Flow-banding and agglomeratic textures in the metafelsites support their volcanic origin. Effects of metamorphism resulted in a variety of grain size and micrographic intergrowth.

8.2. The Stavoren Granophyre is truly magmatic, which follows from the intrusive relationships into Rooiberg Felsite and the granophyric intergrowth types.

8.3. The Stavoren Granophyre in the area under consideration probably crystallized from a partial melt extracted from the felsites on metamorphism by the Rustenburg Layered Suite. A co-magmatic origin could also be postulated.

8.4. The Klipkloof Granite, which intruded below a cover sequence of Stavoren Granophyre is an aplitic phase of the Nebo Granite.

8.5. The Nebo Granite displays a large differentiation trend on binary variation diagrams, while the Klipkloof Granite plots randomnly near the end of the Nebo Granite trend.

8.6. The relationship between the Nebo and Klipkloof Granites is not simple, which is obvious from some variation diagrams where the latter does not conform to the Nebo Granite trend. This is evidently caused by late-stage alteration of the Klipkloof Granite.

8.7. Trace element data indicates that the Klipkloof Granite is highly differentiated and therefore a possible target

for tin mineralization. No tin mineralization is, however, present in the Klipkloof Granite of this area, which is ascribed to the removal of the uppermost portions of the granite by erosion.

8.8. The granites of the Zaaiplaats area are characterized by post crystallization metasomatism, which resulted in the tin mineralization of the area (Coetzee, 1984). The albitized Klipkloof Granite has the same Rb-Ba-Sr pattern as the Zaaiplaats granites, but the normal Klipkloof granites show a different pattern with lower Rb values. The trend of the normal, unmineralized Klipkloof granites, which are only slightly metasomatized, appear to represent the normal fractionation pattern for the Bushveld Granite. These two different trends can thus be used to identify metasomatized granites and therefore areas of possible tin mineralization.

8.9. The Bushveld granites are characteristic A-type granites.

8.10. Mineralization in the Lebowa Granite Suite of the area occurs below impermeable Klipkloof Granite sills and is related to the intrusion of late Klipkloof Granite aplite dykes, which carried the ore-bearing fluids.

REFERENCES

Abbot, R.N., 1978. Peritectic reactions in the system An-Ab-Or-Qz-H_2O. Can. Min., 16, 245-256.

Bailey, J.C. 1977. Fluorine in granitic rocks and melts: A review. Chem. Geol., 19, 1-42.

Barker, D.S., 1971. Quartz- feldspar intergrowths: granophyre, myrmekite, and graphic granite. Unpuplished ms. In: Feldspar Minerals, J.V. Smith, Vol 2, Springer, Berlin. 690pp.

Barker, D.S., 1970. Compositions of granophyre, myrmekite and graphic granite. Bull. geol. Soc. Am., 81, 3339-3350.

Barsukov, V.L., 1957. The geochemistry of tin. Geochem. Int., 1, 41-51.

Bayer, G., 1974. Crystal chemistry of thorium -section 90A. In: Handbook of Geochemistry. Wedepohl, K.H. (Ed.). Springer.

Biste, M., 1979. Die Anwendung geochemischer Indikatoren auf die Zinn-Hoeffigkeit herzynischer Granite in Sued-Sardinien. Berl. Geowiss. Abh., 18, 1-109.

Borisenok, L.A. and Saukov, A.A., 1960. Geochemical cycle of gallium. Intern. Geol. Congr., 21st, Rept. Session, Norden Part 1,96.

Bowen, N.L., 1945. Phase equilibria bearing on the origin and differentiation of alkaline trends. Am. J. Sci., 243-A, 75-89.

Burton, J.D., 1972. In: Handbook of Geochemistry (31-D-1). Wedepohl, K.H. (Ed.), Springer.

Button, A., 1973. A regional study of the stratigraphy and development of the Transvaal basin in the eastern and southeastern Transvaal. Ph.D. thesis (unpubl.), Univ. of the Witwatersrand, 510pp.

Chappel, B.W. and White, A.J.R., 1974. Two contrasting granite types. Pacific Geology, 8, 173-174.

Chorlton, L.B. and Martin, R.F., 1978. The effect of boron on the granite solidus. Can. Min., 16, 239-244.

Clementson, I.M., 1979. Orientation rock and soil sampling survey over the molybdenite occurence on Varschwater 23JS. Rand Mines Report.

Clubley-Armstrong, A.R., 1977. The geology of the Selonsriver area, north of Middelburg, Transvaal, with special reference to the structure of the regions southeast of the Dennilton Dome. M.Sc. thesis (unpubl.) Univ. of Pretoria, 106pp.

Clubley-Armstrong, A.R. and Sharpe, M.R., 1979. The structural evolution of the Dennilton Dome and its relationship to the intrusion of the Bushveld Complex. Trans. geol. Soc. S. Afr., 82. 23-37.

Cocco, G., Fanfani, L. and Zanazzi, P.F., 1972. Rubidium section, Vol II/4, In: Handbook of Geochemistry, Wedepohl, K.H.(Editor), Springer.

Coetzee, J., 1984. A geochemical and petrological investigation of the low-grade tin deposits in the Bobbejaankop Granite at the Zaaiplaats tin mine. M.Sc. thesis (unpubl.), Univ. of Pretoria.

Collins, W.J., Beams, S.D., White, A.J.R. and Chappell, B.W., 1982. Nature and origin of A-type granites with particular reference to southeastern Australia. Contrib. Mineral. Petrol., 80, 189-200.

Crocker, I.T., Walraven, F. and Hammerbeck, E,C.I., 1977. Report on molybdenite mineralization on Varschwater 23JS, Nebo district. Geol. Surv. S. Afr., Report 32 (open file).

Dana, E.S., 1932. A textbook of mineralogy. Fourth Edition, revised and enlarged by W.E. Ford. John Wiley

and Sons. New York. 851pp.

Day, H.W. and Fenn, P.M., 1982. Estimating the P-T-X_{H2O} conditionsduring crystallization of low calcium granites. J.Geol., 90, 485-507.

Deer, W.A., Howie, R.A. and Zussman, J., 1962a. Rock forming minerals, volume 1 (ortho- and ring silicates). Longmans, Green, London, 333pp.

Degenhardt, H., 1957. Untersuchungen zur geochemischen Verteilung des Zirkoniums in der Lithosphaere. Geochim. Cosmochim. Acta. VII, 279.

Desborough, G.A., Ludington, S.D. and Sharp, W.N., 1980. Redskin Granite: a rare-metal-rich Precambrian pluton, Colorado, USA. Min. Mag., 43, 959-965.

Dietrich, R.V., 1962. Advanced study of feldspar. In Norsk Geologisk Tidsskrift Bind 42. Christie, OHJ (Red.), Oslo, Kopenhagen.

Durasova, N.A. and Barsukov, V.L., 1973. The behaviour of tin in liquating boron-bearing silicate melts. Geochem. Int., 10, 920-922.

El Bouseily, A.M. and El Sokkary A.A., 1975. The relation between Rb, Ba and Sr in granitic rocks. Chem. Geol.,16, 207-219.

Eugster, H.P. and Wones, D.R., 1962. Stability relations of the ferruginous biotite, annite. J. Petrol.,3, 82-125.

Flinter, B.H., 1971. Tin in acid granitoids: the search for a geochemical scheme for mineral exploration. In: Geochemical Exploration. Can. Inst. Min., Spec. Vol.,11, 323-330.

Flinter, B.H., Hesp, W.R. and Rigby, D., 1972. Selected geochemical, mineralogical and petrological features of granitoids of the New England Complex, Australia, and their relation to Sn, W, Mo and Cu mineralization.

Econ. Geol.,67, 1241-1262.

Fourie, P.J., 1969. Die geochemie van granitiese gesteentes van die Bosveldstollingskompleks. D.Sc. thesis (unpubl.), Univ. of Pretoria, 289pp.

Gain, S.B., 1979. Report on a geological and geochemical survey on the farms Varschwater 23JS, Tafelkop 120JS, Tussenin 21JS, Mooiplaats 121JS and Boekenhoutkloof 124JS. Mining Corporation Report.

Glyuk, D.S., Bazarova, S.B. and Trufanova, L.G., 1977. Ezhegodnik Sibirsk Inst Geochim. (yearbook Siberian Inst. Geochem. for 1976), 170-175.

Groves, D.I. and McCarthy, T.S., 1978. Fractional crystallization and the origin of tin in granitoids. Mineral. Dep.,13, 11-26.

Haapala, I., 1977. Petrography and geochemistry of the Eurajoki stock, a rapakivi-granite complex with greisen-type mineralization in south-western Finland. Finland. Geol. Survey. Bull.,286, 128pp.

Hahn-Weinheimer, P. and Ackermann, H., 1967. Geochemical investigation of differentiated granite plutons of the southern Black Forest II. The zoning of the Marlsburg Granite pluton as indicated by the elements titanium, zirconium, phosphorus, strontium, barium, rubidium, potassium and sodium. Geochim. Cosmochim. Acta.,31, 2197-2218.

Hall, A., 1967. The distribution of some major and trace elements in feldspars from the Rones and Ardra granite complexes, Donegal, Ireland. Geochim. Cosmochim. Acta.,31, 835-847.

Hall, A.L., 1913. The geology of the country southwest of Lydenburg. Geol. Surv. S. Afr., explanation of sheet no.11.

Hara, I., etal., 1980. Distribution patterns of quartz in

granites evidence of their high-temperature deformation during cooling. N. Jb. Min. Hh., 20-30.

Hattingh, P.J., 1977. Die struktuur van die Bosveldkompleks in die Groblersdal-Lydenburg-Belfast gebied soos afgelei uit 'n regionale gravitasie-opname. Inst. geol. Res. Bushveld Complex, Res. Rept. 8.

Hawley, C.C. and Wobus, R.A., 1977. General geology and petrology of the precambrian crystalline rocks, Park and Jefferson Counties, Colorado. U.S. Geol. Surv. Prof. Paper. 608-B, 73pp.

Heier, K.S. and Brooks, C., 1966. Geochemistry and genesis of the Heemskirk granite, West Tasmania. Geochim. Cosmochim. Acta. 30, 633-643.

Heier, K.S. and Rogers, J.J.W., 1963. Radiometric determination of thorium, uranium and potassiumin basalts and in two magmatic differentiation series. Geochim. Cosmochim. Acta. 27, 137-154.

Hesp, W.R., 1971. Correlations between the tin content of granitic rocks and their chemical and mineralogical composition. In: Geochemical Exploration. Can. Inst. Min.. Spec. Vol.11, 341-353.

Hesp, W.R. and Rigby, D., 1972. The transport of tin in acid igneous rocks. Pacific Geology.4, 135-152.

Hesp, W.R. and Rigby, D., 1974. Some geochemical aspects of of tin mineralization in the Tasman Geosincline. Mineral. Deposita.9, 49-60.

Hesp, W.R. and Rigby, D., 1975. Aspects of tin metallogenesis in the Tasman Geosincline, Eastern Australia, as reflected by cluster and factor analyses. Jnl. Geochem. Expl..4, 331-347.

Hine, R., Williams,I.S., Chappel, B.W. and White, A.J.R., 1978. Contrasts between I- and S-type granitoids of the Kosciusko Batholith. J. Geol. Soc. Aust..

25, 219-234.

Hosking, K.F.G., 1968. The relation between primary deposits and granitic rocks. In: A technical conference on tin, Fox, W. (editor), International tin council, Haymarket, London 1967, 267-311.

Hunter, D.R., 1973. The localization of tin mineralization with reference to South Africa. Minerals. Sci. Engng..5, 53-77.

Hyndman, D.W., 1981. Controls on source and depth of emplacement of granitic magma. Geology. 9, 244-249.

Ianova, G.F., 1963. Content of tin, tungsten and molybdenum in granites enclosing tin-tungsten deposits. Geochemistry.5, 492-500.

Ivanova, G.F., 1969. Conditions of formation of tungsten and molybdenum minerals in hydrothermal processes. Geokhimiya. 1969, 411-415.

Ishihara, S., 1981. The granitoid series and mineralization. Econ. Geol.. 75th Ann. Vol., 458-484.

James, R.S. and Hamilton, D.L., 1969. Phase relations in the system $NaAlSi_3O_8$-$KAlSi_3O_8$-$CaAl_2Si_2O_8$-SiO_2 at 1 kilobar water vapor pressure. Contr. Mineral. Petrol.. 21, 111-141.

Jahns, R.H. and Burnham, C.W., 1969. Experimental studies of pegmatite genesis: I. A model for the derivation and crystallization of granitic pegmatites. Econ. Geol.. 64, 843-864.

Jahns, R.H. and Tuttle, O.F., 1963. Origin of igneous aplites. Abstracts for 1962: Geol. Soc. Am. Spec. Paper. 73, 177-178.

Janardan Rao, Y., Murthy, I.S.N. and Sree Ramulu, C., 1973. Sphene coronites from Hyberabad Granites, Andhra Pradesh, India. Contr. Mineral. Petrol..41, 57-60.

Juniper, D.N. and Kleeman, J.D., 1979. Geochemical charac-

terization of some tin-mineralizing granites of New South Wales. J. Geochem. Explor., 11, 321-333.

Köhler, A. and Raaz, F., 1951. Ueber eine neue Berechnung und graphische Darstellung von Gesteinsanalysen. N. Jb. Min. Mh., 247-263.

Kolbe, P., 1966. Geochemical investigation of the Cape Granite, South-Western Cape Province, South Africa. Trans. geol. Soc. S. Afr., 69, 161.

Kolbe, P. and Taylor, S.R., 1966. Major and trace element relationships in granodiorites and granites from Australia and South Africa. Contrib. Mineral. Petrol., 12, 202-222.

Kuroda, P.K. and Sandell, E.B., 1954. Geochemistry of molybdenum. Geochim. Cosmochim. Acta., 6, 35-63.

Lameyre, J. and Bowden, P., 1982. Plutonic rock types series: discrimination of various granitoid series and related rocks. J. Volcanol. Geotherm. Res., 14, 169-186.

Larsen, E.S. and Gottfried, D., 1961. Distribution of uranium in rocks and minerals of Mesocoic batholiths in Western United States. U.S. geol. Surv. Bull., 1070-C, 63-102.

Leake, B.E., 1978. Nomenclature of amphiboles. Am. Mineral., 63, 1023-1052.

Lenthall, D.H., 1975. Aspects of the geochemistry of the acid phase of the central and eastern Bushveld Complex. Econ. Geol. Res. Unit., Univ Witwatersrand, Johannesburg, Info. Circ., 99, 20pp.

Lenthall, D.H. and Hunter, D.R., 1977. The geochemistry of the Bushveld Granites in the Potgietersrus tin-field. Prec. Res., 5, 359-400.

Loiselle, M.C. and Wones, D.R., (in prep). Characteristics and models for the origin of A-type granites.

Lombaard, B.V., 1932. The felsites and their relations in the Bushveld Complex. Trans. geol. Soc. S. Afr.,35, 125-190.

Lombaard, B.V., 1934. On the differentiation and relationships of the rocks of the Bushveld Complex. Trans. geol. Soc. S. Afr., 37.

Lombaard, A.F., 1949. Die geologie van die Bosveldkompleks langs Bloedrivier. Trans. geol. Soc. S. Afr., 52, 343-376.

Lombaard, B.V., 1932. The felsites and their relations in the Bushveld Complex. Trans. geol. Soc. S. Afr.,35, 125-190.

Luth, W.C., Jahns, R.H. and Tuttle, O.F., 1964. The granite system at pressures of 4 to 10 kilobars. J. Geophysical. Research. 69, 759-773.

MacCaskie, D.R., 1983. Differentiation of the Nebo Granite (Main Bushveld Granite), South Africa. Ph.D. thesis (unpubl.) Univ. of Oregon, 146pp.

Maaloe, S. and Wyllie, P.J., 1975. Water content of a granite magma deduced from the sequence of crystallization determined experimentally with water-undersaturated conditions. Contrib. Mineral. Petrol., 52, 175-191.

Manning, D.A.C., 1981. The effect of fluorine on the liquidus phase relationships in the system Qz-Ab-Or with excess water at 1 kb. Contrib. Mineral. Petrol., 76, 206-215.

Martin, R.F. and Bonin, B., 1976. Water and magma genesis: the association hypersolvus granite- subsolvus granite. Can. Mineral., 14, 228-237.

McCarthy, T.S. and Hasty, R.S., 1976. Trace element distribution patterns and their relationship to the crystallization of granitic melts. Geochim. Cosmochim. Acta.,40, 1351-1358.

Mishchenko, V.S., Kuts, V.P. and Orlova, L.A., 1966. The geochemistry of gallium in high-temperature post-magmatic processes. Geochem. Int., 3, 330-.

Mogarovskiy, V.V. and Mel'nichenko, A.K., 1968. Distribution of niobium and tantalum in the granitoids of the Gissar Pluton, Central Tadzhikistan. Geochem. Intern.,5, 893-.

Nell, J., 1984. Geochemical and thermodynamic controls in the formation of mineral assemblages from the metamorphic aureole of the Bushveld Complex in the Potgietersrus area. M.Sc. thesis (unpubl.), Univ. of Pretoria, 332pp.

Nemec, D., 1975. Genesis of tourmaline spots in leucocratic granites. N. Jb. Miner. Mh.,H7, 308-317.

Nockolds, S.R. and Allen, R., 1953. The geochemistry of some igneous rock series. Geochim. Cosmochim. Acta.,4, 105-142.

Norrish, K. and Hutton, J.J., 1969. An accurate X-ray spectrographic method for analyses of a wide range of geological samples. Geochim. Cosmochim. Acta, 33, 431-453.

Oelsner, O.W., 1952. Die pegmatitisch- pneumatolytischen Lagerstätten des Erzgebirges. Freiberger Forsch.-H.,4.

Olade, M.A., 1980. Geochemical characteristics of tin-bearing and tin-barren granites, Northern Nigeria. Econ. Geol.,75, 71-82.

Pagel, M., 1982. The mineralogy and geochemistry of uranium, thorium, and rare-earth elements in two radio-active granites of the Vosges, France. Min. Mag., 46, 149-161.

Parry, W.T. and Downey, L.M., 1982. Geochemistry of hydrothermal chlorite replacing igneous biotite. Clays and Clay Minerals,30, 81-90.

Pitcher, W.S., 1979. The nature, ascent and emplacement of granitic magmas. J. geol. Soc. London, 136, 627-662.

Pupin, J.P., 1980. Zircon and granite petrology. Contr. Mineral. Petrol., 73, 207-220.

Recknagel, R., 1909. On the origin of the South African tin deposits. Trans. geol. Soc. S. Afr., 12, 168-203.

Rogers, J.J.W. and Ragland, P.C., 1961. Variation of thorium and uranium in selected granitic rocks. Geochim. Cosmochim. Acta, 25, 99-109.

Rogers, J.J.W., Ragland, P.C., Nishimori, R.K., Greenberg, J.K. and Hauck, S.A., 1978. Varieties of granitic uranium deposits and favourable exploration areas in the eastern United States. Econ. Geol., 73, 1539-1555.

Rye, D.M. and Roy, R.F., 1978. The distribution of thorium, uranium and potassium in archean granites from northeastern Minnesota. Am. J. Sci., 278, 354-378.

Sattran, V. and Klominsky, J., 1970. Petrometallogenic series of igneous rocks and the endogenous ore deposits in the Czechoslovak part of the Bohemian Massif. Sbornik. Geologickych. Ved., 12, 65-154.

Schloemer, H., 1962. Hydrothermal-syntetische gemeinsame Kristallization von Orthoklas und Quartz, II. Radex Rundschau. 4, 157-173.

Schust, F., Striegler, R. and Oemler, M., 1970. Bemerkungen zur räumlichen Verteilung von Turmalin-Quarz-Knollen im Eiberstocker Granitmassiv. Zeitschr. Angew. Geol., 16, 113-122.

Sharpe, M.R., Brits, R. and Engelbrecht, J.P., 1983. Rare Earth and trace element evidence pertaining to the petrogenesis of 2.3 GA old continental andesites and other volcanic rocks from the Transvaal Sequence,

South Africa. Inst. geol. Res. Bushveld Complex. Res. Rept. 40.

Smith, J.V., 1974. Feldspar Minerals. II-Chemical and textural properties. Springer. Berlin. 690pp.

Smith, J.V. and MacKenzie, W.S., 1955. The alkali feldspars. II. A simple X-ray technique for the study of alkali feldspars. Amer. Mineral., 40, 733-747.

Smith, T.E. and Turek, A., 1976. Tin-bearing potential of some Devonian granitic rocks in S.W. Nova Scotia. Mineral. Deposita,11, 234-245.

Spry, A., 1979. Metamorphic textures. Pergamon Press. Oxford. 350pp.

Steiner, J.C., Jahns, R.H. and Luth, W.C., 1975. Crystallization of alkali feldspar and quartz in the haplogranite system $NaAlSi_3O_8$-$KAlSi_3O_8$-SiO_2-H_2O at 4 kb. Geol. Soc. Am. Bull., 86, 83-98.

Stemprok, M., 1970. Geochemical association of tin. In: Technical Conference on Tin, 2nd, Bangkok 1969, Fox, W.(Editor), Internat. Tin Council, 1, 118-124.

Stone, M., 1982. The behaviour of tin and some other trace elements during granite differentiation, West Cornwall, England. 339-355. In: Metallization associated with acid magmatism (MAWAM), Evans, A.M.(Editor), Wiley.

Strauss, C.A., 1954. The geology and mineral deposits of the Potgietersrust tin-fields. Geol. Surv. S. Afr., Mem. 46, 241pp.

Strauss, C.A. and Truter, F.C., 1944. The Bushveld granites in the Zaaiplaats tin mining area. Trans. geol. Soc. S. Afr.,47, 47-77.

Streckeisen, A.L., 1973. Plutonic rocks: classification and nomenclature recommended by the IUGS subcommision of the systematics of igneous rocks. Geotimes,

18, 26-30.

Strydom, J.H., 1983. Geochemiese en mineralogiese verspreidingspatrone in die wandgesteentes van tindraende ertsliggame in die Zaaiplaatsmyn, Potgietersrusdistrik. M.Sc. thesis (unpubl.) Univ. of Pretoria, 137pp.

Tauson, L.V. and Kozlov, V.D., 1973. Distribution functions and ratios of trace element concentrations as estimates of the ore-bearing potential of granites. In: Geochemical Exploration 1977, London, Inst. Mining. Metallurgy., 37-44.

Taylor, R.G., 1979. Geology of Tin Deposits. Elsevier Scientific Publishing Company. Amsterdam. 543pp.

Taylor, S.R., 1964. Abundance of chemical elements in the continental crust: a new table. Geochim. Cosmochim. Acta..28, 1273-1285.

Teuscher, E.O., 1936. Umwandlungserscheinungen an Gesteinen des Granitmassivs von Eibenstock-Neudek. Min. petrogr. Mitt.. 47, 273-312.

Thornton, C.P. and Tuttle, O.F., 1960. Chemistry of igneous rocks. I: Differentiation index. Am. J. Sci..258, 664-684.

Tindle, A.G. and Pearce, J.A., 1981. Petrogenetic modelling of in situ fractional crystallization in the zoned Loch Doon Pluton, Scotland. Contrib. Mineral. Petrol.. 78, 196-207.

Tischendorf, G., 1977. Geochemical and petrographic characteristics of silicic magmatic rocks associated with rare-element mineralization. Int. Geol. Cong. Prog.. MAWAM. 2, 41-96. M. Stemprok, L.Burnol and G. Tischendorf (Ed.). Prague.

Tröger, W.E., 1969. Optische Bestimmung der gesteinsbildenden Minerale. Teil II. Schweitzerbartsche Verlagsbuchhandlung, Stuttgart. 822pp.

Turekian, K.K. and Wedepohl, W.H., 1961. Distribution of the elements in some major units of the earth's crust. Bull. Geol. Soc. Am.,72, 175-192.

Tuttle, O.F., 1952. Origin of the contrasting mineralogy of extrusive and plutonic salic rocks. J. Geol., 60, 107-124.

Tuttle, O.F. and Bowen, N.L., 1958. Origin of granite in the light of experimental studies in the system $NaAlSi_3O_8$-$KAlSi_3O_8$-SiO_2-H_2O. Geol. Soc. Am. Mem., 74, 153pp.

Twist, D., 1984. Geochemical evolution of the Rooiberg acid lavas in the Loskop Dam area, southeastern Bushveld. Inst. geol. Res. Bushveld Complex, Res. Rept. 45.

Van de Pijpekamp, B., 1982. Petrological criteria for establishing the tin potential in granitoid complexes. 273-278. In: Metallization associated with acid magmatism (MAWAM), Evans, A.M. (Editor), Wiley.

Van Straaten, P.A., 1980. Rand Mines report on a geochemical survey of the farms Varschwater 23JS, Tafelkop 120JS, Tussenin 21JS, Mooiplaats 121JS, Boekenhoutkloof 124JS and Welverdiend 24JS.

Vlasov, K.A., 1966. Geochemistry of Rare Elements. Israel Progr. Sci. Transl., Jerusalem. 688pp.

Von Gruenewaldt, G., 1966. The geology of the Bushveld Igneous Complex east of the Kruis River cobalt occurence, north of Middelburg, Transvaal. M.Sc. thesis, Univ. Pretoria (unpubl.). 104pp.

Von Gruenewaldt, G., 1968. The Rooiberg Felsite north of Middelburg and its relation to the Layered Sequence of the Bushveld Complex. Trans. geol. Soc. S. Afr.,71, 153-172.

Von Gruenewaldt, G., 1971. A petrographical and mineralogical investigation of the rocks of the Bushveld Igneous

Complex in the Tauteshoogte-Roossenekal area of the Eastern Transvaal. D.Sc. dissertation (unpubl.) Univ. of Pretoria, 228pp.

Von Gruenewaldt, G., 1972. The origin of the roof-rocks of the Bushveld Complex between Tauteshoogte and Paardekop in the Eastern Transvaal. Trans. geol. Soc. S. Afr.,75, 121-134.

Wagner, P.A., 1929. The platinum deposits and mines of South Africa. Oliver and Boyd, London, Edinburgh. 326pp.

Walraven, F., 1976. Notes on the late-stage history of the western Bushveld Complex. Trans. geol. Soc. S. Afr., 79, 13-21.

Walraven, F., Burger, A.J. and Allsopp, H.L., 1981. Summary of age determinations carried out during the period April 1979 to March 1980. Ann. Geol. Surv. S. Afr., 15.

Walraven, F., 1982. Textural, geochemical and genetical aspects of the granophyric rocks of the Bushveld Complex. Ph.D. thesis (unpubl.) Univ. of the Witwatersrand, 251pp.

Watson, E.B., 1979. Zircon saturation in felsic liquids: Experimental results and applications to trace element geochemistry. Contr. Mineral. Petrol.,70, 407-419.

Wedepohl, K.H., 1969. 74-F-2, Handbook of Geochemistry, Wedepohl, K.H. (Ed.), Springer.

White, D.E., 1940. The molybdenite deposits of the Recontre East area, Newfoundland. Econ. Geol., 35, 967-995.

White, A.J.R. and Chappel, B.W., 1982. Granitoid types and their distribution in southeast Australia. In: Roddick J. (Ed.). Circumpacific plutonism. Geol. Soc. Am. Mem.

Whitfield, J.M., Rogers, J.J.W. and Adams, J.A.S., 1959. The relationship between the petrology and the thorium and uranium contents of some granitic

rocks. Geochim. Cosmochim. Acta. 17, 248-271.

Willemse, J. and Frick, C., 1970. Stroomroof en die invloed van verskuiwings op die geomorphologie in die opvanggebied van die Steelpoortrivier in Oos-Transvaal. Trans. geol. Soc. S. Afr., 73, 159-171.

Wilson, M.R. and Akerblom, G.V., 1982. Geological setting and geochemistry of uranium-rich granites in the Proterozoic of Sweden. Min. Mag.,46, 233-245.

Wolhuter, L.E., 1954. The geology of the country surrounding Loskopdam, Transvaal. M.Sc. thesis (unpubl.). Univ. Pretoria. 66pp.

Wyllie, P.J., Huang, W.L., Stern, C.R. and Maaloe, S., 1976. Granitic magmas: possible and impossible sources, water contents, and crystallization sequences. Can. J. Earth Sci., 13, 1007-1019.

Yeates, A.N., Wyatt, B.W. and Tucker, D.H., 1982. Application of gamma-ray spectrometry to prospecting for tin and tungsten granites, particularly within the Lachlan Fold Belt, New South Wales. Econ. Geol.,77, 1725-1738.

APPENDIX 1 (MICROPROBE ANALYSES)

Sample No.	Rocktype
GN-12A	Nebo Granite
GN-16	Nebo Granite
VW4-60,15	Nebo Granite
GK-38	Fine- medium-grained Klipkloof Granite
GN-16	Nebo Granite
GK-27	Porphyritic Klipkloof Granite
GGr-142	Fine- to medium-grained Klipkloof Granite
GR-212	Magnetite-rich granophyre
GR-232	Microgranophyre of the Stavoren Granophyre
GR-43A	Metafelsite
GR-52	Metafelsite

MICROPROBE ANALYSES

Mineral Sample No.	Plagio=clase GN-12A	Plagio=clase rim GN-16	Plagio=clase core GN-16	Plagio=clase VW4-60,15	Plagioclase GK-38		Biotite GN-16	Ferro-edenite GN-16	Biotite VW4-60,15	Ferro-edenite VW4-6015	Biotite GK-27	Chlorite GK-38	Chlorite GGr-142
SiO_2	66,86	67,61	64,93	67,19	68,41	67,77	35,38	43,18	36,18	43,03	36,41	29,69	29,06
TiO_2	0,00	0,00	0,00	0,00	0,00	0,00	3,01	1,11	2,47	1,09	2,22	0,37	1,23
Al_2O_3	19,53	19,72	21,40	20,70	19,28	19,37	11,56	6,13	12,04	5,48	11,86	15,99	12,39
FeO*	0,22	0,26	0,25	0,16	0,15	0,12	35,62	31,43	34,28	31,18	35,36	32,42	36,69
MnO	0,00	0,00	0,00	0,00	0,00	0,00	0,29	0,50	0,31	0,48	0,42	0,20	0,28
MgO	0,00	0,00	0,00	0,00	0,00	0,00	0,43	0,68	0,33	1,09	0,33	1,02	0,99
CaO	1,02	0,92	2,03	0,65	0,23	0,15	0,10	10,37	0,06	10,25	0,09	0,29	0,09
Na_2O	10,42	10,90	9,93	10,89	11,29	11,32	0,14	1,84	0,10	1,83	0,09	0,15	0,24
K_2O	0,75	0,26	0,59	0,36	0,10	0,20	8,66	1,24	8,51	0,88	8,02	2,10	1,92
Cr_2O_3	0,00	0,00	0,00	0,00	0,00	0,00	0,15	0,16	0,16	0,16	0,17	0,20	0,15
NiO	0,00	0,00	0,00	0,00	0,00	0,00	0,19	0,23	0,18	0,23	0,25	0,22	0,19
Total	98,80	99,67	99,13	99,95	99,46	98,93	95,53	96,87	94,62	95,70	95,22	82,65	83,23

*Total Fe as FeO

STRUCTURAL FORMULAE

Number of O	32	32	32	32	32	32	22	23	22	23	22	28	22
Si	11,88	11,89	11,54	11,77	12,01	11,97	5,87	7,06	6,00	7,11	6,01	6,97	5,50
Al	4,09	4,09	4,48	4,27	3,99	4,03	2,26	1,18	2,35	1,07	2,31	4,43	2,77
Ti	0,00	0,00	0,00	0,00	0,00	0,00	0,38	0,14	0,31	0,14	0,28	0,07	0,18
Fe^{2+}	0,03	0,04	0,04	0,02	0,02	0,02	4,95	4,30	4,75	4,31	4,88	6,37	5,81
Mn	0,00	0,00	0,00	0,00	0,00	0,00	0,04	0,07	0,04	0,07	0,06	0,04	0,04
Mg	0,00	0,00	0,00	0,00	0,00	0,00	0,11	0,17	0,08	0,27	0,08	0,36	0,28
Cr	0,00	0,00	0,00	0,00	0,00	0,00	0,02	0,02	0,02	0,02	0,02	0,04	0,02
Ni	0,00	0,00	0,00	0,00	0,00	0,00	0,03	0,03	0,02	0,03	0,03	0,04	0,03
Ca	0,19	0,17	0,39	0,12	0,04	0,03	0,02	1,82	0,01	1,82	0,02	0,07	0,02
Na	3,59	3,72	3,42	3,70	3,84	3,88	0,04	0,58	0,03	0,59	0,03	0,07	0,09
K	0,17	0,06	0,13	0,08	0,02	0,05	1,83	0,26	1,80	0,19	1,69	0,63	0,46
$\frac{Mg}{Mg + Fe}$	-	-	-	-	-	-	0,022	0,038	0,017	0,059	0,016	0,053	0,046
Ab	95,0	95,6	89,8	96,9	99,0	99,2	Sid -14,1	-	Sid -16,2	-	Sid -13,7	-	-
An	5,0	4,4	10,2	3,1	1,0	0,8	Ann -83,8	-	Ann -82,1	-	Ann -84,7	-	-
							Phlog- 1,8	-	Phlog- 1,4	-	Phlog- 1,4	-	-
							East- 0,3	-	East- 0,3	-	East- 0,2	-	-

MICROPROBE ANALYSES

Mineral	Olivine	Clino= pyroxene	Clino= pyroxene	Clino= pyroxene	Clino= pyroxene	Sphene	Magnetite rim= med by sphene	Magnetite not rim= med by sphene	Chlorite
Sample No.	GR-212	GR-212	GR-232	GR-43A	GR-52	GR-52	GR-52	GR-52	GR-43A
SiO_2	30,06	46,94	47,71	51,54	50,08	30,01	0,00	0,00	28,05
TiO_2	0,22	0,41	0,17	0,15	0,44	32,47	1,38	0,56	0,31
Al_2O_3	0,25	0,49	0,29	0,35	1,53	2,73	0,86	0,59	15,15
FeO*	66,46	29,00	25,43	12,72	13,46	Fe_2O_3-4,35	88,94	89,56	27,53
MnO	1,07	0,47	2,42	0,16	0,80	0,29	0,36	0,33	0,15
MgO	0,20	0,19	0,19	11,77	9,57	0,15	0,16	0,19	14,43
CaO	0,21	20,99	21,96	22,23	22,68	27,89	0,00	0,14	0,13
Na_2O	0,12	0,30	0,19	0,20	0,34	0,13	0,00	0,00	0,16
K_2O	0,10	0,09	0,08	0,05	0,13	0,07	0,00	0,00	0,31
Cr_2O_3	0,24	0,17	0,19	0,15	0,19	0,15	0,20	0,15	0,17
NiO	0,23	0,23	0,25	0,23	0,21	0,26	0,06	0,06	0,24
Total	99,16	99,28	98,88	99,55	99,43	98,50	91,96	91,58	86,63

*Total Fe as FeO

STRUCTURAL FORMULAE

Number of O	4	6	6	6	6	19,5	4	4	28
Si	1,01	1,96	1,99	1,97	1,94	3,91	0,00	0,00	6,09
Al	0,01	0,02	0,01	0,02	0,07	0,42	0,05	0,04	3,88
Ti	0,06	0,01	0,01	0,00	0,01	3,19	0,05	0,02	0,05
Fe^{2+}	1,88	1,01	0,89	0,41	0,44	0,43	3,78	3,85	5,00
Mn	0,03	0,02	0,09	0,01	0,03	0,03	0,02	0,01	0,03
Mg	0,01	0,01	0,01	0,67	0,55	0,03	0,01	0,01	4,67
Cr	0,01	0,01	0,01	0,00	0,01	0,02	0,01	0,01	0,03
Ni	0,01	0,01	0,01	0,01	0,01	0,03	0,00	0,00	0,04
Ca	0,01	0,94	0,98	0,91	0,94	3,90	0,00	0,01	0,03
Na	0,01	0,02	0,02	0,02	0,03	0,03	0,00	0,00	0,07
K	0,00	0,00	0,00	0,00	0,01	0,01	0,00	0,00	0,09
$\frac{Mg}{Mg + Fe}$	0,005	0,010	0,011	0,620	0,556	0,065	-	-	0,483
Mg	0,5	0,5	0,5	33,7	28,5	-	-	-	-
Fe	99,5	51,5	47,3	20,6	22,8	-	-	-	-
Ca	-	48,0	52,2	45,7	48,7	-	-	-	-

APPENDIX 2 (MAJOR ELEMENT ANALYSES)

I MAJOR ELEMENT ANALYSES OF NEBO GRANITE

Sample No.	GR-98*	GR-115*	GN-53*	GN-1*	GN-56	GN-52	GN-58A	GN-58	GN-51	GN-44	GGr-95	GGr-214	GGr-255	GN-50	GN-4	GN-8	GN-9	GN-12	GN-12A
SiO_2	71,39	68,98	69,45	72,77	71,45	71,87	71,93	71,10	72,17	71,96	73,29	72,70	73,74	74,33	74,38	74,13	74,10	74,72	74,77
TiO_2	0,44	0,42	0,42	0,29	0,38	0,34	0,33	0,33	0,32	0,29	0,25	0,26	0,23	0,22	0,21	0,20	0,19	0,19	0,20
Al_2O_3	12,06	12,52	12,56	11,66	12,10	12,16	12,27	12,46	12,32	11,87	11,78	12,16	11,69	11,55	11,77	11,72	11,56	11,40	11,40
FeO	4,93	5,99	6,00	3,94	4,56	4,39	4,04	4,18	4,02	3,74	4,03	3,47	3,32	3,19	2,99	3,04	2,95	2,86	2,99
MnO	0,08	0,09	0,09	0,06	0,09	0,09	0,08	0,09	0,07	0,08	0,05	0,06	0,05	0,06	0,05	0,05	0,03	0,04	0,04
MgO	0,00	0,00	0,00	0,02	0,02	0,02	0,00	0,02	0,09	0,07	0,01	0,11	0,00	0,00	0,00	0,00	0,15	0,00	0,00
CaO	1,53	1,65	1,69	1,06	1,48	1,27	1,10	1,43	1,18	1,12	0,76	1,13	0,92	0,83	0,96	0,81	0,62	0,40	0,89
Na_2O	3,39	3,73	3,71	3,68	3,51	3,71	3,62	3,78	3,73	3,74	3,15	3,76	3,65	3,73	3,76	3,97	3,57	3,77	3,68
K_2O	4,94	4,48	4,64	4,53	4,98	4,90	5,13	4,87	5,00	4,94	5,01	4,88	5,15	4,73	5,00	5,12	4,99	4,90	5,21
P_2O_5	0,04	0,05	0,04	0,02	0,05	0,04	0,04	0,05	0,04	0,03	0,03	0,02	0,02	0,02	0,02	0,01	0,02	0,02	0,02
Cr_2O_3	0,03	0,03	0,04	0,03	0,04	0,05	0,05	0,04	0,05	0,05	0,04	0,04	0,05	0,03	0,04	0,05	0,04	0,05	0,04
NiO	0,01	0,01	0,01	0,01	0,00	0,01	0,00	0,00	0,02	0,00	0,01	0,00	0,01	0,00	0,01	0,00	0,00	0,00	0,01
LOI	0,30	0,42	0,45	0,74	0,42	0,42	0,33	0,47	0,40	0,29	0,86	0,52	0,47	0,43	0,36	0,33	0,92	0,71	0,49
H_2O^-	0,10	0,10	0,26	0,22	0,21	0,19	0,21	0,19	0,20	0,39	0,27	0,23	0,22	0,22	0,26	0,30	0,23	0,15	0,20
Total	99,24	98,47	99,36	99,03	99,29	99,46	99,13	99,01	99,61	98,57	99,54	99,34	99,52	99,34	99,81	99,73	99,37	99,21	99,94
CIPW NORMS																			
Q	28,09	24,64	24,44	30,79	27,68	27,56	27,73	26,47	27,54	28,36	32,50	28,86	30,27	32,10	30,80	29,33	32,11	32,59	31,19
or	29,49	26,99	27,74	27,30	29,78	29,30	30,74	29,26	29,84	29,84	30,08	29,25	30,76	38,32	29,79	30,53	30,01	29,42	31,02
ab	29,00	32,18	31,78	31,75	30,07	31,75	31,08	32,49	31,86	32,29	27,07	32,23	31,21	32,01	32,05	32,03	30,72	31,85	29,82
an	3,15	4,27	3,97	1,93	2,58	2,06	2,08	2,68	2,12	1,04	3,24	1,92	0,32	0,78	0,47	0,00	0,81	0,00	0,00
ns	0,00	0,00	0,00	0,00	0,00	0,00	0,00	0,00	0,00	0,00	0,00	0,00	0,00	0,00	0,00	0,00	0,00	0,00	0,00
di	3,80	3,37	3,80	2,94	4,02	3,58	2,89	3,72	3,12	3,96	0,38	3,21	3,72	2,89	3,75	3,51	1,92	1,72	3,85
hy	4,02	5,77	5,51	3,43	3,58	3,62	3,48	3,30	3,54	2,70	4,92	2,89	2,18	2,43	1,73	2,40	3,07	2,83	2,06
ac	0,00	0,00	0,00	0,00	0,00	0,00	0,00	0,00	0,00	0,00	0,00	0,00	0,00	0,00	0,00	1,60	0,00	0,49	1,34
mt	1,48	1,81	1,80	1,19	1,37	1,32	1,21	1,26	1,20	1,11	1,21	1,03	1,00	0,95	0,89	0,11	0,89	0,62	0,23
il	0,84	0,82	0,80	0,56	0,74	0,64	0,63	0,63	0,61	0,57	0,48	0,50	0,43	0,43	0,41	0,38	0,36	0,37	0,39
cm	0,05	0,05	0,06	0,05	0,06	0,07	0,07	0,06	0,07	0,07	0,06	0,06	0,08	0,05	0,06	0,07	0,06	0,07	0,06
ap	0,09	0,11	0,10	0,05	0,12	0,10	0,08	0,12	0,09	0,07	0,07	0,05	0,04	0,05	0,05	0,03	0,04	0,04	0,04
D.I.	86,58	83,81	83,96	89,85	87,53	88,60	89,55	88,23	89,24	90,49	89,64	90,34	92,24	92,43	92,64	91,89	92,84	93,86	92,04
MODAL ANALYSES																			
Quartz	29,57	26,60	26,30	32,20	29,38	29,09	29,15	28,17	29,14	30,12	34,56	30,70	32,19	33,70	32,65	31,74	33,82	34,44	33,61
Orthoclase	30,68	25,97	27,24	28,69	31,11	30,77	32,47	30,54	31,42	31,68	29,55	30,82	32,77	30,13	31,76	32,56	32,06	31,42	33,13
Plagioclase	28,88	33,59	32,57	30,96	29,52	30,67	30,02	32,37	31,07	30,43	27,99	31,65	28,58	30,24	29,89	30,19	28,93	29,64	27,75
Hornblende	10,89	10,97	11,74	8,17	10,01	9,49	8,39	8,94	8,39	7,79	3,95	6,85	6,48	5,96	5,72	5,53	5,21	4,52	5,53
Biotite	0,00	2,90	2,18	0,00	0,00	0,00	0,00	0,00	0,00	0,00	3,98	0,00	0,00	0,00	0,00	0,00	0,00	0,00	0,00

* Granite from intrusion breccia

IIA MAJOR ELEMENT ANALYSES OF NEBO GRANITE

Sample No.	GN-16	GN-60	GGr-260	VW4-31,0	VW4-35,5	VW4-40,75	VW4-53,0	VW4-60,15	VW4-71,7	VW4-81,5
SiO_2	74,30	75,13	74,94	73,87	74,55	74,53	75,08	76,01	75,26	75,85
TiO_2	0,19	0,19	0,12	0,22	0,18	0,18	0,13	0,13	0,17	0,13
Al_2O_3	11,43	11,43	11,43	11,57	11,61	11,46	11,81	11,48	11,65	11,89
FeO	3,17	2,58	2,64	2,92	2,48	2,38	2,41	1,92	2,06	1,35
MnO	0,05	0,03	0,03	0,04	0,04	0,04	0,04	0,03	0,03	0,02
MgO	0,00	0,00	0,00	0,00	0,00	0,00	0,00	0,00	0,00	0,00
CaO	0,94	0,89	0,41	1,20	0,80	0,85	0,37	0,41	0,70	0,31
Na_2O	3,58	3,61	3,79	3,64	3,67	3,73	3,45	3,60	4,18	3,90
K_2O	5,17	5,18	4,97	5,39	5,63	5,46	5,75	5,70	5,24	5,59
P_2O_5	0,02	0,03	0,02	0,02	0,03	0,02	0,01	0,01	0,01	0,01
Cr_2O_3	0,04	0,05	0,05	0,05	0,05	0,05	0,04	0,04	0,05	0,04
NiO	0,00	0,01	0,01	0,00	0,00	0,00	0,00	0,00	0,00	0,00
LOI	0,63	0,40	0,57	0,64	0,40	0,43	0,58	0,41	0,33	0,50
H_2O^-	0,22	0,18	0,32	0,16	0,23	0,30	0,21	0,15	0,14	0,17
Total	99,74	99,71	99,30	99,72	99,67	99,43	99,88	99,89	99,82	99,76
CIPW NORMS										
Q	31,24	32,27	32,54	29,60	30,48	31,12	31,54	33,15	31,21	32,31
or	30,90	30,88	29,82	32,16	33,56	32,65	34,28	33,87	31,14	33,32
ab	30,29	30,16	31,62	29,80	28,64	28,93	28,98	27,54	30,97	30,28
an	0,00	0,00	0,00	0,00	0,00	0,00	0,00	0,00	0,00	0,00
ns	0,00	0,00	0,00	0,00	0,24	0,33	0,00	0,43	0,74	0,48
di	4,06	3,81	1,76	5,28	3,44	3,69	1,60	1,76	3,04	1,31
hy	1,94	1,31	2,71	1,15	1,69	1,40	2,35	1,77	1,24	1,13
ac	0,30	0,58	0,83	1,19	1,49	1,43	0,41	1,15	1,23	0,81
mt	0,80	0,48	0,38	0,28	0,00	0,00	0,52	0,00	0,00	0,00
il	0,36	0,36	0,23	0,41	0,34	0,34	0,25	0,25	0,33	0,25
cm	0,06	0,08	0,07	0,08	0,07	0,07	0,05	0,06	0,07	0,07
ap	0,05	0,07	0,04	0,04	0,06	0,04	0,03	0,02	0,03	0,02
D.I.	92,43	93,31	93,99	91,57	92,68	92,70	94,80	94,55	93,32	95,92
MODAL ANALYSES										
Quartz	33,42	34,48	-	32,21	32,75	33,30	33,57	-	32,78	33,89
Orthoclase	32,96	33,06	-	34,38	36,03	35,04	36,86	-	33,42	36,01
Plagioclase	27,51	27,93	-	27,56	27,15	27,78	26,27	-	31,03	29,68
Hornblende	6,13	4,54	-	5,87	4,09	3,90	3,33	-	2,79	0,44
Biotite	0,00	0,00	-	0,00	0,00	0,00	0,00	-	0,00	0,00

IIB MAJOR ELEMENT ANALYSES OF MEDIUM- TO COARSE-GRAINED KLIPKLOOF GRANITE

Sample No.	VW4-48,85	GN-28	GN-33	GN-35	GN-40	GGr-146	GK-53	GGr-358	GGr-363
SiO_2	74,63	76,47	76,65	75,39	76,25	74,62	75,03	75,60	75,73
TiO_2	0,14	0,08	0,09	0,11	0,09	0,09	0,09	0,09	0,09
Al_2O_3	11,99	11,29	11,28	11,26	11,01	11,70	11,14	11,11	11,08
FeO	2,53	1,91	2,20	2,14	1,97	2,15	3,13	2,70	2,37
MnO	0,06	0,02	0,01	0,03	0,02	0,01	0,01	0,01	0,01
MgO	0,00	0,00	0,00	0,00	0,00	0,43	0,00	0,01	0,01
CaO	0,51	0,47	0,33	0,36	0,61	0,92	0,94	0,64	0,78
Na_2O	4,33	4,03	3,47	3,82	3,51	3,39	3,24	3,25	3,43
K_2O	4,72	4,80	4,70	5,04	5,01	5,24	4,95	5,09	4,90
P_2O_5	0,01	0,01	0,01	0,01	0,01	0,01	0,01	0,01	0,00
Cr_2O_3	0,03	0,03	0,03	0,04	0,04	0,04	0,04	0,04	0,05
NiO	0,00	0,00	0,00	0,00	0,00	0,00	0,00	0,01	0,01
LOI	0,65	0,75	0,77	0,54	0,74	0,96	0,98	0,84	0,83
H_2O^-	0,20	0,21	0,22	0,26	0,12	0,44	0,21	0,29	0,26
Total	99,80	100,07	99,76	99,00	99,38	100,00	99,77	99,69	99,55
				CIPW NORMS					
Q	29,84	34,33	37,00	33,62	35,52	32,15	34,64	35,31	35,23
or	28,17	28,62	28,12	30,31	30,05	31,39	29,64	30,53	29,41
ab	35,76	31,60	29,72	30,41	29,15	29,09	27,77	27,85	29,49
an	0,00	0,00	1,32	0,00	0,00	1,26	1,27	0,72	0,35
ns	0,00	0,35	0,00	0,24	0,00	0,00	0,00	0,00	0,00
di	2,22	2,04	0,26	1,58	2,69	2,83	3,02	2,13	3,16
hy	2,38	1,69	2,68	2,26	1,34	2,38	2,47	2,39	1,37
ac	1,06	1,14	0,00	1,29	0,83	0,00	0,00	0,00	0,00
mt	0,23	0,00	0,66	0,00	0,18	0,65	0,94	0,81	0,72
il	0,27	0,15	0,17	0,22	0,17	0,18	0,17	0,17	0,18
cm	0,05	0,04	0,05	0,06	0,06	0,06	0,05	0,07	0,08
ap	0,02	0,02	0,02	0,02	0,02	0,01	0,03	0,03	0,01
D.I.	93,78	94,56	94,84	94,33	94,72	92,63	92,05	93,69	94,13
				MODAL ANALYSES					
Quartz	31,90	36,09	38,25	35,51	37,69	-	-	36,97	37,11
Orthoclase	30,05	30,69	29,87	32,53	32,28	-	-	32,66	31,48
Plagioclase	34,24	31,02	28,95	29,36	27,36	-	-	25,75	27,39
Hornblende	3,83	2,21	2,43	2,62	2,69	-	-	4,65	4,04
Biotite	0,00	0,00	0,53	0,00	0,00	-	-	0,00	0,00

III MAJOR ELEMENT ANALYSES OF PORPHYRITIC KLIPKLOOF GRANITE

Sample No.	GK-20B	GK-25	GK-27	GK-29	GK-39	GK-42	GGr-129	GGr-131	GGr-143	GGr-145	GGr-167	GGr-181	GGr-184	GGr-193	GGr-194	GGr-195	GGr-196
SiO_2	75,36	74,98	74,63	74,60	74,47	74,71	74,40	74,09	74,97	74,60	75,06	75,13	74,99	75,31	75,34	75,18	75,14
TiO_2	0,11	0,11	0,12	0,12	0,13	0,12	0,15	0,14	0,11	0,12	0,11	0,12	0,10	0,11	0,10	0,16	0,15
Al_2O_3	11,77	11,74	11,64	11,69	11,59	11,36	11,56	11,62	11,60	11,74	11,66	11,52	11,51	11,59	11,28	11,27	11,15
FeO	2,48	2,28	2,52	2,42	2,32	2,27	2,99	2,58	2,44	2,05	2,14	2,40	2,61	2,44	2,53	2,74	3,24
MnO	0,04	0,04	0,04	0,05	0,03	0,04	0,05	0,03	0,04	0,03	0,03	0,03	0,03	0,03	0,04	0,04	0,01
MgO	0,00	0,00	0,00	0,00	0,00	0,00	0,17	0,26	0,58	0,49	0,04	0,00	0,00	0,01	0,00	0,02	0,03
CaO	0,54	0,21	0,64	0,58	0,62	0,51	0,52	0,81	0,53	0,55	0,66	0,53	0,51	0,46	0,30	0,60	0,39
Na_2O	3,95	3,60	3,80	3,73	3,54	3,29	3,54	3,23	3,45	3,58	3,85	3,50	4,13	3,45	3,64	3,35	3,21
K_2O	5,24	5,23	5,25	5,37	5,27	5,32	5,00	5,59	5,21	4,98	4,92	5,29	4,66	5,33	5,19	5,07	4,92
P_2O_5	0,01	0,01	0,00	0,01	0,01	0,01	0,00	0,01	0,01	0,00	0,00	0,01	0,01	0,00	0,01	0,01	0,01
Cr_2O_3	0,04	0,03	0,03	0,03	0,03	0,03	0,03	0,03	0,03	0,04	0,04	0,04	0,04	0,03	0,04	0,03	0,03
NiO	0,00	0,00	0,00	0,00	0,00	0,00	0,00	0,00	0,00	0,00	0,00	0,00	0,00	0,00	0,00	0,00	0,00
LOI	0,72	0,57	0,65	0,63	0,91	0,68	0,80	1,00	0,76	0,79	0,80	0,77	0,90	0,77	0,45	0,82	0,58
H_2O^-	0,24	0,23	0,14	0,18	0,29	0,22	0,18	0,15	0,15	0,23	0,22	0,06	0,21	0,11	0,22	0,16	0,22
Total	100,50	99,03	99,46	99,41	99,21	98,56	99,39	99,54	99,88	99,20	99,53	99,40	99,70	99,64	99,14	99,45	99,08

CIPW NORMS

Q	31,17	32,96	30,88	30,92	32,31	34,06	32,44	31,54	32,28	32,55	32,31	33,01	31,73	33,21	32,99	34,33	35,47
or	31,19	31,45	31,41	32,16	31,76	32,14	30,00	33,56	31,11	29,96	29,49	31,70	27,90	31,89	31,05	30,39	29,49
ab	31,57	30,99	31,03	30,64	30,58	28,45	30,42	27,76	29,47	30,85	33,07	30,07	33,74	29,56	31,05	28,72	27,56
an	0,00	0,45	0,00	0,00	0,17	0,57	0,91	0,73	0,78	1,28	0,00	0,08	0,00	0,39	0,00	1,03	1,91
ns	0,13	0,00	0,00	0,00	0,00	0,00	0,00	0,00	0,00	0,00	0,00	0,00	0,00	0,00	0,00	0,00	0,00
di	2,37	0,52	2,85	2,52	2,58	1,78	1,46	2,86	1,57	1,23	2,92	2,25	2,26	1,70	1,28	1,74	0,00
hy	1,97	2,66	2,10	2,15	1,58	2,01	3,53	2,45	3,78	3,22	1,29	1,84	2,59	2,25	2,56	2,60	4,19
ac	1,33	0,00	1,33	1,17	0,00	0,00	0,00	0,00	0,00	0,00	0,01	0,00	1,51	0,00	0,11	0,00	0,00
mt	0,00	0,69	0,09	0,14	0,70	0,69	0,90	0,78	0,73	0,62	0,64	0,72	0,02	0,73	0,69	0,82	0,97
il	0,22	0,22	0,24	0,23	0,24	0,23	0,30	0,27	0,22	0,22	0,21	0,23	0,20	0,21	0,20	0,31	0,28
cm	0,05	0,05	0,05	0,04	0,05	0,05	0,04	0,04	0,05	0,06	0,05	0,06	0,05	0,04	0,07	0,04	0,05
ap	0,01	0,01	0,01	0,03	0,03	0,01	0,01	0,01	0,02	0,01	0,01	0,02	0,01	0,01	0,02	0,02	0,01
D.I.	93,93	95,40	93,33	93,72	94,66	94,65	92,86	92,86	92,86	93,35	94,87	94,77	93,36	94,66	95,08	93,44	92,51

MODAL ANALYSES

Quartz	33,31	34,93	29,04	33,21	34,23	35,78	34,37	33,73	34,63	-	34,31	34,91	33,90	34,95	34,79	35,82	37,31
Orthoclase	33,44	32,88	33,64	34,49	34,08	34,54	31,52	36,03	33,40	-	31,59	34,01	29,73	34,21	33,28	32,51	29,54
Plagioclase	30,16	29,27	29,13	28,63	28,17	26,36	28,83	25,59	27,91	-	30,92	27,50	32,34	27,23	28,51	27,05	27,47
Hornblende	3,11	1,15	8,21	3,69	3,54	3,34	4,28	4,66	4,08	-	3,20	3,60	4,05	3,63	3,43	4,63	2,17
Biotite	0,00	1,79	0,00	0,00	0,00	0,00	1,03	0,00	0,00	-	0,00	0,00	0,00	0,00	0,00	0,00	3,53

MAJOR ELEMENT ELEMENT ANALYSES OF PORPHYRITIC KLIPKLOOF GRANITE

Sample No.	GGr-237	GK-61	GK-63	GK-66	GK-67	GGr-254	GGr-261	GGr-261A
SiO_2	75,22	75,37	75,44	74,49	74,48	74,28	74,89	75,52
TiO_2	0,09	0,12	0,12	0,13	0,17	0,11	0,13	0,14
Al_2O_3	11,84	11,98	11,49	11,35	11,70	11,59	11,37	11,39
FeO	1,94	2,37	2,72	2,96	3,11	2,78	3,02	3,04
MnO	0,01	0,01	0,02	0,04	0,06	0,05	0,02	0,02
MgO	0,35	0,00	0,00	0,01	0,02	0,01	0,02	0,06
CaO	0,12	0,49	0,67	0,78	0,42	0,86	0,78	0,86
Na_2O	3,70	3,65	3,63	3,15	3,50	3,57	2,96	2,99
K_2O	5,28	5,26	4,77	5,39	5,22	4,99	5,47	5,50
P_2O_5	0,01	0,01	0,01	0,01	0,02	0,02	0,02	0,01
Cr_2O_3	0,04	0,04	0,05	0,04	0,03	0,05	0,04	0,04
NiO	0,00	0,00	0,00	0,00	0,00	0,02	0,01	0,00
LOI	0,44	0,70	0,83	0,97	0,63	0,96	0,87	0,84
H_2O^-	0,21	0,31	0,21	0,31	0,24	0,25	0,30	0,25
Total	99,25	100,31	99,96	99,63	99,60	99,54	99,90	100,66
			CIPW NORMS					
Q	32,72	32,18	33,94	33,29	32,10	32,17	34,24	34,19
or	31,74	31,30	28,46	32,38	31,24	29,99	32,70	32,59
ab	31,87	31,09	31,05	27,10	29,95	30,74	25,36	25,35
an	0,10	0,76	0,98	0,91	0,80	0,85	1,61	1,47
ns	0,00	0,00	0,00	0,00	0,00	0,00	0,00	0,00
di	0,41	1,42	2,08	2,59	1,03	3,02	1,91	2,41
hy	2,33	2,22	2,36	2,49	3,51	2,07	2,91	2,73
ac	0,00	0,00	0,00	0,00	0,00	0,00	0,00	0,00
mt	0,57	0,71	0,81	0,89	0,93	0,84	0,91	0,91
il	0,17	0,23	0,23	0,25	0,33	0,22	0,25	0,26
cm	0,06	0,07	0,07	0,06	0,05	0,07	0,06	0,06
ap	0,02	0,03	0,02	0,03	0,05	0,04	0,05	0,03
D.I.	96,33	94,57	93,45	92,77	93,29	92,90	92,30	92,14
			MODAL ANALYSES					
Quartz	34,42	33,69	35,40	35,02	34,13	33,90	35,75	35,76
Orthoclase	34,16	33,56	30,36	34,65	32,27	32,02	34,95	34,88
Plagioclase	29,69	29,28	29,55	24,84	28,23	28,88	23,72	23,54
Hornblende	1,75	3,48	4,71	5,51	3,18	5,22	5,60	5,84
Biotite	0,00	0,00	0,00	0,00	2,23	0,00	0,00	0,00

IV MAJOR ELEMENT ANALYSES OF FINE- TO MEDIUM-GRAINED KLIPKLOOF GRANITE

	VW4-6,3	VW4-90,0	VW4-92,4	VW4-98,2	VW4-107,8	GK-5	GK-10	GK-13	GK-17
SiO_2	75,29	76,54	74,98	75,01	74,84	75,20	74,70	74,40	74,82
TiO_2	0,13	0,13	0,13	0,09	0,12	0,10	0,09	0,12	0,23
Al_2O_3	11,79	12,07	11,86	11,95	11,91	11,97	11,75	11,84	11,48
FeO	2,49	1,04	1,99	1,98	1,93	1,98	2,41	2,68	2,78
MnO	0,03	0,01	0,03	0,04	0,04	0,02	0,02	0,05	0,06
MgO	0,00	0,00	0,00	0,00	0,00	0,00	0,00	0,00	0,00
CaO	0,23	0,18	0,81	0,69	0,61	0,40	0,61	0,51	0,44
Na_2O	4,42	4,94	3,62	4,09	4,07	4,30	4,36	4,21	3,52
K_2O	4,78	4,47	5,62	5,17	5,19	5,06	4,69	4,86	5,33
P_2O_5	0,01	0,01	0,00	0,01	0,01	0,00	0,00	0,00	0,01
Cr_2O_3	0,04	0,03	0,04	0,04	0,05	0,04	0,04	0,04	0,03
NiO	0,00	0,00	0,00	0,00	0,00	0,01	0,00	0,00	0,00
LOI	0,53	0,39	0,83	0,63	0,62	0,71	0,28	0,73	0,69
H_2O^-	0,22	0,20	0,21	0,22	0,29	0,23	0,55	0,24	0,30
Total	99,96	100,01	100,12	99,92	99,68	100,02	99,50	99,68	99,69
				CIPW NORMS					
Q	31,01	32,48	30,79	30,25	30,51	30,62	30,47	29,79	32,41
or	28,46	26,57	33,52	30,79	31,05	30,18	28,09	29,09	31,92
ab	34,31	37,38	29,98	33,01	32,75	33,69	34,75	34,25	29,73
an	0,00	0,00	0,00	0,00	0,00	0,00	0,00	0,00	0,00
ns	0,38	0,91	0,00	0,13	0,19	0,38	0,23	0,00	0,00
di	0,96	0,76	3,58	3,04	2,66	1,77	2,71	2,26	1,91
hy	3,07	0,96	0,82	1,32	1,36	1,91	2,07	2,72	2,52
ac	1,48	0,63	0,80	1,20	1,16	1,19	1,44	1,56	0,37
mt	0,00	0,00	0,20	0,00	0,00	0,00	0,00	0,02	0,65
il	0,24	0,25	0,25	0,18	0,22	0,19	0,18	0,24	0,44
cm	0,06	0,05	0,06	0,06	0,07	0,06	0,06	0,06	0,04
ap	0,03	0,01	0,01	0,01	0,02	0,01	0,01	0,01	0,02
D.I.	93,78	96,43	94,29	94,05	94,31	94,49	93,31	93,13	94,06
				MODAL ANALYSES					
Quartz	32,61	33,13	33,17	32,46	32,58	32,35	32,47	32,03	34,34
Orthoclase	30,39	28,50	36,06	33,03	33,34	32,37	29,95	31,03	34,21
Plagioclase	33,81	38,39	27,84	31,71	31,63	33,06	33,91	32,74	27,21
Hornblende	3,21	0,00	2,94	2,82	2,47	2,25	3,69	4,22	4,25
Biotite	0,00	0,00	0,00	0,00	0,00	0,00	0,00	0,00	0,00

V

MAJOR ELEMENT ANALYSES OF FINE- TO MEDIUM-GRAINED KLIPKLOOF GRANITE

Sample No.	GK-18	GK-19	GK-20A	GK-21	GK-22	GK-23	GK-24	GK-26	GK-30	GK-34	GK-38	GK-41	GGr-126	GGr-136	GGr-142	GGr-144	GGr-153	GGr-156
SiO_2	75,31	74,73	74,83	75,62	74,85	75,11	75,25	74,47	74,60	74,93	74,67	74,52	74,89	74,67	74,92	74,57	74,65	75,35
TiO_2	0,11	0,12	0,14	0,12	0,11	0,10	0,09	0,10	0,11	0,10	0,09	0,13	0,08	0,11	0,11	0,11	0,12	0,10
Al_2O_3	11,86	11,75	11,94	11,82	11,84	11,92	11,81	11,70	11,89	11,86	11,73	11,66	11,99	11,74	11,65	11,68	11,71	11,77
FeO	1,79	2,93	2,38	2,14	2,32	1,94	2,21	2,54	2,13	2,09	2,07	2,19	1,96	2,30	2,27	2,21	2,09	2,03
MnO	0,03	0,03	0,05	0,04	0,06	0,02	0,03	0,02	0,05	0,02	0,02	0,04	0,02	0,03	0,04	0,04	0,03	0,02
MgO	0,00	0,00	0,00	0,00	0,00	0,00	0,00	0,03	0,00	0,00	0,00	0,00	0,02	0,55	0,38	0,37	0,34	0,31
CaO	0,59	0,82	0,61	0,57	0,59	0,58	0,29	0,50	0,59	0,79	0,57	0,55	0,52	0,64	0,55	0,58	0,59	0,62
Na_2O	4,03	4,08	3,89	4,16	4,01	4,03	4,40	3,43	3,71	3,38	3,76	3,72	4,09	4,01	3,96	3,58	3,36	3,79
K_2O	5,11	4,46	5,21	5,10	5,08	5,08	4,52	5,40	5,21	5,19	5,25	5,34	4,88	4,73	4,93	5,12	5,55	4,90
P_2O_5	0,01	0,01	0,01	0,00	0,00	0,00	0,00	0,01	0,01	0,01	0,01	0,01	0,00	0,01	0,00	0,01	0,00	0,00
Cr_2O_3	0,03	0,03	0,03	0,03	0,03	0,02	0,04	0,03	0,03	0,03	0,03	0,03	0,04	0,04	0,04	0,03	0,04	0,03
NiO	0,00	0,00	0,00	0,00	0,00	0,00	0,00	0,00	0,00	0,00	0,00	0,00	0,00	0,00	0,00	0,00	0,00	0,00
LOI	0,72	0,89	0,68	0,53	0,68	0,70	0,60	0,79	0,75	0,82	0,81	0,67	0,89	0,80	0,80	0,74	0,90	0,70
H_2O^-	0,19	0,21	0,17	0,17	0,20	0,24	0,24	0,33	0,14	0,18	0,23	0,24	0,19	0,10	0,16	0,17	0,14	0,21
Total	99,78	100,06	99,94	100,30	99,77	99,74	99,48	99,35	99,22	99,40	99,24	99,10	99,57	99,73	99,81	99,21	99,52	99,83

CIPW NORMS

Q	31,34	31,55	30,57	31,07	30,56	30,96	31,45	32,28	31,66	33,51	31,59	31,35	31,18	30,78	31,04	32,07	31,91	32,46
or	30,51	26,60	31,02	30,26	30,31	30,40	27,09	32,45	31,30	31,16	31,56	32,12	29,29	28,26	29,48	30,79	33,30	29,26
ab	32,96	34,83	32,71	32,50	33,00	33,40	36,02	29,51	31,92	29,07	31,71	30,78	34,98	34,31	32,83	30,84	28,85	32,39
an	0,00	0,60	0,00	0,00	0,00	0,00	0,00	0,61	0,40	1,89	0,00	0,00	0,00	0,08	0,00	0,65	0,48	0,66
ns	0,07	0,00	0,00	0,32	0,00	0,00	0,04	0,00	0,00	0,00	0,00	0,00	0,00	0,00	0,00	0,00	0,00	0,00
di	2,60	3,09	2,65	2,50	2,63	2,60	1,28	1,67	2,27	1,79	2,53	2,42	2,31	2,62	2,36	1,91	2,12	2,11
hy	1,17	2,15	1,77	1,79	1,97	1,34	2,56	2,45	1,54	1,69	1,46	1,81	1,37	2,98	2,87	2,80	2,43	2,27
ac	1,07	0,00	0,45	1,29	1,15	1,00	1,32	0,00	0,00	0,00	0,57	1,08	0,11	0,00	0,96	0,00	0,00	0,00
mt	0,00	0,88	0,49	0,00	0,12	0,07	0,00	0,76	0,64	0,62	0,33	0,12	0,53	0,69	0,19	0,66	0,63	0,60
il	0,22	0,24	0,27	0,22	0,21	0,18	0,17	0,20	0,21	0,20	0,18	0,25	0,16	0,21	0,22	0,22	0,23	0,20
cm	0,05	0,04	0,05	0,05	0,05	0,03	0,05	0,04	0,04	0,04	0,05	0,05	0,06	0,06	0,05	0,04	0,05	0,05
ap	0,01	0,02	0,02	0,00	0,00	0,00	0,00	0,02	0,01	0,02	0,01	0,02	0,00	0,01	0,00	0,02	0,00	0,00
D.I.	94,81	92,99	94,30	93,83	93,87	94,76	94,57	94,25	99,99	93,74	94,87	94,25	95,45	93,35	93,35	93,70	94,06	94,11

MODAL ANALYSES

Quartz	33,49	-	32,62	32,99	32,81	32,61	33,38	33,99	33,47	35,24	33,71	33,59	33,09	33,33	33,66	34,23	34,20	34,51
Orthoclase	32,77	-	33,23	32,42	32,45	32,23	28,92	34,80	33,60	33,18	33,89	34,50	31,40	30,23	31,59	33,07	35,86	31,39
Plagioclase	31,66	-	30,51	31,67	31,28	32,21	35,01	27,28	29,93	28,75	29,63	28,89	33,04	32,60	31,37	29,28	26,84	31,11
Hornblende	2,09	-	3,65	2,94	3,47	2,95	2,70	3,94	3,02	2,84	2,79	3,04	2,50	3,86	3,40	3,45	3,12	3,02
Biotite	0,00	-	0,00	0,00	0,00	0,00	0,00	0,00	0,00	0,00	0,00	0,00	0,00	0,00	0,00	0,00	0,00	0,00

VI MAJOR ELEMENT ANALYSES OF FINE- TO MEDIUM-GRAINED KLIPKLOOF GRANITE

Sample No.	GGr-166	GGr-168	GGr-177	GGr-178	GGr-182	GGr-185	GGr-197	GGr-224	GK-51	GK-59	GK-62	GK-64	GK-65	GGr-152	GGr-155	GGr-172	GGr-179	GGr-183
SiO_2	74,74	75,39	75,18	74,68	74,56	75,88	74,04	75,05	75,25	75,96	75,20	75,21	75,54	76,06	76,37	75,53	75,79	74,71
TiO_2	0,11	0,11	0,13	0,12	0,09	0,08	0,13	0,08	0,11	0,11	0,12	0,11	0,10	0,11	0,10	0,08	0,09	0,12
Al_2O_3	11,84	11,79	11,75	11,93	11,87	11,97	11,75	11,83	11,69	11,88	11,79	11,72	11,99	11,78	11,90	11,85	11,99	11,79
FeO	2,83	1,59	2,39	2,21	1,77	1,32	2,70	2,22	2,29	0,97	2,42	2,50	1,99	1,74	1,99	2,35	1,75	2,57
MnO	0,06	0,03	0,02	0,03	0,02	0,03	0,04	0,02	0,01	0,01	0,03	0,01	0,01	0,08	0,06	0,02	0,01	0,01
MgO	0,05	0,10	0,21	0,02	0,00	0,10	0,42	0,36	0,05	0,00	0,00	0,01	0,00	0,00	0,00	0,10	0,00	0,05
CaO	0,47	0,74	0,29	0,49	0,53	0,63	0,53	0,47	0,79	0,35	0,59	0,68	0,44	0,51	0,15	0,56	0,26	0,49
Na_2O	5,29	3,68	4,33	3,84	3,93	3,43	3,56	3,85	3,64	2,61	3,77	3,54	3,68	3,72	3,89	4,45	4,16	3,44
K_2O	2,85	5,14	4,16	5,06	5,20	5,41	5,06	5,12	4,93	7,05	5,26	5,06	5,45	5,32	4,98	4,16	4,88	5,01
P_2O_5	0,00	0,00	0,00	0,01	0,00	0,01	0,00	0,00	0,01	0,02	0,01	0,02	0,03	0,02	0,03	0,01	0,01	0,01
Cr_2O_3	0,03	0,04	0,04	0,04	0,04	0,03	0,03	0,04	0,05	0,05	0,04	0,05	0,04	0,04	0,04	0,05	0,04	0,03
NiO	0,00	0,00	0,00	0,00	0,00	0,00	0,00	0,00	0,01	0,01	0,01	0,01	0,02	0,01	0,01	0,00	0,01	0,00
LOI	1,13	0,92	0,63	0,69	0,96	0,92	0,78	0,66	0,84	0,62	0,59	0,95	0,63	0,66	0,64	0,58	0,62	1,03
H_2O^-	0,12	0,13	0,42	0,11	0,15	0,14	0,22	0,24	0,15	0,14	0,22	0,26	0,21	0,25	0,25	0,22	0,25	0,24
Total	99,52	99,66	99,55	99,23	99,12	99,95	99,26	99,94	99,82	99,78	100,05	100,13	100,13	100,30	100,41	99,96	99,86	99,50
CIPW NORMS																		
Q	31,34	32,84	32,53	31,54	30,98	33,72	32,23	31,63	33,14	33,32	31,41	33,22	31,90	32,78	33,43	31,85	32,03	33,60
or	17,11	30,81	24,97	30,39	31,33	32,34	30,52	30,63	29,49	42,05	31,28	30,21	32,43	31,62	29,58	24,75	29,14	30,14
ab	45,52	31,54	37,23	33,02	32,76	29,35	30,78	32,77	31,16	22,08	31,60	30,24	31,36	31,14	33,08	37,98	34,81	29,65
an	0,16	0,49	0,33	0,35	0,00	1,29	1,17	0,00	1,00	0,00	0,00	1,17	0,10	0,00	0,27	0,07	0,00	1,95
ns	0,00	0,00	0,00	0,00	0,00	0,00	0,00	0,00	0,00	0,00	0,00	0,00	0,00	0,00	0,00	0,00	0,00	0,00
di	1,96	2,83	0,94	1,84	2,39	1,59	1,34	2,08	2,53	1,43	2,55	1,88	1,70	2,15	0,30	2,36	1,10	0,40
hy	2,80	0,76	2,98	1,90	1,29	1,11	2,83	1,91	1,69	0,39	1,87	2,20	1,60	1,26	2,43	2,03	1,80	3,20
ac	0,00	0,00	0,00	0,00	1,01	0,00	0,00	0,19	0,00	0,18	0,49	0,00	0,00	0,45	0,00	0,00	0,66	0,00
mt	0,85	0,48	0,70	0,66	0,03	0,39	0,82	0,56	0,69	0,21	0,48	0,75	0,60	0,30	0,59	0,70	0,19	0,77
il	0,21	0,20	0,24	0,22	0,17	0,15	0,25	0,16	0,21	0,22	0,24	0,21	0,20	0,20	0,19	0,16	0,18	0,23
cm	0,05	0,06	0,06	0,06	0,05	0,04	0,05	0,05	0,07	0,07	0,06	0,07	0,06	0,06	0,06	0,07	0,06	0,04
ap	0,00	0,00	0,01	0,01	0,00	0,01	0,01	0,01	0,03	0,05	0,02	0,04	0,06	0,04	0,06	0,03	0,03	0,02
D.I.	93,97	95,18	94,73	94,95	95,07	95,41	93,53	95,03	93,79	97,45	94,29	93,67	95,69	95,55	96,10	94,59	95,98	93,39
MODAL ANALYSES																		
Quartz	32,72	34,83	34,18	33,28	33,18	35,37	-	33,61	34,22	35,41	-	35,40	33,72	34,88	34,96	33,64	33,86	35,03
Orthoclase	17,75	33,17	26,59	32,58	33,69	34,93	-	32,83	31,19	45,51	-	30,36	34,89	34,07	31,78	26,30	31,29	31,70
Plagioclase	44,87	30,05	36,08	31,08	31,17	28,55	-	30,54	30,19	19,09	-	29,55	28,99	29,21	31,29	36,43	33,34	29,27
Hornblende	4,69	1,96	3,18	3,08	1,98	1,16	-	3,03	4,40	0,00	-	4,71	2,42	1,87	1,98	3,64	1,53	3,13
Biotite	0,00	0,00	0,00	0,00	0,00	0,00	-	0,00	0,00	0,00	-	0,00	0,00	0,00	0,00	0,00	0,00	0,90

MAJOR ELEMENT ANALYSES OF FINE- TO MEDIUM-GRAINED KLIPKLOOF GRANITE

MAJOR ELEMENT ANALYSES OF ALBITIZED KLIPKLOOF GRANITE

Sample No.	GGr-257	GGr-258	GGr-259	GGr-213	GGr-236	GGr-300	VW4-93,35	VW4-96,0	GK-11	GK-14	GK-31	GK-32	GK-36	GK-37	GK-52	GGr-175	GGr-176	GGr-256
SiO_2	75,42	75,17	73,72	75,03	75,39	49,98	75,54	75,23	75,48	76,07	74,71	75,11	75,26	75,72	75,49	76,70	76,49	75,55
TiO_2	0,08	0,17	0,11	0,19	0,11	0,01	0,09	0,09	0,05	0,03	0,08	0,08	0,05	0,07	0,11	0,07	0,06	0,06
Al_2O_3	11,88	11,57	11,80	11,67	11,54	14,05	11,78	11,90	12,18	13,07	12,02	12,08	12,28	12,23	11,84	11,98	12,03	12,16
FeO	1,69	2,87	2,71	2,62	2,76	1,13	1,77	1,99	1,43	0,61	1,83	1,89	1,32	1,39	1,91	1,34	1,38	1,56
MnO	0,03	0,03	0,05	0,03	0,01	0,02	0,04	0,03	0,02	0,01	0,02	0,02	0,01	0,01	0,02	0,02	0,01	0,01
MgO	0,00	0,04	0,00	0,45	0,00	0,00	0,00	0,00	0,00	0,00	0,00	0,00	0,00	0,00	0,00	0,00	0,00	0,00
CaO	0,65	0,41	0,92	0,44	0,16	14,77	0,83	0,75	0,59	0,24	0,70	0,64	0,68	0,52	0,67	0,52	0,40	0,65
Na_2O	3,85	4,30	3,62	3,53	3,57	2,24	4,39	4,42	4,90	5,12	3,86	3,72	4,14	4,33	3,85	4,62	4,40	4,16
K_2O	5,25	4,06	5,17	5,07	5,18	8,58	4,95	4,87	4,53	5,20	5,00	5,00	4,75	4,63	5,14	4,28	4,49	4,73
P_2O_5	0,01	0,02	0,01	0,01	0,00	0,07	0,00	0,00	0,00	0,01	0,01	0,01	0,01	0,00	0,02	0,01	0,01	0,00
Cr_2O_3	0,04	0,05	0,05	0,04	0,04	0,01	0,04	0,05	0,03	0,04	0,03	0,03	0,03	0,02	0,04	0,03	0,03	0,04
NiO	0,00	0,01	0,00	0,00	0,00	0,02	0,00	0,00	0,00	0,00	0,00	0,00	0,00	0,00	0,00	0,00	0,00	0,01
LOI	0,74	0,67	0,87	0,40	0,54	4,35	0,75	0,65	0,38	0,39	0,81	0,78	0,71	0,63	0,63	0,35	0,32	0,65
H_2O^-	0,21	0,26	0,27	0,22	0,27	0,21	0,18	0,19	0,20	0,20	0,15	0,18	0,17	0,22	0,16	0,13	0,14	0,20
Total	99,85	99,63	99,30	99,70	99,57	95,44	100,36	100,17	99,79	100,99	99,22	99,54	99,41	99,77	99,88	100,05	99,76	99,78
							CIPW NORMS											
Q	31,71	32,87	30,72	33,34	33,46	-	31,13	30,37	30,33	28,38	31,70	32,87	31,82	31,71	31,95	32,58	32,72	31,89
or	31,36	24,30	31,12	30,35	31,01	-	29,43	28,95	26,98	30,59	30,06	30,01	28,47	27,68	30,67	25,39	26,73	28,24
ab	32,20	36,84	31,15	30,23	30,60	-	33,18	34,28	37,76	38,11	33,25	32,00	35,51	37,06	32,52	37,96	37,09	35,56
an	0,00	0,28	0,71	1,06	0,15	-	0,00	0,00	0,00	0,00	0,71	1,51	0,92	0,23	0,00	0,00	0,00	0,55
ns	0,00	0,00	0,00	0,00	0,00	-	0,69	0,45	0,72	1,06	0,00	0,00	0,00	0,00	0,00	0,08	0,00	0,00
di	2,87	1,51	3,46	0,99	0,54	-	3,67	3,32	2,62	1,01	2,49	1,49	2,19	2,12	2,87	2,28	1,76	2,41
hy	0,81	2,91	1,71	2,80	3,15	-	0,62	1,16	0,62	0,35	1,03	1,38	0,52	0,63	0,97	0,70	0,93	1,28
ac	0,61	0,00	0,00	0,00	0,00	-	1,06	1,21	0,82	0,37	0,00	0,00	0,00	0,00	0,29	0,80	0,37	0,00
mt	0,20	0,86	0,82	0,78	0,81	-	0,00	0,00	0,00	0,00	0,55	0,51	0,39	0,42	0,43	0,00	0,23	0,47
il	0,16	0,33	0,21	0,37	0,21	-	0,16	0,18	0,10	0,05	0,16	0,15	0,10	0,13	0,20	0,13	0,11	0,12
cm	0,06	0,07	0,07	0,06	0,06	-	0,05	0,07	0,05	0,06	0,04	0,05	0,04	0,04	0,06	0,05	0,05	0,06
ap	0,02	0,04	0,02	0,02	0,01	-	0,01	0,00	0,00	0,02	0,02	0,02	0,02	0,00	0,05	0,02	0,01	0,00
D.I.	95,27	94,00	93,00	93,92	95,08	-	93,74	93,60	95,06	97,08	95,01	94,88	95,81	96,44	95,14	95,94	96,54	95,68
							MODAL ANALYSES											
Quartz	33,90	34,33	-	34,86	35,83	-	-	32,22	31,67	28,85	33,39	-	-	33,41	33,99	34,43	-	33,55
Orthoclase	33,74	25,74	-	32,24	31,54	-	-	30,97	28,90	32,80	32,26	-	-	29,71	32,93	27,20	-	30,29
Plagioclase	30,38	35,31	-	28,93	28,65	-	-	33,92	38,43	38,37	31,86	-	-	35,84	30,51	37,46	-	34,42
Hornblende	2,00	4,64	-	3,44	0,68	-	-	2,91	1,03	0,00	2,50	-	-	1,07	2,59	0,92	-	1,76
Biotite	0,00	0,00	-	0,55	3,32	-	-	0,00	0,00	0,00	0,00	-	-	0,00	0,00	0,00	-	0,00

VIII

MAJOR ELEMENT ANALYSES OF ROOIBERG FELSITE

Sample No.	F-60	F-61	F-62	F-63	F-65	F-66	F-67	F-68	F-71	GR-236	GR-264	GR-265	GR-267	GR-269	GR-270	GR-155F
SiO_2	70,38	69,94	70,04	70,44	70,88	71,03	70,71	67,04	71,79	69,05	70,20	69,55	67,80	68,11	67,77	72,28
TiO_2	0,35	0,33	0,35	0,35	0,34	0,34	0,34	0,52	0,34	0,35	0,35	0,34	0,51	0,53	0,53	0,34
Al_2O_3	11,27	11,07	11,28	11,32	11,55	11,38	11,37	12,00	11,49	11,56	11,66	11,57	11,80	11,90	11,83	11,52
FeO	6,31	4,51	5,04	5,17	5,51	5,96	5,57	8,31	5,21	6,87	6,46	6,54	7,86	7,16	7,34	5,50
MnO	0,05	0,13	0,13	0,11	0,08	0,06	0,09	0,16	0,08	0,17	0,14	0,18	0,15	0,12	0,12	0,11
MgO	0,03	0,22	0,16	0,05	0,00	0,06	0,02	0,19	0,01	0,09	0,02	0,12	0,19	0,30	0,30	0,07
CaO	0,85	2,32	1,89	1,49	1,15	1,01	1,25	1,88	1,47	1,49	1,87	1,49	2,31	2,16	2,33	1,44
Na_2O	4,09	3,39	3,02	3,30	3,04	3,92	3,76	4,63	4,49	3,66	3,49	3,53	3,36	4,61	3,54	3,69
K_2O	4,69	4,07	4,43	4,77	5,09	4,42	4,56	3,45	4,08	4,61	4,70	4,78	4,15	3,49	4,41	4,40
P_2O_5	0,05	0,04	0,05	0,04	0,05	0,05	0,05	0,13	0,05	0,05	0,07	0,07	0,14	0,14	0,15	0,04
Cr_2O_3	0,04	0,02	0,03	0,03	0,04	0,03	0,03	0,03	0,04	0,03	0,05	0,03	0,04	0,05	0,04	0,04
NiO	0,00	0,00	0,00	0,00	0,00	0,00	0,00	0,00	0,00	0,00	0,01	0,01	0,01	0,00	0,01	0,01
LOI	0,51	2,71	2,00	1,43	0,85	0,29	0,75	0,30	0,02	0,46	0,13	0,55	0,31	0,19	0,22	0,29
H_2O^-	0,15	0,25	0,32	0,18	0,18	0,23	0,20	0,06	0,15	0,12	0,10	0,19	0,12	0,15	0,11	0,16
Total	98,77	99,00	98,74	98,68	98,76	98,78	98,70	98,70	99,22	98,51	99,25	98,95	98,75	98,91	98,70	99,89

CIPW NORMS

Q	24,91	29,84	30,63	28,91	29,45	27,15	27,34	19,97	26,01	24,59	25,95	25,27	24,62	21,32	23,03	28,99
or	28,22	25,04	27,15	29,00	30,75	26,27	27,53	20,73	24,29	27,78	27,98	28,72	24,93	20,91	26,47	26,11
ab	32,55	29,84	26,48	28,74	26,25	33,69	32,49	39,74	36,71	31,58	29,78	30,38	28,88	39,48	30,44	31,32
an	0,00	3,10	4,29	2,07	2,92	0,41	0,71	1,80	0,00	1,52	2,30	1,64	4,93	1,49	3,40	1,90
ns	0,00	0,00	0,00	0,00	0,00	0,00	0,00	0,00	0,00	0,00	0,00	0,00	0,00	0,00	0,00	0,00
di	3,56	7,54	4,50	4,69	2,31	3,91	4,70	6,04	6,28	5,01	5,91	4,82	5,14	7,41	6,47	4,42
hy	6,86	2,46	4,57	4,22	5,82	5,65	4,70	7,88	3,64	6,59	5,25	6,34	7,79	5,81	6,57	4,80
ac	2,35	0,00	0,00	0,00	0,00	0,00	0,00	0,00	1,40	0,00	0,00	0,00	0,00	0,00	0,00	0,00
mt	0,71	1,38	1,54	1,56	1,67	1,79	1,69	2,49	0,85	2,07	1,93	1,97	2,36	2,15	2,20	1,64
il	0,67	0,66	0,70	0,68	0,67	0,66	0,67	1,00	0,65	0,68	0,67	0,66	0,99	1,02	1,02	0,66
cm	0,05	0,04	0,04	0,05	0,05	0,05	0,05	0,04	0,06	0,04	0,07	0,04	0,05	0,07	0,06	0,06
ap	0,11	0,10	0,12	0,09	0,11	0,11	0,13	0,31	0,11	0,13	0,16	0,15	0,32	0,33	0,35	0,10
D.I.	85,68	84,72	84,26	86,65	86,45	87,41	87,35	80,44	87,01	83,95	83,72	84,37	78,43	81,71	79,93	86,42

MODAL ANALYSES

Quartz	-	32,72	32,59	30,65	31,64	29,90	29,44	22,06	28,41	26,98	27,64	27,49	-	23,11	25,01	-
Orthoclase	-	25,41	27,77	30,31	30,08	25,34	27,96	19,03	25,18	27,19	28,90	28,76	-	21,02	26,78	-
Plagioclase	-	30,84	27,86	27,17	25,84	31,09	29,70	37,97	34,44	29,03	27,69	27,88	-	37,58	29,76	-
Hornblende	-	11,05	11,79	11,90	8,47	9,19	11,39	17,86	11,98	13,73	15,79	13,69	-	18,32	18,47	-
Biotite	-	0,00	0,00	0,00	4,00	4,50	1,54	3,10	0,00	3,09	0,00	2,20	-	0,00	0,00	-

IX MAJOR ELEMENT ANALYSES OF STAVOREN MICROGRANOPHYRE

Sample No.	GRF-2	GR-133	GR-220	GR-221	GR-225	GR-229	GR-230	GR-231	GR-234	GR-240	GR-134	GR-135	GR-241	GR-242
SiO_2	73,52	73,49	73,22	72,96	72,94	73,48	73,47	73,46	72,84	73,60	73,79	73,77	74,02	73,61
TiO_2	0,25	0,25	0,25	0,24	0,24	0,24	0,25	0,24	0,25	0,24	0,24	0,25	0,24	0,24
Al_2O_3	11,60	11,65	11,60	11,75	11,82	11,63	11,77	11,65	11,50	11,70	11,59	11,57	11,68	11,53
FeO	3,47	3,31	3,87	4,35	4,35	3,44	3,48	3,56	4,07	3,55	3,89	3,86	3,34	3,41
MnO	0,08	0,11	0,05	0,08	0,08	0,12	0,10	0,08	0,08	0,06	0,13	0,09	0,03	0,05
MgO	0,10	0,00	0,00	0,00	0,00	0,00	0,00	0,00	0,00	0,00	0,00	0,03	0,00	0,01
CaO	0,62	0,85	0,84	0,40	0,39	0,71	0,59	0,62	0,52	0,62	0,52	0,70	0,43	0,48
Na_2O	3,62	3,93	3,47	3,35	4,04	3,74	3,50	3,67	2,26	3,82	3,23	3,06	3,63	3,10
K_2O	5,25	5,36	5,40	5,01	5,01	5,36	5,34	5,38	6,96	5,16	5,39	5,74	5,35	5,56
P_2O_5	0,01	0,01	0,01	0,02	0,02	0,01	0,01	0,02	0,01	0,02	0,03	0,02	0,03	0,02
Cr_2O_3	0,03	0,03	0,04	0,04	0,04	0,04	0,02	0,02	0,03	0,03	0,04	0,03	0,03	0,03
NiO	0,00	0,00	0,00	0,00	0,00	0,00	0,00	0,00	0,01	0,00	0,01	0,02	0,00	0,00
LOI	0,51	0,24	0,41	0,50	0,48	0,43	0,47	0,41	0,43	0,43	0,41	0,36	0,41	0,64
H_2O	0,13	0,08	0,10	0,10	0,12	0,11	0,16	0,17	0,06	0,12	0,09	0,12	0,13	0,20
Total	99,19	99,31	99,26	98,80	99,53	99,31	99,16	99,28	99,02	99,35	99,36	99,62	99,32	98,88
CIPW NORMS														
Q	30,03	28,42	29,62	31,56	27,75	29,00	30,36	29,34	30,46	29,42	31,66	31,09	30,52	32,22
or	31,43	31,96	32,32	30,13	29,91	32,05	32,01	32,17	41,74	30,87	32,22	34,20	31,96	33,51
ab	30,87	30,37	29,70	28,81	33,20	30,34	30,02	30,36	19,35	31,77	27,59	26,07	30,67	26,76
an	0,00	0,00	0,12	1,90	0,00	0,00	0,64	0,00	0,71	0,00	1,22	0,90	0,00	1,14
ns	0,00	0,23	0,00	0,00	0,00	0,00	0,00	0,00	0,00	0,00	0,00	0,00	0,00	0,00
di	2,71	3,72	3,60	0,00	1,67	3,11	1,98	2,69	1,63	2,67	1,09	2,20	1,76	1,04
hy	3,28	2,78	2,93	5,61	5,02	3,18	3,40	3,36	4,34	3,26	4,48	3,83	3,31	3,77
ac	0,17	1,97	0,00	0,00	1,20	1,46	0,00	0,92	0,00	0,84	0,00	0,00	0,38	0,00
mt	0,96	0,00	1,15	1,31	0,70	0,30	1,04	0,61	1,22	0,63	1,17	1,15	0,81	1,03
il	0,48	0,48	0,47	0,46	0,46	0,47	0,48	0,47	0,47	0,46	0,46	0,47	0,46	0,45
cm	0,04	0,04	0,05	0,05	0,05	0,06	0,04	0,04	0,04	0,05	0,05	0,05	0,05	0,04
ap	0,02	0,03	0,03	0,04	0,04	0,02	0,03	0,04	0,03	0,04	0,06	0,05	0,07	0,04
D.I.	92,34	90,75	91,64	90,49	90,87	91,39	92,39	91,88	91,55	92,06	91,47	91,35	93,15	92,49
MODAL ANALYSES														
Quartz	-	-	31,62	33,91	31,05	31,42	-	-	33,37	31,51	33,87	33,24	33,00	34,23
Orthoclase	-	-	34,4	28,59	28,87	34,20	-	-	42,75	32,87	32,64	35,58	32,79	34,56
Plagioclase	-	-	26,35	28,87	31,58	28,05	-	-	15,91	29,23	25,94	23,57	28,34	24,98
Hornblende	-	-	7,65	2,28	3,01	6,35	-	-	3,84	6,42	4,16	5,75	3,24	3,69
Biotite	-	-	0,00	6,38	5,51	0,00	-	-	4,16	0,00	3,40	1,89	2,65	2,56

MAJOR ELEMENT ANALYSES OF STAVOREN GRANOPHYRE

Sample No.	GR-43	GR-84	GGr-10
SiO_2	74,29	73,02	74,14
TiO_2	0,24	0,24	0,27
Al_2O_3	12,02	11,80	11,57
FeO	3,10	3,88	3,04
MnO	0,08	0,08	0,05
MgO	0,00	0,00	0,07
CaO	0,97	1,16	0,42
Na_2O	4,00	3,87	3,30
K_2O	5,26	4,74	5,01
P_2O_5	0,02	0,02	0,01
Cr_2O_3	0,03	0,03	0,03
NiO	0,00	0,00	0,00
LOI	0,25	0,43	0,93
H_2O	0,15	0,15	0,17
Total	100,41	99,42	99,01
CIPW NORMS			
Q	28,28	29,14	33,82
or	31,05	28,35	30,22
ab	32,54	33,12	28,52
an	0,00	0,84	1,99
ns	0,00	0,00	0,00
di	4,14	4,13	0,03
hy	1,97	2,70	3,91
ac	1,12	0,00	0,00
mt	0,36	1,15	0,92
il	0,46	0,47	0,52
cm	0,04	0,05	0,05
ap	0,05	0,04	0,03
D.I.	91,87	90,61	92,56
MODAL ANALYSES			
Quartz	30,67	30,86	35,62
Orthoclase	33,12	29,98	30,85
Plagioclase	30,42	31,01	28,48
Hornblende	5,81	8,17	2,40
Biotite	0,00	0,00	2,67

X MAJOR ELEMENT ANALYSES OF STAVOREN GRANOPHYRE

Sample No.	GGr-93	GGr-94	GGr-96	GG-54	GG-55	GG-57	GR-69	GR-70	GR-132A	GR-132	GR-150	GR-151	GR-262	GR-263	GR-266	GR-268	GR-155G
SiO_2	73,86	73,92	75,00	74,49	74,48	74,34	73,69	73,95	77,78	73,92	74,30	73,54	73,11	73,46	74,71	73,47	74,24
TiO_2	0,24	0,23	0,24	0,26	0,24	0,26	0,23	0,23	0,02	0,24	0,23	0,24	0,25	0,23	0,24	0,23	0,29
Al_2O_3	11,57	11,57	11,59	11,69	11,97	11,61	11,47	11,57	11,47	11,64	11,53	11,60	11,54	11,32	11,58	11,31	11,47
FeO	3,33	3,16	3,04	3,17	2,95	3,43	3,17	3,13	0,65	3,39	3,08	3,70	4,05	3,80	3,06	3,61	3,47
MnO	0,06	0,06	0,02	0,03	0,02	0,07	0,07	0,07	0,02	0,06	0,04	0,08	0,08	0,13	0,06	0,06	0,05
MgO	0,00	0,04	0,07	0,05	0,62	0,00	0,00	0,00	0,00	0,00	0,00	0,00	0,02	0,00	0,00	0,02	0,00
CaO	0,83	0,83	0,44	0,56	0,25	0,70	0,79	0,90	0,25	0,65	0,91	0,80	0,46	0,92	0,67	0,79	0,79
Na_2O	3,57	3,60	3,71	3,77	3,23	3,68	3,69	3,84	3,81	3,96	3,89	3,82	3,18	2,67	3,85	3,57	3,43
K_2O	5,29	4,56	5,06	5,06	5,28	5,18	5,07	4,93	5,15	5,15	4,89	5,19	5,87	6,24	4,94	4,93	5,51
P_2O_5	0,01	0,01	0,02	0,02	0,03	0,01	0,02	0,02	0,01	0,02	0,02	0,02	0,02	0,03	0,02	0,02	0,03
Cr_2O_3	0,03	0,02	0,04	0,04	0,04	0,05	0,03	0,04	0,03	0,05	0,05	0,05	0,05	0,05	0,05	0,04	0,05
NiO	0,00	0,00	0,01	0,02	0,01	0,01	0,00	0,01	0,00	0,01	0,01	0,01	0,02	0,01	0,00	0,00	0,00
LOI	0,64	1,14	0,50	0,31	0,64	0,33	0,70	0,72	0,22	0,29	0,36	0,32	0,30	0,55	0,35	0,95	0,30
H_2O^-	0,12	0,12	0,21	0,13	0,19	0,12	0,17	0,19	0,02	0,12	0,11	0,09	0,09	0,14	0,15	0,19	0,21
Total	99,55	99,26	99,95	99,60	99,95	99,79	99,10	99,60	99,43	99,50	99,42	99,46	99,04	99,55	99,68	99,19	99,84
								CIPW NORMS									
Q	30,43	33,07	31,74	31,05	32,81	30,65	30,79	30,47	36,44	29,10	30,69	28,96	29,74	31,10	31,30	31,47	30,73
or	31,63	27,46	29,98	30,15	31,46	30,81	30,46	29,51	30,69	30,67	29,18	30,93	35,16	37,29	29,40	29,69	32,75
ab	30,42	31,03	31,51	32,16	27,52	31,04	31,30	32,47	30,54	31,49	32,42	31,05	26,98	22,84	32,33	30,75	28,49
an	0,00	2,03	1,01	0,02	1,07	0,00	0,00	0,00	0,00	0,00	0,00	0,00	0,00	0,48	0,00	0,29	0,00
ns	0,00	0,00	0,00	0,00	C-0,56	0,00	0,00	0,00	0,34	0,00	0,00	0,00	0,00	0,00	0,00	0,00	0,00
di	3,67	1,88	0,93	2,34	0,00	3,04	3,46	3,89	1,08	2,83	3,98	3,46	1,94	3,51	2,90	3,18	3,34
hy	2,25	3,07	3,36	2,74	5,12	2,71	2,30	1,98	0,39	3,31	1,89	3,24	4,24	3,08	2,37	2,97	2,63
ac	0,15	0,00	0,00	0,00	0,00	0,24	0,41	0,38	0,39	2,03	0,72	1,36	0,22	0,00	0,43	0,00	0,64
mt	0,92	0,95	0,91	0,95	0,88	0,90	0,75	0,75	0,00	0,00	0,56	0,42	1,11	1,14	0,70	1,09	0,71
il	0,47	0,45	0,46	0,49	0,46	0,49	0,44	0,44	0,05	0,46	0,45	0,46	0,48	0,43	0,46	0,44	0,56
cm	0,04	0,04	0,06	0,05	0,06	0,07	0,04	0,06	0,04	0,08	0,07	0,07	0,07	0,07	0,07	0,06	0,08
ap	0,02	0,02	0,04	0,05	0,06	0,03	0,04	0,05	0,02	0,04	0,04	0,05	0,05	0,07	0,04	0,05	0,07
D.I.	92,49	91,56	93,22	93,36	91,78	92,51	92,55	92,45	97,68	91,26	92,29	90,94	91,88	91,23	93,03	91,91	91,98
								MODAL ANALYSES									
Quartz	32,52	30,76	33,48	32,86	35,24	32,64	32,90	-	37,73	-	32,87	31,31	32,78	33,27	33,27	33,33	-
Orthoclase	33,75	29,01	31,15	32,17	31,28	32,85	32,48	-	33,06	-	31,07	32,89	35,37	39,97	31,35	31,55	-
Plagioclase	27,48	34,44	30,26	29,52	28,69	28,23	28,74	-	29,22	-	30,27	28,67	24,01	19,10	30,02	28,04	-
Hornblende	6,27	5,81	3,42	5,48	0,39	6,31	5,89	-	0,00	-	5,80	7,14	3,52	7,68	5,37	7,10	-
Biotite	0,00	0,00	1,72	0,00	4,43	0,00	0,00	-	0,00	-	0,00	0,00	4,36	0,00	0,00	0,00	-

XI MAJOR ELEMENT ANALYSES OF META FELSITE

Sample No.	GR-10	GR-12	GR-41	GR-48	GR-49	GRL-52	GR-53	GR-55	GR-58	GR-59	GR-60	GR-61	GR-62	GR-66	GR-68	GR-70	GR-71	GR-72
SiO_2	69,65	73,35	66,31	65,48	73,34	66,13	72,87	70,84	73,43	72,14	71,78	70,32	69,92	73,88	71,63	71,31	70,18	68,45
TiO_2	0,36	0,22	0,73	0,74	0,25	0,73	0,28	0,43	0,48	0,50	0,37	0,53	0,46	0,23	0,37	0,48	0,23	0,46
Al_2O_3	12,20	12,34	11,96	12,04	11,66	11,95	11,89	11,86	11,32	12,32	11,58	11,29	11,82	11,18	11,51	12,03	15,12	11,82
FeO	5,64	3,33	8,42	10,22	3,97	8,50	3,86	6,20	3,84	3,65	5,28	6,95	5,79	4,16	5,35	4,52	1,85	7,23
MnO	0,10	0,05	0,12	0,10	0,06	0,12	0,07	0,09	0,04	0,05	0,10	0,05	0,05	0,05	0,10	0,11	0,05	0,14
MgO	0,23	0,17	0,23	0,42	0,00	0,38	0,00	0,27	1,10	0,89	0,02	1,02	0,33	0,00	0,00	0,74	0,35	0,35
CaO	2,12	1,56	2,28	2,60	0,83	2,83	1,00	1,80	1,22	1,68	1,22	1,52	1,32	0,92	1,41	1,83	1,58	1,89
Na_2O	3,18	3,35	3,46	5,03	3,76	4,37	3,81	3,24	3,10	2,56	3,95	2,22	3,31	3,28	3,88	2,77	6,47	4,26
K_2O	5,05	4,28	4,11	3,16	4,86	3,59	4,84	4,27	3,86	4,54	4,66	4,28	5,48	4,97	4,63	4,52	3,12	4,52
P_2O_5	0,07	0,04	0,18	0,20	0,02	0,19	0,02	0,13	0,13	0,13	0,07	0,14	0,14	0,02	0,05	0,12	0,11	0,14
Cr_2O_3	0,03	0,04	0,05	0,03	0,03	0,02	0,04	0,04	0,07	0,05	0,04	0,07	0,03	0,03	0,03	0,06	0,03	0,02
NiO	0,00	0,00	0,00	0,00	0,00	0,00	0,01	0,01	0,00	0,01	0,01	0,01	0,00	0,00	0,00	0,01	0,00	0,00
LOI	0,42	0,44	0,35	0,15	0,82	0,13	0,33	0,32	0,71	0,80	0,17	0,69	0,33	0,37	0,23	0,62	0,56	0,11
H_2O	0,13	0,13	0,23	0,13	0,16	0,05	0,17	0,13	0,16	0,18	0,17	0,17	0,12	0,14	0,11	0,14	0,21	0,11
Total	99,18	99,30	98,43	100,30	99,76	98,99	99,19	99,63	99,46	99,50	99,42	99,26	99,10	99,23	99,30	99,26	99,86	99,50
										CIPW NORMS								
Q	25,53	32,85	22,60	15,81	30,30	18,61	18,61	29,10	35,23	33,90	26,92	33,31	24,86	32,57	27,06	31,50	17,09	20,07
or	30,22	25,60	24,80	18,83	29,20	21,42	21,42	25,43	23,14	27,21	27,75	25,69	32,79	29,74	27,61	27,09	18,61	26,85
ab	27,26	28,69	29,89	42,87	32,34	37,39	37,39	27,58	26,55	22,00	33,73	19,03	28,35	28,08	33,11	23,73	55,20	35,87
an	4,16	6,06	5,04	0,97	0,57	2,41	2,41	5,25	5,33	7,58	0,10	6,70	1,24	1,11	0,34	7,16	3,06	0,00
ns	0,00	0,00	0,00	0,00	0,00	0,00	0,00	0,00	C-0,12	C-0,45	0,00	C-0,60	0,00	0,00	0,00	0,00	0,00	0,00
di	5,29	1,29	4,69	9,46	3,10	9,25	9,25	2,54	0,00	0,00	4,94	0,00	3,95	3,00	5,68	1,09	3,54	7,47
hy	4,94	3,93	8,51	7,40	2,85	6,50	6,50	7,08	7,17	6,39	4,06	11,11	5,84	3,71	3,71	6,77	1,22	6,17
ac	0,00	0,00	0,00	0,00	0,00	0,00	0,00	0,00	0,00	0,00	0,00	0,00	0,00	0,00	0,00	0,00	0,00	0,35
mt	1,69	1,00	2,54	2,75	1,07	2,54	2,54	1,85	1,15	1,10	1,58	2,09	1,73	1,25	1,60	1,36	0,54	1,97
il	0,70	0,42	1,42	1,42	0,49	1,39	1,39	0,81	0,92	0,97	0,71	1,02	0,89	0,43	0,71	0,92	0,43	0,88
cm	0,04	0,05	0,07	0,05	0,04	0,03	0,03	0,06	0,10	0,08	0,06	0,11	0,04	0,05	0,05	0,10	0,05	0,03
ap	0,17	0,10	0,44	0,46	0,04	0,45	0,45	0,30	0,29	0,31	0,15	0,34	0,32	0,06	0,12	0,28	0,25	0,33
D.I.	83,01	87,14	77,30	77,50	91,84	77,42	90,69	82,11	84,92	83,12	88,40	78,03	85,99	90,39	87,79	82,32	90,90	82,79
										MODAL ANALYSES								
Quartz	27,73	33,89	25,16	-	31,99	20,95	-	31,18	37,35	33,93	28,88	34,21	27,09	34,28	29,02	32,57	19,63	22,77
Orthoclase	31,01	26,24	22,08	-	31,01	20,92	-	24,11	23,08	28,23	29,06	22,03	33,89	31,12	28,88	27,90	18,45	27,63
Plagioclase	27,81	33,21	31,83	-	30,06	36,14	-	30,24	31,69	29,82	30,32	25,69	25,58	25,86	29,84	29,09	59,47	31,81
Hornblende	13,46	6,67	16,31	-	6,97	22,01	-	11,50	6,72	8,04	11,77	10,67	12,05	8,01	12,28	10,46	2,47	17,80
Biotite	0,00	0,00	4,64	-	0,00	0,00	-	2,99	1,18	0,00	0,00	7,42	1,41	0,76	0,00	0,00	0,00	0,00

XII

	MAJOR ELEMENT ANALYSES OF META FELSITE							
Sample No.	GR-73	GR-80	GR-81	GR-82A	GR-82B	GR-85	GR-86	GR-103
SiO_2	70,79	64,74	68,02	68,44	67,87	67,06	66,92	69,82
TiO_2	0,39	0,79	0,66	0,61	0,66	0,68	0,67	0,59
Al_2O_3	11,73	12,03	12,61	11,59	12,21	12,51	12,11	11,42
FeO	6,11	9,44	7,28	7,40	7,07	7,74	7,96	6,78
MnO	0,08	0,16	0,05	0,06	0,07	0,06	0,12	0,06
MgO	0,13	0,84	0,16	0,36	0,45	0,42	0,49	0,17
CaO	1,47	3,35	1,96	1,23	1,65	2,39	2,27	1,61
Na_2O	3,57	4,06	5,15	5,76	4,75	5,06	4,76	5,16
K_2O	4,28	3,27	3,39	3,86	3,00	3,09	3,90	2,94
P_2O_5	0,09	0,25	0,18	0,15	0,15	0,17	0,16	0,15
Cr_2O_3	0,04	0,02	0,04	0,04	0,02	0,03	0,02	0,03
NiO	0,01	0,00	0,01	0,00	0,00	0,01	0,00	0,00
LOI	0,44	0,17	0,14	0,17	0,61	0,36	0,26	0,48
H_2O^-	0,18	0,13	0,13	0,28	0,17	0,11	0,12	0,15
Total	99,31	99,25	99,78	99,95	98,68	99,69	99,76	99,36
	CIPW NORMS							
Q	28,15	18,00	18,87	18,29	22,47	18,30	17,01	23,54
or	25,60	19,48	20,09	22,89	18,09	18,35	23,17	17,62
ab	30,56	34,66	43,69	38,26	40,99	43,05	40,45	42,89
an	3,39	5,01	1,32	0,00	3,20	2,35	0,16	0,00
ns	0,00	0,00	0,00	1,31	0,00	0,00	0,00	0,00
di	3,00	8,83	6,44	4,54	3,62	7,41	8,86	6,31
hy	6,44	9,10	5,70	8,74	7,83	6,49	6,30	5,52
ac	0,00	0,00	0,00	4,40	0,00	0,00	0,00	1,19
mt	1,83	2,80	2,16	0,00	2,13	2,30	2,36	1,40
il	0,76	1,51	1,26	1,16	1,27	1,30	1,27	1,14
cm	0,05	0,03	0,05	0,06	0,03	0,04	0,04	0,04
ap	0,22	0,59	0,41	0,35	0,36	0,40	0,38	0,34
D.I.	84,31	72,13	82,65	79,44	81,55	79,69	80,63	84,05
	MODAL ANALYSES							
Quartz	30,29	20,73	20,15	20,01	24,73	-	-	25,60
Orthoclase	24,40	18,11	20,08	23,21	15,63	-	-	17,52
Plagioclase	31,11	36,39	41,93	40,07	42,67	-	-	41,05
Hornblende	10,79	24,79	17,86	16,72	13,16	-	-	15,85
Biotite	3,43	0,00	0,00	0,00	3,83	-	-	0,00

	MAJOR ELEMENT ANALYSES OF GRANODIORITE (DIEPKLOOF GRANOPHYRE)			
Sample No.	GR-67	GR-78	GR-79	GR-200
SiO_2	63,73	65,60	63,58	64,99
TiO_2	0,68	0,62	0,71	0,69
Al_2O_3	13,16	12,95	13,36	13,38
FeO	9,36	8,17	9,73	8,00
MnO	0,16	0,17	0,19	0,12
MgO	0,39	0,24	0,00	0,00
CaO	3,17	2,60	3,34	2,68
Na_2O	4,77	4,11	3,97	4,13
K_2O	3,07	4,12	3,52	3,52
P_2O_5	0,06	0,05	0,08	0,07
Cr_2O_3	0,02	0,02	0,02	0,03
NiO	0,00	0,00	0,02	0,00
LOI	0,54	0,51	0,30	0,73
H_2O^-	0,13	0,14	0,17	0,20
Total	99,24	99,30	98,99	98,54
	CIPW NORMS			
Q	14,04	17,38	16,49	19,08
or	18,40	24,63	21,05	21,26
ab	40,89	35,23	34,03	35,76
an	5,47	4,77	8,38	7,73
ns	0,00	0,00	0,00	0,00
di	8,86	7,01	7,01	4,83
hy	8,06	7,19	7,19	7,36
ac	0,00	0,00	0,00	0,00
mt	2,80	2,45	2,92	2,42
il	1,31	1,19	1,36	1,35
cm	0,03	0,04	0,03	0,04
ap	0,15	0,12	0,19	0,17
D.I.	73,33	77,25	71,58	76,10
	MODAL ANALYSES			
Quartz	16,09	19,49	17,09	-
Orthoclase	16,75	23,70	19,26	-
Plagioclase	42,92	36,27	38,39	-
Hornblende	24,15	19,50	24,56	-
Biotite	0,11	1,06	0,74	-

	MAJOR ELEMENT ANALYSES OF ANOMALOUS GRANITES						
Sample No.	GR-45	GR-160	GGr-107	GGr-140	GGr-191	GGr-215	VW4-50,8
SiO_2	75,58	75,75	75,15	72,12	69,88	77,80	76,75
TiO_2	0,14	0,13	0,24	0,25	0,43	0,19	0,04
Al_2O_3	11,69	11,35	10,85	12,31	11,83	10,01	12,76
FeO	2,14	2,66	1,81	3,92	6,94	2,80	1,60
MnO	0,04	0,06	0,05	0,06	0,08	0,07	0,02
MgO	0,00	0,01	1,08	0,81	0,25	0,31	0,00
CaO	0,27	1,67	4,29	1,65	2,13	0,21	0,26
Na_2O	2,71	4,24	3,93	3,17	2,97	2,20	8,93
K_2O	6,15	3,13	0,89	4,45	3,79	4,97	0,44
P_2O_5	0,04	0,03	0,00	0,06	0,06	0,03	0,01
Cr_2O_3	0,01	0,04	0,04	0,03	0,03	0,05	0,04
NiO	0,00	0,00	0,00	0,00	0,01	0,01	0,00
LOI	0,35	0,37	0,97	0,78	0,89	0,63	0,44
H_2O^-	0,24	0,14	0,11	0,15	0,15	0,27	0,22
Total	99,36	99,58	99,41	99,76	99,44	99,55	101,51
	CIPW NORMS						
Q	-	35,55	40,35	30,49	30,37	44,09	28,24
or	-	18,68	5,35	26,61	22,76	29,74	2,61
ab	-	36,18	33,81	27,13	25,51	18,90	62,60
an	-	2,73	9,48	6,27	7,86	0,89	0,00
ns	-	0,00	0,00	0,00	0,00	C-0,69	2,60
di	-	4,84	9,90	1,36	2,17	0,00	1,09
hy	-	0,84	0,00	6,30	8,25	4,33	1,77
ac	-	0,00	0,00	0,00	0,00	0,00	0,95
mt	-	0,79	0,55	1,17	2,08	0,84	0,00
il	-	0,25	0,46	0,48	0,82	0,37	0,08
cm	-	0,05	0,06	0,05	0,04	0,07	0,06
ap	-	0,08	0,00	0,14	0,14	0,07	0,02
D.I.	-	90,41	79,52	84,24	78,64	92,74	93,45
	MODAL ANALYSES						
Quartz	-	37,94	-	32,26	31,18	46,11	26,61
Orthoclase	-	18,68	-	27,33	21,23	29,52	1,85
Plagioclase	-	38,50	-	31,71	30,57	20,05	70,64
Hornblende	-	4,90	-	8,71	14,63	0,00	0,92
Biotite	-	0,00	-	0,00	2,40	4,34	0,00

XIII MAJOR ELEMENT ANALYSES OF PSEUDO-GRANOPHYRE

Sample No.	GR-56	GR-57	GR-114	GR-162	GR-163	GR-1	GR-212	GR-249
SiO_2	71,13	70,90	74,17	74,31	74,51	71,21	74,39	75,11
TiO_2	0,37	0,39	0,24	0,27	0,26	0,38	0,26	0,24
Al_2O_3	11,82	11,65	11,79	11,95	11,73	11,64	11,69	11,68
FeO	5,54	5,47	3,17	3,53	3,27	4,99	3,07	2,89
MnO	0,12	0,10	0,05	0,05	0,05	0,08	0,07	0,07
MgO	0,00	0,02	0,00	0,00	0,00	0,00	0,00	0,00
CaO	1,45	1,62	0,80	0,86	0,85	1,55	1,05	1,08
Na_2O	4,29	4,42	4,08	3,94	3,87	3,96	3,56	3,78
K_2O	4,44	4,48	4,98	4,62	4,72	4,88	5,15	4,82
P_2O_5	0,05	0,05	0,02	0,03	0,03	0,04	0,01	0,01
Cr_2O_3	0,04	0,03	0,03	0,04	0,04	0,03	0,00	0,00
NiO	0,00	0,00	0,00	0,00	0,00	0,00	0,01	0,00
LOI	0,17	0,18	0,35	0,25	0,31	0,35	0,21	0,42
H_2O^-	0,23	0,10	0,12	0,17	0,22	0,13	0,13	0,12
Total	99,65	99,41	99,80	100,02	99,86	99,24	99,60	100,22
			CIPW NORMS					
Q	24,75	23,67	29,12	30,66	31,31	25,5	-	-
or	26,39	26,68	29,64	27,38	28,08	29,18	-	-
ab	36,36	35,27	33,12	33,47	32,91	33,07	-	-
an	0,00	0,00	0,00	1,29	0,70	0,00	-	-
ns	0,00	0,00	0,00	0,00	0,00	0,00	-	-
di	6,20	6,95	3,45	2,53	2,96	6,68	-	-
hy	3,68	3,82	2,47	3,00	2,43	2,87	-	-
ac	0,19	2,15	1,44	0,00	0,00	0,70	-	-
mt	1,54	0,55	0,22	1,05	0,98	1,14	-	-
il	0,71	0,76	0,46	0,51	0,50	0,72	-	-
cm	0,06	0,04	0,04	0,05	0,06	0,04	-	-
ap	0,11	0,11	0,04	0,06	0,07	0,10	-	-
D.I.	87,51	85,62	91,88	91,51	92,30	87,74	-	-
			MODAL ANALYSES					
Quartz	26,90	26,45	31,42	31,95	32,87	27,93	-	-
Orthoclase	27,47	27,76	31,55	29,00	29,85	30,65	-	-
Plagioclase	33,04	33,04	31,32	32,18	31,11	29,91	-	-
Hornblende	12,61	12,77	5,73	6,89	6,19	11,35	-	-
Biotite	0,00	0,00	0,00	0,00	0,00	0,00	-	-

MAJOR ELEMENT ANALYSES OF PRE-BUSHVELD SILLS

Sample No.	GH-29	GH-148	GH-202	GH-152	GH-204	GH-216	GH-253
SiO_2	48,02	52,15	51,04	48,84	52,77	51,01	48,65
TiO_2	0,79	0,32	0,68	1,00	0,60	0,60	1,38
Al_2O_3	16,28	10,26	15,26	13,91	9,83	8,72	12,43
FeO	12,84	9,73	11,11	12,91	8,53	9,52	10,72
MnO	0,22	0,18	0,20	0,21	0,16	0,23	0,27
MgO	7,26	16,86	8,16	8,52	11,21	13,22	4,85
CaO	8,68	5,42	8,14	10,18	11,77	14,06	17,73
Na_2O	1,60	0,75	1,81	1,71	1,89	1,26	1,53
K_2O	1,52	0,98	0,78	1,00	0,83	0,12	0,66
P_2O_5	0,14	0,06	0,12	0,10	0,04	0,04	0,28
Cr_2O_3	0,06	0,32	0,05	0,05	0,21	0,26	0,01
NiO	0,03	0,09	0,03	0,04	0,04	0,05	0,02
LOI	1,00	1,65	1,07	0,45	1,32	0,32	1,00
H_2O^-	0,19	0,17	0,16	0,16	0,14	0,07	0,21
Total	98,63	98,94	98,61	99,08	99,34	99,58	99,74
			CIPW NORMS				
Q	0,00	2,87	3,76	0,00	1,14	0,00	0,30
or	9,19	5,94	4,74	5,96	5,01	0,71	3,93
ab	13,87	6,57	15,73	14,63	16,35	10,74	13,09
an	33,52	22,35	31,96	27,73	16,18	17,89	25,43
di	7,95	3,95	7,06	18,68	34,65	41,78	50,18
hy	25,50	54,11	31,70	22,77	22,53	22,13	0,00
wo	0,00	0,00	0,00	0,00	0,00	0,00	0,52
ol	4,12	0,00	0,00	4,13	0,00	2,28	0,00
mt	3,89	2,96	3,37	3,87	2,58	2,84	3,21
il	1,53	0,63	1,32	1,92	1,16	1,15	2,66
cm	0,08	0,48	0,08	0,08	0,31	0,39	0,02
ap	0,33	0,18	0,28	0,23	0,09	0,10	0,65
D.I.	23,06	15,38	24,22	20,59	22,50	11,45	17,33
			MODAL ANALYSES				
-	-	-	-	-	-	-	-
-	-	-	-	-	-	-	-
-	-	-	-	-	-	-	-
-	-	-	-	-	-	-	-
-	-	-	-	-	-	-	-

APPENDIX 3 (TRACE ELEMENT ANALYSES)

Appendix 3 I TRACE ELEMENT ANALYSES OF NEBO GRANITE

Sample No.	GR-98*	GR-115*	GN-53*	GN-1*	GN-56	GN-52	GN-58A	GN-58	GN-51	GN-44	GGr-95	GGr-214	GGr-255	GN-50	GN-4	GN-8	GN-9	GN-12	GN-12A
Ba	2618	2210	2294	1280	2139	1534	1808	1935	1770	1174	1187	1137	540	633	737	590	521	546	554
Rb	138	149	147	114	124	180	158	143	164	169	166	170	232	228	180	225	210	226	255
Sr	167	148	144	68	132	91	103	128	109	84	66	84	31	49	54	37	25	34	32
Y	38	72	71	53	50	73	56	54	54	64	79	57	114	106	68	94	98	94	75
Zr	441	599	607	481	576	569	620	524	537	467	463	396	408	396	355	385	352	375	346
Nb	15	33	27	21	25	28	23	21	23	23	30	21	39	32	24	28	31	32	36
La	29	81	59	79	48	59	59	57	57	68	77	76	106	83	85	122	101	114	83
Ce	50	145	118	141	94	123	106	108	105	140	147	146	210	170	170	239	206	221	158
Nd	35	81	73	76	60	81	68	70	67	85	88	84	127	114	100	139	124	133	89
Th	10	23	19	20	14	18	12	18	18	21	25	22	41	32	25	35	39	37	32
U	2	4	5	5	2	5	3	7	7	4	8	5	12	7	4	10	9	8	9
Hf	8	8	11	8	8	9	7	11	9	10	11	5	11	9	13	10	11	12	11
Ga	18	21	21	19	18	21	20	19	19	20	21	19	22	21	20	21	20	21	20
Sc	2	3	2	1	2	2	2	1	1	2	1	2	1	1	2	1	1	1	1
Zn	102	105	109	49	113	138	110	118	122	86	58	73	76	88	65	71	70	64	69
Cu	20	1	5	25	1	5	1	5	8	6	16	3	5	6	3	7	5	3	14
Ni	6	5	6	11	5	7	7	6	7	12	11	9	9	7	12	16	12	11	9
Pb	21	15	14	17	21	33	20	30	30	20	20	20	25	25	20	24	23	25	21
Mo	0	9	6	2	3	1	2	4	3	1	27	2	2	1	2	3	2	2	32
W	1	6	6	4	6	6	7	6	5	8	10	8	13	10	7	7	7	5	7
Sn	0	5	0	1	0	2	2	0	0	2	0	0	6	6	3	5	6	6	5
ELEMENT RATIOS																			
K/Rb	297	250	262	330	333	226	270	283	253	243	251	238	184	172	231	189	197	180	170
K/Sr	246	251	267	553	313	447	414	316	392	488	630	483	1378	801	769	1149	1657	1196	1353
K/Ba	16	17	17	29	19	27	24	21	23	35	35	36	79	62	56	72	80	75	78
Ca/Sr	66	80	85	112	81	100	77	80	78	96	83	97	214	122	128	158	179	85	200
Ti/Zr	6,0	4,2	4,2	3,6	4,0	3,6	3,2	3,8	3,6	3,7	3,2	3,9	3,4	3,3	3,5	3,1	3,2	3,0	3,5
Rb/Sr	0,8	1,0	1,0	1,7	0,9	2,0	1,5	1,1	1,5	2,0	2,5	2,0	7,5	4,7	3,3	6,1	8,4	6,7	8,0
Ba/Rb	19,0	14,8	15,6	11,2	17,3	8,5	12,3	12,7	10,8	7,0	7,2	6,7	2,3	2,8	4,1	2,6	2,5	2,4	2,2
Ba/Sr	15,7	14,9	15,9	18,8	16,2	16,9	14,1	18,8	16,2	14,0	18,0	13,5	17,5	12,9	13,7	15,9	20,9	16,1	17,3
Zr/Nb	29,4	18,2	22,5	22,9	23,0	20,3	27,0	25,0	23,3	20,3	15,4	18,9	10,5	12,4	14,8	13,8	11,4	11,7	9,6
Th/U	5,0	5,8	3,8	4,0	7,0	3,6	4,0	2,6	2,6	5,3	3,1	4,4	3,4	4,6	6,3	3,5	4,3	4,6	3,6

* Granite from intrusion breccia

TRACE ELEMENT ANALYSES OF NEBO GRANITE

Sample No.	GN-16	GN-60	GGr-260	VW4-31,0	VW4-35,5	VW4-40,75	VW4-53,0	VW4-60,15	VW4-71,70	VW4-81,5
Ba	533	578	208	573	600	574	469	449	527	462
Rb	259	235	235	236	240	235	281	255	229	242
Sr	32	37	15	31	31	33	23	26	37	19
Y	95	87	167	114	83	92	74	40	80	61
Zr	315	323	215	368	315	321	175	180	270	241
Nb	34	30	24	39	33	34	26	19	26	33
La	95	98	102	87	103	75	241	74	177	36
Ce	177	188	186	182	206	154	484	149	317	68
Nd	102	112	130	110	119	94	254	80	153	43
Th	34	34	42	37	32	28	62	34	41	33
U	8	9	9	7	4	8	11	8	7	6
Hf	7	9	7	11	9	10	5	7	9	5
Ga	21	27	21	20	20	21	22	20	20	20
Sc	1	1	0	2	2	1	1	0	1	0
Zn	70	52	47	64	60	58	71	53	53	49
Cu	11	4	11	8	8	10	2	3	4	4
Ni	13	8	4	11	10	10	6	7	9	12
Pb	24	21	28	24	21	20	28	18	21	21
Mo	119	4	1	9	7	9	6	3	3	8
W	11	8	10	10	8	8	34	6	6	5
Sn	7	2	6	3	8	6	6	2	7	3
ELEMENT RATIOS										
K/Rb	166	183	175	190	195	193	170	185	190	192
K/Sr	1342	1162	2749	1443	1506	1372	2075	1818	1175	2442
K/Ba	81	74	198	78	78	79	102	105	83	100
Ca/Sr	212	173	197	279	186	185	116	114	136	117
Ti/Zr	3,6	3,5	3,3	3,6	3,4	3,4	4,5	4,3	3,8	3,2
Rb/Sr	8,1	6,4	15,7	7,6	7,7	7,1	12,2	9,8	6,2	12,7
Ba/Rb	2,1	2,5	0,9	2,4	2,5	2,5	1,7	1,8	2,3	1,9
Ba/Sr	16,7	15,6	13,9	18,5	19,4	17,4	20,4	17,3	14,3	24,4
Zr/Nb	9,3	10,8	9,0	9,4	9,5	9,4	6,7	9,5	10,4	7,3
Th/U	4,3	3,8	4,7	5,3	8,0	3,5	5,6	4,3	5,9	5,5

TRACE ELEMENT ANALYSES OF MEDIUM- TO COARSE-GRAINED KLIPKLOOF GRANITE

Sample No.	VW4-48,85	GN-28	GN-33	GN-35	GN-40	GGr-146	GK-53	GGr-358	GGr-363
Ba	324	137	191	162	145	152	152	155	174
Rb	248	262	251	258	244	280	259	266	259
Sr	25	12	6	14	13	6	11	10	7
Y	93	136	122	177	137	180	150	150	136
Zr	199	251	282	282	230	360	263	263	272
Nb	32	25	38	20	33	78	47	47	52
La	124	79	126	95	130	68	135	205	119
Ce	239	152	242	192	262	127	245	351	229
Nd	134	91	131	141	146	79	127	167	120
Th	63	41	45	45	44	67	50	48	55
U	17	14	12	11	12	18	18	15	9
Hf	9	9	10	11	7	14	6	9	9
Ga	25	24	23	22	22	28	25	24	25
Sc	1	0	0	0	0	0	0	0	1
Zn	76	53	44	44	37	40	96	69	43
Cu	6	0	0	1	1	5	0	1	2
Ni	8	7	13	8	11	10	6	8	9
Pb	24	18	6	20	21	40	31	18	5
Mo	1	7	0	1	2	2	41	18	5
W	6	10	8	13	10	13	13	10	10
Sn	2	7	5	8	7	20	8	7	9
ELEMENT RATIOS									
K/Rb	158	152	155	162	170	155	159	159	157
K/Sr	1567	3322	6505	2987	3200	7248	3734	4228	5814
K/Ba	286	291	204	258	287	286	270	273	234
Ca/Sr	147	282	396	185	338	1104	615	461	802
Ti/Zr	4,2	1,9	1,9	2,3	2,3	1,5	2,1	2,1	2,0
Rb/Sr	9,9	21,8	41,8	18,4	18,7	46,7	23,5	26,6	37,0
Ba/Rb	1,3	0,5	0,8	0,6	0,6	0,5	0,6	0,6	0,7
Ba/Sr	13,0	11,5	32,0	11,6	11,2	25,3	13,9	15,6	24,9
Zr/Nb	6,2	10,0	7,4	14,1	7,0	4,6	5,6	5,6	5,2
Th/U	3,7	2,9	3,8	4,1	3,7	3,7	2,8	3,2	6,1

III TRACE ELEMENT ANALYSES OF PORPHYRITIC KLIPKLOOF GRANITE

Sample No.	GK-20B	GK-25	GK-27	GK-29	GK-39	GK-42	GGr-129	GGr-131	GGr-143	GGr-145	GGr-167	GGr-181	GGr-184	GGr-193	GGr-194	GGr-195	GGr-196
Ba	269	262	93	133	187	177	214	259	130	134	189	186	148	142	273	335	246
Rb	254	278	320	320	294	276	248	308	314	290	245	249	267	289	260	229	233
Sr	13	15	13	12	11	15	14	9	12	12	18	19	11	11	15	16	11
Y	140	136	204	157	134	148	144	104	153	117	137	158	153	127	138	177	131
Zr	272	320	308	272	307	339	351	316	275	342	276	310	218	313	280	324	292
Nb	47	32	36	41	42	42	40	25	60	39	49	34	55	38	29	37	51
La	115	118	95	96	89	107	145	93	71	55	113	87	161	110	61	45	73
Ce	213	218	197	199	185	214	274	178	141	119	212	177	297	206	135	110	119
Nd	125	118	133	128	110	128	166	98	91	73	123	124	159	118	90	97	83
Th	55	49	53	51	48	50	50	45	55	46	54	48	63	48	47	49	49
U	20	19	16	16	16	17	12	20	19	13	10	13	18	18	16	14	8
Hf	10	10	8	9	10	9	10	11	9	12	8	8	8	9	10	9	10
Ga	24	24	25	25	24	24	24	24	26	25	25	23	25	23	23	21	22
Sc	0	0	0	0	0	0	0	0	0	0	0	0	0	0	0	0	0
Zn	60	58	58	65	58	64	69	39	56	44	46	42	60	74	43	75	17
Cu	1	0	1	0	0	1	2	3	0	15	1	3	0	0	3	1	3
Ni	12	10	13	9	12	13	9	7	8	12	8	12	7	8	15	10	12
Pb	20	24	27	25	29	31	28	8	24	145	23	23	23	26	18	27	15
Mo	7	17	4	5	2	2	3	2	6	2	1	2	5	2	14	1	0
W	8	12	11	8	8	8	8	8	14	9	11	12	11	6	6	11	11
Sn	3	1	6	10	0	3	8	30	5	3	6	1	6	8	6	8	10
ELEMENT RATIOS																	
K/Rb	171	156	136	139	149	160	167	151	138	142	167	176	145	153	166	184	175
K/Sr	3347	2895	3351	3713	3976	2941	2964	5154	3605	3443	2268	2311	3513	4024	2871	2631	3710
K/Ba	162	166	468	335	234	249	194	179	333	308	216	236	261	312	158	126	166
Ca/Sr	299	101	354	348	406	245	267	648	318	330	264	201	334	301	144	270	255
Ti/Zr	2,4	2,1	2,3	2,6	2,5	2,1	2,6	2,7	2,4	2,1	2,4	2,3	2,8	2,1	2,1	3,0	3,1
Rb/Sr	19,5	18,5	24,6	26,7	26,7	18,4	17,7	34,2	26,2	24,2	13,8	13,1	24,3	26,3	17,3	14,3	21,2
Ba/Rb	1,1	1,0	0,3	0,4	0,6	0,6	0,9	0,8	0,4	0,5	0,8	0,8	0,6	0,5	1,1	1,5	1,1
Ba/Sr	20,7	17,5	7,2	11,2	17,0	11,9	15,4	28,9	10,8	11,2	10,5	9,8	13,5	13,0	18,2	21,0	22,5
Zr/Nb	5,8	10,0	8,6	6,6	7,3	8,1	8,8	12,6	4,6	8,8	5,6	9,1	4,0	8,2	9,7	8,8	5,7
Th/U	2,8	2,6	3,3	3,2	3,0	2,9	4,2	2,3	2,9	3,5	5,4	3,7	3,5	2,7	2,9	3,5	6,1

IV TRACE ELEMENT ANALYSES OF PORPHYRITIC KLIPKLOOF GRANITE

Sample No.	GGr-237	GK-61	GK-63	GK-66	GK-67	GGr-254	GGr-261	GGr-261A
Ba	133	188	187	320	412	165	246	242
Rb	329	298	255	232	243	283	294	297
Sr	6	11	9	17	25	11	8	7
Y	156	150	112	171	115	124	123	122
Zr	339	274	245	270	388	210	284	282
Nb	49	58	48	38	26	37	57	57
La	280	98	82	278	193	194	161	157
Ce	253	192	166	457	346	338	287	282
Nd	232	130	89	254	180	150	136	135
Th	49	50	46	47	46	47	42	40
U	6	18	12	7	10	11	6	5
Hf	13	9	9	2	10	8	11	11
Ga	27	19	25	22	21	25	23	24
Sc	0	0	0	0	0	0	1	1
Zn	11	66	47	91	96	52	52	52
Cu	1	0	4	2	1	5	0	2
Ni	12	8	7	8	6	5	8	10
Pb	5	33	18	34	38	35	34	33
Mo	3	4	11	2	12	7	7	10
W	8	11	12	13	11	9	11	10
Sn	6	3	8	5	8	7	18	18
ELEMENT RATIOS								
K/Rb	133	147	155	193	178	146	155	154
K/Sr	7303	3971	4396	2633	1734	3767	6483	5701
K/Ba	329	232	212	140	105	251	184	188
Ca/Sr	144	321	536	330	121	563	702	885
Ti/Zr	1,6	2,6	2,9	2,9	2,6	3,1	2,7	3,0
Rb/Sr	54,8	27,1	28,3	13,6	9,7	25,7	36,8	42,4
Ba/Rb	0,4	0,6	0,7	1,4	1,7	0,6	0,8	0,8
Ba/Sr	22,2	17,2	20,8	18,8	16,5	15,0	34,7	30,8
Zr/Nb	6,9	4,7	5,1	7,1	14,9	5,7	4,9	5,0
Th/U	8,2	2,8	3,8	6,7	4,6	4,3	7,0	8,0

TRACE ELEMENT ANALYSES OF FINE- TO MEDIUM-GRAINED KLIPKLOOF GRANITE

	VW4-6,3	VW4-90,0	VW4-92,4	VW4-98,2	VW4-107,8	GK-5	GK-10	GK-13	GK-17
Ba	297	229	238	71	201	266	192	241	194
Rb	260	240	269	466	264	234	238	264	257
Sr	14	10	12	8	15	16	7	20	18
Y	157	132	204	150	145	134	143	109	176
Zr	327	211	276	269	223	135	217	302	287
Nb	21	36	41	52	48	13	52	25	37
La	82	81	66	80	102	134	94	86	133
Ce	170	187	135	154	217	260	183	167	285
Nd	124	131	91	86	135	143	97	101	201
Th	47	53	55	49	56	46	54	49	58
U	18	12	23	22	20	15	22	14	15
Hf	11	9	11	11	9	8	9	10	11
Ga	24	24	24	27	25	25	27	23	22
Sc	0	0	0	0	1	0	0	0	0
Zn	56	11	66	59	67	63	37	63	64
Cu	29	3	1	2	13	1	3	1	5
Ni	12	7	12	9	10	12	14	13	13
Pb	18	5	28	33	21	31	9	20	25
Mo	5	1	7	1	6	2	4	1	2
W	18	12	16	11	14	10	14	11	9
Sn	6	5	6	7	4	6	0	6	8
ELEMENT RATIOS									
K/Rb	153	155	173	92	163	180	164	153	172
K/Sr	2834	3711	3889	5360	2872	2626	5563	2018	2458
K/Ba	134	162	196	604	214	158	203	167	228
Ca/Sr	118	130	486	621	293	180	627	184	176
Ti/Zr	2,4	3,7	2,8	2,0	3,2	4,4	2,5	2,4	4,8
Rb/Sr	18,6	24,0	22,4	58,3	17,6	14,6	34,0	13,2	8,1
Ba/Rb	1,2	1,0	0,9	0,2	0,8	1,1	0,8	0,9	0,8
Ba/Sr	21,3	23,0	19,9	8,9	13,5	16,7	27,4	12,1	10,8
Zr/Nb	15,6	5,9	6,7	5,2	4,6	10,4	4,2	12,1	7,8
Th/U	2,6	4,4	2,4	2,2	2,8	3,1	2,5	3,5	3,9

TRACE ELEMENT ANALYSES OF FINE- TO MEDIUM-GRAINED KLIPKLOOF GRANITE

Sample No.	GK-18	GK-19	GK-20A	GK-21	GK-22	GK-23	GK-24	GK-26	GK-30	GK-34	GK-38	GK-41	GGr-126	GGr-136	GGr-142	GGr-144	GGr-153	GGr-156
Ba	215	230	295	111	204	229	232	191	100	115	150	103	212	202	164	123	99	87
Rb	251	230	259	312	243	246	228	281	356	294	275	302	219	235	269	307	301	329
Sr	14	10	15	13	11	10	10	11	9	7	10	11	11	13	12	9	14	10
Y	136	159	150	154	170	152	152	136	159	152	114	161	129	162	171	156	139	178
Zr	302	104	352	343	291	285	292	278	300	294	325	243	229	293	291	264	267	244
Nb	31	29	50	27	53	50	29	50	51	46	55	43	47	55	42	47	46	67
La	91	61	118	96	100	87	96	105	116	44	100	74	83	97	99	83	90	79
Ce	171	138	207	195	193	180	193	188	217	89	178	159	158	177	192	161	176	151
Nd	95	120	115	121	107	103	126	99	119	59	86	106	87	113	118	96	99	95
Th	52	54	50	44	51	51	58	51	53	48	54	48	44	53	50	48	53	54
U	22	19	18	15	19	20	27	18	20	18	19	15	13	13	16	13	17	25
Hf	10	6	12	9	12	8	10	9	9	10	12	7	11	7	10	10	10	10
Ga	24	23	25	24	26	26	27	27	27	26	26	25	26	25	25	26	25	26
Sc	0	0	0	0	0	0	0	0	0	0	0	0	0	0	0	0	0	0
Zn	56	67	66	59	69	72	43	77	64	31	54	61	39	62	66	64	51	35
Cu	4	4	0	1	3	0	10	2	0	2	0	0	3	3	2	0	0	1
Ni	11	12	15	11	12	12	12	9	13	13	9	11	10	8	9	6	10	9
Pb	32	9	24	27	16	18	34	30	27	11	14	28	16	26	30	24	24	16
Mo	8	60	6	1	7	3	15	59	1	1	3	0	2	14	15	1	0	1
W	10	10	10	8	13	13	12	7	12	10	10	8	11	11	15	9	9	13
Sn	6	7	7	8	5	6	7	10	4	5	5	5	3	4	1	8	5	8
ELEMENT RATIOS																		
K/Rb	169	161	167	138	173	171	165	159	121	146	158	147	185	170	152	138	153	124
K/Sr	3027	3700	2880	3258	3830	4219	3754	4072	4803	6154	4354	4028	3685	3018	3411	4726	3291	4067
K/Ba	197	161	146	382	207	184	162	235	432	375	290	430	191	194	250	346	465	467
Ca/Sr	303	590	293	316	386	418	209	327	472	813	410	360	340	354	330	464	303	446
Ti/Zr	2,2	6,9	2,4	2,1	2,3	2,1	1,8	2,2	2,2	2,0	1,7	3,2	2,1	2,3	2,3	2,5	2,7	2,5
Rb/Sr	14,3	23,0	17,3	24,0	22,1	24,6	22,8	25,6	39,6	42,0	27,5	27,5	19,9	18,1	22,4	34,1	21,5	32,9
Ba/Rb	0,9	1,0	1,1	0,4	0,8	0,9	1,0	0,7	0,3	0,4	0,6	0,3	1,0	0,9	0,6	0,4	0,3	0,3
Ba/Sr	15,4	23,0	19,7	8,5	18,5	23,0	23,2	17,5	11,2	16,4	15,1	9,5	19,3	15,6	13,8	13,8	7,1	8,7
Zr/Nb	9,7	3,6	7,0	12,7	5,5	5,7	10,1	5,6	5,9	6,4	5,9	5,7	4,9	5,3	6,9	5,6	5,8	3,6
Th/U	2,4	2,8	2,8	2,7	2,7	2,6	2,1	2,8	2,7	2,7	2,8	3,2	3,4	4,1	3,1	3,7	3,1	2,2

TRACE ELEMENT ANALYSES OF FINE- TO MEDIUM-GRAINED KLIPKLOOF GRANITE

Sample No.	GGr-166	GGr-168	GGr-177	GGr-178	GGr-182	GGr-185	GGr-197	GGr-224	GK-51	GK-59	GK-62	GK-64	GK-65	GGr-152	GGr-155	GGr-172	GGr-179	GGr-183
Ba	224	254	253	232	161	211	210	246	158	405	109	168	231	177	171	203	290	208
Rb	183	225	201	237	272	334	238	340	280	329	329	291	247	313	278	231	221	280
Sr	11	11	11	17	12	8	14	7	7	10	14	8	14	9	9	10	15	10
Y	99	131	130	165	101	168	147	136	146	139	196	217	114	111	113	144	118	156
Zr	105	176	152	203	213	332	363	260	236	302	307	309	231	311	191	395	390	308
Nb	22	33	29	23	45	36	49	52	50	26	60	46	11	66	50	29	15	50
La	116	102	41	94	77	61	154	87	77	57	105	122	71	82	85	75	145	111
Ce	233	181	63	215	143	102	293	164	141	112	200	254	137	102	150	141	218	211
Nd	128	113	53	162	76	90	169	93	80	99	122	160	91	47	90	78	145	123
Th	59	48	54	58	45	29	45	45	51	31	49	50	39	58	46	48	39	53
U	14	16	8	19	17	6	15	5	16	10	20	13	17	20	25	19	16	21
Hf	5	5	6	3	8	13	15	12	11	8	10	12	10	11	6	12	12	13
Ga	23	25	23	23	26	25	24	28	26	23	25	26	25	25	26	25	25	26
Sc	0	0	0	0	0	0	1	0	0	0	0	0	1	0	0	0	0	0
Zn	11	22	40	57	27	18	124	28	43	11	49	66	60	6	9	60	56	41
Cu	1	4	3	1	3	0	1	9	2	4	2	1	10	1	2	28	5	2
Ni	8	8	8	9	7	8	9	12	10	10	8	7	7	7	6	6	11	10
Pb	6	7	7	23	10	8	28	9	13	30	27	6	27	11	6	7	15	6
Mo	2	0	1	7	1	2	8	2	2	2	2	2	2	1	7	5	2	13
W	8	8	11	12	8	8	11	11	14	14	14	11	10	11	9	9	6	11
Sn	2	6	7	2	2	4	5	6	2	4	9	0	8	8	4	7	5	1
ELEMENT RATIOS																		
K/Rb	240	190	172	177	159	135	176	125	146	178	133	144	183	141	149	149	183	148
K/Sr	3991	3880	3140	3472	3595	5616	2997	6069	5850	5848	3116	5248	3231	4906	4597	3449	2702	4161
K/Ba	196	168	137	181	268	213	200	173	259	144	400	250	196	249	242	170	140	200
Ca/Sr	308	484	190	208	318	567	273	483	813	252	303	612	226	408	120	403	125	353
Ti/Zr	6,3	3,8	5,1	3,5	2,5	1,4	2,1	1,8	2,8	2,2	2,3	2,1	2,6	2,1	3,1	1,2	1,8	2,3
Rb/Sr	16,6	20,5	18,3	13,9	22,7	41,8	17,0	48,6	40,0	32,9	23,5	36,4	17,6	34,8	30,9	23,1	14,7	28,0
Ba/Rb	1,2	1,1	1,3	1,0	0,6	0,6	0,9	0,7	0,6	1,2	0,3	0,6	0,9	0,6	0,6	0,9	1,3	0,7
Ba/Sr	20,5	23,1	23,1	13,7	13,5	26,5	15,1	35,1	22,7	40,5	7,9	21,1	16,6	19,7	19,0	20,3	19,4	20,8
Zr/Nb	4,8	5,3	5,2	8,8	4,7	9,2	7,4	5,0	4,7	11,6	5,1	6,7	21,0	4,7	3,8	13,6	26,0	6,2
Th/U	4,2	3,0	6,8	3,1	2,6	4,8	3,0	9,0	3,2	3,1	2,5	3,8	2,3	2,9	1,8	2,5	2,4	2,5

TRACE ELEMENT ANALYSES OF FINE- TO MEDIUM-GRAINED KLIPKLOOF GRANITE

Sample No.	GGr-257	GGr-258	GGr-259	GGr-213	GGr-236	GGr-300
Ba	170	132	179	1116	209	342
Rb	339	194	258	153	322	443
Sr	10	14	12	86	7	26
Y	191	218	151	36	130	346
Zr	271	497	246	433	365	166
Nb	65	30	37	27	51	0
La	178	64	58	52	116	26
Ce	314	140	124	100	123	79
Nd	168	116	80	60	68	64
Th	48	57	47	28	49	68
U	22	17	13	7	5	10
Hf	10	16	8	9	14	9
Ga	28	24	25	19	26	31
Sc	0	0	0	0	0	3
Zn	7	53	57	41	17	-
Cu	1	1	4	3	2	-
Ni	6	8	7	12	13	-
Pb	9	20	89	18	6	16
Mo	2	3	5	1	1	11158
W	13	17	11	3	12	18
Sn	5	4	5	4	6	1
ELEMENT RATIOS						
K/Rb	129	174	166	275	133	161
K/Sr	4358	2407	3578	489	6142	2739
K/Ba	256	255	240	38	206	208
Ca/Sr	903	211	1065	37	165	4090
Ti/Zr	1,8	2,1	2,7	2,6	1,8	0,4
Rb/Sr	33,9	13,9	21,5	1,8	46,0	17,0
Ba/Rb	0,5	0,7	0,7	7,3	0,7	0,8
Ba/Sr	17,0	9,4	14,9	13,0	29,8	13,2
Zr/Nb	4,2	16,6	6,6	16,0	7,2	-
Th/U	2,2	3,4	3,6	4,0	9,8	6,8

TRACE ELEMENT ANALYSES OF ALBITIZED KLIPKLOOF GRANITE

VW4-93,35	VW4-96,0	GK-11	GK-14	GK-31	GK-32	GK-36	GK-37	GK-52	GGr-175	GGr-176	GGr-256
67	57	13	185	47	36	40	7	59	1	16	33
499	451	600	654	505	506	627	669	391	606	441	643
8	9	7	15	9	9	9	9	10	6	4	9
80	165	129	94	150	147	168	149	203	122	111	158
271	317	213	202	263	293	292	294	295	203	215	277
58	59	61	27	52	49	85	71	55	68	46	88
81	64	155	68	80	86	77	50	115	38	53	72
134	131	95	135	147	162	137	89	224	72	59	121
52	80	45	74	78	87	62	26	130	33	55	55
33	46	46	55	53	47	57	53	49	54	46	63
18	21	14	19	8	20	27	18	22	29	9	29
10	14	11	14	11	11	13	17	13	7	12	13
31	28	29	33	28	28	30	31	27	30	28	32
0	1	0	0	0	0	0	0	0	0	0	0
81	54	17	20	31	39	16	14	58	14	14	19
1	3	0	11	2	3	6	0	0	0	0	6
9	10	13	15	10	15	9	6	8	6	6	6
43	32	29	22	23	41	25	20	34	31	21	30
2	1	1	4	2	1	2	0	1	0	0	2
8	10	11	11	10	12	10	8	14	13	10	14
11	6	8	6	15	10	117	14	5	17	9	34
ELEMENT RATIOS											
82	89	63	66	82	82	63	57	109	59	85	61
5139	4490	5369	2876	4611	4609	4379	4273	4270	5920	9323	4360
614	709	2891	233	883	1152	985	5494	724	35520	2331	1189
747	600	607	115	560	512	544	416	482	624	720	520
2,0	1,7	1,4	0,9	1,8	1,6	1,0	1,4	2,2	2,1	1,7	1,3
62,4	50,1	85,7	43,6	56,1	56,2	69,7	74,3	39,1	101,0	110,3	71,4
0,1	0,1	0,0	0,3	0,1	0,1	0,1	0,0	0,2	0,0	0,0	0,1
8,4	6,4	1,9	12,3	5,3	4,1	4,4	0,8	6,0	0,3	4,0	3,7
4,7	5,4	3,5	7,5	5,1	6,0	3,4	4,1	5,4	3,0	4,7	3,1
1,8	2,2	3,3	2,9	6,6	2,4	2,1	2,9	2,2	1,9	5,1	2,2

TRACE ELEMENT ANALYSES OF ROOIBERG FELSITE

Sample No.	F-60	F-61	F-62	F-63	F-65	F-66	F-67	F-68	F-71	GR-236	GR-264	GR-265	GR-267	GR-269	GR-270	GR-155F
Ba	1004	885	926	981	1020	1018	953	954	862	943	1059	1048	935	970	919	1037
Rb	210	192	200	208	247	192	192	126	163	210	198	205	151	127	192	177
Sr	36	31	45	38	75	55	53	123	82	40	115	51	158	130	142	99
Y	56	65	67	64	58	60	62	60	62	79	66	72	58	55	54	63
Zr	428	427	429	430	450	430	437	381	437	418	431	427	386	362	359	436
Nb	22	23	21	24	23	22	22	20	22	21	22	21	20	18	19	22
La	76	69	68	73	68	70	72	68	69	76	68	73	60	64	59	74
Ce	142	125	129	145	128	129	136	127	136	137	132	140	124	118	113	132
Nd	76	70	72	78	75	70	74	69	77	80	73	82	69	63	60	76
Th	25	23	25	25	27	24	24	21	24	21	25	24	22	22	21	26
U	5	7	6	9	5	7	7	8	7	7	5	6	5	4	6	8
Hf	11	7	9	9	8	11	9	6	10	8	8	8	9	9	8	9
Ga	19	20	20	18	19	19	20	17	19	19	19	19	20	19	19	18
Sc	6	8	8	5	7	6	6	15	6	8	7	8	12	12	12	6
Zn	23	154	138	152	141	55	73	142	114	320	231	263	181	110	81	-
Cu	6	12	3	4	10	1	2	11	12	1	8	14	32	4	15	-
Ni	16	9	16	14	6	6	8	16	6	5	9	4	5	6	6	-
Pb	14	32	29	30	29	19	20	24	19	20	43	37	31	29	29	41
Mo	2	1	1	2	1	3	2	2	2	2	3	2	4	3	1	2
W	11	10	8	7	7	4	8	8	10	7	10	6	8	8	7	5
Sn	5	0	0	6	4	4	7	3	7	7	2	2	0	1	0	2

ELEMENT RATIOS

K/Rb	185	176	184	190	171	191	197	227	208	182	197	194	228	228	191	206
K/Sr	1081	1090	817	1042	563	667	714	233	413	957	339	778	218	223	258	369
K/Ba	39	38	40	40	41	36	40	30	39	41	37	38	37	30	40	35
Ca/Sr	170	539	302	282	110	132	170	110	129	268	117	210	105	120	118	105
Ti/Zr	4,9	4,6	4,9	4,9	4,5	4,7	4,7	8,2	4,7	5,0	4,9	4,8	7,9	8,8	8,9	4,7
Rb/Sr	5,8	6,2	4,4	5,5	3,3	3,5	3,6	1,0	2,0	5,3	1,7	4,0	1,0	1,0	1,4	1,8
Ba/Rb	4,8	4,6	4,6	4,7	4,1	5,3	5,0	7,6	5,3	4,5	5,3	5,1	6,2	7,6	4,8	5,9
Ba/Sr	27,9	28,5	20,6	25,8	13,6	18,5	18,0	7,8	10,5	23,6	9,2	20,5	5,9	7,5	6,5	10,5
Zr/Nb	19,5	18,6	20,4	17,9	19,6	19,5	19,9	19,1	19,9	19,9	19,6	20,3	19,3	20,1	18,9	19,8
Th/U	5,0	3,3	4,2	2,8	5,4	3,4	3,4	2,6	3,4	3,0	5,0	4,0	4,4	5,5	3,5	3,3

TRACE ELEMENT ANALYSES OF STAVOREN MICRO-GRANOPHYRE

Sample No.	GRF-2	GR-133	GR-220	GR-221	GR-225	GR-229	GR-230	GR-231	GR-234	GR-240	GR-134	GR-135	GR-241	GR-242
Ba	1210	1253	1346	1107	967	1286	1255	1210	1378	1198	1237	1265	1201	1252
Rb	214	206	263	298	270	210	206	235	322	183	242	255	219	230
Sr	43	67	65	48	36	59	55	46	52	57	60	59	43	48
Y	79	75	79	79	79	76	78	85	77	79	83	78	96	91
Zr	531	529	520	530	532	523	526	525	527	542	519	528	509	522
Nb	26	28	27	27	25	28	27	27	27	26	28	28	27	26
La	84	86	82	95	87	91	86	90	84	94	88	87	126	134
Ce	163	164	160	173	161	168	164	173	163	168	163	168	234	248
Nd	95	96	89	98	93	100	90	104	95	102	96	97	136	141
Th	28	27	27	29	27	26	27	29	24	28	27	28	28	26
U	10	7	8	5	7	5	7	10	7	9	8	5	5	8
Hf	11	10	10	9	15	9	10	11	8	12	12	11	10	14
Ga	20	19	20	20	21	20	20	20	19	21	18	21	21	19
Sc	0	1	0	0	0	0	0	0	0	0	1	0	0	0
Zn	123	145	103	137	104	229	187	197	122	91	244	212	76	68
Cu	5	12	10	12	9	12	9	4	8	4	14	9	4	1
Ni	15	9	10	13	10	13	11	9	9	11	7	7	5	6
Pb	35	49	30	30	19	39	34	38	21	19	20	48	24	31
Mo	2	0	3	3	3	1	2	2	1	3	2	0	3	1
W	9	7	12	7	6	7	9	9	9	8	7	8	12	14
Sn	11	3	8	5	12	3	1	8	2	8	4	5	6	7
K/Rb	203	216	170	140	154	212	215	190	179	234	185	187	203	201
K/Sr	1011	664	690	866	1155	754	806	971	1111	751	746	807	1033	961
K/Ba	36	36	33	38	43	35	35	37	42	36	36	38	37	37
Ca/Sr	104	91	93	59	78	87	76	97	72	78	63	85	72	72
Ti/Zr	2,8	2,8	2,9	2,7	2,7	2,8	2,9	2,7	2,8	2,7	2,8	2,8	2,8	2,8
Rb/Sr	5,0	3,1	4,0	6,2	7,5	3,6	3,7	5,1	6,2	3,2	4,0	4,3	5,1	4,8
Ba/Rb	5,7	6,1	5,1	3,7	3,6	6,1	6,1	5,1	4,3	6,5	5,1	5,0	5,5	5,4
Ba/Sr	28,1	18,7	20,7	23,1	26,9	21,8	22,8	26,3	26,5	21,0	20,6	21,4	27,9	26,1
Zr/Nb	20,4	18,9	19,6	19,6	21,3	18,7	19,5	19,4	19,5	20,8	18,5	18,9	18,9	20,1
Th/U	2,8	3,9	3,4	5,8	3,9	3,9	3,9	2,9	3,4	3,1	3,4	5,6	5,6	3,3

TRACE ELEMENT ANALYSES OF STAVOREN GRANOPHYRE

Sample No.	GR-43	GR-84M	GGr-10
Ba	1319	3197	1201
Rb	169	150	195
Sr	64	144	42
Y	82	48	87
Zr	493	554	549
Nb	24	17	47
La	83	46	67
Ce	161	99	137
Nd	97	49	92
Th	28	13	29
U	10	4	7
Hf	10	13	10
Ga	21	17	19
Sc	0	1	0
Zn	130	94	108
Cu	5	6	8
Ni	8	8	7
Pb	30	21	20
Mo	1	1	2
W	7	7	11
Sn	0	4	4
K/Rb	258	262	213
K/Sr	682	273	990
K/Ba	33	12	35
Ca/Sr	109	56	72
Ti/Zr	2,9	2,6	3,0
Rb/Sr	2,6	1,0	4,6
Ba/Rb	7,8	21,3	6,2
Ba/Sr	20,6	22,2	28,6
Zr/Nb	20,5	32,6	11,7
Th/U	2,8	3,3	4,1

TRACE ELEMENT ANALYSES OF STAVOREN GRANOPHYRE

Sample No.	GGr-93	GGr-94	GGr-96	GG-54	GG-55	GG-57	GR-69	GR-70	GR-132A	GR-132	GR-150	GR-151	GR-262	GR-263	GR-266	GR-268	GR-155G
Ba	1196	1024	1121	1201	1087	1299	1144	1152	1232	1258	1105	1234	1324	1350	1173	1098	1439
Rb	219	168	176	193	190	175	192	188	228	228	196	221	264	279	200	208	260
Sr	71	58	58	69	41	79	46	44	53	58	47	60	51	38	53	25	55
Y	72	75	78	107	83	75	76	85	35	79	79	83	71	77	72	73	55
Zr	478	414	467	496	474	511	489	529	285	510	536	540	500	470	536	495	543
Nb	21	32	25	27	27	23	27	27	4	26	30	28	26	24	25	27	20
La	75	84	77	140	80	72	89	91	42	86	93	78	58	86	85	79	54
Ce	145	158	144	215	155	149	170	175	70	166	174	154	118	171	161	158	106
Nd	83	93	90	130	89	89	97	102	40	99	102	90	72	96	96	89	62
Th	25	30	26	28	26	26	28	30	11	25	29	28	26	26	29	26	19
U	7	9	7	8	6	7	7	8	6	6	8	7	8	7	6	7	5
Hf	7	6	14	8	10	14	10	10	10	9	12	7	11	7	12	12	11
Ga	20	20	21	20	19	20	19	20	18	19	20	20	20	18	20	19	17
Sc	1	0	1	0	0	0	1	0	0	0	0	0	0	1	0	1	0
Zn	116	104	87	97	72	79	108	198	69	117	55	232	251	166	147	84	-
Cu	3	6	6	4	3	11	0	16	9	12	1	8	19	7	6	3	-
Ni	7	6	7	11	8	9	5	9	4	13	7	7	11	8	8	7	-
Pb	31	34	26	19	25	49	31	48	18	32	24	56	36	34	41	24	30
Mo	2	3	2	3	2	2	2	1	3	5	2	3	2	0	4	2	0
W	6	6	8	11	8	5	7	8	4	9	12	13	11	13	11	8	6
Sn	7	6	3	3	5	2	2	5	2	4	6	0	5	12	4	4	24
									ELEMENT RATIOS								
K/Rb	200	225	239	218	231	246	219	218	187	187	207	195	185	186	205	197	176
K/Sr	618	653	724	609	1069	544	915	930	807	737	864	718	955	1363	774	1637	832
K/Ba	37	37	37	35	40	33	37	36	35	34	37	35	37	38	35	37	32
Ca/Sr	84	103	55	58	44	64	124	147	34	81	139	96	65	174	91	228	103
Ti/Zr	3,0	3,3	3,1	3,1	3,0	3,1	2,8	2,6	0,4	2,8	2,6	2,7	3,0	2,9	2,7	2,8	3,2
Rb/Sr	3,1	2,9	3,0	2,8	4,6	2,2	4,2	4,3	4,3	3,9	4,2	3,7	5,2	7,3	3,8	8,3	4,7
Ba/Rb	5,5	6,1	6,4	6,2	5,7	7,4	6,0	6,1	5,4	5,5	5,6	5,6	5,0	4,8	5,9	5,3	5,5
Ba/Sr	16,8	17,7	19,3	17,4	26,5	16,4	24,9	26,2	23,2	21,7	23,5	20,6	26,0	35,5	22,1	43,9	26,2
Zr/Nb	22,8	12,9	18,7	18,4	17,6	22,2	18,1	19,6	71,3	19,6	17,9	19,3	19,2	19,6	18,3	18,3	27,2
Th/U	3,6	3,3	3,7	3,5	4,3	3,7	4,0	3,8	1,8	4,2	3,6	4,0	3,3	3,7	4,8	3,7	3,8

TRACE ELEMENT ANALYSES OF META FELSITE

Sample No.	GR-10	GR-12	GR-41	GR-48	GR-49	GRL-52	GR-53	GR-55	GR-58	GR-59	GR-60	GR-61	GR-62	GR-66	GR-68	GR-70	GR-71	GR-72
Ba	1237	887	1006	726	1224	856	1544	868	1257	1325	1048	1297	1290	1057	1192	1124	1283	988
Rb	139	171	147	115	140	140	183	182	139	167	148	180	172	168	146	169	98	139
Sr	118	130	208	154	56	169	82	143	156	203	89	177	101	62	113	199	869	123
Y	72	42	51	52	66	52	83	59	24	25	57	21	52	71	55	27	23	50
Zr	374	243	345	356	581	359	453	367	313	358	409	318	314	471	422	321	145	353
Nb	22	14	18	18	25	18	26	17	9	9	19	8	15	24	20	10	2	17
La	67	49	57	55	79	54	79	64	36	37	65	42	69	82	57	40	41	51
Ce	153	93	112	104	154	99	152	110	68	71	123	75	122	156	107	79	68	103
Nd	85	53	63	55	83	52	93	72	36	37	68	37	68	91	66	38	37	57
Th	19	19	16	20	24	21	23	23	14	18	18	9	16	26	18	19	4	17
U	4	2	6	6	8	7	6	5	2	4	4	0	4	8	5	4	3	6
Hf	7	6	4	6	13	7	9	8	6	9	11	5	7	8	11	7	4	6
Ga	18	16	17	19	20	18	21	18	13	15	19	13	17	18	19	14	17	19
Sc	9	4	15	13	0	11	1	12	9	9	7	10	11	2	5	9	1	11
Zn	67	23	129	62	62	64	210	110	41	63	155	53	43	68	115	66	77	118
Cu	1	1	42	26	24	25	23	12	12	4	19	12	52	3	27	15	20	19
Ni	8	7	7	12	6	11	11	7	29	24	5	25	12	6	6	23	10	6
Pb	12	11	24	12	19	17	41	25	7	15	64	10	13	17	27	16	41	25
Mo	0	1	2	2	3	2	4	3	1	1	3	0	0	1	3	1	1	2
W	8	2	2	5	8	7	9	5	5	5	5	10	4	6	6	5	3	8
Sn	0	1	0	6	5	2	3	4	0	0	0	0	6	5	0	0	0	0

ELEMENT RATIOS

K/Rb	302	208	232	228	288	213	220	195	230	226	261	197	264	246	263	222	264	270
K/Sr	355	273	164	170	720	176	490	248	205	186	435	201	450	665	340	189	30	305
K/Ba	34	40	34	36	33	35	26	41	25	28	37	27	35	39	32	33	20	40
Ca/Sr	129	86	79	122	107	121	88	91	56	60	99	62	94	107	90	66	13	111
Ti/Zr	5,8	5,4	12,7	12,5	2,6	12,2	3,7	7,0	9,2	8,4	5,4	10,0	8,8	2,9	5,3	9,0	9,5	7,8
Rb/Sr	1,2	1,3	0,7	0,8	2,5	0,8	2,2	1,3	0,9	0,8	1,7	1,0	1,7	2,7	1,3	0,9	0,1	1,1
Ba/Rb	8,9	5,2	6,8	6,3	8,7	6,1	8,4	4,8	9,0	7,9	7,1	7,2	7,5	6,3	8,2	6,7	13,1	7,1
Ba/Sr	10,5	6,8	4,8	4,7	21,9	5,1	18,8	6,1	8,1	6,5	11,8	7,3	12,8	17,0	10,5	5,6	1,5	8,0
Zr/Nb	17,0	17,4	19,2	19,8	23,2	19,9	17,4	21,6	34,8	40,0	21,5	40,0	20,9	19,6	21,1	32,1	72,5	20,8
Th/U	4,8	9,5	2,7	3,3	3,0	3,0	3,8	4,6	7,0	4,5	4,5	-	4,0	3,3	3,6	4,8	1,3	2,8

XII

TRACE ELEMENT ANALYSES OF META FELSITE

Sample No.	GR-73	GR-80	GR-81	GR-82A	GR-82B	GR-85	GR-86	GR-103
Ba	1026	815	901	801	696	627	934	742
Rb	152	119	123	137	111	143	143	128
Sr	103	174	148	74	93	190	131	115
Y	59	49	50	49	53	56	54	47
Zr	374	325	365	353	378	386	366	349
Nb	21	16	21	18	20	21	18	19
La	65	56	65	56	54	35	56	46
Ce	128	104	115	91	104	68	103	99
Nd	73	61	55	50	59	52	60	52
Th	24	17	20	21	19	22	21	17
U	7	4	8	6	5	5	4	4
Hf	9	6	10	7	15	8	6	4
Ga	19	18	19	16	19	21	18	18
Sc	10	13	8	9	14	13	13	10
Zn	62	143	58	62	74	88	87	101
Cu	13	67	9	6	4	1	27	2
Ni	9	7	8	17	11	4	8	8
Pb	19	27	13	12	10	17	10	12
Mo	3	1	4	3	2	3	1	1
W	10	4	5	4	4	12	6	3
Sn	2	3	0	0	0	5	0	0
ELEMENT RATIOS								
K/Rb	234	179	229	234	224	179	226	191
K/Sr	345	264	190	433	268	135	247	212
K/Ba	35	27	31	40	36	41	35	33
Ca/Sr	103	234	95	120	128	91	125	101
Ti/Zr	6,3	12,7	10,9	10,4	10,5	10,6	11,0	10,1
Rb/Sr	1,5	0,7	0,8	1,9	1,2	0,8	1,1	1,1
Ba/Rb	6,8	6,9	7,3	5,9	6,3	4,4	6,5	5,8
Ba/Sr	10,0	4,7	6,1	10,8	7,5	3,3	7,1	6,5
Zr/Nb	17,8	20,3	17,4	19,6	18,9	18,4	20,3	18,4
Th/U	3,4	4,3	2,5	3,5	3,8	4,4	5,3	4,3

TRACE ELEMENT ANALYSES OF GRANODIORITE (DIEPKLOOF GRANOPHYRE)

Sample No.	GR-67	GR-78	GR-79	GR-200
Ba	992	1674	1426	1298
Rb	124	182	166	120
Sr	184	211	251	209
Y	74	59	68	57
Zr	308	533	390	303
Nb	22	25	27	21
La	64	63	71	61
Ce	129	117	140	116
Nd	80	63	77	67
Th	24	22	22	20
U	5	5	6	7
Hf	3	6	10	4
Ga	22	20	23	22
Sc	7	5	8	6
Zn	197	297	175	116
Cu	16	46	19	44
Ni	8	7	5	4
Pb	22	50	26	18
Mo	3	3	0	2
W	4	5	6	6
Sn	2	0	2	3
ELEMENT RATIOS				
K/Rb	205	188	176	243
K/Sr	138	162	116	140
K/Ba	26	20	21	23
Ca/Sr	124	89	96	92
Ti/Zr	13,3	7,0	10,9	13,7
Rb/Sr	0,7	0,9	0,7	0,6
Ba/Rb	8,0	9,2	8,6	10,8
Ba/Sr	5,4	7,9	5,7	6,2
Zr/Nb	14,0	21,3	14,4	14,4
Th/U	4,8	4,4	3,7	2,9

TRACE ELEMENT ANALYSES OF ANOMALOUS GRANITES

Sample No.	GR-45	GR-160	GGr-107	GGr-140	GGr-191	GGr-215	VW4-50,8
Ba	1089	2366	158	1007	1084	947	52
Rb	212	89	35	104	79	124	28
Sr	59	218	206	164	124	44	18
Y	41	34	22	52	64	57	213
Zr	346	183	186	259	455	318	252
Nb	15	9	4	15	22	18	16
La	68	29	20	66	73	111	21
Ce	105	60	46	127	130	207	62
Nd	53	37	28	71	72	120	80
Th	18	11	5	22	20	25	72
U	6	4	0	2	3	6	28
Hf	-	1	6	9	11	7	15
Ga	-	16	11	17	20	16	31
Sc	4	4	9	7	9	1	0
Zn	45	75	18	32	31	32	17
Cu	10	4	7	3	6	16	19
Ni	0	6	17	6	8	9	9
Pb	15	15	7	11	10	15	8
Mo	0	1	1	0	1	2	17
W	1	3	5	5	3	8	19
Sn	0	0	3	0	0	0	3
ELEMENT RATIOS							
K/Rb	241	292	211	355	398	333	130
K/Sr	865	119	36	224	254	937	203
K/Ba	47	11	47	37	29	44	70
Ca/Sr	33	55	150	72	124	34	104
Ti/Zr	2,4	4,3	7,7	5,8	5,7	3,6	1,0
Rb/Sr	3,4	0,4	0,2	0,6	0,6	2,8	1,6
Ba/Rb	5,1	26,6	4,5	9,7	13,7	7,6	1,9
Ba/Sr	18,5	10,9	0,8	6,1	8,7	21,5	2,9
Zr/Nb	23,1	20,3	46,5	17,3	20,7	17,7	15,8
Th/U	3,0	2,8	-	11,0	6,7	4,2	2,6

TRACE ELEMENT ANALYSES OF PSEUDO-GRANOPHYRE

Sample No.	GR-56	GR-57	GR-114	GR-162	GR-163	GR-1	GR-212	GR-249
Ba	1094	1171	1221	1309	1344	1102	1358	1200
Rb	148	134	209	134	147	151	136	173
Sr	99	113	86	64	63	99	80	74
Y	56	49	88	55	69	53	73	69
Zr	432	386	496	499	428	413	420	500
Nb	20	16	26	22	27	17	25	25
La	61	48	99	51	83	50	113	111
Ce	114	98	188	117	155	106	190	181
Nd	67	61	113	65	91	62	101	92
Th	20	11	30	22	21	18	24	26
U	6	2	8	5	5	7	7	6
Hf	10	8	12	9	6	10	-	-
Ga	19	18	21	19	19	18	-	-
Sc	6	5	0	0	0	5	2	1
Zn	113	106	84	57	103	166	80	153
Cu	24	18	1	11	14	30	3	5
Ni	13	9	6	7	4	9	0	0
Pb	28	27	22	17	24	42	15	23
Mo	3	3	2	0	1	3	1	2
W	9	8	7	9	9	4	4	5
Sn	4	3	0	5	2	1	0	7
K/Rb	249	277	198	286	267	268	314	231
K/Sr	372	329	481	599	622	409	534	541
K/Ba	34	32	34	29	29	37	32	33
Ca/Sr	105	103	67	97	97	113	95	105
Ti/Zr	5,1	6,1	2,9	3,2	3,6	5,5	3,7	2,9
Rb/Sr	1,5	1,2	2,4	2,1	2,3	1,5	1,7	2,3
Ba/Rb	7,4	8,7	5,8	9,8	9,1	7,3	10,0	6,9
Ba/Sr	11,1	10,4	14,2	20,5	21,3	11,1	17,0	16,2
Zr/Nb	21,6	24,1	19,1	22,7	15,9	24,3	16,8	20,0
Th/U	3,3	5,5	3,8	4,4	4,2	2,6	3,4	4,3

TRACE ELEMENT ANALYSES OF PRE-BUSHVELD SILLS

GH-29	GH-148	GH-202	GH-152	GH-204	GH-216	GH-253
677	314	275	450	165	32	174
70	46	40	41	40	2	29
335	141	203	181	99	60	116
29	12	23	25	20	20	43
129	61	107	56	64	39	186
9	0	6	0	4	4	17
11	11	13	0	8	6	24
26	14	24	2	21	0	58
8	1	8	0	1	8	29
0	3	6	1	4	1	8
0	1	3	1	4	2	4
6	7	3	1	0	0	4
20	25	11	14	11	9	20
44	38	44	50	60	66	43
85	80	67	-	-	-	-
32	14	9	-	-	-	-
114	585	123	-	-	-	-
5	5	8	6	4	5	4
0	0	0	0	0	0	12
0	0	0	0	0	0	0
0	0	0	0	0	0	4
180	177	162	202	172	498	189
38	58	32	46	70	17	47
19	26	24	18	42	31	32
187	277	289	405	856	1687	1100
36,7	31,5	38,1	107,1	56,3	92,3	44,5
0,2	0,3	0,2	0,2	0,4	0,0	0,3
9,7	6,8	6,9	11,0	4,1	16,0	6,0
2,0	2,2	1,4	2,5	1,7	0,5	1,5
14,3	-	17,8	-	16,0	9,8	10,9
-	3,0	2,0	1,0	1,0	0,5	2,0

MAP OF SAMPLE LOCALITIES EAST OF GROBLERSDAL

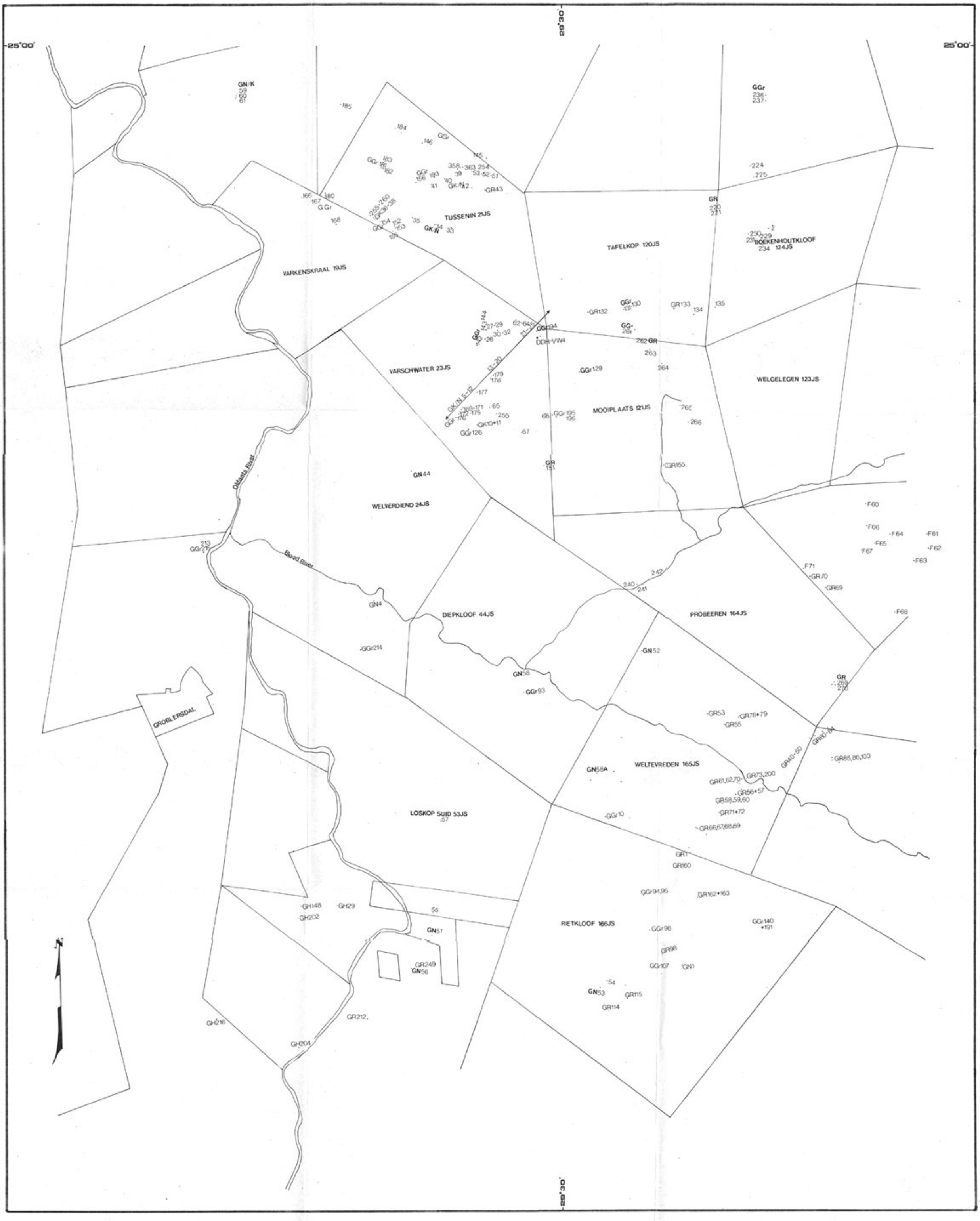

THE GEOLOGY OF THE BUSHVELD COMPLEX AND METAMORPHOSED TRANSVAAL SEQUENCE SEDIMENTARY ROCKS EAST OF GROBLERSDAL

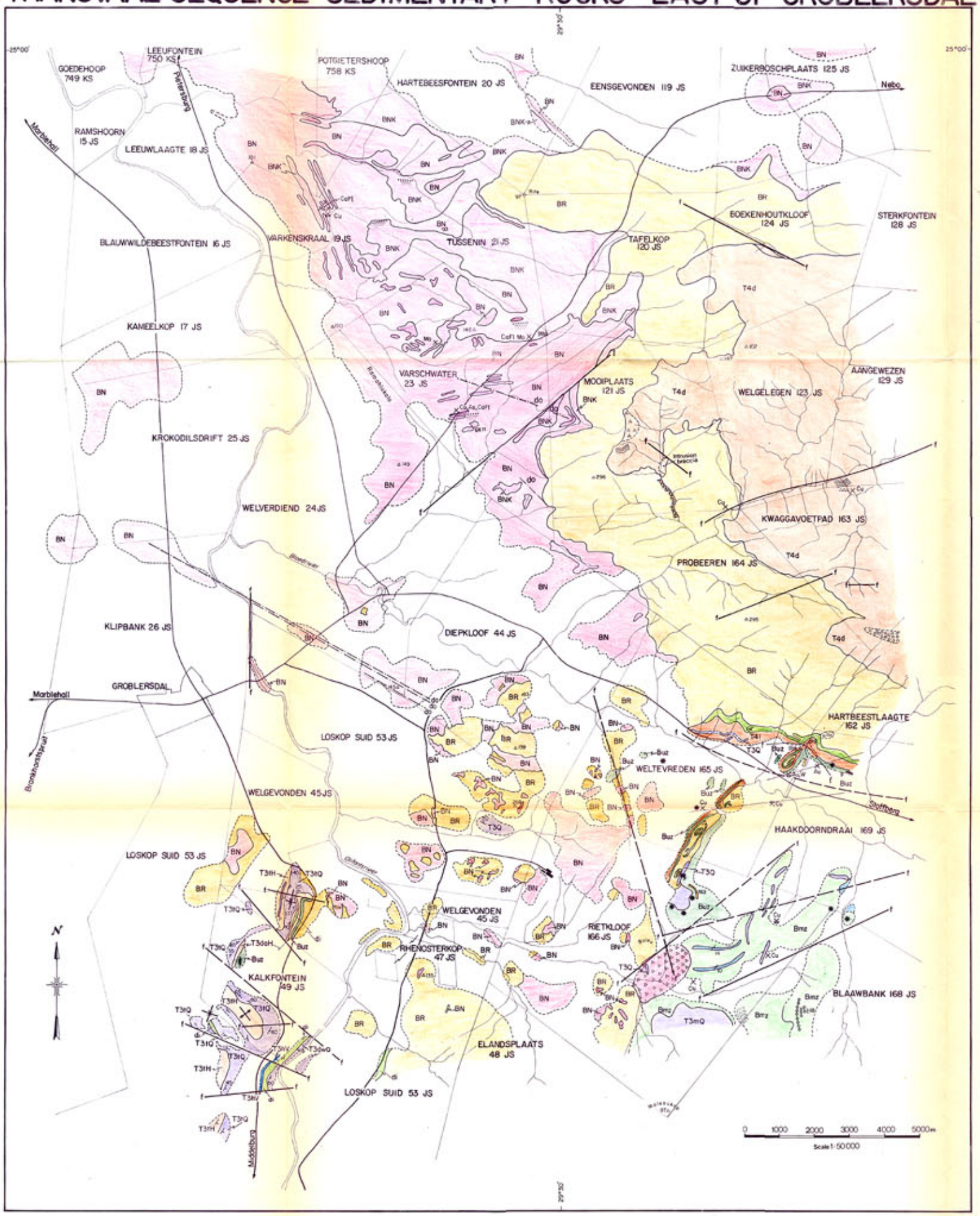

	ALLUVIUM, SOIL COVER AND CULTIVATED LAND			
do	DOLERITE			
	GRANITE AND INTRUSION BRECCIA	NEBO GRANITE	LEBOWA GRANITE SUITE	BUSHVELD COMPLEX
BNK	KLIPKLOOF GRANITE			
BN	NEBO GRANITE			
BR	STAVOREN GRANOPHYRE		RASHOOP GRANOPHYRE SUITE	
Gr	GRANODIORITE		RUSTEBURG LAYERED SUITE	
Buz	DIORITE	UPPER ZONE		
Buz	MAGNETITE GABBRO			
Bmz	GABBRO AND NORITE	MAIN ZONE		
Bmz	ANORTHOSITE			
do	METABASITE		MARICO DIABASE SUITE	
T4d	FELSITE (f flowbanded; a amygdaloidal; c agglomerate)	SELONS RIVER FORMATION	ROOIBERG GROUP (T4)	TRANSVAAL SEQUENCE
T4l	METAFELSITE			
T3Q	QUARTZITE - UNDIFFERENTIATED		PRETORIA GROUP (T3)	
T3mQ	QUARTZITE	MAGALIESBERG FORMATION		
T3dwQ	QUARTZITE	DWAAL HEUWEL FORMATION		
T3hV	ANDESITE LAVA	HEKPOORT FORMATION		
T3tQ	QUARTZITE	TIMEBALL HILL FORMATION		
T3tH	HORNFELS WITH INTERCALATED QUARTZITE			

- NODULES IN GRANITE
- MAGNETITE PLUG
- FRACTURE
- FAULT
- DIP AND STRIKE OF STRATA
- SYNCLINAL STRUCTURE
- ANTICLINAL STRUCTURE
- ABANDONED MINES
- PROSPECT
- SOLID AND INFERRED GEOLOGICAL CONTACT
- MAIN ROAD
- HOMESTEAD
- RIVERS AND STREAMS
- TRIGONOMETRICAL BEACON
- FARM BOUNDARIES